LEABHARLANN CHOLÁISTE NA TRÍONÓIDE, BAILE ÁTHA CLIATH | TRINITY COLLEGE LIBRARY DUBLIN
Ollscoil Átha Cliath | The University of Dublin

Terms and Conditions of Use of Digitised Theses from Trinity College Library Dublin

Copyright statement

All material supplied by Trinity College Library is protected by copyright (under the Copyright and Related Rights Act, 2000 as amended) and other relevant Intellectual Property Rights. By accessing and using a Digitised Thesis from Trinity College Library you acknowledge that all Intellectual Property Rights in any Works supplied are the sole and exclusive property of the copyright and/or other IPR holder. Specific copyright holders may not be explicitly identified. Use of materials from other sources within a thesis should not be construed as a claim over them.

A non-exclusive, non-transferable licence is hereby granted to those using or reproducing, in whole or in part, the material for valid purposes, providing the copyright owners are acknowledged using the normal conventions. Where specific permission to use material is required, this is identified and such permission must be sought from the copyright holder or agency cited.

Liability statement

By using a Digitised Thesis, I accept that Trinity College Dublin bears no legal responsibility for the accuracy, legality or comprehensiveness of materials contained within the thesis, and that Trinity College Dublin accepts no liability for indirect, consequential, or incidental, damages or losses arising from use of the thesis for whatever reason. Information located in a thesis may be subject to specific use constraints, details of which may not be explicitly described. It is the responsibility of potential and actual users to be aware of such constraints and to abide by them. By making use of material from a digitised thesis, you accept these copyright and disclaimer provisions. Where it is brought to the attention of Trinity College Library that there may be a breach of copyright or other restraint, it is the policy to withdraw or take down access to a thesis while the issue is being resolved.

Access Agreement

By using a Digitised Thesis from Trinity College Library you are bound by the following Terms & Conditions. Please read them carefully.

I have read and I understand the following statement: All material supplied via a Digitised Thesis from Trinity College Library is protected by copyright and other intellectual property rights, and duplication or sale of all or part of any of a thesis is not permitted, except that material may be duplicated by you for your research use or for educational purposes in electronic or print form providing the copyright owners are acknowledged using the normal conventions. You must obtain permission for any other use. Electronic or print copies may not be offered, whether for sale or otherwise to anyone. This copy has been supplied on the understanding that it is copyright material and that no quotation from the thesis may be published without proper acknowledgement.

PRODUCTION AND CHARACTERISATION OF SPRAY DRIED PARTICULATE SYSTEMS FOR PULMONARY DRUG DELIVERY

Presented by

Shadeed Gad, B.Sc. (Pharm.), M.P.S.E., M. Sc. (Pharm.).

being a thesis submitted for the degree of
Doctor of Philosophy in Pharmaceutics

at the

University of Dublin, Trinity College

under the direction and supervision of

Anne Marie Healy, B.Sc. (Pharm.), Ph.D., M.P.S.I.

and

Professor Owen I. Corrigan,
B.Sc. (Pharm.) (N.U.I.), M.A., Ph.D. (N.U.I.), F.T.C.D., F.P.S.I.

July, 2009

TRINITY COLLEGE
2 7 JUL 2011
LIBRARY DUBLIN
THES S
9268

DECLARATION

This thesis is submitted by the undersigned to the University of Dublin, Trinity College, for examination for the degree of Doctor of Philosophy. This thesis has not been submitted as an exercise for a degree at any other university. It is entirely the work of the undersigned author, except where duly acknowledged. This manuscript was completely written by the undersigned author, with the aid of editorial advice from Dr. Anne Marie Healy and Professor O. I. Corrigan.

I agree that the Library may lend or copy the thesis upon request. This permission covers only single copies made for study purposes, subject to normal conditions of acknowledgement.

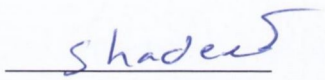

Shadeed Gad

TABLE OF CONTENTS

Acknowledgements I

Presentations associated with this thesis II

Abbreviations and Symbols III

Summary VIII

INTRODUCTION

Origin and Scope 1

Chapter 1: Introduction 3

1.1 Pulmonary Drug Delivery 3

1.1.1 Advantages of pulmonary delivery 3

1.1.2 Optimal site of deposition for treatment of lung diseases 4

1.1.3 Fate of inhaled particles 5

1.1.4 Preparation of particles suitable for pulmonary delivery 5

1.1.5 Types of inhalers 8

1.2 Tuberculosis inhalation therapy 10

1.2.1 Feasibility of pulmonary delivery of antitubercular drugs 11

1.2.2 Limits on the amount of drug delivered by dry powder inhalers 13

1.2.3 Preparation of inhaled antitubercular drugs 13

1.2.3.1 Porous particles for pulmonary delivery of antitubercular drugs 14

1.2.3.2 Other methods of preparation of inhaled antitubercular drugs 15

1.3 Spray-drying 16

1.4 Changes of solid-state on processing 20

1.4.1 Introduction 20

1.4.2 Solid-state changes during spray drying 20

1.5 Pharmaceutical salts 22

1.5.1 Basic definitions 22

1.5.2 Salt formation 22

1.5.3 Basic properties of salts 24

1.5.4 Thermal analysis and combined techniques for characterisation of salts 25

1.5.5 Ammonium salts 26

1.6 Co-crystals, definition and examples 27

1.6.1 Characterisation of co-crystals 28

1. 6.2.1 Melting Point 28

1.6.2.2 Stability 29

1.7 Background to drugs/ excipients used in the current work 30

EXPERIMENTAL

Chapter 2: Materials and Methods

2.1 Materials 35

2.2 Methods 37

2.2.1 Spray-drying 37

2.2.2 Thermogravimetric analysis (TGA) 37

2.2.3 Differential scanning calorimetry (DSC) 37

2.2.4 Scanning electron microscopy (SEM) 38

2.2.5 Powder X-ray diffraction (XRD) 38

2.2.6 Particle size analysis 39

2.2.7 Density Measurements 39

2.2.8 Particle Surface Area Measurement 39

2.2.9 Fourier transform infrared spectroscopy (FTIR) 40

2.2.10 *In Vitro* Aerosol Characterisation 40

2.2.11 Preparation of ammonium salts 41

2.2.12 Determination of degradation product of p-aminosalicylic acid 41

2.2.13 Ammonia Assay 42

2.2.14 Elemental Analysis 43

2.2.15 Nuclear Magnetic Resonance Spectra 43

2.2.16 Micronisation of p-aminosalicylic acid 43

2.2.17 Dynamic vapour sorption 43

2.2.18 *In vitro* drug deposition and aerodynamic particle size analysis 44

2.2.19 UV analysis 44

2.2.20 pH measurement 45

2.2.21 Preparation of physical mixtures 45

2.2.22 Statistical analysis 45

2.2.23 Karl Fischer titration 46

RESULTS AND DISCUSSION

Chapter 3: Spray-dried p-aminosalicylic acid systems **47**

3.1 Introduction 47
3.2 PAS systems spray-dried from ethanol 48
3.3 Preparation of ammonium salt of PAS 60
3.4 PAS/ammonium carbonate systems spray-dried from ethanol 61
3.4.1 Morphological properties of spray dried composite 62
3.4.2 Physicochemical properties of spray dried composite 66
3.4.2.1 Thermal behaviour of the spray dried composite 66
3.4.2.2 X-ray powder diffraction studies 71
3.4.2.3 Infrared spectra 75
3.4.2.4 ^{1}HNMR spectral assignments 76
3.4.2.5 High performance liquid chromatography 79
3.4.3 Stoichiometry of spray dried PAS/ammonium carbonate systems 80
3.4.4 Conclusion 82
3.5 particle characterisation of spray-dried PAS 82
3.6 PAS/ammonium bicarbonate systems spray-dried from ethanol 86
3.7 PAS/ammonium carbonate systems spray-dried from methanol 89
3.8 Spray dried PAS at elevated inlet temperature 93
3.9 PAS/PVP spray dried systems 107
3.10 *In vitro* deposition properties of systems for inhalation purposes 108
3.11 Ammonium salt of PAS spray-dried systems 111
3.11.1 Physicochemical properties of spray dried salt from ethanol 111
3.11.2 *In vitro* deposition properties of spray dried ammonium salt 115
3.11.3 Ammonium salt of PAS spray-dried from water 117
3.11.4 Spray drying of ammonium salt of PAS at higher temperature 120
Conclusion 122

Chapter 4: Spray drying of acidic compounds **124**

4.1 Introduction 124
4.2 Spray-dried benzoic acid systems 125

4.2.1 Introduction 125
4.2.2 Ethanol: water: ammonium carbonate spray-dried systems 125
4.2.2.1 X-ray powder diffraction studies 125
4.2.2.2 Thermal behaviour of spray dried composites 128
4.2.2.3 Infrared spectroscopic studies 130
4.2.2.4 Stoichiometry of spray dried benzoic acid/ammonium carbonate 131
4.2.3 Ethanol: water spray-dried systems 132
4.2.4 Ammonium benzoate spray-dried systems 135
4.3 Spray-dried salicylic acid systems 139
4.3.1 Introduction 139
4.3.2 Spray-dried salicylic acid with ammonium carbonate 139
4.3.2.1 X-ray powder diffraction studies 140
4.3.2.2 Thermal behaviour of spray dried composites 142
4.3.2.3 Infrared spectroscopic studies 143
4.3.2.4 Stoichiometry of the salicylic acid systems 145
4.3.3 Spray-dried salicylic acid without ammonium carbonate 146
4.3.4 Ammonium salicylate spray-dried systems 149
4.3.4.1 Introduction 149
4.3.4.2 Ethanol: water spray-dried system 149
4.3.4.3 Water spray-dried system 153
4.3.4.4 Elemental analysis of spray dried ammonium salicylate 155

4.4- Spray dried pyrazinoic acid 157
4.4.1 Introduction 157
4.4.2 Pyrazinoic acid: ammonium carbonate spray dried systems 157
4.4.2.1 Stoichiometry of spray dried pyrazinoic acid systems 160
4.4.3 Ammonium salt of pyrazinoic acid spray dried systems 161

4.5 Spray-dried sulfacetamide systems 165
4.5.1 Introduction 164
4.5.2 spray-dried sulfacetamide with ammonium carbonate 164
4.5.3 Preparation of ammonium salt of sulfacetamide 159
4.5.4 Solid-state of spray-dried ammonium salt of sulfacetamide 170

4.5.5 spray-dried sulfacetamide without ammonium carbonate 173

4.6 Spray-dried sulfamethizole systems 175
4.6.1 Introduction 175
4.6.2 spray-dried sulfamethizole with ammonium carbonate 175
4.6.2.1 Chemical composition of spray dried samples 177
4.6.2.1.1 Infrared spectroscopic studies 177
4.6.2.1.2 Elemental analysis 178
4.6.2.2 Effect of feed concentration 180
4.6.3 spray-dried sulfamethizole without ammonium carbonate 184
Conclusion 187

Chapter 5: Spray-dried anti-tubercular agents systems 189

5.1 Introduction 189
5.2 Spray-dried isoniazid systems 191
5.2.1 Introduction 191
5.2.2 Isoniazid systems spray-dried from methanol/butyl acetate 191
5.2.3 Water: Methanol: butyl acetate solvent systems 193
5.2.4 Spray-dried excipients systems 195
5.2.4.1 Introduction 195
5.2.4.2 PVP spray-dried systems 196
5.2.4.3 HP- β-CD spray-dried systems 196
5.2.5 Isoniazid/ HP- β-CD spray-dried systems 197
5.2.6 Moisture sorption-desorption study for isoniazid/ HP-β-CD (1:9) 201
5.2.7 Isoniazid/PVP systems spray-dried from methanol/butyl acetate 203
5.2.8 Particle characterisation of spray-dried isoniazid 207
5.2.9 *In vitro* deposition properties of systems for inhalation purposes 211
Conclusion 213

5.3 Spray-dried rifampicin systems 214
5.3.1 Introduction 214
5.3.2 Complexation of rifampicin 215
5.3.3 Spray dried complex systems 216

5.3.4 Other rifampicin spray dried system 218
5.3.5 Physicochemical and morphological characterisation of spray dried rifampicin 219
5.3.6 Dissolution study 225
5.3.7 *In vitro* drug deposition of spray dried complex 226
Conclusion 228
5.4 Spray-dried pyrazinamide systems 229
5.4.1 Introduction 229
5.4.2 Pyrazinamide spray dried without excipient 230
5.4.3 Pyrazinamide /PVP spray-dried systems 231
Conclusion 234

Chapter 6: General Discussion 235

6.1 Introduction 235
6.2 Production of novel solid-state upon spray drying of acidic compounds 237
6.2.1 Stoichiometry of the PAS/ammonium carbonate spray-dried systems 239
6.2.2 Solid-state characteristics of the acidic compounds/ammonium carbonate 240
6.2.3 Stoichiometry of the acidic compounds/ammonium carbonate 243
6.3 Spray drying of ammonium salts 244
6.4 Morphological characteristics of recovered particles 246
6.5 spray drying of active pharmaceutical ingredient/excipient combinations 251
6.6 Aerosolisation performance of spray dried particles 252
6.7 Main findings 257
6.8 Future work 258

References **259**

Appendices

Appendix 1 – Spray drying conditions for different systems 282

Appendix 2 – Calibration curves 299

ACKNOWLEDGEMENTS

I would like to express my deep sense of gratitude to my supervisor Dr. Anne Marie Healy for her valuable guidance, supervision and helpful suggestions throughout my research project.

My deep thanks are due to Prof. Owen Corrigan for his valuable supervision as well as helpful and guiding advice throughout my research project. I am grateful to Dr. Lidia Tajber for all her help, valuable discussions and suggestions.

I am deeply indebted to Dr. Ahmad Barham, Dr. Frederic Tewes and Dr. Vincent Caron whose help, suggestions and encouragement helped me in practical work. I am also particularly grateful to Dr. Vincent Caron for taking the time to proof-read chapters in this thesis.

I would also like to extend my thanks to the academic, secretarial and technical staff of Pharmaceutics and Pharmaceutical Technology and in particular to Patrick Quinlan, Brian O'Reilly and Conan Murphy for their assistance during the course of my research. Many thanks to Liesa Eckhardt for her help with poster presentations. I also wish to thank Neal Leddy of the Centre for Microscopy and Analysis for his expertise and help with SEM and to Ann Connolly of school of chemistry, UCD, for her help with elemental analysis.

I would like to thank my colleagues for their friendship and support over the years: Alecia Barry, Evelyn O'Shea, Sibylle Endter, Lenka Horalkova, Arun Katheri, Xue Li, Maria Ines Amaro, Bo Liu, Anita Umerska, Hanumantha Kurapati, Janani Swaminathan, Orla Ní Ógáin, Katie Ryan, Tao Zhang, Lorraine Nolan, Krystoff Paluch, Christine Grossjohann and Stefano Bianco. A special thank you is extended to Orla Ní Ógáin, and Lorraine Nolan for introducing me to the 'world of porous particles and being very helpful in my initial year starting into my research.

I would like to acknowledge my wife, Reham, my kids Mohamed and Renad for giving me a reason to work. I would also like to thank my extended family and friends for encouragement, and support.

PRESENTATIONS ASSOCIATED WITH THIS THESIS

S. Gad, L. Tajber, A.M. Healy and O. I. Corrigan. "Production and Characterisation of Spray Dried p-aminosalicylic acid for Targeting to the Lungs" All-Ireland Pharmacy Schools Conference, Royal College of Surgeons, Dublin, April 2007.

Gad, S., Tajber, L., Healy, A. M. and Corrigan, O .I. "Physicochemical properties of p-aminosalicylic acid / salt spray dried microparticles designed for pulmonary delivery". British Association for Crystal Growth/Irish Association for Crystal Growth Conference, Dublin, 2007.

ABBREVIATIONS AND SYMBOLS

-	to
%	percent
~	Approximately
±	plus or minus
®	Registered trademark
AC	ammonium carbonate
AHC	ammonium bicarbonate
Air	compressed air drying medium
B.P.	British Pharmacopoeia
BA	n-butyl acetate
BOC	benzoic acid
bρ	bulk density
C	carbon
C_f	concentration of feed solution
CFC	chloroflurocarbon
CHN	elemental analysis
CI	Carr's Compressibility Index
cm	centimetres
CM	closed mode configuration of spray dryer
C_s	solubility of solute
Cu	copper
d	particle diameter
$d_{0.5}$	particle diameter corresponding to the 50% point on the cumulative percent undersize curve
d_a	aerodynamic diameter
dm/dt	the mass variation vs time
DPI	dry powder inhaler
DSC	differential scanning calorimetry
DVS	Dynamic vapour sorption
EC	efficiency cyclone
ED	emitted dose
EtOH	ethanol solvent

Exo	exothermic direction
FPD	fine particle dose
FPF	fine particle fraction
FTIR	Fourier transform infrared spectroscopy
g	grams
GDH	L-glutamate dehydrogenase
GSD	geometric standard deviation
H	hydrogen
H_20	water
HFC	hydrofluorocarbon
HPEC	high performance efficiency cyclone
HPLC	high performance liquid chromatography
HP-ß-CD	hydroxypropyl-ß-cyclodextrin
hr	hour/hours
INH	isoniazid
IR	infrared
J/g	joules per gram
K	degrees Kelvin
K_a	acid dissociation constant
KBr	potassium bromide
KF	Karl Fisher titration
KGA	α-ketoglutaric acid
kPa	kilopascals
kV	kilovolts
l/min	litres per minute
LPNP	large porous particles containing nanoparticles
LPP	large porous particles
m	metres
M	molar
m.p.	melting point
mA	milliamperes
MDI	metered dose inhaler
MeOH	methanol
mg	milligram

min	minute/minutes
ml	millilitres
mm	millimetres
MMAD	mass median aerodynamic diameter
$MMAD_e$	experimental mass median aerodynamic diameter
MMI	marple miller cascade impactor
Mw	weight average molecular weight
N	nitrogen
n	number of replicates
N_2	nitrogen gas
NADPH	nicotinamide adenine dinucleotide phosphate
NGI	next generation impactor
nm	nanometres
NMR	Nuclear magnetic resonance
non-p	non-porous
NP	nanoparticles
NP	nanoparticles
NPMPs	nanoporous microparticles
°	degree
O	oxygen
°C	degree Celsius
OM	open mode configuration of spray dryer
P	porous
p	total vapour pressure
p_A	partial vapour pressure of A
PAS	p-aminosalicylic acid
pH	minus log of hydrogen ion concentration
Ph. Eur.	European Pharmacopoeia
pH_{max}	the pH of maximum solubility
pK_a	acid dissociation constant
pMDI	pressurised metered dose inhaler
PVP	polyvinylpyrrolidone
PZD	pyrazinamide
Q	flow rate

R	gas constant
r	particle radius
r.p.m	revolutions per minute
r^2	correlation of coefficient
RC	regular cyclone
RD	recovered dose
RF	respirable fraction
RH	relative humidity
RIF	rifampicin
RSD	relative standard deviation
r_t	retention time
S_0	intrinsic solubility
SAC	salicylic acid
SD	spray dried
sd	standard deviation
sec	seconds
SEM	scanning electron microscopy
S_T	total solubility
SV	sample volume
T	temperature
t	time
T_g	glass transition temperature
TG	thermogravimetric analysis
TGA	thermogravimetric analysis
TI	twin impinger
T_m	melting temperature/point
TV	total assay volume
$t\rho$	tap density
™	trademark
U.S.P.	United States Pharmacopoeia
V	molar volume
v/v	volume per volume
V_m	molar volume
w/v	weight per volume
w/w	weight in weight

x	mole fraction
XRD	X-ray diffraction (powder)
α	alpha
β	beta
γ	gamma
δ	delta
ΔH	change in enthalpy
ΔH_c	enthalpy of crystallisation
ΔH_f	enthalpy of fusion
ε	millimolar extinction coefficient for NADPH at 340nm
θ	angle of incidence
μg	micrograms
μl	microlitres
μm	micrometer
ρ	density

SUMMARY

The work presented in this thesis concerns the application of a particle engineering technology, one-step spray drying method, to produce porous particles of antitubercular drugs, suitable for inhalation and to study the effect of spray drying on acidic model drugs and their ammonium salts. Five antitubercular drugs in addition to four acidic model drugs and their ammonium salts were selected for analysis. The spray drying process employed involved the spray drying of a solution of drug or excipient with or without a pore-forming agent (for example ammonium carbonate) to produce the desired nanoporous microparticles (NPMPs). Recovered particles were visualised by scanning electron microscopy. The physicochemical characteristics of the unprocessed and spray dried samples were compared in terms of solid-state characterisation; thermal behaviour, residual solvent content, powder x-ray diffraction and Fourier Transform Infrared Spectroscopy. Elemental analysis, nuclear magnetic resonance and HPLC were carried out for selected samples to evaluate the chemical structure of certain spray dried samples. Micromeritic characteristics of selected systems were investigated. These included evaluation of specific surface area, particle size, bulk and tapped densities. In-vitro deposition of powders was evaluated.

The spray drying process used in this project involved spray drying solutions of active pharmaceutical ingredients or active pharmaceutical ingredients with excipient from co-solvent systems. The co-solvent system consists of two volatile solvents of different boiling points, one being a good solvent for the spray dried compound and the other is a poor solvent. A pore forming agent, ammonium carbonate or ammonium bicarbonate, were also incorporated into certain spray dried systems. Generally, solvent composition had a significant effect on morphological characteristics of the recovered particles. For hydrophobic drugs (p-aminosalicylic acid) the solvent compositions of ethanol/water, ethanol/water/ammonium carbonate and methanol/ water/ammonium carbonate appeared to be suitable for production of porous particles. On the other hand, methanol/butyl acetate and water/methanol/butyl acetate solvent systems appeared suitable for hydrophilic compounds (PVP, hydroxypropyl-ß-cyclodextrin, isoniazid/PVP, isoniazid/ hydroxypropyl-ß-cyclodextrin, pyrazinamide/PVP).

p-Aminosalicylic acid was initially investigated and spray-dried from a feed system comprising ethanol/water or methanol/water solvent systems with or without ammonium

carbonate or ammonium bicarbonate, as a process enhancer. The morphology of recovered particles was dependant on spray drying parameters/conditions, which included changes in the blowing agent employed, solvent and solvent concentration, drying inlet temperature, drying gas and changes in feed concentration. Spray dried p-aminosalicylic acid/ammonium carbonate demonstrated superior aerodynamic properties relative to micronised p-aminosalicylic acid.

The solid state of p-aminosalicylic acid was altered on spray drying with ammonium carbonate or ammonium bicarbonate, the new solid state was produced regardless of the solvent used. The stoichiometry of the recovered particles could be p-aminosalicylic acid: ammonia: water 2:1:0.5. This was different from previous studies by our research group, which showed that process enhancers were evaporated upon spray drying. Extensive studies on production and characterisation of the new solid state using different acidic model drugs revealed that the production of a new solid state was dependent on the interaction between the acidic compound and ammonium carbonate. The solid state of spray dried acidic compounds/ammonium carbonate was altered upon spray drying whenever the compound reacts with ammonium carbonate. However, in absence of such interaction, there was no alteration in solid state of co-spray dried acidic compound/ammonium carbonate.

Nanoporous microparticles (NPMPs) of isoniazid were not produced on spray drying from methanol/butyl acetate or water/methanol/butyl acetate systems. However, NPMPs of isoniazid/excipient were produced from these solvent systems, the excipients used were polyvinylpyrrolidone and Hydroxypropyl-β- cyclodextrin. Particle characterisation of recovered NPMPs showed favorable characteristics for pulmonary delivery including particle size, surface area and in-vitro deposition, compared to micronised isoniazid. This suggests potential for future work and development of these systems, as a therapeutically used antitubercular drug suitable for pulmonary delivery.

Methanol: butyl acetate solvent system was used to spray dry NPMPs of pyrazinamide/PVP; future work will necessitate studying pharmacokinetics of the co-spray dried systems to develop pyrazinamide formulation suitable for pulmonary delivery.

NPMPs of rifampicin were not produced on spray drying of rifampicin/ hydroxypropyl-ß-cyclodextrin. However, using hydroxypropyl-ß-cyclodextrin as a complexing agent for

rifampicin resulted in a definite improvement in solubility and dissolution of rifampicin in comparison to the starting material. The particle size of spray-dried complex was seen to fall within the optimal 1-5μm region and using NGI the aerodynamic properties of the particle were also seen to be favourable.

INTRODUCTION

Origin and scope

Pulmonary delivery of antitubercular agents would be a vast improvement on treatment of tuberculosis because this would help in targeting to alveolar macrophages which are used by the mycobacteria as a safe site for their prolonged survival (Pandey, 2005).
Dry powder inhalers (DPIs) are widely accepted as an alternative to pressurised metered-dose inhalers and nebulisers for pulmonary drug delivery (Timsina et al, 1994). DPIs present many advantages over other aerosol generating systems. The possibility of generating aerosols from drug particles without the use of volatile propellants makes them environmentally friendly and also easy to operate. They are portable and relatively inexpensive with improved physicochemical stability of the drugs as a result of the dry state in the formulation (Zeng et al, 2001).

The challenge of any inhalation delivery system is the generation of particles with acceptable micromeritic characteristics. Production of porous particles by spray drying represents a particle engineering solution to generate particles suitable for inhalation; this is one of the objectives of this thesis. The principal advantage of using porous particles for pulmonary delivery is that they have a relatively low aerodynamic diameter, which is the physical property that can lead to more efficient deep lung delivery of a therapeutic drug substance. Spray drying has been used as a method of particle production for inhalation therapy. Frequently spray drying results in the production of amorphous materials (Corrigan et al., 1984).

Tajber (2005) reported a novel spray drying method to prepare porous particles, by spray drying an ethanolic solution containing an active drug substance (budesonide or sulfadimidine) and a dissolved process enhancer (ammonium carbonate). The produced particles were amorphous porous particles. Previous studies of our research group involved the application of this spray drying process to a number of active pharmaceutical ingredients, excipients and active pharmaceutical ingredients /excipients combinations. Studies showed that the respirable fractions obtained for produced porous particles of budesonide (a corticosteroid used as an anti-inflammatory and immunosuppressive agent) were higher than those achieved for micronised budesonide particles (Mc Donald, 2005). Porous particles of

sulfadimidine and sulfamerazine also showed superior aerodynamic properties in comparison with the raw material and non-porous spray dried materials (Nolan et al, 2006). Generally, extensive studies of our research group showed that this spray drying process can produce nanoporous microparticles with low densities and high surface areas. In the current work, we aimed to examine the application of the spray drying method to different antitubercular agents to see if NPMPs could be produced using the previously described spray drying process.

It should be noted that previous studies of our research group on spray drying of several compounds with process additive, ammonium carbonate, showed that ammonium carbonate was removed upon spray drying. In the present project, we aimed to co-spray dry ammonium carbonate with compounds with which it has potential to react.

The scope of this thesis was therefore:

- ✓ To study the feasibility of using the spray-drying method to prepare porous particles of antitubercular drugs and to investigate particle characteristics that are important in terms of pulmonary delivery, for example, particle size, bulk and tapped density, surface area and in-vitro deposition. The rational for investigation of antitubercular agents, while their oral dose is in grams, is that several studies found in literatures reported that this dose is reduced by inhalation.
- ✓ To process a series of acidic compounds and their ammonium salts (non-pulmonary specific drugs) using spray drying technology, in an attempt to study the potential alteration of the solid state of acidic compounds upon spray drying with ammonium carbonate. These initial investigations would form the basis for further research on production of porous particles by spray drying of ammonium salts of drugs.
- ✓ To evaluate the effect of various spray drying process conditions on the morphology of porous particles.

Chapter 1: Introduction

1.1 Pulmonary Drug Delivery

Inhalation is a very old method of drug delivery, the ancient Egyptians inhaled vapours to treat a variety of diseases (Bailey and Berkland, 2009), and in the 20th century, it became a basis of respiratory care, known as aerosol therapy (Rau, 2005). The inhalation route offers an enormous absorptive surface area in the range 35–140 m^2, thin (0.2 μm) and highly vascularised epithelium, which leads to high bioavailability. Furthermore, in most societies oral inhalation is well accepted by the general population (Byron, 1990). Unlike the oral route of drug administration, pulmonary administration is not subject to first pass metabolism. Therefore, expensive biotechnology derived drugs such as the recombinant human deoxyribonuclease (rhDNase) for the treatment of cystic fibrosis or toxic chemotherapeutics are ideal candidates for local pulmonary administration (Sharma et al. 2001). The inhalation route of administration is also preferred for bronchoactive drugs as less amount of drug is required than for oral ingestion, more rapid onset of action occurs and there are fewer side effects as compared to other routes (Chodosh et al. 2001).

1.1.1 Advantages of pulmonary delivery

Generally, local delivery is advantageous; the potential therapeutic advantages of local delivery include reduced systemic side effects and higher dose levels of the applicable medication at the site of drug action (Bennett et al, 2002). This fact is also applicable to the lungs, where local delivery of medication to the lungs is highly desirable (Sham et al, 2004) because targeted delivery to the lungs can achieve high, localised concentrations of drugs while avoiding systemic toxicities. This is due to the fact that inhaled drugs are localised to the target organ, therefore, it allows for a lower dose than is necessary with systemic delivery (e.g. oral salbutamol 2-4 mg is therapeutically equivalent to 100-200 μg by MDI) (Labris and Dolovich, 2003). In addition, by avoiding the gastro-intestinal tract, side effects often associated with high oral doses e.g. up to 12 g daily for p-aminosalicylic acid (Peloquin et al. 1999) can be avoided. Furthermore, since the lungs are directly targeted, hence, total body doses are lower, leading to a decrease of potential drug resistance build-up.

The lungs are more permeable to macromolecules than any other portal of entry into the body (Patton, 1996); they are more permeable to small molecules in comparison to the gastrointestinal tract (Schanker, 1978). Moreover, the pulmonary route should be regarded

as a potential alternative for the delivery of drugs that are inadequately absorbed after oral administration (Tronde et al., 2003).

Another advantage of inhalation therapy is rapid absorption, where small molecules are absorbed in few seconds after inhalation, therefore, inhalation therapy can be used to treat several symptoms that come on suddenly or require quick response. Bronchoconstriction, nausea, cardiovascular crises, panic, sleep induction, anxiety and Parkinson's lock-up are some of the rapid-onset conditions that can be managed with inhaled medicines (Hung, et al., 1995, Tan et al., 1996 and Masood et al., 1996).

Based on this discussion, it is obvious that inhalation delivery of drugs could help to increase patient compliance, while increasing local concentrations of the drug with a practical and convenient inhalation system (Tsapis et al. 2003).

1.1.2 Optimal site of deposition for treatment of lung diseases

The therapeutic effect of aerosolised drugs is dependent on distribution of drug within the lung. If inhaled particles are delivered to a part of the lung devoid of the targeted disease or receptor, the effectiveness of therapy may be compromised (Labiris and Dolovich, 2003). Since the main advantage of pulmonary delivery is the reduction of dose through increasing local concentration of drug at the site of action, the appropriate amount of drug must be deposited past the oropharyngeal region to achieve therapeutic effectiveness. The site of deposition, which is on central or peripheral airways and whether the distribution of the inhaled drug is uniform or non-uniform, may also play a role in an inhaled drug's effectiveness (Labiris and Dolovich, 2003). For example, in treatment of lung infection, where infection starts in the smaller airways, the bronchioles, and moves into the larger airways, successful therapy would require a uniform distribution of the antimicrobial agent on the conducting airways. For example, chronic lung infection with *Pseudomonas aeruginosa* resides in the airway lumen with limited invasion of the lung parenchyma (Baltimore et al., 1989). Successful therapy would theoretically require the antimicrobial agent to be evenly distributed on the conducting airways. On the other hand, those restricted to the alveolar region would benefit from peripheral deposition.

Another important issue in investigation of optimal site of deposition is the receptors. Ruffin et al., (1978) reported that two inhalation techniques were performed to obtain airway and diffuse airway deposition of histamine aerosol. A radiotracer method was used to confirm the patterns of aerosol deposition and to measure the dose of histamine aerosol in the airways. In five subjects, the effect of cumulative doses of histamine aerosol given

either centrally or diffusely to the airways was measured. Histamine aerosol deposited in the large airways was more effective in increasing airway obstruction that was diffusely deposited histamine aerosol, suggesting that the receptors mediating the action of histamine reside mainly in the large airways and that surface concentration of a drug affects response (Ruffin et al., 1978).

1.1.3 Fate of inhaled particles

Clearance or absorption is the fate of pulmonary delivered drugs (Labiris and Dolovich, 2003). Inhaled particles accumulated in the conducting airways are cleared through mucociliary clearance and, the airway epithelium may absorb a small fraction. Ciliated epithelium starts from the trachea to the terminal bronchioles. It is covered by two layers of mucus secreted from epithelial cells and submucosal glands: a low-viscosity periciliary or sol layer covered by a high-viscosity gel layer. Insoluble particles are trapped in the high viscosity layer and are moved toward the pharynx by the upward movement of mucus generated by the metachronous beating of cilia (Labiris and Dolovich, 2003).

In addition to mucociliary clearance, inhaled particles can be absorbed. Due to the large surface area of the alveolar epithelium and the short air to blood pathway, the lung is permeable to many substances, and therefore pulmonary deposition of aerosols represents an efficient, rapid and non-invasive alternative for the delivery of many drugs (Lahnstein et al., 2008). Hydrophilic particles cross via extracellular pathways, such as tight junctions, or by active transport via endocytosis, while lipophilic particles pass easily through the airway epithelium via passive transport (Stone et al., 1991).

1.1.4 Preparation of particles suitable for pulmonary delivery

Hickey, (1998) reported that pharmaceutical aerosols must be in the respirable size range to bypass deposition in the mouth and throat, and deposit in the periphery of the lung. Hence, aerosol particle size is very important in defining the dose deposited and the distribution of drug aerosol in the lung (Labris and Dolovich, 2003). Therefore, particle size of inhaled particles influences the clinical effectiveness of the drug. Smyth and Hickey (2003) reported that large size particles (approximately 10 μm and above) are generally accepted to be "nonrespirable" and will tend to deposit in the oropharyngeal and upper regions of the respiratory tract. This occurs particularly when the drug is inhaled from a dry powder inhaler or metered dose inhaler. Such particles are swallowed, thus producing negligible, if any, therapeutic response. Particles of sizes ranging from 1-5 μm are

deposited in the small airways and alveoli. Over 50% of the 3 μm diameter particles are deposited in the alveolar region. Those less than 3 μm have about an 80% chance of reaching lower airways and 50-60% chance of deposition in the alveoli (Labris and Dolovich, 2003).

Most therapeutic aerosols consist of a wide range of particle sizes, so a number of parameters usually define the particle size of sample. Mass median diameter is the particle diameter that divides the frequency distribution in half; fifty percent of the aerosol mass has particles with a larger diameter, and fifty percent of the aerosol mass has particles with a smaller diameter. Geometric standard deviation (GSD) is a measure of the variability of the particle diameters within the aerosol. A GSD of 1 indicates a mono-disperse aerosol, while a GSD of >1.2 indicates a hetero-disperse aerosol.

As shown previously, aerodynamic diameter of a particle is important in prediction of the performance of a particle. The smaller the aerodynamic diameter is, the larger is the probability of deposition far down into the lungs upon inhalation. Porous particles represent a particle engineering solution to improve lung deposition and potentially bioavailability of dry powder drugs. As it is a way of achieving low aerodynamic diameter (Chan, 2006). Low aerodynamic diameter can also be achieved by the use of physically small particles, elongated particles, and particles of rough surface (Chan, 2006).

Small particles have the disadvantage of strong interparticulate cohesive forces and poor dispersibility and may also exhibit poor flow properties (French et al., 1996). In contrast, porous particles have considerably better flow properties than more compact particles, they have low particle densities due to hollowness; therefore, have low aerodynamic diameters. Besides the fact that they are more readily handled and disaggregate, they have a longer residence time in the lung than small particles (Edwards, et al., 1997).

A number of different processes are found in literature for the preparation of porous particles. Porous particles were produced by spray-freeze drying (Maa et al., 1999). Two recombinant therapeutic proteins, deoxyribonuclase (rhDNase) and anti-IgE monoclonal antibody (anti-IgE MAb), were employed and formulated with different carbohydrate excipients. The recovered particles were compared to non-porous dimpled spherical particles produced by spray-drying in terms of aerodynamic properties. The results showed that the high surface area low density porous particles demonstrated a significantly higher fine particle fraction compared to non-porous particles.

Vanbever et al. (1999) prepared large porous particles of insulin, albuterol or estradiol in combinations with excipients (lactose and dipalmitoylphosphatidylcholine) using spray-drying process. Water soluble excipients and/or drug were dissolved in distilled water and

water insoluble excipients and/or drug were dissolved in 95% EtOH, and combined to give an overall 87% EtOH feed material with a total solid content of 0.1% w/v. Characterisation of spray-dried samples showed that increasing dipalmitoylphosphatidylcholine concentration resulted in an increase in volume diameter and a decrease in density of particles, potentially as a result of the surface activity of dipalmitoylphosphatidylcholin and its tendency to adsorb on the droplet surface (Chow et al., 2007). Particles produced had geometric diameters of 3 – 15 μm and tapped densities of 0.04 – 0.6 g/cm^3. It was also reported that particles with high porosity showed excellent emitted dose of ~96 %.

Straub et al. (2005) used ammonium bicarbonate as a volatile pore-forming agent to produce porous particles by spray-drying, These studies involved spray-drying a water-in-oil emulsion containing poly-d,l-lactide-co-glycolide, 1,2-diarachidoyl-*sn*-glycero-3-phosphocholine in methylene chloride, and ammonium bicarbonate in water.

Previous studies by members of our research group involved the preparation of porous particles by spray drying. Tajber (2005) prepared porous particles of budesonide and sulfadimidine, by a novel spray drying process. The study involved spray drying ethanolic solutions of the drugs and a blowing agent (ammonium carbonate). It was hypothesised that during the drying process, ammonium carbonate decomposed into volatile ammonia, water and carbon dioxide and together with the ethanol vapour, was removed with the drying medium producing excipient-free porous particles. Tajber, (2005) also compared the respirable dose of the recovered porous particles of budesonide to that of micronised budesonide, where a significant increase of respirable dose was reported for the porous particles in comparison to the micronised particles.

Li (2005) successfully processed different excipients (hydroxypropyl-β-cyclodextrin and polyvinylpyrrolidone) into porous particles. The process involved spray drying from different solvent systems for example methanol/butyl acetate or methanol/butyl acetate/ water.

Another researcher from our group, McDonald (2005) produced porous particles of budesonide and bendroflumethiazide with and without the incorporation of the process additive, ammonium carbonate, in addition, the author reported that solvent composition of water/ethanol; water/ethanol/ammonium carbonate; water/methanol/ammonium carbonate were successful in producing porous particles.

Generally, the importance of the spray drying method invented and used by our research group in comparison to other published processes for production of porous particle by spray drying, is that other methods necessitated the inclusion of emulsion stabilisers and

additives to improve either the stability of the spray dried emulsion and/or maintain the porosity of the particles (Straub et al., 2005), while porous particles produced by Tajber, 2005 and McDonald, 2005 were excipient-free. It should also be noted that *in vitro* dry powder inhaler deposition measurements and aerodynamic particle size analysis of porous particles of budesonide confirmed the potential and suitability of porous particles for pulmonary delivery (McDonald, 2005).

1.1.5 Types of inhalers

There are three major types of inhalers; nebulisers, metered dose inhalers (MDIs) and dry powder inhalers (DPIs). Each type of inhaler uses a different delivery mechanism, therefore, requires different types of drug formulations.

Nebulisers are a historic technology for pulmonary delivery; they have been used for many years to treat asthma and other respiratory disease. It is a device for turning a solution of a drug into a mist of particles (Zeng et al., 2001). The potential advantages of using nebulisers for pulmonary delivery of different drugs include their simplicity, the fact that generation of relatively small droplets is easy and doses as high as 1 g can be delivered. However, they are not historically portable devices and have traditionally been limited to the treatment of hospitalised or non-ambulatory patients. Traditionally, nebulisers are mainly used when patients cannot use other devices and for delivering large doses of bronchodilators and medicaments that it is not possible to formulate into MDIs or powder formulation.

Two types of nebuliser are available, jet and ultrasonic nebulisers. Air-jet nebulisers use compressed jets of high velocity air to shear a bulk suspension or solution into a liquid film at the spray nozzle. The film then collapses under surface tension (Tiano and Dalby, 1996) forming droplets that are aerosolised and inhaled by the patient. The other type of nebulisers is ultrasonic nebulisers; this type does not require the use of a carrier gas. Ultrasonic nebulisers utilise a vibrating piezoelectric crystal, which causes cavitation bubble formation at the surface of the solution or suspension (Tiano and Dalby, 1996). This generates a dense mist when droplets effervesce from the turbulent medium, which is inhaled by the patient.

Metered dose inhaler (MDI) is another inhalation device, it was first introduced in 1955 (Stefely, 2002). MDIs are pressurised vessels and contain drug dissolved or suspended in a liquid propellant. When actuated, the device releases a metered volume of drug and propellant through a valve system.

The main advantage of MDI is that it overcame the problems of the hand-bulb nebuliser and it has been introduced as the primary device for outpatient treatment of asthma (Labiris and Dolovich, 2003). Moreover, MDIs combine the practical benefits of small size, portability, convenience and are relatively inexpensive (Stefely, 2002). Furthermore, the dose in MDIs can be delivered in a few seconds, unlike nebulisers, where delivery of the dose takes several minutes (Newman, 2005). However, the limitations of MDIs have also been known for years. Drug delivery is dependent on the patient's inhaler technique. Reports of inhaler misuse are commonplace in the literature, and failure to coordinate or synchronise actuation with inhalation is the most important problem patients have with MDIs (Newman, 2005). The misuse of MDIs can result in a suboptimal lung deposition (Newman et al., 1991). Limited dosing range is a major disadvantage of MDIs, for example, the Spinhaler® (Aventis) was first introduced for the delivery of sodium cromoglicate because it was not possible for a pMDI to accommodate the large (20 mg) required dose of sodium cromoglycate for each administration (Chrystyn, 2007). Another drawback of MDIs is the use of a blend of chlorofluorocarbon (CFC) as propellants. CFCs have been banned because of their effect on the ozone layer, but now it is possible to use hydrofluroalkanes (HFAs) 134a and 227 instead. Currently, several marketed products contain HFA-134a, including QVAR (beclomethasone dipropionate, 3M Pharmaceuticals, Minneapolis, MN) and Ventolin HFA (albuterol, GSK Inc, RTP, NC) (Smyth and Hickey, 2003).

Dry powder inhaler (DPI) is another aerosol generation system, which has been developed to generate a dry aerosol without using propellants. DPIs are mainly breath-actuated devices that deliver a dry powder drug through shear-induced aerosolisation (Richardson et al., 2007). DPIs have some advantages over MDIs and nebulisers. DPIs are portable, easy to operate, they have no propellant and the dispersion of drug particles and entrainment from DPIs are brought about by the patient's inhalation efforts (Zeng et al., 2001). Moreover, they are low-cost devices with improved stability of the formulation because of the dry state (Bosquillon et al., 2001) and unlike MDIs they are environmentally friendly.

Different types of DPIs are available, which fall into three device categories: single-unit dose inhalers, multi-dose reservoir inhalers and multi-unit dose inhalers.

Generally, the drug in single-unit dose inhaler is supplied in individual single-dose capsules, the capsule must be inserted into the inhaler before use. The drug is usually formulated as micronised drug particles mixed with lactose or a suitable carrier. Different single-unit dose inhalers are available, for example, Spinhaler® and HandiHaler®. In the Spinhaler®, the capsule is placed into a holder located on top of a propeller. Two metal

needles pierce the walls of the capsule by actuating the device (Zeng et al., 2001). Another single-unit DPI, the HandiHaler®, has recently been developed for inhalation delivery. It consists of a plastic device to inhale medication. A capsule of powdered medication is placed in the device and like in the Spinhaler® is pierced by a needle on actuation. The HandiHaler® is breath activated. The portable size, efficiency and convenience make the HandiHaler® a desirable method for inhalation treatment.

Multi-dose reservoir inhalers in which a bulk supply of drug is preloaded into the device. Astra Zeneca introduced the first multi-dose inhaler, the Turbohaler®. In this device, a disposable reservoir is employed to meter the drug on priming the inhaler. The dosing unit consists of a disc with a group of conical holes and the powder is pushed into them by scrapers upon rotation of the dosing unit. Up to 200 doses can be delivered by this device.

Multi-unit dose inhalers in which several single doses are individually sealed and discharged each time the device is actuated, for example, Aerohaler™ (Boehringer-Ingelheim) (Chrystyn, 2007).

1.2 Tuberculosis inhalation therapy

Antitubercular inhaled therapy is a convenient way of delivering antitubercular agents to the lungs. The importance of the area under discussion arises from the fact that tuberculosis continues to be an important killer disease causing three million deaths annually (Smith et al., 2004). Tuberculosis is a chronic infectious disease caused by the bacterium *Mycobacterium tuberculosis,* and the lungs are the primary site of infection. Gelperina, (2005) reported that about one third of the world population is infected with *Mycobacterium tuberculosis* in a latent or active form, which results in more than 8 million new cases and 2 million deaths annually. The infection is acquired by inhalation of infectious airborne particles, which were expelled by patients with active pulmonary or laryngeal tuberculosis. The expelled particles can remain suspended in the air for several hours, allowing exposure to a susceptible person.

Although potentially curative treatments and vaccines are available, tuberculosis remains the foremost cause of preventable deaths in the world. This could be because drug therapy of pulmonary tuberculosis is associated with a number of significant disadvantages. The main drawback of current treatment is the dose, where more than 80% of tuberculosis cases are of pulmonary tuberculosis and high drug doses are required to be administered due to the fact that the total dose reach the lungs after oral administration is small in comparison to the oral dose. Moreover, this small fraction is cleared in a matter of a few

hours; therefore, antitubercular drugs should be administered on a regular basis, a regimen that the majority of patients find difficult to adhere to (Pandey and Khuller, 2005a). The other negative aspect of the current treatment is related to the fact that it is a long process, which requires daily administration of oral or injected combinations of antibiotics for periods of at least six months and may take up to two years for drug-resistant tuberculosis therapy (Fox et al. 1999). Thomas, (2002) reported that patients may terminate treatment due to many factors including unwanted side effects or alleviation of primary symptoms. Incomplete treatment subsequently can make the disease more difficult to treat (Goldman et al., 2007) as it is associated with many therapeutic problems, particularly, the appearance of multidrug-resistant strains of *M. tuberculosis*, which exhibit resistance to the major antitubercular drugs (isoniazid and rifampicin).

Pulmonary tuberculosis is the most common form of this disease, therefore, development of methods for delivering antitubercular drugs directly to the lungs via the inhalation route is a rational therapeutic objective, as the simplest route of drug delivery to the lungs is the inhalation rout (Dessanges, 2001). The advantages of inhalation therapy include direct delivery to the site of action, targeting to alveolar macrophages harboring the mycobacteria, reduced systemic toxicity and improved patient compliance. It is well established that inhaled delivery systems enhance the efficacy of antitubercular drugs; therefore, several studies have proposed the use of inhalable delivery systems for chemotherapy of tuberculosis (Zahoor et al, 2005; Hirota et al., 2007; Sharma et al., 2007).

From an historical point of view, Pedanus Discorides (a Greek pharmacist) introduced the concept of inhaled fumigation during the first century (Pandey and Khuller, 2005a). Antiseptic aerosol therapy, e.g. boiling tar vapours, became a popular antituberculosis medication in the middle of the 20th century, while it barely had any therapeutic value (Dessanges, 2001). From that time, antitubercular inhaled therapy has come to a stage of experimental reality with potential clinical use.

1.2.1 Feasibility of pulmonary delivery of antitubercular drugs

Oral dose of antitubercular drugs is in grams, the usual adult dose of rifampicin is 8 to 12 mg/kg. Isoniazid usual adult dose is 5 mg/kg, to a maximum of 300 mg, daily by mouth and pyrazinamide dose is 15 to 20 mg/kg daily (maximum 2 g daily) (Reynolds, et al., 1996). This fact raises important questions about the feasibility of production of pulmonary delivered formulation containing antitubercular drugs and if the powders could be delivered in realistic doses.

Initially, targeted delivery of antitubercular drugs to the infected cells is an important tool for reducing the required oral dose. It should be noted that the high oral daily dose of antitubercular agents is needed due to several reasons; one of these reasons is the fact that drugs reach target tissues through the systemic circulation. This is in contrast to the inhalation route of administration, which allows the delivery of relatively small dose of drug directly to the lung. Therefore, targeting the drug to the lungs (the primary site of infection) may result in a high therapeutic ratio when compared to standard oral delivery. In addition, the exposed surface area of the lungs is extremely large, estimated to approximate the area of a tennis court (Edwards, et al., 1998). Accordingly, it is theoretically feasible to prepare and investigate pulmonary delivered antitubercular drugs.

Moreover, different studies are reported in the literature which evaluated the pharmacokinetics and pharmacodynamics of different inhalation systems containing antitubercular drugs. Generally, these studies showed that the inhalation doses of antitubercular drugs were reduced in comparison with the oral dose of the equivalent drug. The antibacterial effect of the nanoparticle bound three antitubercular drugs (rifampicin, isoniazid and pyrazinamide) administered via respiratory route was investigated in guinea pigs (Pandey, et al., 2003). The authors reported that single nebulisation of antitubercular drugs co-encapsulated in poly (DL-lactide-co-glycolide) nanoparticles to guinea pigs resulted in sustained therapeutic drug levels in the plasma for 6-8 days and in the lungs for up to 11 days. On nebulisation of nanoparticles to infected guinea pigs at every 10th day, no tubercle bacilli could be detected in the lung after only five doses of treatment, whereas 46 daily doses of orally administered drug were required to obtain an equivalent therapeutic benefit.

In another study, Katiyar et al., (2008) studied the pharmacokinetics of inhalation versus oral doses of antitubercular drugs. Briefly, a group of six healthy volunteers aging from 20-50 received antitubercular drugs (isoniazid 15 mg, rifampicin 30 mg and pyrazinamide 75 mg with lactose as carrier) using a dry powder inhaler, the particle size was 1-10 μm and mass median aerodynamic diameter was 2.79 μm. Another group received oral tablets contain rifampicin 500 mg, isoniazid 250 mg and pyrazinamide 1250 mg. The results showed that the mean concentrations of isoniazid, pyrazinamide and rifampicin in epithelial lining fluid were 220, 15 and 83 times higher in the inhaled group than those in the oral group. It could be concluded that pulmonary delivery is a promising, non-invasive route for the administration of antitubercular drugs.

Furthermore, the reduction in total body dose of p-aminosalicylic acid by inhalation was reported by Tsapis et al., (2003), who investigated the pharmacokinetic parameters of

inhaled particles of p-aminosalicylic acid. The authors reported that the total body dose of the prepared particles of p-aminosalicylic acid was approximately 11 mg/kg via the lungs compared to an estimated value of 57 mg/kg for oral dosing of the drug in humans. Therefore, the dose was reduced to less than 20% of the oral dose.

It is obvious from previous studies that inhalation delivery of antitubercular drugs can potentially allow for a reduction in total dose delivered while providing for higher local and similar peak systemic drug concentrations as compared to those obtained by higher oral dose.

1.2.2 Limits on the amount of drug delivered by dry powder inhalers

The use of dry powder inhalation has become popular in recent years. Nevertheless, most dry powder inhalers (DPIs) deliver relatively low doses, for example, the Intal® spincaps (Aventis) are the highest quantity available dry powder inhalers, at 20 mg (Young et al., 2004). But several high dose medicaments could potentially be delivered as dry powders by inhalation. Young et al., (2004) reported that the Actispire® by Britannia Pharmaceuticals (Redhill, UK) is suitable for high dose delivery (e.g., 20–250 mg of a synthetic lung surfactant). This device uses a pressurised gas to aerosolise micronised powder contained in the individual vial. Young et al., (2004) studied the performance of this inhaler, which is designed to deliver high doses using pumactant as a model powder. Pumactant (a synthetic lung surfactant consisting of a phospholipid mixture) is amorphous, highly cohesive, has a high moisture affinity (6.2% w/w at 45% RH) and has a particle size ($d_{0.9}$) of 2.92 μm. The authors studied the effect of loaded dose on dry powder delivery and can pressure on aerosolisation efficiency. The results showed that the relationship between loaded dose and delivered dose was linear (r^2 = 0.96, for loaded doses of 0–250 mg). In addition, analysis of the aerosolisation efficiency using a Marple Miller type impactor suggested fine particle fractions of about 30% using canister pressures of 8–14 bars. The authors concluded that the device may be a useful tool in delivering high-dose medicaments, as a carrier-free formulation, to the deep lung.

1.2.3 Preparation of inhaled antitubercular drugs

Several studies have proposed the use of inhalable delivery systems for chemotherapy of tuberculosis; the ideas of these studies are better given under the following headings:

1.2.3.1 Porous particles for pulmonary delivery of antitubercular drugs

Porous particles have been identified that may be useful in inhalation therapy. These particles have low mass density, which leads to more efficient aerosolisation. There are a number of parameters which must be taken into consideration during formulation of inhaled powder either porous or non-porous particles. These include mass median aerodynamic diameter (MMAD) and geometric standard deviation (GSD).The MMAD of an aerosol refers to the particle diameter that has 50% of the aerosol mass residing above and 50% of its mass below it. GSD is a measure of the variability of the particle diameters within the aerosol (Labris and Dolovich, 2003). Aerodynamic diameter of a particle is important in prediction of the behaviour of a particle in airflow streams. The smaller the aerodynamic diameter is, the larger is the probability of deposition far down into the lungs on inhalation e.g., in the alveoli. Due to the larger geometric diameter, porous particles have considerably better flowing properties than more compact particles having the same aerodynamic diameter. Therefore, by formulation of hollow or porous particles, the dry powders can be delivered into the lungs with a simple inhaler (Sung et al., 2007). Besides the fact that porous particles are more readily handled and disaggregate, they have a longer residence time in the lung than small particles (Edwards, et al. 1997). In addition to good flowability pattern of porous particles, the use of porous particles has other advantages, for example, such particles will become easier to dose and mix. Moreover, the porosity associated with these materials will be likely to result in increases dissolution rates.

Different studies are reported in the literature which showed the use of porous particles for pulmonary drug delivery, Tsapis et al., (2003) formulated porous particles of p-aminosalicylic acid (antitubercular agent) for inhalation therapy. The produced particles were physically stable over four weeks at elevated temperatures. It should be noted that physical stability is considered as an important aspect for practical therapy. These particles were administered by insufflation to rats; plasma drug concentrations peaked at 15 min, and the maximum plasma concentration was 11±1 μg/ml. The concentration in the lung lining fluid was 148±62 μg/ml at 15 min. Tissue concentrations were 65±20 μg/ml at 15 min and 3.2±0.2 μg/ml at 3 h. The drug was cleared within three hours from the lung lining fluid and plasma but was still present at therapeutic concentrations in the lung tissue. The authors suggested that similar particles containing other antitubercular agents could potentially be used for inhalation therapy of tuberculosis, for examples, rifampicin, aminoglucosides or fluoroquinolones.

In another study, Garcia-Contreras et al., (2007) formulated low density porous capreomycin sulphate particles for inhalation therapy. It should be noted that capreomycin is an antitubercular agent used for multidrug-resistant tuberculosis, but due to its severe side effects, it is limited therapeutically. Briefly, a solution containing 80% capreomycin sulphate and 20% L-leucine in 50% ethanol was spray-dried using a Niro Mobile Minor spray dryer at an inlet temperature of 189 to 192°C. The produced particles had a mass median aerodynamic diameter of 4.99 ± 0.02 μm and fine particle fractions (FPF< 5.8 μm and FPF< 3.3 μm) of 47.7% ± 0.7% and 8.8% ± 0.5%, respectively. Pharmacokinetic studies revealed that plasma concentrations of the drug measured for the guinea pigs that received the insufflated particles were comparable to that for groups of guinea pigs after intravenous or intramuscular administration in the period 2 to 6 hours. Furthermore, the rate of clearance of pulmonary delivered capreomycin was at a lower rate in comparison to i.v. or i.m. administration, resulting in a significantly longer effect.

1.2.3.2 Other methods of preparation of inhaled antitubercular drugs

Preparation of porous particles was not the only method found in literature for preparation of pulmonary delivered antitubercular drugs, formulation of nanoparticles was another method for preparation of particles containing antitubercular drugs suitable for inhalation.

Nanoparticles are defined as submicron (< 1μm) colloidal particles. This definition includes monolithic nanoparticles (nanospheres) in which the drug is adsorbed, dissolved, or dispersed throughout the matrix and nanocapsules in which the drug is confined to an aqueous or oily core surrounded by a shell-like wall (Gelperina et al., 2005). Generally, nanoparticle formulations are a particularly interesting approach to pulmonary delivery given the uptake of nanoparticles by macrophages and other cells of the immune system. The advantages of using nanoparticles for pulmonary delivery of antitubercular drugs include high carrier capacity, feasibility of incorporation of both hydrophilic and hydrophobic drugs and feasibility of different routes of administration, including inhalation. Furthermore, nanoparticles can be designed to allow sustained drug delivery; in this case, nanoparticles can adhere a longer time onto the mucosal surface and in that way increase the absorption of drug (Jacobs and Muller, 2002). These properties of nanoparticles may lead to reduction of the dosing frequency and may resolve the problem of patient non-compliance, which is one of the major problems in treatment of tuberculosis.

The effectiveness of pulmonary drug delivery using nanoparticles was demonstrated in a number of studies (Gelperina et al., 2005). Pandey et al., (2003) prepared poly (DL-lactide-co-glycolide) -nanoparticles by the multiple emulsion technique, co-encapsulating rifampicin, isoniazid and pyrazinamide. Upon aerosolisation, the MMAD was found to be 1.88 μm and thus suitable for lung delivery. The formulation was nebulised to guinea pigs, evaluated in terms of the pharmacokinetic parameters of each drug and the effect on guinea pigs infected with tuberculosis. A single nebulisation of the formulation to guinea pigs was able to maintain a therapeutic drug concentration in the plasma for 6–8 days and in the lungs for 9–11 days. The elimination half-life and mean residence time of the drugs were prolonged compared to oral administration. The relative and absolute bioavailability of encapsulated drugs was improved compared to unprocessed antitubercular drugs. Further improvement of this formulation was made by Sharma et al., (2004) who used lectin-coated poly (DL-lactide-co-glycolide) -nanoparticles as carrier for antitubercular drugs. Upon nebulisation of the new formulation to guinea pigs, therapeutic drug concentrations were maintained in the plasma for 6–15 days. *In vivo* studies showed that three doses of the coated nanoparticles had equal chemotherapeutic benefit to five doses of uncoated poly (DL-lactide-co-glycolide) –nanoparticles, clearly indicating the advantage of lectin conjugation in poly (DL-lactide-co-glycolide) –nanoparticles.

1.3 Spray Drying

With the rapidly growing popularity of pulmonary drug delivery, there is an increasing demand to develop particles suitable for inhalation as the challenge of any inhalation delivery system is the generation of particles with acceptable range of particle sizes. These particles should be in the respirable size range (<5 μm). Therefore, a wide variety of particle technologies have used over the past decade (Chow et al., 2007). Micronisation is typically a method of particle size reduction without sophisticated attributes. The main objective of the micronisation process is to achieve a proper particle size. This perspective has changed as new drug delivery approaches are developed. More advanced therapeutic approaches have created complex requirements for dosage forms that can only be met by particles that are formulated for different purposes such as targeted drug delivery and modification of release pattern of different medicaments.

Spray drying offers an alternative approach to the generation of pharmaceutical solids. The recovered materials can have unique functional properties, for example compressibility, density, solubility, aerodynamic particle size, which can impact on future processability,

and may be optimised to suit a particular drug delivery system, for example pharmaceutical aerosols. This one-step process can be used to produce dry powders from solutions, suspensions or emulsions, with greater control over particle size, morphology and powder density than destructive methods of powder production, such as milling or micronisation. The physical properties and *in vitro* inhalation behaviour of mechanically micronised and spray-dried disodium cromoglycate were compared by Vidgrén et al. (1987). Spray-dried particles were found to be smaller than micronised particles, and regarding aerosolisation performance, spray-dried disodium cromoglycate proved superior to micronised disodium cromoglycate.

Masters, (1991) reported the advantages of using spray drying. These include: spray drying is applicable to both heat sensitive and heat resistant material due to the fact that the exposure to the heat during drying process is instant, the operation is continuous and easy and a wide range of dryer designs are available with extensive flexibility. Furthermore, the specification of powder quality remains constant throughout the entire drying operation.

On the other hand, spray drying may alter the solid-state characteristics such as crystal form or habit and may render the material amorphous as found for sodium cromoglicate and salbutamol sulphate (Vidigrén et al., 1987; Chawla *et al.*, 1994). Amorphous materials have the advantages of increased solubility and dissolution rates (Corrigan, 1995). However, this change in solid state may be considered as a drawback as amorphous materials are hygroscopic, more cohesive and difficult to flow and disperse (Chan and Chew, 2003).

The disadvantages of spray drying also include high costs of installation, poor thermal efficiency unless very high inlet temperatures are used which may lead to product degradation and unacceptable low process yields. Another common problem with a spray dryer is wall deposits, caused by large droplets hitting the chamber wall before they are dry, which can happen because of a change in feed properties, a wear or blockage problem in the atomiser or recirculation patterns in the gas flow (Oakley, 1997).

Figure 1.1 shows the spray dryer used in this project. Generally, the drying process proceeds as follows: liquid form (solution or suspension) of the drug is first atomised into a spray of droplets as it passes through a nozzle, after that followed by contacting the droplets with a circulation of hot gas in a drying chamber. In the drying chamber, solvent is evaporated. Powder mixed with gas passes through to the cyclone separator, where they are separated. Gas and very fine powder pass to the filter, where fine powder is retained, while gas is removed through an exhaust. The separated powder is collected in the

collecting vessel. It should be noted that spray drying may include the use of flammable, organic solvents; in this case, the spray-dryer should run in closed mode. The closed mode is based on recycling and reusing a gaseous medium, which can be an inert gas, for example, nitrogen (Masters, 1991), and in this case, gas passes through a cooler unit, where solvent condenses and is collected for recycling/discard).

Figure 1.1 Buchi Mini Spray Dryer B-290

There are several reports indicating the application of spray drying in the production of powder formulations for inhalation (Chawla et al., 1994 and Stahl et al., 2002).

Corrigan et al., (2006a) investigated this process as a means to produce particles suitable for inhalation. Briefly, salbutamol sulphate was spray dried as a 10% (w/v) aqueous solution and as a 0.6% (w/v) solution from ethanolic solvent consisting of 75% ethanol and 25% water, ipratropium bromide was spray dried as a 5% (w/v) aqueous solution, salbutamol sulphate/ipratropium bromide systems were co-spray dried from 5% (w/v) aqueous solutions, the resulting particles were collected and analyzed. This method produced microspherical particles which, for many of the systems, deposited in the lower region of the twin stage impinger indicating that they were in the respirable range. The authors concluded that spray drying is a successful method for production of particles suitable for pulmonary delivery.

In another study, Corrigan et al., (2006b) co-spray dried salbutamol sulphate/chitosan, the recovered particles were X-ray amorphous. Twin impinger analysis of the produced

particles indicated good in-vitro deposition of the microparticulates and potential for pulmonary delivery.

Spray-drying was also used by Mizoe et al, (2007) to produce particles suitable for inhalation; the drug used was pranlukast hemihydrate (a cysteinyl leukotriene receptor-1 antagonist). The solution was prepared by dissolving the drug in a solution of aqueous bicarbonate and ethanol 1:1. Mannitol was dissolved in water for use as the carrier. The spray-dried particles were collected and analysed. This method produced particles with a mean diameter of approximately 2 μm, which is within the respirable range. The microparticles, being mostly mannitol, were dissolved in water, reportedly leaving behind a suspension of insoluble nanoparticles within the size range of 100 and 430 nm. Hence, the particles produced by this process would rapidly dissolve on the surface of the pulmonary epithelium, leaving behind drug nanoparticles that can slowly dissolve and release drug for systemic or local action.

Yamamoto et al., (2007) used a spray drying fluidized bed granulator to produce microparticles suitable for inhalation, where, 4.0 g of poly(lactide-co-glycolide) (used as a wall material for the nanospheres) and 2.0 mg of 6-coumarin (used as a fluorescence marker of the nanospheres) was dissolved in 120 ml of acetone: ethanol (2:1). This polymer solution was poured into 300 ml of 10% PVA (was used as a dispersing agent for the emulsion solvent diffusion method) aqueous solution that was stirred at 400 r.p.m. for 5 min and 100 r.p.m. for 2 h to evaporate organic solvent. The produced particles were approximately 250 nm in diameter after evaporation of the organic phase. Lyophilized powder was then suspended in water containing dissolved mannitol (was employed as a filler) and spray dried in a fluidized bed granulation system. In this process, solution is sprayed from the bottom of the reactor into the granulation chamber and the resulting mist was dried by heated air. Dried particles were then entrapped onto a backdrop filter and redispersed into the granulation chamber with a pulsed air jet. Yamamoto et al., (2007) hypothesized that the particles were granulated by the coalescence of wet and dry particle collisions within the granulation chamber. It should be noted that the aerodynamic diameter of the resulting particles was measured to be 1-10 μm.

1.4 Changes of solid-state on processing

1.4.1 Introduction

The properties of a solid material depend not only on the identity of its constituents but also on their arrangement (Stahly, 2007). In particular, crystalline materials are made up of molecules that are arranged in a specific arrangement. These molecules are held together by relatively weak forces, for example, hydrogen bonding and van der Waals interactions (Newman and Byrn, 2003), and are arranged in a fixed repeating array built of unit cells, which is known as a lattice, on the other hand, there is no definite long-range order in the amorphous state (Aaltonen et al., 2009).

Drug compounds and excipients must go through many processes during formulation of the pharmaceutical products and the structure of the materials can change during these processes (Karjalainen et al., 2005). However, processing-induced transformations during pharmaceutical manufacturing are well known but difficult to predict and often difficult to control (Morris et al., 2001). For example, grinding is an often used pharmaceutical process to reduce particle size and to accelerate the solubility of materials. Grinding usually makes material more amorphous and it can also change the polymorphic form of a material. The polymorph change of anhydrous caffeine from metastable form I to the stable form II by grinding has been reported (Pirttimäki et al., 1993). Other processes which may change the solid state of the pharmaceutical compounds are granulation and drying, where temperature and air humidity have large effects on the material (Karjalainen et al., 2005).

Another example of common phase transformation during processing is the dehydration of a hydrated crystal, the structure of hydrated forms of compound drugs may change to dehydrated forms during drying. This could be due to high temperature and relatively low humidity during the process. For example, theophylline, which is a frequently used model compound in pharmaceutical processing studies, forms a monohydrate that readily dehydrates in a dry atmosphere or elevated temperatures to anhydrous theophylline (Morris et al., 2001).

1.4.2 Solid-state changes during spray drying

The spray drying is of particular interest for considerations of solid-state changes. Generally, rapid drying processes, such as spray drying are likely to increase the level of crystal defects and these in turn will be reflected in the thermal properties of the material

(Corrigan, 1995). The nature of spray drying is such that physical and chemical changes can occur in materials. The process involves the transformation of feed material from a liquid state to a dried powder by spraying the material into a drying gas (Chidavaenzi et al., 1997). Spray drying may results in alterations in the energy of the spray dried solid components ranging from disordering of the crystal lattice, elimination of crystallinity, formation of polymorphic forms to complex formation (Corrigan, 1995).

A further point of interest is that spray drying involves a high degree of atomisation, leading to the formation of high surface area droplets. During the drying process the solvent will evaporate, and the size of the droplet decreases. Drying will continue at a constant rate as long as the droplet surface is saturated with solvent transferred through diffusion and convection within the droplet to the surface of the droplet (Masters, 1991). With continued evaporation the solvent content decreases and the drug solidifies. The time for a solute to reach saturation at the droplet surface can vary and the precipitated solute may not crystallise immediately when its solubility limit is reached at the droplet surface leading to characteristic times associated with crystal growth, nucleation and polymorphic transitions. Spray drying has a high potential for the production of metastable crystal forms. Corrigan, (1995) reported that frequently the spray drying results in high energy amorphous products. An example that demonstrates the change of solid state upon spray drying is processing of lactose which reported by Chidavaenzi et al., (1997), who showed that spray drying of 10g/100ml lactose solution yielded amorphous lactose due to rapid solidification, while, the spray dried sample at equilibrium solubility (20g/100ml) yielded a solid form that was 91% amorphous lactose, probably due to nucleation sites that may have remained. The 30 and 40g/100ml lactose suspensions produced spray dried products consisting of much higher amorphous lactose content than the amount that was dissolved. The crystalline part of these products was found to be anhydrous α-lactose, except for the 40 g/100ml sample which consisted of both anhydrous α-lactose and α-monohydrate. Another example is spray drying of sulfamethoxazole with excipients, which resulted in an alteration of the crystal form of the drug, either to a different polymorphic form or to an amorphous form (Takenaka *et al.*, 1981).

1.5 Pharmaceutical salts

Salts are most commonly used to modify undesirable traits of a drug substance, most typically the solubility or the dissolution rate. Therefore salts are widely distributed, Stahl and Wermuth, (2002) reported that an estimated half of all the pharmacologically active molecules used in medicinal therapy are administrated as salts. Therefore, understanding how salts are formed and characterisation of solid-state of drug salts are important for the development of pharmaceutical formulations. Generally, thermal analysis, X-ray diffraction, solubility, sorption-desorption and stability studies are useful techniques for the characterisation of the salt candidates.

1.5.1 Basic definitions

Addressing pharmaceutical salts necessitates using basic chemical definitions, for example, pH and pKa.

pH is defined as the negative of the logarithm of the hydronium ion concentrations (Carstensen, 1998). The definition of pH in equation form is

$$pH = -\log [H^{1+}]$$

where, $[H^{1+}]$ means the molar concentration of hydronium ions, M = moles / litre

pKa is defined as the negative log of the acid dissociation constant, Ka. The definition of pH in equation form is

$$pKa = -\log Ka$$

1.5.2 Salt formation

Salt formation is the most common and effective method of improvement of solubility and dissolution rates of acidic and basic drugs (Serajuddin, 2007). It constitutes an acid -base reaction, this reaction involves either a proton transfer or neutralisation reaction, wherein, a drug candidate forms strong ionic interaction with an oppositely charged counterion. Numerous counterions are available for preparation of pharmaceutical salts, for example, common acidic counterions like hydrochloric, sulphuric and acetic acids for basic drugs, and alkaline counterions like sodium, potassium and magnesium for acidic drugs (Bastin et al., 2000).

Generally, acids react with bases to form a salt and water. This is called a neutralisation reaction and takes the following form:

$$HA + BOH \text{ --> } BA + H_2O$$

Salts may be prepared by chemical reaction between strong acid and strong base, for example reaction of hydrochloric acid and sodium hydroxide. When strong acids and strong bases react, the products are salt and water. In this case the acid and the base neutralise each other, so the solution will be neutral and the ions that are formed will not react with the water found in the media. On the other hand, strong acid may react with a weak base, for example the reaction of hydrochloric acid and ammonia. The reaction between a strong acid and a weak base also produces a salt, but water is not usually formed because weak bases tend not to be hydroxides. In this case, the water solvent may react with the cation of the salt to reform the weak base. In addition a salt may be formed by reaction between a weak acid and a weak base, for example, reaction of hypochlorous acid with ammonia, in this case the pH of the solution formed from the reaction of a weak acid with a weak base depends on the relative strengths of the reactants.

A further point of interest is that the aqueous solubility of acidic drugs as a function of pH determines whether the compound will form suitable salts or not (Serajuddin and Pudipeddi, 2002). Serajuddin, (2007) reported that the free acid would be the equilibrium species at a pH below the pH of its maximum solubility (pH_{max}). In addition, the acid would convert to a salt only if it is equilibrated with a solution at a pH above pH_{max} by adding a sufficient quantity of an alkali. The relevant equations below and above pH_{max} are given below (Chowhan, 1978):

$$S_T, \text{acid}(pH \prec pH_{max}) = [AH]_s + [A^-] = [AH]_s\left(1 + \frac{Ka}{[H3O^+]}\right)$$
$$= [AH]_s(1 + 10^{pH\text{-}pKa})$$

$$S_T, \text{salt}(pH \succ pH_{max}) = [A^-]_s + [AH] = [A^-]_s\left(1 + \frac{[H_3O^-]}{Ka}\right)$$
$$= [A^-]_s(1 + 10^{pKa\text{-}pH})$$

Where, AH and A^- represent free acid and salt forms of the compound, respectively. pH_{max} is the pH of maximum solubility of the acid, (S_T) is the total solubility and the subscript "s" represents the saturation species.

It should be noted that the solid phase coexist in equilibrium with a saturated solution at pH_{max}, both acid and salt forms. On the other hand, the solid phase at $pH < pH_{max}$ is the free acid and the solid phase at $pH > pH_{max}$ is the salt.

Serajuddin, (2007) reported that the concept of the pH of maximum solubility of certain compound (pH_{max}) plays a major role in determining whether a salt would be formed or not, and, in case it is formed, whether it would remain or would convert to the corresponding free acidic form. Serajuddin, (2007) also showed the effect of intrinsic solubility of the acid and its pK_a on pH_{max}, and consequently on salt formation, where an increase in intrinsic solubility and decreases in pK_a of the acidic drug will decrease pH_{max} and, therefore, favour salt formation.

Salt formation may also be affected by the solvent system used during synthesis process; Wermuth and Stahl (2002) reported that pharmaceutical salts are usually prepared from organic solvents, which, in turn, may affect the solubility of a drug by increasing solubility of unionised species or decreasing solubility of the salt form (Serajuddin and Pudipeddi, 2002). Accordingly, an increase in intrinsic solubility in an organic co-solvent will increase pH of maximum solubility for a basic drug, consequently favouring salt formation (Kramer and Flynn, 1972). A further point of interest is the effect of organic solvents on drug ionisation by suppressing the dielectric constant (Izutsu, 1990). Therefore, the positive effect of organic solvents on salt formation may be negated by the decreased ionisation (Serajuddin, 2007).

1.5.3 Basic properties of salts

The basic properties of salts include melting point, which could be measured by Differential Scanning Calorimetry (DSC). Determination of melting point of salts is important because very low melting point salts are not suitable for purification, handling, processing (Giron, 2003). In addition, the choice of the counterion allows modification of the characteristics of the molecule. Therefore, different counterions of the same salt have different melting points.

Another important characteristic of salts is the solubility; although the majority of the salts are developed to enhance the aqueous solubility of drug substances (Bastin et al., 2000), but hydrophobic salts are shown to be of choice for certain formulations. Jashani and Byron, (1996) compared aerosolisation performance of three salts (sulphate, adipate and stearate) and the free base of albuterol. All powders were micronised. Albuterol adipate had the highest aqueous solubility (353 mg/ml), followed by albuterol sulphate (250 mg/ml), albuterol free base (15.7 mg/ml) and albuterol stearate (0.6 mg/ml). Only the sulphate was found to be hygroscopic at relative humidity RH >93%. The authors reported that for inhaler performance in a high humidity environment, the hydrophobic stearate was found the best.

Chemical stability is another basic characteristic of the salt candidate; it depends on the solid-state of the salt form and also on the polymorphic form (Walkling et al., 1983). The amorphous state is particularly critical for stability. Hygroscopicity of salts is a key factor in determination of the stability, York, (1983) reported that the water vapour sorption properties of pharmaceutical materials are recognised as critical factors in determining their storage, stability, processing and application performance. Sorption-desorption isotherms are measured as the mass change observed during the change of the relative humidity. X-ray diffraction during such studies is very important (Giron et al., 2002).

1.5.4 Thermal analysis and combined techniques for characterisation of salts

Thermal analysis is a group of techniques in which a property of the sample is measured against time or temperature while the temperature of the sample, in a specified atmosphere is heated or cooled at a fixed rate of temperature change or hold at constant temperature. Differential scanning calorimetry is a fast and sensitive type of thermal analysis. But it is always useful to use Thermogravimetric Analysis (TGA), X-ray diffraction (XRD) and Fourier Transform Infrared (FTIR) for proper interpretation of DSC scans.

Combined techniques are usually helpful in characterisation of salts, for example, thermogravimetry coupled with mass spectroscopy (TG-MS) is generally very useful when salt forms contain high amount of entrapped residual solvents which play a role in the solubility results or which are bound as solvate or hydrated forms.

Thermal analysis and combined techniques are efficient for the detection of unexpected phase transitions and for the comparison of different forms of salts. Giron, (2002) used TG-MS and combined techniques with X-ray diffraction for interpretation of the DSC curves of a malonate. The author reported that DSC scan showed a dual melting with

intermediate crystallisation, which would be wrongly attributed to a polymorphic behaviour. However, the high amount of mass loss found by thermogravimetric analysis showed a decomposition which was easily attributed to the loss of malonic acid by TG-MS, FT-IR and X-ray diffraction with heating cell. The base was the product formed after recrystallisation. And the second DSC peak is the melting peak of the base.

Based on all previous discussion, it could be concluded that no single analysis will be sufficient to characterise the solid state of salt, but proper characterisation requires several analytical methods and the results should be interpreted together.

1.5.5 Ammonium salts

An ammonium salt is a product of a reaction between ammonia, NH_3, and various acids. The general reaction for formation is

$$NH_3 + HX \rightarrow NH_4X.$$

These compounds are addition products of ammonia and the acid. For this reason, their formulas are sometimes written as $[H(NH_3)]X$.

All ammonium salts decompose into ammonia and the acid when heated (Frenkel et al., 1995). Their stability, however, varies according to the nature of the acid. Salts of weak acids decompose at lower temperatures than do salts of strong acids.

Furthermore, Frenkel et al., (1995) reported that the ability of ammonium salts to undergo thermal decomposition is well known. This decomposition process can proceed both in the solid phase by the heating of the dry salt in a stream of inert gas and in the liquid phase by heating the aqueous solution of the salt. Dehn and Heuse, (1907) reported that decompositions of the hydrate ammonium salts involve the expulsion of water followed by the dissociation of ammonia. The authors gave example of mono-ammonium oxalate, which is stable to 70° C; at higher temperatures, it begins to lose its water of crystallisation and at 140° C, it forms oxamic acid.

The application of the decomposition of ammonium salts was described for the industrial isolation of nicotinic acid from ammonium nicotinate (Frenkel et al., 1990). In addition, Chuck and Zacher, (2000) found that an aqueous solution of ammonium nicotinate can be converted to nicotinic acid by spray-drying. Briefly, an aqueous solution of ammonium nicotinate solution was sprayed into a fluidized-bed spray-dryer (Niro FSD™-4. diameter 1.2 m, height 2.5 m), at an inlet temperature of 220°C and the outlet temperature was 100° C. The drying gas used was nitrogen. This produced a free-flowing product comprising 89% by weight nicotinic acid. The recovered particles had a bulk density of 0.4 kg/l and a

mean particle size of 451 μm. The ammonia, together with the water, escapes in the exhaust gas of the spray-dryer.

Moreover, Frenkel et al., (1995) suggested that decomposition of ammonium salts can serve as the basis for the practically waste-free method for the isolation of some carboxylic acids widely applied in the pharmaceutical industry.

In the current work, ammonium salts were spray dried using novel spray drying method. Generally, the recovered particles from spray drying of ammonium salts of p-aminosalicylic acid and pyrazinoic acid were uniform, crystalline and either porous particles or aggregates of microcrystalline particles within the size range of 2-5 μm, these particle characteristics are desirable for inhalation system.

1.6 Co-crystals, definition and examples

Crystal engineering has emerged into the pharmaceutical formulation with its importance in the pharmaceutical co-crystallisation of drug compounds; the main advantage of crystal engineering is that it is a method to improve solubility, dissolution, moisture sorption and compressibility of drug compounds without altering the pharmacological activity of the drug (Basavoju et al., 2006). Stahly, (2007) has documented the widespread existence of co-crystals of drug molecules. However, co-crystals are often discovered by accident (Rane and Anderson, 2008).

Co-crystals can be considered unique crystalline solids containing multiple components (two or more components) that form a unique crystalline structure having unique properties (Stahly, 2007). Such co-crystals will have different properties than that of crystals made from each constituent alone (Stahly, 2007). In addition, pharmaceutical co-crystal is a special type of co-crystals and is defined as a co-crystal that is formed between an active pharmaceutical ingredient, either ionic or neutral form, and a co-crystal former.

Co-crystals can be thought of as representing a continuum of structure with salts at one end and crystals containing multiple, non-ionised components at the other. Schultheiss and Newman, (2009) reported that although salt formation is frequently used to modify the physical properties of active ingredients, but, a major limitation within this approach is that the drug substance must possess a suitable (basic or acidic) ionisable site. The alternative means of controlling drug properties by co-crystal formation (two or more components held together by freely reversible, non-covalent interactions), where any drug substance could be co-crystallised. The importance of this aspect is that it helps complement existing methods by reintroducing molecules that had limited pharmaceutical profiles based on

their non-ionisable functional groups. However, co-crystals are underutilised solids that greatly expand the possibilities for finding a developable solid form of an active pharmaceutical ingredient.

Several examples of co-crystals may be found in the literature. The use of co-crystals to alter the properties of pharmaceutically active compounds was reported by Krantz et al., (1946), who found that the stoichiometric (1:1) co-crystal containing the sodium salt of theophylline and glycine increased the water solubility of the drug. In addition, a clinical study using the co-crystal showed that it was tolerated in man and elicited the typical theophylline response. Another example of co-crystal is the co-crystal of caffeine-gentisic acid that had stoichiometry of 1:1 and 1:2 (caffeine-gentisic acid) which was made by Higuchi and Pitman, (1973), those materials altered the dissolution rate of caffeine, reducing the rate of dissolution of caffeine. This was important for the slow release of caffeine.

Hydrates and solvates are also types of co-crystals (Rane and Anderson, 2008), which have been frequently reported. Sometimes they are the preferred solid form for development, for example in the commercial products made from cefadroxil (a monohydrate), paroxetine hydrochloride (a hemihydrate) (Rane and Anderson, 2008).

It should be noted that co-crystal formation is not restricted to applications in the pharmaceutical industry but also finds utility in synthetic chemistry (Zukerman-Schpector and Tiekink, 2008), and in the generation of optical materials (Friščić and MacGillivray, 2005).

1.6.1 Characterisation of co-crystals

1. 6.1.1 Melting Point

Schultheiss and Newman, (2009) reported that melting point is a basic physical property, which is the temperature at which the solid phase is at equilibrium with the liquid phase. Differential scanning calorimetry (DSC) is a thermal technique, which can be used for determination of melting points. It gives comprehensive melting point data, in comparison to the standard melting point apparatus, because additional thermal data such as the enthalpy of fusion can be determined. These data are important for characterisation of different polymorphic forms.

Determination of melting point is usually used for the purpose of characterisation and quality control studies, for example, purity identification. In addition, the melting point is

important due to the fact that melting point is directly correlated to the log of solubility (Jain and Yalkowsky, 2001) Therefore, determination of the melting point of co-crystal would be useful.

1.6.1.2 Stability

Stability is defined as the capacity of a drug compound to remain within established specifications to maintain its identity, strength, quality and purity. In fact, stability of drug is of great importance since it becomes less effective as it undergoes degradation. Therefore, stability is a seriously studied parameter during the development of a new compound. In addition, different types of stability need to be considered depending on the structure and characteristics of the molecule (Schultheiss and Newman, 2009). Generally, chemical and physical stability data are commonly obtained at accelerated stability conditions to determine shelf life. Water content of a compound should be analysed as it may lead to form changes and degradation.

Thermal studies are very important, especially for hydrates and thermally labile compounds (Schultheiss and Newman, 2009). High temperature is a common method used to determine the chemical and physical stability based on accelerated stability studies. Pop et al., (2009) discovered a new co-crystal of tiotropium fumarate with fumaric acid, and found to be the most stable solid form of tiotropium fumarate. The structure comprises a 2:1 salt of the diacid co-crystallised with a free fumaric acid moiety. The authors reported that the co-crystal is more stable than the corresponding simple 1:1 salt. In another study, Chen et al., (2007) reported that exposure of a co-crystal of a monophosphate salt with phosphoric acid for 8-week exposure at 60 °C resulted in no detectable degradation or form change.

Variankaval et al., (2006) prepared different co-crystals of L-883555 (a phosphodiesterase-IV inhibitor) and L-tartaric acid. The authors reported that DSC scans showed a single melting endotherm for stoichiometries close to 0.5:1 tartaric acid/L-883555. On the other hand, DSC scans showed additional thermal events for the other stoichiometries. When the two complexes with stoichiometries of 0.7:1 and 0.89:1 tartaric acid/L-883555 were heated above the first DSC endotherm, titration and NMR analysis showed values equivalent to the 0.5:1 stoichiometry, which indicate loss of some of the tartaric acid. In addition these results were confirmed by TG-IR and XRD. The authors concluded that the 0.5:1 tartaric acid/L-883555 stoichiometry was the most thermally stable.

1.7 Background to drugs/ excipients used in the current work

1.7.1 *p*- Aminosalicylic acid

Generic and additional names: para-aminosalicylic acid; PAS
CAS name: 4-Amino-2-hydroxybenzoic acid, *CAS registry:* 65-49-6
Molecular formula: $C_7H_7NO_3$ and *Molecular weight:* 153.14

p-Aminosalicylic acid is commonly known as PAS, it is used therapeutically as an antitubercular agent. PAS one of the first antibiotics found to be effective in the treatment of tuberculosis in the 1940s (Rengarajan *et al.*, 2004). However, PAS causes gastrointestinal toxicity leading to poor patient compliance (Rengarajan *et al.*, 2004), in addition, the oral dose of PAS is 8 - 12 grams per day in 2 or 3 divided doses (Reynolds, *et al.,* 1996). As more easily tolerated antibiotics became available, PAS usage diminished considerably. Nevertheless, PAS reemerged in antitubercular therapy due to the appearance of a widespread epidemic of multidrug-resistant tuberculosis, which has necessitated the use of alternatives to the first-line antitubercular agents that are used routinely in short-course chemotherapy regimens (Dye et al., 2002). When given orally, aminosalicylic acid is absorbed and peak plasma concentrations occur after about 1 - 4 hours. Aminosalicylate diffuses widely through body tissues and fluids, about 50 to 70% of the acid is bound to plasma proteins. Aminosalicylate is metabolised in the intestine and liver primarily by acetylation. Urinary excretion is rapid and 80% or more of a dose is excreted within 24 hours; 50% or more of the dose is excreted as the acetylated metabolite. The half-life of aminosalicylic acid is about 1 hour (Reynolds, et al., 1996).

It is available as a white or practically white, bulky powder, which darkens on exposure to light and air. It is odourless or has a slight acetous odour. It is slightly soluble in water and in ether, soluble in alcohol, practically insoluble in benzene (U.S.P, 2007). Its melting point is 139-141°C (Whittel, 1948). PAS is an acidic compound, according to Merck Index, it has a pKa value of 3.25 and the pH of 0.1% aqueous solution of p-aminosalicylic acid is 3.5. The structure of PAS is given in Figure 1.2.

In the current work PAS was spray dried using different spray drying parameters/conditions, and the recovered particles were extensively investigated in terms of physicochemical and morphological characteristics. In addition, the ammonium salt of PAS was prepared according to the method of Forbes et al., (1995) for comparative purposes.

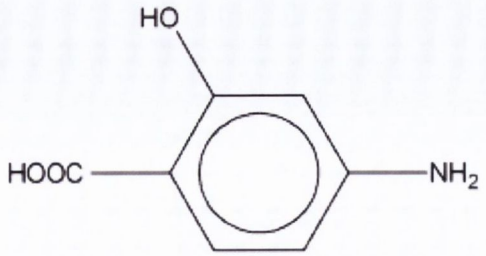

Figure 1.2 – Structure of *p*- aminosalicylic acid

1.7.2 Isoniazid

Chemical Name: Isonicotinohydrazide

CAS Registry: 54-85-3

Molecular Formula: $C_6H_7N_3O$ and Molecular Weight: 137.1

Isoniazid is used therapeutically as an antitubercular agent. It appears as colorless or white crystals or white, crystalline powder. It is odourless and is slowly affected by exposure to air and light. It is freely soluble in water, sparingly soluble in alcohol, slightly soluble in chloroform and very slightly soluble in ether (USP, 2007). Isoniazid was supplied as crystalline powder. Its melting point is 170-173°C (U.S.P, 2007). The structure of isoniazid is given in Figure 1.3.

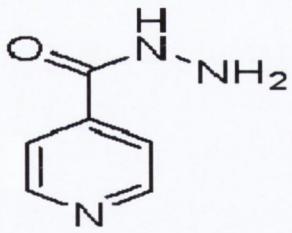

Figure 1.3– Structure of isoniazid

1.7.3 Rifampicin

Molecular Formula: $C_{43}H_{58}N_4O_{12}$

Molecular Weight:822.9

CAS Registry: 13292-46-1

Rifampicin is used therapeutically as an antitubercular drug. It is a reddish-brown, crystalline powder, slightly soluble in water, soluble in methanol, slightly soluble in

acetone and in alcohol (B.P. 2008). It has pKa values of 1.7 and 7.9. The structure of rifampicin is given in Figure 1.4 below.

Due to the complex structure of rifampicin, it exhibits polymorphism and exists in two polymorphic forms, i.e. form I and form II (Pelizza et al., 1977).

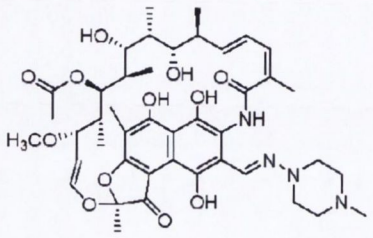

Figure 1.4 – Structure of rifampicin

1.7.4 Pyrazinamide

Chemical Name: Pyrazine-2-carboxamide

CAS Registry: 98-96-4

Molecular Formula: $C_5H_5N_3O$ and Molecular Weight:123.1

Pyraziamide is used therapeutically as an antitubercular drug. It is available as white to practically white, odourless or practically odourless, crystalline powder. It is sparingly soluble in water; slightly soluble in alcohol, in ether and in chloroform (U.S.P. 2007). Its melting point is 188-191°C (U.S.P. 2007). The structure of pyrazinamide is given in Figure 1.5.

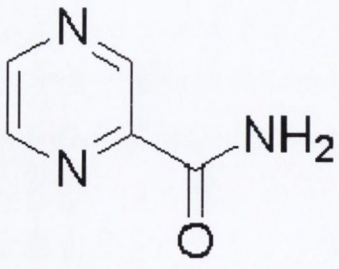

Figure 1.5 – Structure of pyrazinamide

1.7.5 Ammonium Carbonate

Ammonium carbonate is an ammonium salt with an empirical formula $(NH_4)_2CO_3$. It consists of a mixture of ammonium bicarbonate and ammonium carbonate, and is obtained by subliming a mixture of ammonium sulphate and calcium carbonate. It may also be prepared by bringing ammonia and carbon dioxide together in aqueous. Ammonium carbonate is a colourless, hard, translucent, crystalline masses or powder, which has a strong odour of ammonia and a sharp taste. On exposure to air it loses ammonia and carbon dioxide and becomes opaque. It is slowly soluble in 4 parts of water and volatilises at 60°C (Merck Index, 1989).

1.7.6 Ammonium bicarbonate

Ammonium bicarbonate is a white, crystalline powder with a slight odour of ammonia that can dissolve in water to give a mildly alkaline solution. Ammonium bicarbonate decomposes at 36-60 °C into ammonia, carbon dioxide and water vapour in an endothermic process. The aqueous solution of this salt liberates carbon dioxide on exposure to air or on heating.

1.7.6 Polyvinylpyrrolidone (PVP)

PVP is used in a variety of pharmaceutical formulations, but is used primarily in solid dosage forms. It is commercially available in a range of molecular weights from 10,000 to 1,300,000 $g \cdot mol^{-1}$. It is white or yellowish-white, hygroscopic powder or flakes, freely soluble in water, in ethanol (96%) and in methanol, very slightly soluble in acetone (B.P., 2008). It is used as excipient in many pharmaceutical dosage forms, for example tablets. The molecular weight of PVP used in this thesis was 40,000. The structure of PVP is given in Figure 1.6.

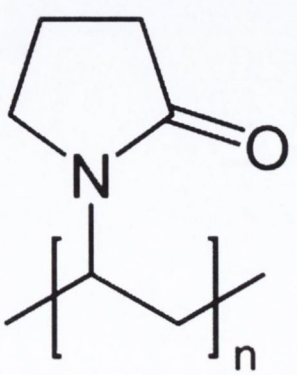

Figure 1.6 – Structure of PVP

1.7.8 Hydroxylpropyl-β- cyclodextrin (HP-β-CD)

Cyclodextrins are a family of cyclic oligosaccharides composed of seven glucose units arranged in a donut-shaped ring. Pharmaceutical use of cyclodextrins include solubility, bioavailability or stability enhancements, odour/taste masking and prevention of admixture incompatibilities (Davis and Brewster, 2004). The mechanism of solubility enhancement of lipophilic drugs may be by inclusion complexation, within the more hydrophobic cavity of the cyclodextrin. 2-hydroxypropyl-ß-cyclodextrin (HP-ß-CD) is modified from the naturally occurring cyclodextrin ß-CD through substitution of hydroxypropyl groups. Modification improves the water solubility and the toxicity profile of the cyclodextrin. The structure of HP-β-CD is given in Figure 1.7.

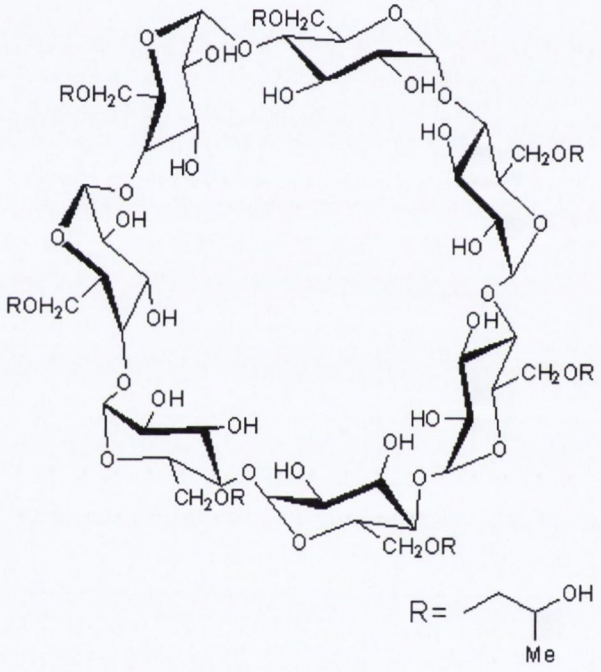

Figure 1.7 – Structure of HP-β-CD

EXPERIMENTAL

Experimental

2 Material and methods

2.1 Materials

Material (abbreviation or chemical formula)	Supplier/ manufacturer
Acetonitrile, HPLC Grade	Lab Scan Analytical Sciences, Ireland
Ammonia Assay Kit	Sigma, Ireland
Ammonium carbonate ($(NH_4)_2CO_3$)	Sigma, Ireland
Ammonium hydrogen carbonate (NH_4HCO_3)	Rectapur – Prolabo, France
Ammonium benzoate	Fluka, USA
Ammonium salicylate	Gentaur, Belgium
Benzoic acid	Sigma, USA
Butyl acetate, extra pure	Merck, Germany
Citric acid monohydrate ($C_6H_8O_7.H_2O$)	BDH Laboratory Supplies, UK
Compressed air	Haug Kompressoren, Germany
Dimethylsulphoxide-D6	Apollo Scientific, UK
Ethanol (EtOH)	Cooley distillery, Ireland
Hydranal (Karl-Fisher titration reagent)	Riedel-de-Haën, Germany
Hydrochloric Acid 32 % extra pure	Riedel-de-Haën, Germany
Hydroxypropyl-β- cyclodextrin (HP-β-CD)	Sigma, Ireland
Isoniazid	Sigma, Germany
L-glutamate dehydrogenase solution	Sigma, Ireland
Liquid nitrogen	Air Products, Ireland
Methanol (MeOH)	Lab Scan Analytical Sciences, Ireland
Methanol anhydrous (Karl-Fisher titration reagent)	Merck
Methanol, HPLC grade	Lab Scan Analytical Sciences, Ireland
Nitrogen gas (high purity, oxygen free)	BOC Gases, Ireland
p -Amino salicylic acid (PAS)	Aldrich, Germany

Polyvinylpyrrolidone PVP-40 – Ave. MW 40,000	Sigma, Ireland
Polyvinylpyrrolidone PVP-K15 – Ave. MW 10,000	Fluka, U.S.A.
Potassium bromide (KBr) IR Grade	Sigma, Ireland
Potassium dihydrogen phosphate (KH_2PO_4)	Merck, Germany
Pyrazinamide (PZA)	Aldrich, Germany
Pyrazinoic acid	Aldrich
Rifampicin	Sigma-Aldrich, Germany
Salicylic acid	BDH, England
Sodium hydroxide pellets (NaOH), extra pure	Riedel de Haën, Germany
Sulfacetamide	Sigma, Germany
Sulfamethizole	Sigma, Ireland
Tetraoctylammonium bromide	Fluka
Water, deionised	Purite Prestige Analyst HP water
Water, HPLC grade	Purite Prestige Analyst HP water

2.2 Methods

2.2.1 Spray Drying

Solutions of the required drug were spray dried using a Büchi B-290 spray dryer (Büchi Laboratoriums-Technik AG, Switzerland). For the purposes of this thesis, systems which were spray dried from a mixture of alcohol and water are described in terms of their alcohol content (volume percentage), with the remaining percentage constituting the water content. For a compound spray dried from 90% (v/v) ethanol, the spray drying solution would constitute 90% (v/v) ethanol and 10% (v/v) water.

The Büchi-290 Mini Spray Dryer allows for spray drying in both a closed mode (CM) and open mode (OM) configuration. Both configurations were employed in the experimental work undertaken. When operating in the closed mode configuration, the Büchi-290 spray dryer was used in conjunction with the Büchi-295 inert loop. This layout is typically chosen when flammable or explosive solvents i.e. organic solvents, toxic products or oxygen sensitive products are being processed. The drying medium (typically an inert gas such as nitrogen) is constantly reused in the drying process through recycling within a closed system. Spray dried powder was collected from the collecting vessel of the spray dryer using a small synthetic bristle brush. A static gun (Zerostat 3; Aldrich) was used as needed, depending on the static nature of the powder. Collected samples were stored in amber or clear glass screw cap jars or clear glass sample tubes in a sealed desiccator containing silica gel, at 4 °C.

2.2.2 Thermogravimetric Analysis (TGA)

TGA was performed using a Mettler TG 50 (Mettler Toledo Ltd., Switzerland) linked to a Mettler MT 5 balance. Data was processed using Mettler Toledo STAR^e software. Samples (approximately 4 - 12 mg) were accurately weighed and analysed using open aluminium pans under nitrogen purge. Samples were generally run at a heating rate of 10°C/minute from 25 – 300 °C, except were otherwise indicated.

2.2.3 Differential Scanning Calorimetric Analysis (DSC)

Differential scanning calorimetry measurements were carried out under nitrogen purge using a Mettler Toledo DSC 821^e (Mettler Toledo Ltd., Switzerland) calorimeter. Samples

(approximately 4 - 10 mg) were accurately weighed using a Mettler MT50 microbalance into 40 µl aluminium pans, which were hermetically sealed with a lid with three vent-holes. Samples were run at a specific heating rate of 10°C/minute under nitrogen purge from 25 – 300 °C (except were otherwise indicated). Mettler Toledo STAR^e software was used for analysis of thermodynamic events.

2.2.4 Scanning Electron Microscopy(SEM)

Visualisation of particle size and morphology was achieved by scanning electron microscopy (SEM). Scanning electron micrographs of powder samples were taken using a Hitachi S-4300N instrument (Hitachi Scientific Instruments Ltd., Japan) variable pressure scanning electron microscope or Tescan Mira XMU Scanning Electron Microscope. The dry powder samples were fixed on an aluminium stub with double-sided adhesive tabs and a 10-nm-thick gold film was sputter coated on the samples before visualisation. The images were formed from the collection of secondary electrons. Samples were visualised at different magnifications.

2.2.5 Powder X- ray Diffraction (XRD)

XRD scans were made on samples in low background silicon mounts, which consisted of cavities 0.5 mm deep and 9 mm in diameter (Bruker AXS, UK). A Siemens D500 diffractometer was used. This consists of a DACO MP wide range goniometer with a 1.0^0 anti-scatter slit and a 0.15^0 receiving slit. The Cu anode X-ray tube was operated at 40 kV and 30 mA in combination with a Ni filter to give monochromatic Cu Kα X-rays. Measurements were taken from 5° to 40° on the 2 theta scale at a step size of 0.05^0 per second for qualitative analysis. Data was processed using XRD Commander Software. A MiniFlex II desktop X-Ray diffractometer was used for XRD scans of salicylic acid, sulfamethizole and sulfacetamide systems. Measurements were taken from 5° to 40° on the 2 theta scale at a step size of 0.05^0 per second for qualitative analysis. XRD was used to calculate the percentage crystallinity of spray dried crystalline powders (de Villiers et al., 1998). The crystallinity of unprocessed materials was assumed to be 100%. From the X-ray diffractograms of the unprocessed and spray dried materials the areas under the strongest peaks was used for the calculations for the crystalline unprocessed and spray dried powders. Data of pyrazinamide polymorphs was processed by Dr. Karsten Rode (School of Physics, Trinity College Dublin) using Topas version 3 software.

2.2.6 Particle Size Analysis

The particle size distribution was determined by laser diffraction using a Malvern Mastersizer 2000 (Malvern Instruments Ltd., Worcs., UK) with the Scirocco 2000 accessory. The dispersive air pressure employed was 2 bar. Samples were generally run at a vibration feed rate of 60%. The particle size of each sample was determined in triplicate, unless otherwise indicated, and expressed in terms of the median diameter (d (0.5)). Results are expressed as mean ± standard deviation (sd).

2.2.7 Density Measurements

Bulk density ($b\rho$) was measured by filling dry powders in a 1 ml graduated syringe (Lennox Laboratory supplies) with a funnel. The weight of the powder required to fill 1 ml graduated syringe was recorded in order to calculate $b\rho$. The tap density ($t\rho$) of the powder was then evaluated by tapping the syringe onto a level surface 100 times. The resultant volume was recorded in order to calculate $t\rho$. The tapped density was calculated as the ratio of the mass to the tapped volume of the sample. Measurements were performed in triplicate unless otherwise indicated, and are expressed as a mean ± standard deviation.

2.2.8 Particle Surface Area Measurement

Surface area analyses were performed using a Micromeritics Gemini 2370 analyzer, with nitrogen gas (BOC) as the analytical (adsorptive) gas and helium (BOC) as the reference gas for free space measurements, as required. Prior to analysis, samples were degassed under nitrogen gas purge, using a Micromeritics FlowPrep 060 degasser for 24 hours at 25 °C, to remove residual moisture and contaminants. Sample weights before and after degassing were recorded. These mild degassing conditions were chosen to avoid any changes in solid state of spray dried p-aminosalicylic acid/ammonium carbonate systems. It should be noted that Maa et al. (1999) reported similar mild degassing conditions (25 °C for 16 hours) for degassing of spray dried samples prior to surface area measurement.
Free space measurements were performed using glass beads of negligible surface area in the reference tube. The number of glass beads used was such that approximate volume balance was achieved, i.e. the measured free space was between -0.5 and +0.5 cm^3. Saturation pressure was determined periodically between analyses. The evacuation

conditions used were as follows: rate of 500 mmHg/min, the evacuation time was 1 minute and the equilibration time was 10 seconds. The amounts of nitrogen gas adsorbed at the relative pressures of 0.05, 0.1, 0.15, 0.2, 0.25 and 0.3 (p/p_0) were determined, and the BET multipoint surface area was calculated. Where it improved the correlation coefficient for the BET plot, the first or last point was omitted. The values presented are the average of three determinations; results are expressed as mean ± sd.

2.2.9 Fourier Transform Infrared Spectroscopy (FTIR)

FTIR was carried out using a Magna – IR 560 Spectrometer E.S.P. (Thermo Electron Corporation, U.S.A.) Fourier Transform Infrared Spectrometer. Potassium bromide (KBr) discs were prepared based on 1 % w/w sample loading. Discs were prepared by grinding the sample with KBr in an agate mortar and pestle, placing the sample in an evacuable KBr die and applying 8 tons of pressure in an IR press. The OMNIC E.S.P. software was used for processing the data.

2.2.10 *In vitro* Aerosol Characterisation

The apparatus used was a twin stage impinger conforming to the specification in the British Pharmacopoeia (2008) and European Pharmacopoeia (2007). The powders were aerosolised using a dry powder inhalation device (Spinhaler®). The aerodynamic particle deposition was investigated using the twin impinger (Model TI-2, Copley) containing 7 and 30 ml of 80% ethanol (in case of p-aminosalicylic acid systems) or water (in case of isoniazid) for stage 1 and 2, respectively. A total of 20 ± 1 mg of powder was loaded into a No. 2 hard gelatin capsule. After the Spinhaler® was connected to the mouthpiece of the twin impinger a capsule was placed in the holder of the device. An air stream of 60 L/min was produced through the system by attaching the outlet of the twin impinger to a vacuum pump for 5 s. The drug in stages 1 and 2, mouthpiece and device was collected by rinsing with fresh solvent. The rinsed solutions were diluted to appropriate volumes and the drug content were determined by an appropriate UV method. Calibration curves for unprocessed and spray dried *p*-aminosalicylic acids, unprocessed and spray dried p-aminosalicylic acid ammonium salt, unprocessed and spray dried isoniazid were constructed (Appendix II). UV measurements were carried out on the Pharmspec UV-1700 UV-Visible spectrophotometer (Shimadzu) using 10 mm quartz cuvettes. Results are expressed in terms of the respirable fraction percentage, calculated on the basis of drug content captured

in stage 2, as the recovered dose. The recovered dose (RD) was defined as the total amount of drug recovered from the capsule, device, mouthpiece, stage 1 and stage 2 of the impinger. All twin impinger studies were carried out in triplicate.

2.2.11 Preparation of ammonium salts

The ammonium salts of p-aminosalicylic acid and pyrazinoic acid were prepared according to the method of Forbes et al. (1995). The preparation process involved the addition of 3.3 ml ammonia solution with a continuous stirring to a suspension of 10 g of the acid in 35 ml ethanol. Ammonium salt of sulfacetamide was prepared by mixing equivalent amounts (1:1 molar) of sulfacetamide and ammonium hydrogen carbonate in ethanol. In all cases the mixture was heated until complete solution had occurred and then allowed to cool for 2 h with stirring. The crystals were filtered and washed twice with 2 ml of ethanol. The recovered product was then stored in amber glass, dried in a desiccator dried at ambient temperature under reduced pressure overnight.

2.2.12 Determination of degradation product of *p*-aminosalicylic acid in the presence of the drug

A HPLC method was adopted to determine 3- aminophenol (the main degradation product of *p*-aminosalicylic acid in the presence of the drug (Jivani et al, 1985). Separation was carried out at ambient temperatures

Chromatographic conditions:

Apparatus: the HPLC used was a Shimadzu LC-10AT VP liquid chromatograph with a Shimadzu L-10A system controller, a Shimadzu SPD-10A UV-VIS detector, a Shimadzu DGU-14 degasser and a SIL-10AD VP auto injector system. Samples were analysed using Shimadzu Class VP software (version 6.10)

Column: Hypersil BDS C18 5μ, 150 mm × 4.6 mm

Flow rate: 1.5 ml/min

Detector: UV at 280 nm

Mobile phase: 55 parts methanol, 45 parts 0.05 M potassium phosphate buffer (pH 7.0) containing 1 mM tetraoctylammonium bromide as ion-pairing agent.

2.2.13 Ammonia Assay

Unprocessed and spray dried samples were analysed using an ammonia assay kit purchased from Sigma-Aldrich, Ireland (product code AA0100). Ammonia reacts with α-ketoglutaric acid (KGA) and reduced nicotinamide adenine dinucleotide phosphate (NADPH) in the presence of L-glutamate dehydrogenase (GDH) to form L-glutamate and oxidised nicotinamide adenine dinucleotide phosphate ($NADP^+$). The decrease in absorbance at 340nm, due to the oxidation of NADPH, is proportional to the ammonia concentration. Approximately 1 mg of the raw material or spray dried samples was accurately weighed and dissolved in 10 ml of water. 1.0 ml of ammonia assay reagent (KGA and NADPH) was accurately transferred into appropriately marked cuvettes. Then, 100 µL of water was added and the contents were mixed immediately, this was referred as a blank reagent. The same procedure was followed to prepare samples or standards with a 100 µL of each sample/standard solution transferred into each cuvette. All cuvettes were incubated for approximately 5 minutes at 25 °C, and the absorbance of each solution was initially measured at 340 nm (using a Shimadzu UV-1700 PharmaSpec spectrophotometer). Following this 10 µL of L-glutamate dehydrogenase solution was added into each cuvette. All cuvettes were again incubated for 5 minutes at 25°C after which time the final absorbance was measured at 340 nm. All measurements were conducted in at least triplicate. Absorbance change was determined for the reagent blank, test, and standard. For each: $\Delta A_{340} = A_{Initial} - A_{Final}$; $\Delta(\Delta A_{340})$Test or Standard= ΔA(Test or Standard) - ΔA(Blank); µg of NH3 /mL of original sample was calculated using the following equation:

$$\frac{(A)(TV)(MW)}{(\varepsilon)(d)(SV)}$$

Where: A= $\Delta(\Delta A_{340})$Test or Standard; TV=total assay volume in mL (1.1 mL); SV=sample volume in mL (0.1 mL); MW=molar weight of ammonia (17 µg/µmole); ε= millimolar extinction coefficient for NADPH at 340nm=6.22 (mL/µmoles)(1/cm), and d (light path)=1 cm.

It should be noted that the limit of detection (LOD) of the assay method used was determined to be 1 µg/mL.

2.2.14 Elemental Analysis

The elemental analysis was carried out using an Exeter Analytical CE440 CHN analyzer. The sample was burned in oxygen and passed over reagents which remove unwanted components and converts the CHN in the sample to CO_2, H_2O and N_2. The quantity of CO_2, H_2O and N_2 present was determined by thermal conductivity detectors. This analysis was carried out by the Department of Chemistry, University College Dublin.

2.2.15 Nuclear Magnetic Resonance Spectra

Nuclear magnetic resonance spectra were recorded on a Bruker, Avance III 400 at a proton frequency of 400.13 MHz and carbon frequency of 100.62 MHz. Dimethylsulphoxide-D6 was used as a solvent for *p*-aminosalicylic samples.

2.2.16 Micronisation of drug compounds

Micronisation of p-aminosalicylic acid and isoniazid was performed using a Jet-O-Mizer fluid energy mill model 00. The drug compound was placed into the vibratory feeder. The vibratory feeder was set at 60.4 maximum vibrations. The vibratory feed rate is the rate at which the material to be micronised enters the Venturi feed and from there enters the grinding chamber where micronisation takes place. The grinding pressure and pusher pressure were set at 40. These settings were carried out as a series of trials where the feed rate was varied.

2.2.17 Dynamic vapour sorption

Dynamic vapour sorption (DVS) is a well-established method for the determination of vapour sorption isotherms. The DVS instrument used for these studies measures the uptake and loss of vapour gravimetrically using a Cahn D200 recording ultra-microbalance with a mass resolution of ±0.1 μg. The high mass resolution and excellent baseline stability allow the instrument to measure the adsorption and desorption of very small amounts of probe molecule. The vapour partial pressure around the sample is controlled by mixing saturated and dry carrier gas streams using electronic mass flow controllers. The temperature is maintained constant ±0.1 °C, by enclosing the entire system in a temperature-controlled incubator. Water vapour isotherms were collected on all samples over a wide humidity range at 25.0 °C. Typically, 18 mg of sample was placed in the sample holder. The sample

holder was then attached to a hang down wire connected to an ultra sensitive microbalance. The temperature was maintained at 25±0.01 °C. The study consisted of two cycles; for the first cycle the relative humidity was increased from 40 to 90% RH in steps of 10% RH for the adsorption isotherm and decreased from 90 to 0% RH in steps of 10% for the desorption isotherm. In the second cycle relative humidity increased from 0 to 90% RH then decreased from 90 to 0% RH. At each relative humidity step, the system controls the RH and monitors the sample weight. The equilibrium weight and temperature are then recorded. For each step, an equilibrium behaviour was established when the mass variation vs time (dm/dt) was equal to 0.002 mg/min for 10 minutes before the partial pressure was increased or decreased.

2.2.18 *In-vitro* drug deposition and aerodynamic particle size analysis

The aerodynamic particle size distribution was measured by a Next Generation Impactor (NGI) operated under pharmacopoeia conditions. The flow rate was adjusted to a pressure drop of 4 kPa, as is typical for inspiration by a patient. Size 3 hard gelatin capsules (Farillon Ltd., U.K.) were filled with the dry powder (approximately 20 ± 2 mg of powder). Capsules were loaded into a HandiHaler® dry powder inhaler (GlaxoSmithKline, Australia). Drug deposition in the device, the throat, all the stages and the filter was determined by HPLC analysis. For accuracy, each test was repeated three times.

The total dose of particles with aerodynamic diameters smaller than 5.0 μm was calculated by interpolation from the cumulative mass against cut-off diameter of the respective stages and considered as the fine particle dose (FPD) (mg) or fine particle fraction (FPF), expressed as a percentage of the emitted dose (ED). The ED was determined as the percentage of total powder mass exiting the capsule and device. The mass median aerodynamic diameter (MMAD) of the particles was defined from the same plot as the particle size at which the line crosses the 50% mark.

2.2.19 UV analysis

UV measurements were carried out on the Pharmspec UV-1700 UV-Visible spectrophotometer (Shimadzu) using 10 mm quartz cuvettes. Absorbance was measured at appropriate wavelengths corresponding to each individual compound, sourced from literature values. Concentrations were determined by reference to a calibration curve

prepared from dilutions of stock solutions of the particular drug. Each stock solution was prepared in triplicate.

2.2.20 pH measurement

pH measurements were carried out using an Orion 420A+ (Thermo Electron Corp., U.S.A.) pH-meter. The pH-meter was calibrated daily using standard buffer solutions (Orion) of pH 4, 7, 10 (± 0.01) which are sufficient to cover the desired pH range.

2.2.21 Preparation of physical mixtures

Glass specimen vials with push-in caps containing accurately weighed quantities of substances were placed in a Turbula mixer (Glen Greston Ltd., Middx, UK) and mixing was carried out for 30 min at 42 revolutions per min. The powder blends were sampled randomly by taking at least three samples from the vial. The results of XRD of the samples were used as a measure for the homogeneity of the powder mixtures. Batches were accepted and used if their XRD scans were similar.

2.2.22 Statistical analysis

Statistical analysis was carried out using Minitab™ statistical software, version 14 (Minitab Inc, USA) and Microsoft® Excel, Office Package.

2.2.22.1 Two sample t-tests

Two sample t-tests were used to compare the means and standard deviations of two independent samples. The test procedure involved defining a null and an alternative hypothesis. The null hypothesis was that the sample means were equal; while the alternative hypothesis was that they were not equal. The test was carried out at a significance level of 0.05, with a p-value less than 0.05 taken as indicating that the observed difference between the means was statistically significant, i.e. rejecting the null hypothesis. This test was used to compare the values obtained for respirable fractions with the control powders for twin impinger studies.

2.2.22.2 Linear regression analysis

Linear regression analysis was used to determine if a linear relationship existed between two variables. This linear relationship can be represented by the following equation:

$$Y = aX + b$$

Where X is the independent variable, Y is the dependent variable and b is the value of Y when X = 0, i.e. the Y-axis intercept. The equation of the line was fitted to the data and the adequacy of the fit was assessed from the r^2 value. The closer this value is to 1, the better the fit.

2.2.23 Karl Fischer titration (KF)

The Karl Fischer titration was carried out with a KF 890 Titrando with Touch Control. The titrant used was Hydranal® Titrant; temperature was room temperature for all samples. Approximately 100 mg of sample was introduced to the reaction cell. The latter contained 25 ml the methanolic KF working medium, and the sample was dissolved by stirring and the volume of titrant consumed was determined in triplicate. For the purpose of calculation of water content of processed samples, the amount of water determined by 1 ml of the titrant was accurately measured in triplicate. Water content of samples was calculated using the following formula:

$$\text{water content} = \frac{\text{volume of titrant consumed(ml)} * \text{f (mg/ml)}}{\text{wieght of sample (mg)}} * 100$$

Where f is the amount of water determined by 1 ml of the titrant.

RESULTS AND DISCUSSION

CHAPTER 3- SPRAY DRIED *p*-AMINOSALICYLIC ACID

3.1 INTRODUCTION

p-Aminosalicylic acid (PAS) needs to be administered in very large amounts, 8 - 12 grams per day in 2 or 3 divided doses (Reynolds, *et al.,* 1996). This is inconvenient to the patient, hence the importance of reducing the drug dosage. Formulation of PAS into porous particles for direct delivery into the lungs was the objective of the study carried out by Tsapis et al. (2003). They formulated PAS as large porous particles containing 95% PAS by weight via spray drying. The apparatus used was a NIRO Atomizer Portable spray-drier system and the solvent composition was 80% (v/v) ethanol/20% (v/v) water. The solid contents of the spray-dried system included 0.025% of dipalmitoyl-sn-glycero-3-phosphocholine and 0.475% of PAS. The pharmacokinetic data reported by Tsapis et al. (2003) indicated that the prepared powder delivered via insufflations reached the systemic circulation within 15 min of delivery to the lungs with a plasma peak concentration of 11±1 μg/ml. The concentration in the lung lining fluid was 148±62 μg/ml at 15min. Tissue concentrations were 65±20 μg/ml at 15 min and 3.2±0.2 μg/ml at 3 h. PAS was cleared within 3 h from the lung lining fluid and plasma but was still present at therapeutic concentrations in the lung tissue and the authors concluded that the total body dose was approximately 11 mg/kg via the lungs compared to an estimated value of 57 mg/kg for oral dosing of PAS in humans.

Tajber (2005) used particle engineering process (spray drying method) to produce porous particles of budesonide (a corticosteroid used as an anti-inflammatory and immunosuppressive agent), the process includes spray drying the drug from an ethanolic solution. Nolan (2008) used this novel method to prepare NPMPs of sulfadimidine. She reported that the recovered porous particles demonstrated superior *in vitro* drug deposition and aerodynamic properties in comparison to sulfadimidine raw material. This method has not been previously applied to PAS, PAS salt or other carboxylic acids and their salts, and as such, this work will provide a base for future application of this novel method using acidic compounds and their salts.

The objective of this study was to spray dry PAS to ascertain if nanoporous microparticles could be produced and subsequently to optimise the processing parameters and spray drying conditions to produce nanoporous microparticles with optimal micromeritic properties. In the current study, the preparation and properties of spray-dried PAS systems with and without process enhancer present were investigated. The particle size and morphology of all the powders produced from the spray-dried PAS systems were analysed

using scanning electron microscopy, and subsequently some of these systems were selected for further characterisation.

3.2 PAS SYSTEMS SPRAY-DRIED FROM ETHANOL

PAS was supplied as a crystalline powder as shown by the presence of well-defined peaks in the X-ray powder diffractogram of the raw material (Figure 3.1b). Spray drying of PAS from different ethanolic solutions was first considered based on previous work of McDonald (2005), Tajber (2005) and Nolan (2008) which illustrated the use of different mass ratios of ethanol/water or methanol/water in the production of nanoporous microparticles of hydrophobic compounds (bendroflumethiazide and budesonide). The inlet temperature was set to 78 °C because the boiling point of ethanol is 78.5 °C. This was the inlet temperature used by Tajber (2005), when ethanolic solutions of budesonide were spray-dried.

The morphology of PAS is presented in Figure 3.1. Generally, large rod-shape particles were observed.

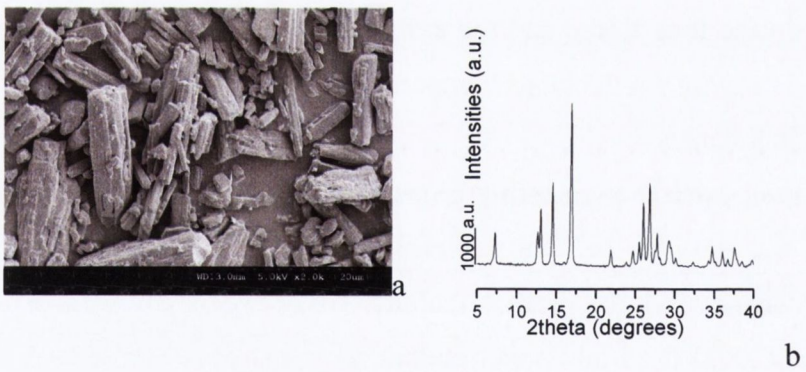

Figure 3.1- (a) SEM micrograph (b) XRD scan of PAS

An investigation into the production of NPMPs of PAS was undertaken; in the current project, the ability of spray drying to produce NPMPs without incorporating a recognised pore-forming agent (i.e. ammonium carbonate) was investigated. It was hypothesized that the inclusion of ethanol in the solvent system, might actually act as the pore-forming agent, resulting in the porous powders (McDonald, 2005).

Various solutions of PAS were prepared in ethanolic solvent and spray-dried using the spray drying parameters given in Appendix I, Table 1. It should be noted that all experiments are listed in Appendix I as discussed in each chapter.

A 1% (w/v) solution of PAS system was spray-dried from 70% (v/v) ethanol. SEM micrographs of the spray-dried material showed that spray drying of this system resulted in porous particles as well as small rod shaped crystals of PAS as shown in Figure 3.2a and at higher magnification in Figure 3.2d, which was different from the large elongated crystals of the unprocessed material (Figure 3.1 a).

The impact of the solvent composition employed was investigated; a 1% (w/v) solution of PAS was spray dried from varying ethanolic concentrations (80%, (v/v) ethanol and 90% (v/v) ethanol). These systems were also spray dried at an inlet temperature of 78 °C, with the spray drying conditions given in Appendix I. As shown in Figure 3.2 the composition of the solvent system had a significant effect on the morphology of the spray dried particles produced. The morphology of the spray dried powder from 80% ethanol was comprised of spherical porous particles and rod shape particles (Figure 3.2 (b)), while increasing ethanol concentration to 90% (v/v) produced rod shape particles similar to those previously produced at the ethanol concentration of 70% and 80% (v/v) ethanol, but with numerous spherical porous particle (Figure 3.2 (c)).

The outlet temperature is the temperature of the air with the solid particles before entering the cyclone. This temperature is the resulting temperature of the heat and mass balance in the drying cylinder and thus cannot be regulated (Training Papers Spray Drying, BÜCHI Labortechnik AG). In general, the outlet temperature varies in these spray dried samples despite the fact that the inlet temperature is the same (Appendix I), this may be attributed to the differences in solvent composition. Prinn et al., (2002) showed that parameters other than inlet air temperature may affect outlet temperature during spray drying process such as liquid feed rate, the atomizing flow rate and solid concentration. In addition, Kent and McLeod, (2007) reported that air moisture may influence outlet temperature.

Filtration removed undisclosed particles, thus improving uniformity of particles. Filtration and spray drying of 1% solution of PAS from 70% (v/v) ethanol resulted in a mixture of spherical particles as well as rod shaped crystals as shown in Figure 3.2e.

From the SEM micrographs of the various spray dried PAS systems, it could be concluded that the morphological characters of spray dried PAS under these conditions was dependent on the ethanol concentration.

Figure 3.2- SEM micrographs of 1% PAS system spray-dried from (a) 70% v/v ethanol, (b) 80% v/v ethanol, (c) 90% v/v ethanol, (d) 70 % v/v ethanol at higher magnification and (e) 70% v/v ethanol (filtered solution). Note the different magnifications.

Inter-batch reproducibility was checked. Different batches of PAS were used to investigate reproducibility of the process, where 1% solution of PAS was spray-dried from two separate 70% ethanol solutions. This approach was important to provide information on the reproducibility of the spray drying process. Examination of the resulted powders showed that the morphological characteristics were similar to those obtained from spray drying of the first batch of PAS. Figure 3.3 shows SEM micrographs of spray-dried PAS (different batches) from 70% ethanol where a mixture of rod shape crystals as well as spherical porous particles were obtained (repeatability was found to be quite good, with very similar SEM micrographs as shown).

It could be concluded that the co-solvent composition have a significant effect on the morphology of the spray dried samples. At co-solvent ratios of 90% (v/v) ethanol, the number of spherical particles of PAS produced was significantly higher in comparison to other spray dried systems. In addition, as observed from the different SEM micrographs of spray dried PAS (a hydrophobic compound) the use of ethanol as a solvent appeared to be promising in terms of production of NPMPs using this spray drying method. This was consistent with the results reported by Nolan et al., (2009) who successfully produced

porous particles of a hydrophobic compound (budesonide) by spray drying from ethanolic solutions.

Figure 3.3- SEM micrographs of 1% PAS system spray-dried from 70% v/v ethanol (a) (Lot: S26559-365) (b) &(c) (Lot: S35728-346).

In the solid phase, PAS has bands in the FTIR spectrum due to N–H antisymmetric and symmetric stretching modes at 3494 and 3387cm^{-1} respectively, and an absorption band at 1659 cm^{-1} due to C=O group (Akkaya, 2006). The spectrum of the spray-dried PAS was identical to that of the starting material; the characteristic signals of PAS were found at the same wavenumbers in the spectra of both processed and unprocessed samples as shown in Table 3.1. This indicates the similarity of vibration in bonding energies of the samples and that processing did not alter the chemical structure of the compound (Figure 3.4). The obvious similarity in finger print region between unprocessed and spray-dried PAS indicated that spray drying did not appear to alter PAS chemically.

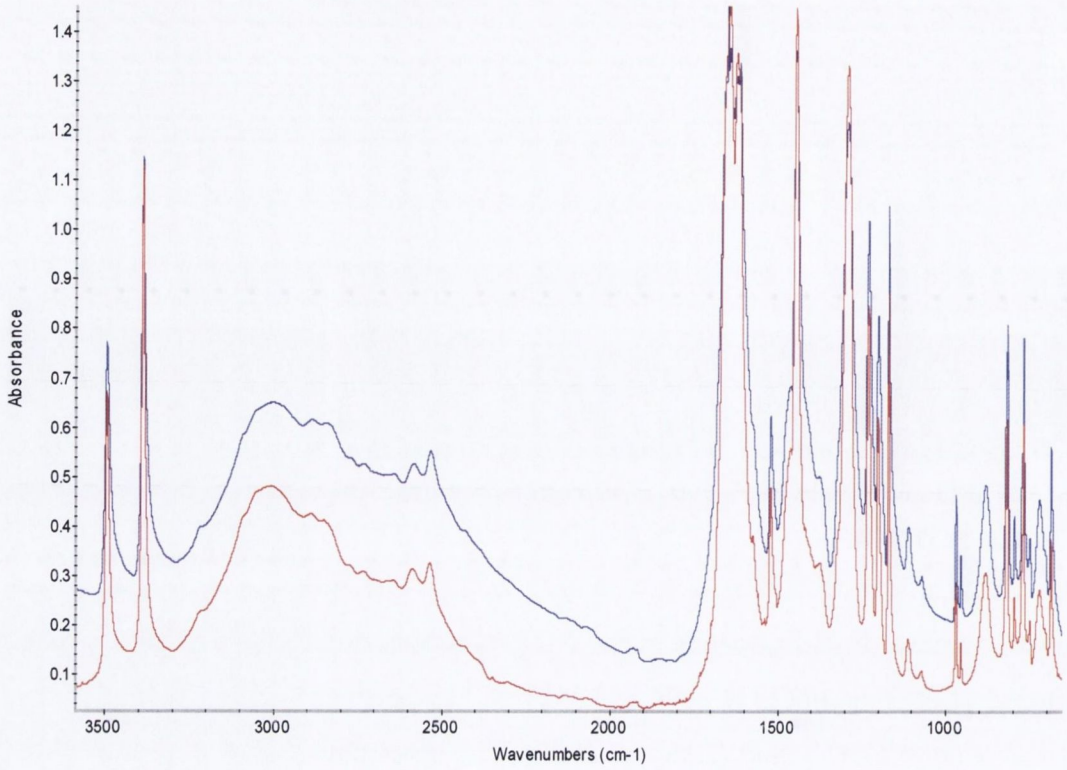

Figure 3.4- FTIR scans of PAS starting material (blue line) PAS system spray-dried from 90% v/v ethanol (red line).

Table 3.1 Summary of FTIR spectra of unprocessed and spray-dried PAS

System	NH signal (cm^{-1})	NH signal (cm^{-1})	OH signal (cm^{-1})	C=O signal(cm^{-1})
PAS raw material	3494	3387	3005	1653
spray-dried PAS	3494	3387	3005	1653

Having established the impact of the ethanol concentration on the morphological characters of the recovered particles, the effect of drug concentration was also investigated. Masters, (1991) reported that increasing feed solids may lead to heavy drying chamber deposits, which may indicate that maximum feed solids may have been exceeded. In addition, many spray dryers operate at low feed solids and comparatively low drying temperatures as these conditions are affected by the feed properties. It should be noted that the solubility of PAS in ethanolic solutions was the limiting factor in the Feed concentration used. The feed concentration of PAS ranged from 1% to 4% (w/v). It should be noted that solubility studies of PAS in different ethanol/water co-solvent system was undertaken. At a co-solvent concentration of 90% (v/v) ethanol a solubility of 42.02 ±0.64

g/l was measured, thus the selection of a 4% (w/v) feed concentration represented a close to saturated state.

Solutions at different concentrations of PAS were spray-dried from 90% ethanol (Appendix I, Table 1). A 3% (w/v) solution of PAS system was spray-dried from 90% (v/v) ethanol. SEM micrographs of the spray-dried material showed that the spray drying of this system resulted mainly in spherical particles either porous or non porous with few rod shape crystalline particles (Figure 3.5b). On the other hand, spray drying of a 4% (w/v) solution of PAS from 90% (v/v) ethanol resulted in crystalline aggregates, spherical porous particles and rod shaped crystals (Figure 3.5c).

It could be concluded that the morphology of spray dried PAS was significantly altered depending on feed concentration.

Figure 3.5- SEM micrographs of (a) 1% PAS (b) 3% PAS (c) 4% PAS system spray-dried from 90% v/v ethanol.

Another solution of 3% (w/v) PAS system was spray-dried from 95% (v/v) ethanol. The morphology of the processed particles was comprised of smooth, non-porous spherical particles and aggregates of crystalline particles with few porous particles as shown in Figure 3.6.

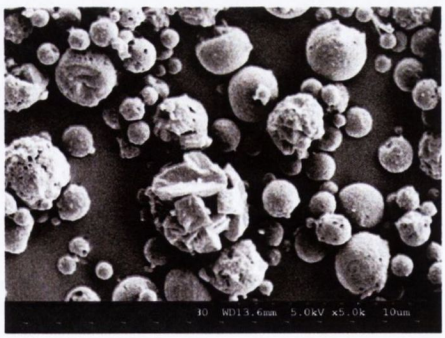

Figure 3.6- SEM micrograph of 3% PAS system spray-dried from 95% v/v ethanol.

Figure 3.7 shows the SEM micrograph of 4% PAS system spray-dried from 100% v/v ethanol. SEM micrographs of the spray-dried material showed that spray drying of this

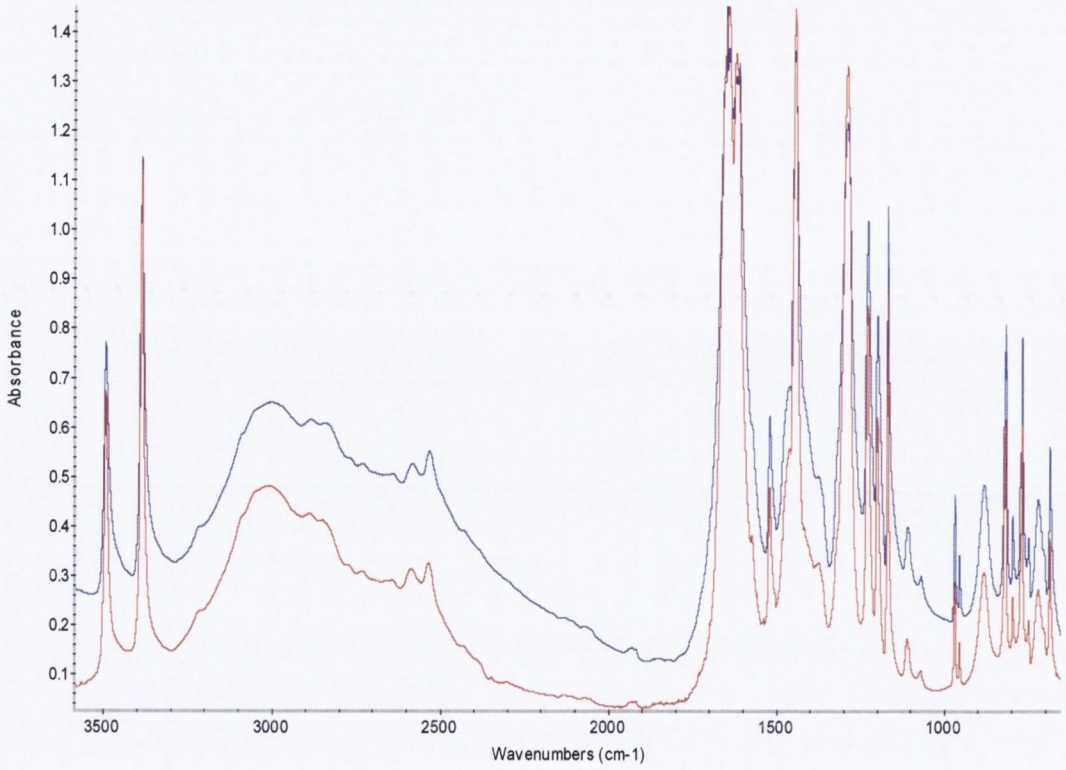

Figure 3.4- FTIR scans of PAS starting material (blue line) PAS system spray-dried from 90% v/v ethanol (red line).

Table 3.1 Summary of FTIR spectra of unprocessed and spray-dried PAS

System	NH signal (cm^{-1})	NH signal (cm^{-1})	OH signal (cm^{-1})	C=O signal(cm^{-1})
PAS raw material	3494	3387	3005	1653
spray-dried PAS	3494	3387	3005	1653

Having established the impact of the ethanol concentration on the morphological characters of the recovered particles, the effect of drug concentration was also investigated. Masters, (1991) reported that increasing feed solids may lead to heavy drying chamber deposits, which may indicate that maximum feed solids may have been exceeded. In addition, many spray dryers operate at low feed solids and comparatively low drying temperatures as these conditions are affected by the feed properties. It should be noted that the solubility of PAS in ethanolic solutions was the limiting factor in the Feed concentration used. The feed concentration of PAS ranged from 1% to 4% (w/v). It should be noted that solubility studies of PAS in different ethanol/water co-solvent system was undertaken. At a co-solvent concentration of 90% (v/v) ethanol a solubility of 42.02 ±0.64

g/l was measured, thus the selection of a 4% (w/v) feed concentration represented a close to saturated state.

Solutions at different concentrations of PAS were spray-dried from 90% ethanol (Appendix I, Table 1). A 3% (w/v) solution of PAS system was spray-dried from 90% (v/v) ethanol. SEM micrographs of the spray-dried material showed that the spray drying of this system resulted mainly in spherical particles either porous or non porous with few rod shape crystalline particles (Figure 3.5b). On the other hand, spray drying of a 4% (w/v) solution of PAS from 90% (v/v) ethanol resulted in crystalline aggregates, spherical porous particles and rod shaped crystals (Figure 3.5c).

It could be concluded that the morphology of spray dried PAS was significantly altered depending on feed concentration.

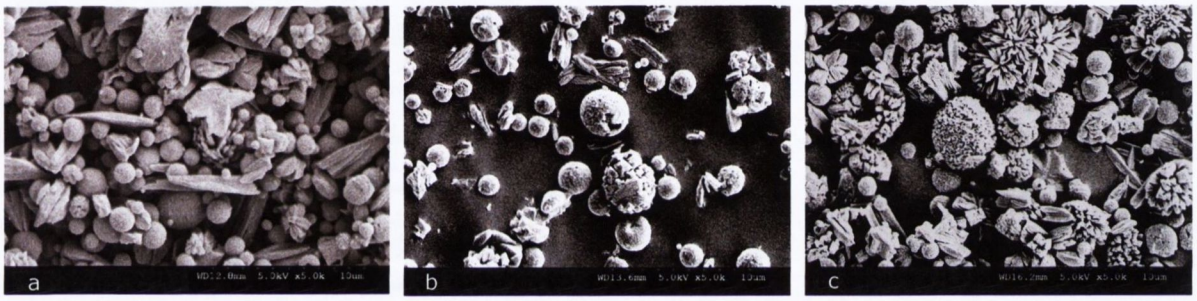

Figure 3.5- SEM micrographs of (a) 1% PAS (b) 3% PAS (c) 4% PAS system spray-dried from 90% v/v ethanol.

Another solution of 3% (w/v) PAS system was spray-dried from 95% (v/v) ethanol. The morphology of the processed particles was comprised of smooth, non-porous spherical particles and aggregates of crystalline particles with few porous particles as shown in Figure 3.6.

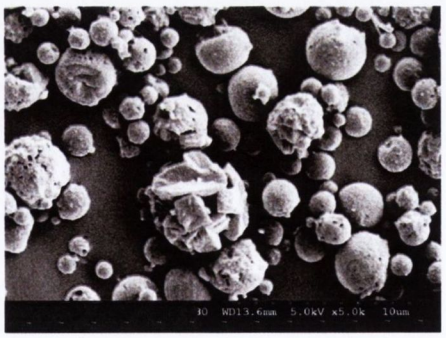

Figure 3.6- SEM micrograph of 3% PAS system spray-dried from 95% v/v ethanol.

Figure 3.7 shows the SEM micrograph of 4% PAS system spray-dried from 100% v/v ethanol. SEM micrographs of the spray-dried material showed that spray drying of this

system resulted in spherical particles with a rough surface texture; these particles vary greatly in size. The spherical particles were non-porous as seen in Figure 3.7. At higher magnification SEM micrographs (Figure 3.7 (b), red box) the formations of distinguishable spherical particles with visible holes were noticed (red box).

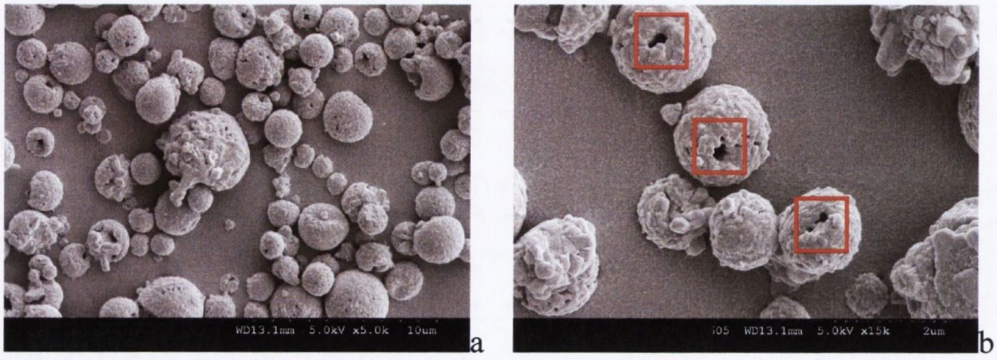

Figure 3.7- SEM micrographs (at different magnifications) of 4% PAS system spray-dried from 100% v/v ethanol, the red boxes show the holes in the spherical particles.

Verreck et al. (2006) reported that PAS is a thermally labile compound, which melts with decomposition. Different literature values of melting point of PAS were found: 149-151°C (Erlenmeyer et al., 1948), 150-151°C (O'Connor, 1948) and 139-141°C (Whittet, 1948) have been reported.

There was a melting endotherm visible on examination of PAS starting material by DSC. Figure 3.8 presents the DSC scans of unprocessed PAS and its spray-dried systems from 70% (v/v) ethanol and 90% (v/v) ethanol. An endothermic peak due to PAS melting was detected at ~140 °C; this was characteristic of PAS melting, as confirmed by the literature value of (139-151°C) (Rotich et al., 2001), with measured enthalpy of fusion of ~369 J/g. The spray-dried samples also showed one endothermic process. PAS spray-dried from 90% (v/v) ethanol showed an endotherm peaking at ~ 140°C, attributed to melting (Figure 3.8b). The DSC thermogram of PAS spray-dried from 70% (v/v) ethanol (Figure 3.8c) showed a melting endotherm, peaking at ~142 °C. The presence of one endothermic event in the DSC scans of spray-dried samples would suggest a crystalline form of spray-dried PAS.

The shapes of TGA scans were similar for PAS unprocessed and spray-dried powders (Figure 3.9). The TG curve for PAS starting material heated in flowing nitrogen at 10 °C/min gives a two-stage mass loss (total 100%) with the discontinuity after about 30% mass loss at close to the melting point of PAS (~140°C) as estimated from DSC thermograms of PAS. It should be noted that The CO_2 content, calculated from the formula

of PAS, is approximately 29%, i.e. close to mass loss at the discontinuity. In addition, the molecular weight of 3-aminophenol (the main degradation product of PAS) is 109.13, which is about 70% of the molecular weight of PAS, that may suggest that PAS degraded to 3-aminophenol in the first stage mass loss. These finding were in agreement with Rotish et al., (2001), who studied thermal behaviour of PAS, the authors reported that TG scan for PAS heated in flowing nitrogen gives a two-stage mass loss (total 100%) with the discontinuity after about 30% mass loss at close to the reported melting point of PAS.

It could be concluded that the decomposition pathway of PAS includes a decarboxylation of the drug with the formation of carbon dioxide as confirmed by different studies found in the literature (Rekker and Nauta, 1948; Roy, 2002; Vasbinder et al., 2004).

TGA registered weight loss of 0.67%, 0.77 and 0.95% over the temperature range of 25 to 100 °C for PAS starting material, spray-dried PAS from 90% (v/v) ethanol and spray-dried PAS from 70% (v/v) ethanol, respectively. The difference in weight loss over the temperature range of 25 to 100 °C between starting material and spray-dried samples could be attributed to residual solvent content in the spray-dried samples, in addition, the difference in weight loss between the spray dried samples may be due to difference in solvent composition. The higher the content of water the more moisture has adsorbed. Further mass loss occurred at ~ 140 °C, corresponding to decomposition in the DSC scan.

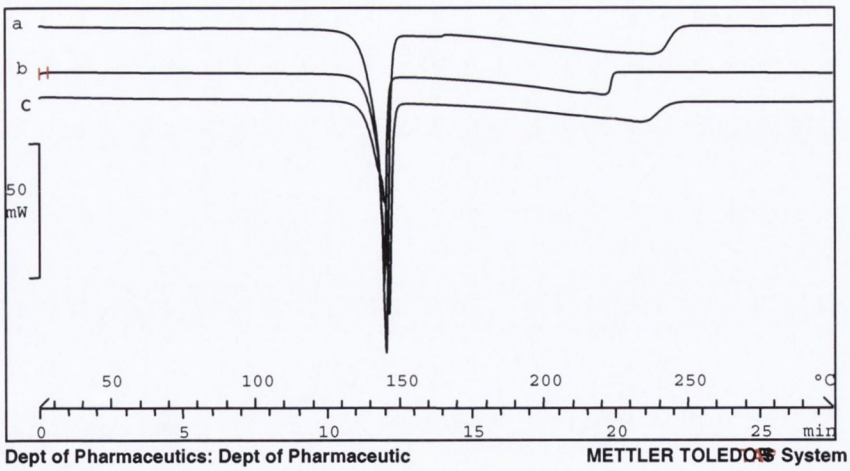

Figure 3.8- DSC scans of (a) PAS starting material and 1% PAS system spray-dried from (b) 90% v/v ethanol (c) 70% v/v ethanol.

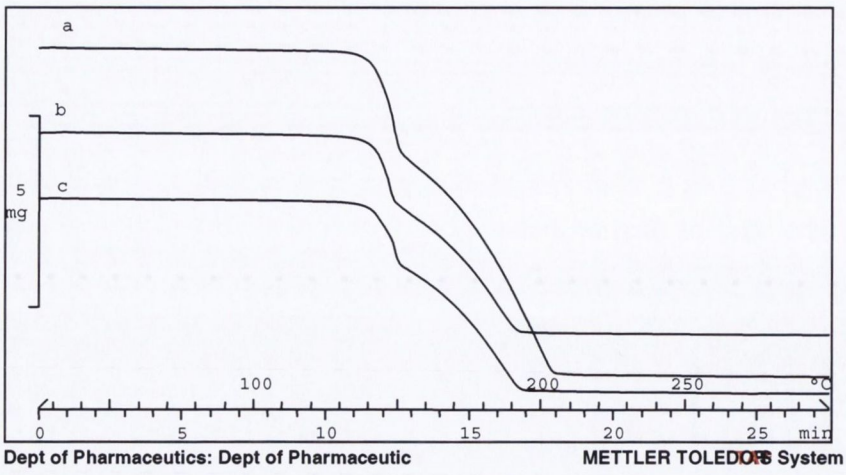

Figure 3.9- TGA scans of (a) PAS starting material and 1% PAS system spray-dried from (b) 90% v/v ethanol (c) 70% v/v ethanol.

Figure 3.10 shows the DSC thermograms obtained for 1, 3 and 4% PAS systems spray-dried from 90% ethanol analysed over the heating range of 25 to 300 °C. The crystalline nature of the spray-dried systems was clear by DSC analysis. Generally, DSC scans of the spray-dried samples showed only one endothermic event. 1% PAS systems spray-dried system showed one endotherm peaking at ~141 °C (Figure 3.10 (a)), attributed to melting, as confirmed by the literature value of (139-151°C) (Rotich et al., 2001). In the DSC thermogram of 3% PAS spray-dried system (Figure 3.10 (b)), a melting endotherm was detected, peaking at 143 °C. An endothermic peak due to PAS melting was detected at ~142 °C on investigation of DSC thermogram of 4% PAS spray-dried system (Figure 3.10 (c)).

It could be concluded that there was no significant changes in thermal behaviour of processed samples in comparison to the starting material upon spray drying under these conditions.

TGA registered weight loss of ~0.7%, ~1% and ~1% over the temperature range of 25 to 100 °C for 1, 3 and 4% PAS systems spray-dried from 90% ethanol, respectively (TGA not shown). This could be attributed to residual solvent content in the samples due to the fact that the boiling points of water and ethanol are within this temperature range, in addition, Nolan (2008) reported that the weight loss over the temperature range of 25 to 100 °C of spray dried samples from ethanol/water co-solvent could be attributed to residual solvent content in the sample. In addition, the differences in residual solvent content between different spray dried samples may be due to differences in solid content of spray dried systems, so it is not surprising that systems containing 3% and 4% of solid retained more solvent in comparison to the spray dried systems contain 1% of total solid.

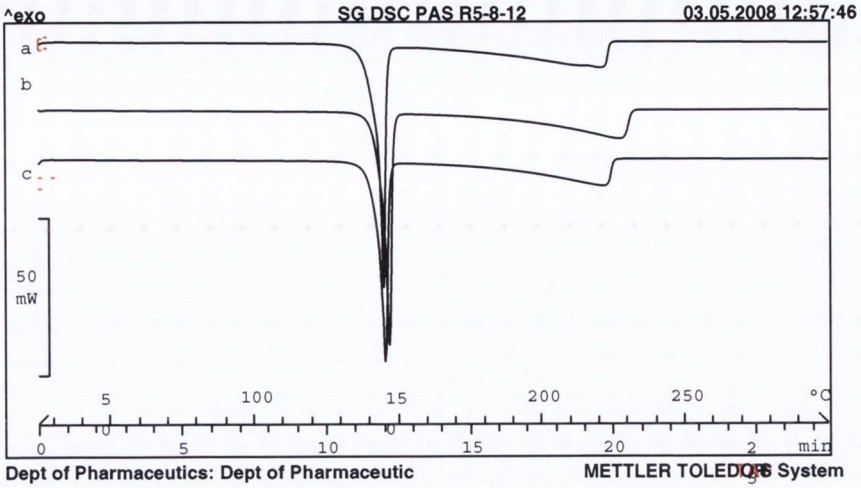

Figure 3.10- DSC scans of (a) 1% PAS (b) 3% PAS (c) 4% PAS system spray-dried from 90% v/v ethanol.

DSC analysis of the 3% PAS system spray-dried from 95% v/v ethanol showed a melting endothermic event peaking at 141.6 °C with its onset at 141.3°C. The TGA curve for the spray-dried sample (Figure 3.11) heated in flowing nitrogen at 10 °C/min gives a two-stage mass loss. TGA scan also shows a weight loss of 0.81% up to 100°C compared to weight loss of 0.67% for the starting material; the difference could be attributed to residual solvent contents in the spray dried sample (Figure 3.11).

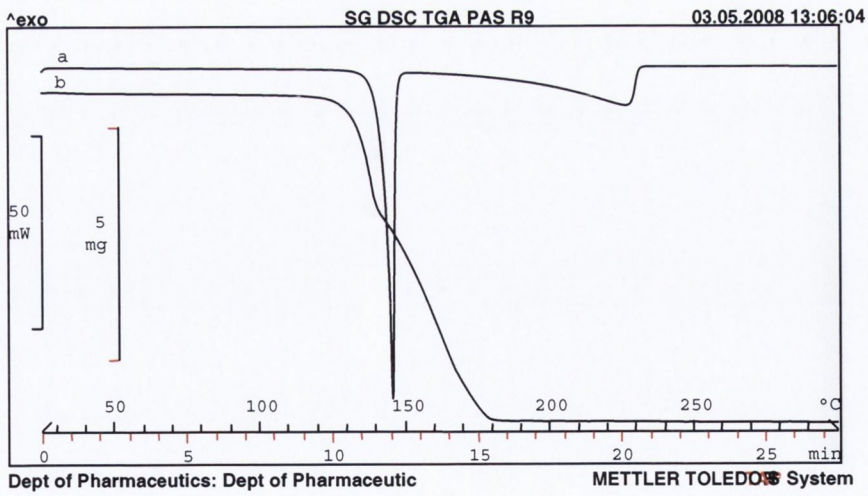

Figure 3.11- (a) DSC and (b) TGA scans of 3% PAS system spray-dried from 95% v/v ethanol.

Figure 3.12 shows the DSC thermogram of 4% PAS system spray-dried from 100% v/v ethanol. It appears to be crystalline, as only one endothermic event, peaking at 141.5°C with the onset at ~140.9 °C was recorded. TGA analysis of the same sample shows a weight loss of 0.89% up to 100°C compared to weight loss of 0.67% over the temperature

range of 25 to 100 °C for PAS starting material, which indicates the presence of residual solvent in the spray-dried sample.

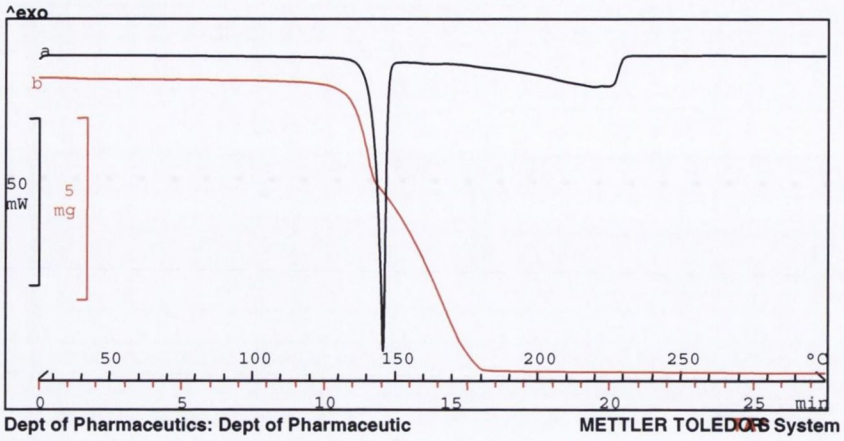

Figure 3.12- (a) DSC and (b) TGA scans of 4% PAS system spray-dried from 100% v/v ethanol.

It is obvious that thermal analysis suggested that the spray-dried samples may be crystalline, as only one endothermic event was observed on examination of DSC scans of spray-dried samples. The onset of the endothermic peak of the spray-dried samples was in good agreement with the observed melting point of the starting material and with the literature value reported by Rotich et al., 2001. It could also be assumed from DSC and TGA that the decomposition pathway of PAS includes a decarboxylation process of the acid with the formation of 3-amiophenol and carbon dioxide, this is in agreement with the finding of Verreck, et al., (2006), who showed that the decomposition pathway of PAS includes a decarboxylation process with the formation of carbon dioxide as shown in the following equation.

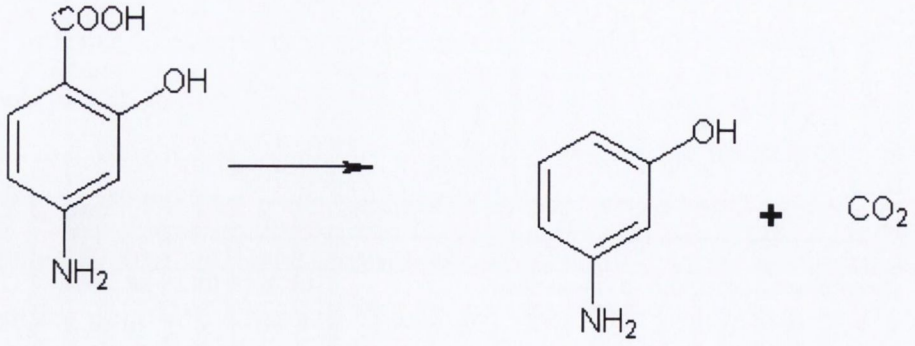

The powder X-ray diffractogram (Figure 3.13) of PAS raw material was typical of a crystalline material. The peak positions were consistent with the XRD spectrum presented by Rotich et al., (2003a) for PAS raw material. XRD analysis demonstrated that the degree of crystallinity of spray-dried PAS was reduced compared to the raw material.

It should be noted that the percentage crystallinity of the spray-dried samples should be considered as relative values as the crystallinity of unprocessed PAS was assumed to be 100%. It should also be noted that Giron et al., (1997) reported that amorphous phase detection by XRD is limited to 5-10%. The combined integrated area under the three sharp peaks positioned at approximately 16.90, 25.95 and 26.75 degrees was taken for calculation. The crystallinity of unprocessed PAS was assumed to be 100%. The combined area under the peaks of 1% PAS spray-dried from 90% v/v ethanol was reduced compared to the starting material. The reduction in crystallinity by XRD was calculated to be about 61%. The combined area under the peaks of 3% PAS spray-dried from 90% v/v ethanol was reduced compared to the starting material. The reduction in crystallinity by XRD was calculated to be about 47%.

This reduction in peak intensities in the diffractograms of spray dried samples could be attributed to a reduction in the crystallite size of the spray dried samples. This was in agreement with Singh et al., (2008), who attributed the decrease in peak intensity in case of nano-sized ZSM-5 (NZ) to a decrease in crystal size.

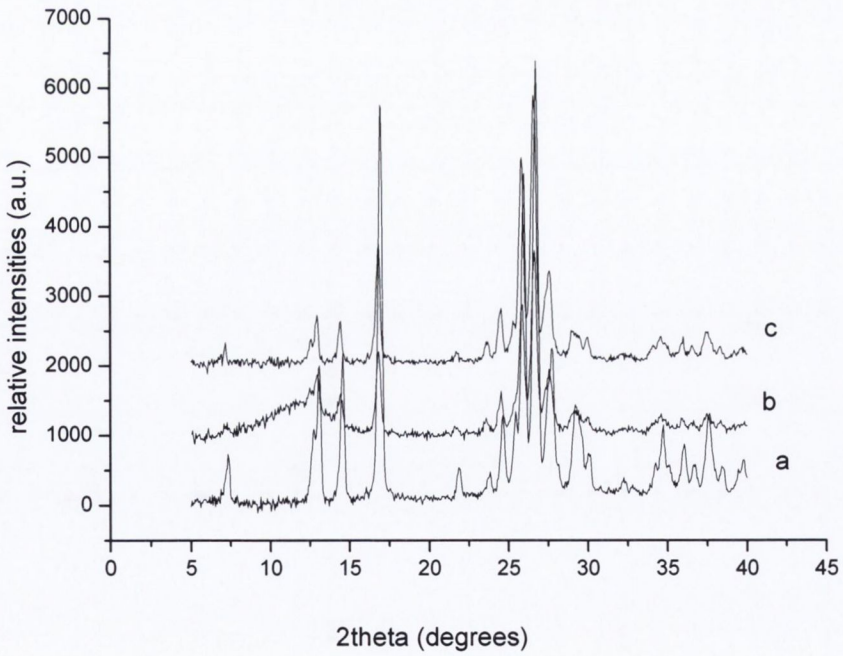

Figure 3.13- XRD scans of (a) PAS starting material (b) 1% (c) 3% PAS system spray-dried from 90% v/v ethanol.

It could be concluded from XRD analysis that spray drying of PAS from ethanolic solution resulted in production of crystalline powder, the XRD pattern of spray-dried samples was

typical of a crystalline powder and the peak positions were compared favourably with the X-ray diffractogram of the unprocessed material.

3.3 Preparation of ammonium salt of PAS

Synthesis of PAS ammonium salt was confirmed by elemental analysis. The results of elemental analysis are shown in Table 3.2. The crystals dried under reduced pressure to give 1.5 g (production yield of 15%). It should be noted that Forbes et al., (1995) reported that the yield of preparation of ammonium salt of PAS was approximately 30%, the difference in yield found in the current work and that reported by Forbes et al., (1995) may be attributed to the difference of the amount of starting material used in the preparation, Forbes et al., (1995) used 100 grams of PAS, while only 10 grams of PAS was used in the current work.

Ammonium salt of aminosalicylic acid is crystalline powder as shown by the presence of well-defined peaks in the X-ray powder diffractogram of the unprocessed material (Figure 3.14b). The morphology of ammonium salt of PAS is presented in Figure 3.14. Generally, large irregular shape particles were observed. The structure of ammonium salt of PAS is shown in Figure 3.14c).

Table 3.2- Elemental analysis of PAS and its salt

Sample		Analysis% w/w		
		C	H	N
PAS	Calculated	54.90	4.61	9.15
ammonium salt of PAS	Calculated	49.41	5.92	16.46
	Found	49.80±0.17	5.79±0.07	15.99±0.49

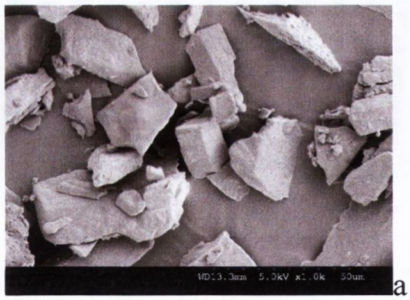

a

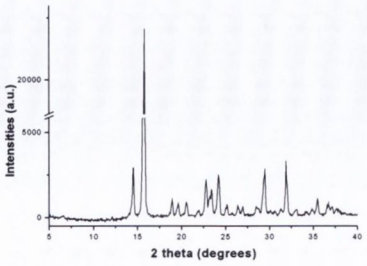

b

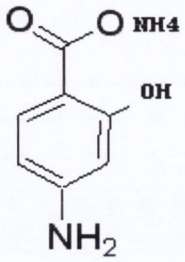

c

Figure 3.14- (a) SEM micrograph (b) XRD scan (c) structure of ammonium salt of PAS

3.4 PAS/ammonium carbonate systems spray-dried from ethanol

As shown earlier, the main objective of this work was to spray dry PAS systems to ascertain if NPMPs could be produced. Tajber (2005) had previously shown that porous particles could be produced by spray drying systems where ammonium carbonate acted as the pore-forming agent. Tajber (2005) spray dried budesonide from ethanolic solution with ammonium carbonate. Tajber (2005) hypothesised that, as ammonium carbonate is insoluble in ethanol and on the other hand budesonide is insoluble in water, a microemulsion-type mixture comprised of an aqueous solution of ammonium carbonate and ethanolic solution of budesonide was formed. The pore-forming agent was volatilised during the spray drying process and together with the evaporated process solvent; these expanding gases were removed with the drying medium to produce essentially excipient-free porous particles.

In another study Mc Donald (2005) used ammonium carbonate as a pore-forming agent in spray drying budesonide and bendroflumethiazide, whereby the pore-forming agent was removed during the drying process by decomposition and volatilisation process. The ammonium carbonate decomposes into ammonia, carbon dioxide and water at temperatures over 59° C, so in a spray drying process operating above this temperature it is postulated that the ammonium carbonate is removed from the spray-dried system with the exhaust gases, therefore producing essentially excipient-free NPMPs.

3.4.1 Morphological properties of spray dried composites

Initially 4% (w/v) solutions of PAS/ammonium carbonate were prepared in 90% (v/v) ethanol and spray-dried at an inlet temperature of 78°C. The ammonium carbonate concentration varied between 3.8% and 20% (weight of solids) as outlined in Appendix I, Table 1. It should be noted that 3.8% ammonium carbonate represents PAS: ammonium carbonate 10:1 molar ratio. As with all the spray drying experiments, the resultant powders were viewed by SEM. SEM micrographs of the spray-dried material showed that spray drying of each of the systems described above resulted in aggregates of rod shape crystals (Figure 3.15).

It could be concluded that the morphological characteristics of powders produced by spray drying of 4% (w/v) solutions of PAS/ammonium carbonate is dependant on ammonium carbonate concentration. The sample produced from the spray drying of 4% (w/v) solution of PAS/ammonium carbonate 80:20 was the most promising in terms of the morphological characteristics. Ideally, uniform and porous particles within the size range of 2-5 μm are desirable for pulmonary delivery.

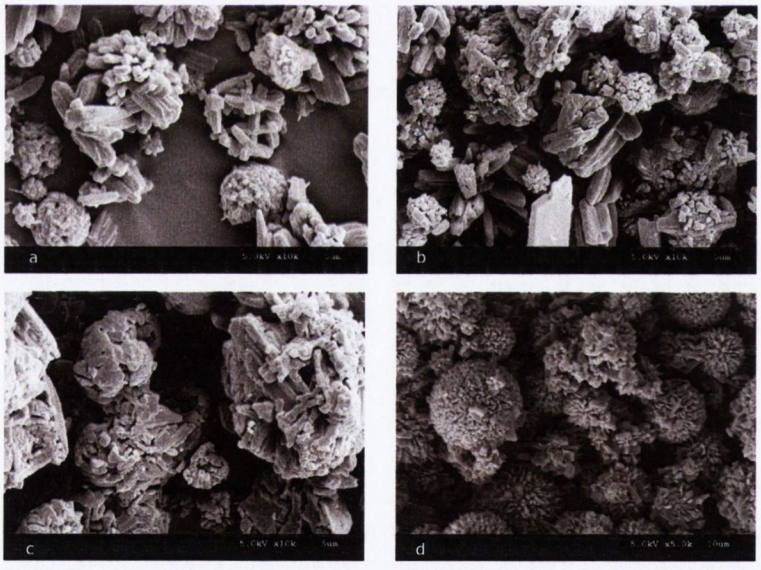

Figure 3.15- SEM micrographs of 4% (w/v) solution of PAS/ammonium carbonate (a) 96.2:3.8 (b) 90: 10 (c) 85: 15 (d) 80: 20 systems spray-dried from 90% v/v ethanol.

Inter-batch reproducibility was checked. Different batch of PAS was used to investigate reproducibility of the process, where 4% solution of PAS/ammonium carbonate 80: 20 was spray-dried from two separate 90% ethanol solutions. This approach was important to provide information on the repeatability of the spray drying process. Examination of the resulted powders showed that the morphological characteristics were similar to those

obtained from spray drying of the first batch of PAS. Figure 3.16 shows SEM micrographs of spray-dried PAS (different batches) from 90% ethanol where aggregates of microcrystalline particles were obtained (repeatability was found to be quite good, with very similar SEM micrographs as shown).

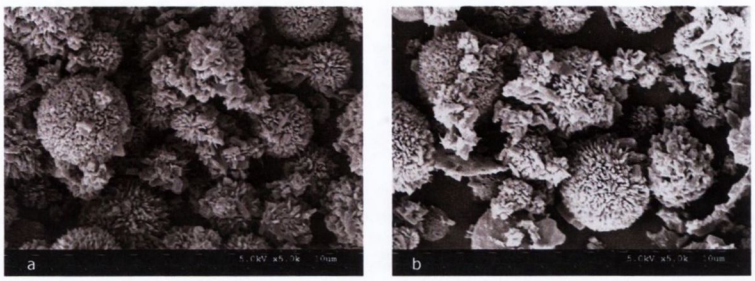

Figure 3.16- SEM micrographs of 4% (w/v) solution of PAS (a) (Lot: S26559-365) (b) (Lot: S35728-346)/ammonium carbonate 80: 20 system spray-dried from 90% v/v ethanol

The effect of total solid concentration was also examined. 3% solutions of PAS/ammonium carbonate were prepared in 90% (v/v) ethanol and spray-dried, using air as a drying gas. The ammonium carbonate concentration was 20%, 27%, 38% and 50% (weight of solids) as outlined in Appendix I, Table 1. The choice of 20% ammonium carbonate was based on the morphological characteristics of 4% PAS/ammonium carbonate 80:20 which showed spherical aggregates of microcrystalline particles. The solution of PAS/ammonium carbonate 73:27 was used as it represents the PAS/ammonia 1:1 according to the ammonia contents reported by the supplier in the product specification sheet, where ammonia contents in ammonium carbonate is 30% of its weight. On the other hand, 38% ammonium carbonate represents PAS: ammonium carbonate 1:1 molar ratio according to the molecular weights of PAS and ammonium carbonate. 50% ammonium carbonate was also used to study the effect of using ammonium carbonate higher than 1:1 PAS: ammonium carbonate. For these systems, the inlet temperature was set at 78°C. Figure 3.17 shows SEM micrographs of the spray-dried 3% (w/v) solution of PAS/ammonium carbonate. Generally, solid crystalline spherical agglomerates of particles were produced upon spray drying of these systems. Investigation of SEM micrographs of different spray dried systems showed that the morphological properties of the spray dried systems were dependent on the amount of ammonium carbonate. It was also noticed that SEM micrographs of the powder produced by spray drying of PAS 80:20 showed uniform, porous spherical microparticles as shown in Figure 3.17a. It could be concluded that the amount of ammonium carbonate employed influenced the morphological characters of spray dried PAS/ammonium carbonate regardless of the total solid concentration

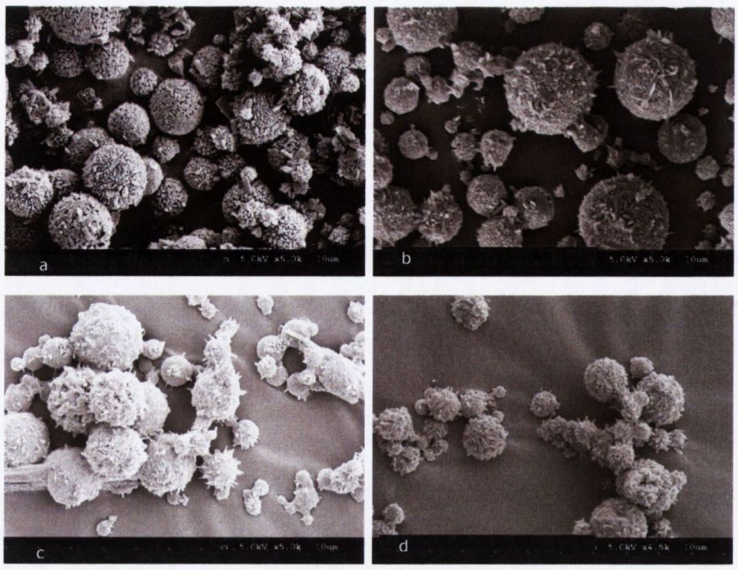

Figure 3.17- SEM micrographs of 3% (w/v) solution of PAS/ammonium carbonate (a) 80:20 (b) 73:27 (c) 62:38 (d) 50:50 systems spray-dried from 90% v/v ethanol.

Inter-batch reproducibility was investigated. Different batch of PAS was used to investigate reproducibility of the process, where 3% solution of PAS/ammonium carbonate was spray-dried from two separate 90% ethanol solutions. Figure 3.18 shows SEM micrographs of 3% (w/v) solution of PAS/ammonium carbonate system spray-dried from 90% v/v ethanol. Repeatability was found to be quite good, with similar SEM micrographs as shown in Figure 3.18 (a) and (b). In addition, at higher magnification SEM micrographs (Figure 3.18 (c)) the formation of distinguishable spherical porous particles and aggregates of crystalline particles were detected.

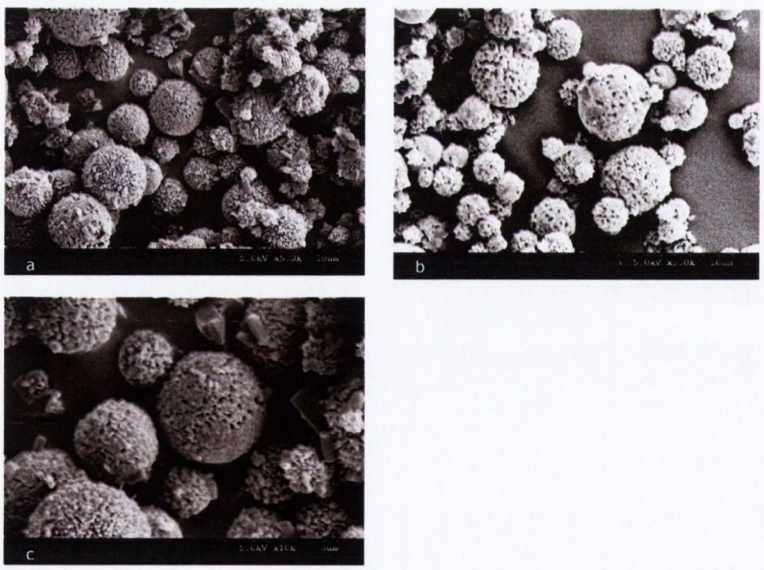

Figure 3.18 SEM micrographs of spray dried 3% solution of PAS /ammonium carbonate 80: 20 systems (Lot: S26559-365) (b) (Lot: S35728-346) and (c) spray dried PAS/ammonium carbonate 80:20 at higher magnification. Note different magnification.

The effect of drying gas was also investigated; a 3% (w/v) solution of PAS/ammonium carbonate was prepared in 90% (v/v) ethanol and spray-dried at an inlet temperature of 78 °C. For this system, nitrogen was used as a drying gas instead of air as in the previous sample. SEM micrographs showed irregular and spherical aggregates of crystalline particles in contrast to porous microparticles and spherical agglomerates of microcrystalline particles produced upon spray drying of the PAS/ammonium carbonate using air as drying gas as shown in Figure 3.19. Nolan (2008) reported that the spray drying mode had an effect on the production of either NPMPs (open mode) or non-porous particles (closed mode) of sulfadimidine and sulfamerazine. McDonald (2005) also studied the effect of spray drying mode on production of NPMPs of bendroflumethiazide, he reported that porous particles were recovered when open mode was used while recovered particle from spray drying using closed mode were non porous. It should be noted that in the open mode the drying gas is discharged after use, on the other hand, in the closed mode the drying gas is continuously recycled. McDonald (2005) reported that the differences in morphology when using different operating modes perhaps due to the fact that when operating in the closed mode the drying gas is recycled through the system so that although the solvent is condensed, the drying gas may not be completely dry of solvent. When operating in the open cycle mode the drying gas exits the system on a continual basis pulling solvent with it. McDonald (2005) anticipated that the gradient for evaporation and thus the driving force may be greater in the open mode, since the solvent is moving into a drier gas.

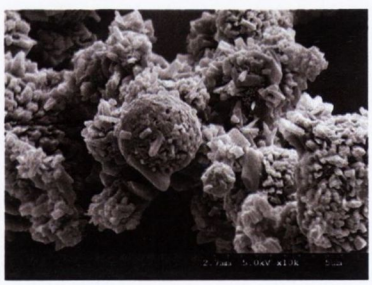

Figure 3.19- SEM micrograph of solution of PAS/ammonium carbonate 80: 20 system spray-dried using nitrogen as drying gas.

3.4.2 Physicochemical properties of spray dried composites

3.4.2.1 Thermal behaviour of the spray dried composites

DSC scan of PAS/ammonium carbonate 80:20 spray-dried from 90% v/v ethanol is shown in Figure 3.20. DSC results showed that the thermal behaviour of PAS/ammonium carbonate 80:20 spray-dried from 90% v/v ethanol differed from that of the starting material: endothermic peak position shifted, the peak broadened and became irregular in shape and asymmetric, and there were differences in the onset temperatures (Figure 3.20). The onset temperature was ~140°C with a measured enthalpy of fusion of ~369 J/g for starting material and 130°C, with a measured enthalpy of fusion of ~318 J/g for the spray-dried sample. The thermal behaviour of the starting material was compared favourably with literature (Rotich et al., 2001), however, the processed material showed different thermal behaviour in comparison to the unprocessed PAS and to the published data.

It should be pointed out that the difference in melting points of the recovered particles compared to those of the unprocessed PAS indicates the formation of new phase upon spray drying. This assumption was based on the fact that the melting point is a basic characteristic for any drug compound and the difference in melting points of processed material compared to those of either of the starting materials strongly indicates the formation of new phases (Basavoju et al., 2006)

A further point of interest illustrated in Figure 3.21 is that the DSC scans of other spray-dried PAS/ammonium carbonate systems showed that thermal properties of the recovered particles were different from that of unprocessed PAS, which may confirm that spray drying of PAS/ammonium carbonate resulted in a new solid state form regardless of the amount of ammonium carbonate used in spray drying process.

Figure 3.22 shows DSC scans of the PAS/ammonium carbonate spray-dried from 90% ethanol and PAS/ammonium carbonate physical mix. DSC analysis of the physical mixture showed broad endothermic event at ~95 °C. This was ascribed to the decomposition process of ammonium carbonate as confirmed by the DSC trace reported by Muehling et al., (1995) for ammonium carbonate. This was followed by endothermic peak at ~132 °C, this was comparable to the endothermic peak of the spray dried sample at ~133°C and the peaks (of both spray dried and physical mix) were irregular in shape and asymmetric. The onset was ~129 °C for the physical mixture and ~130°C for the spray-dried sample. It should be noted that the colour of PAS was darkened by physically mixing with ammonium carbonate, which is perhaps due to possible interactions between PAS and

ammonium carbonate. The shift in the onset of melting of the physical mixture in comparison to unprocessed PAS and the similarities in thermal behaviour of the spray-dried composite and the physical mixture suggest that the complete removal of the process enhancer upon spray drying was uncertain and the spray-dried composite may contain traces of the process enhancer.

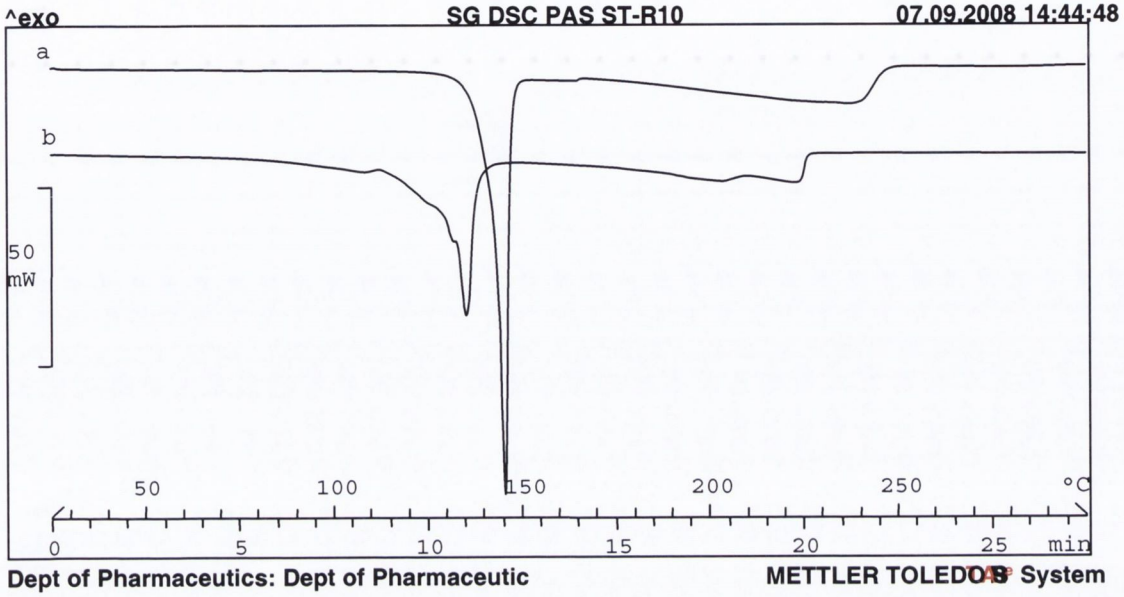

Figure 3.20- DSC scans of (a) PAS starting material (b) PAS/ammonium carbonate spray-dried from 90% v/v ethanol.

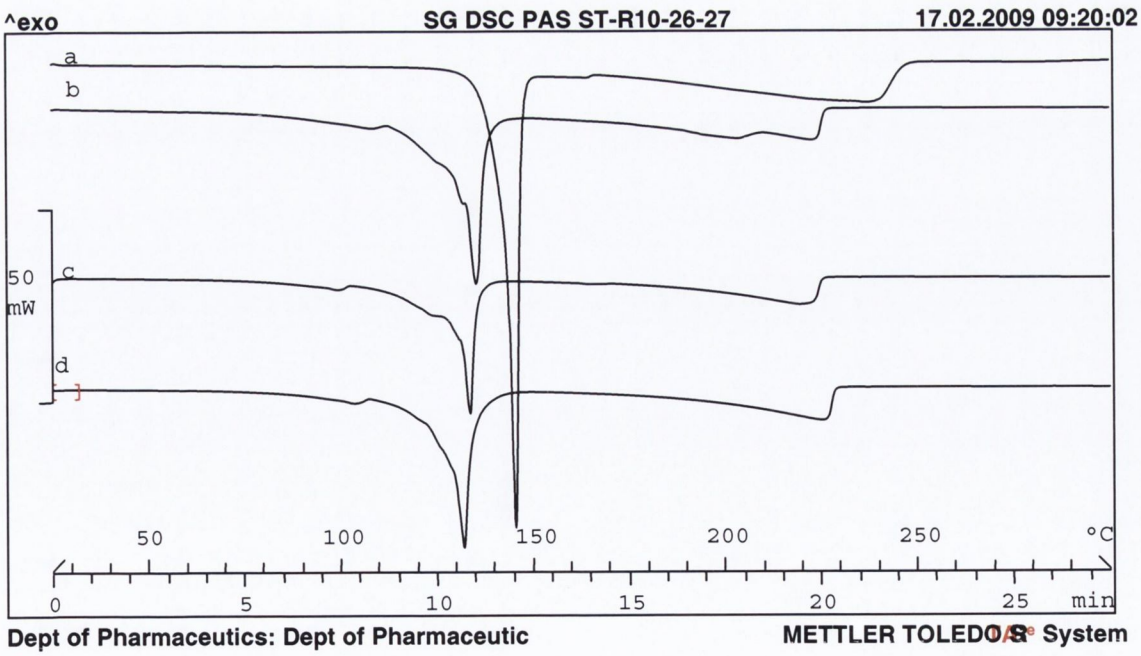

Figure 3.21- DSC scans of (a) PAS starting material and PAS/ammonium carbonate (b) 80:20 (c) 73:27 (d) 62:38 spray-dried from 90% v/v ethanol.

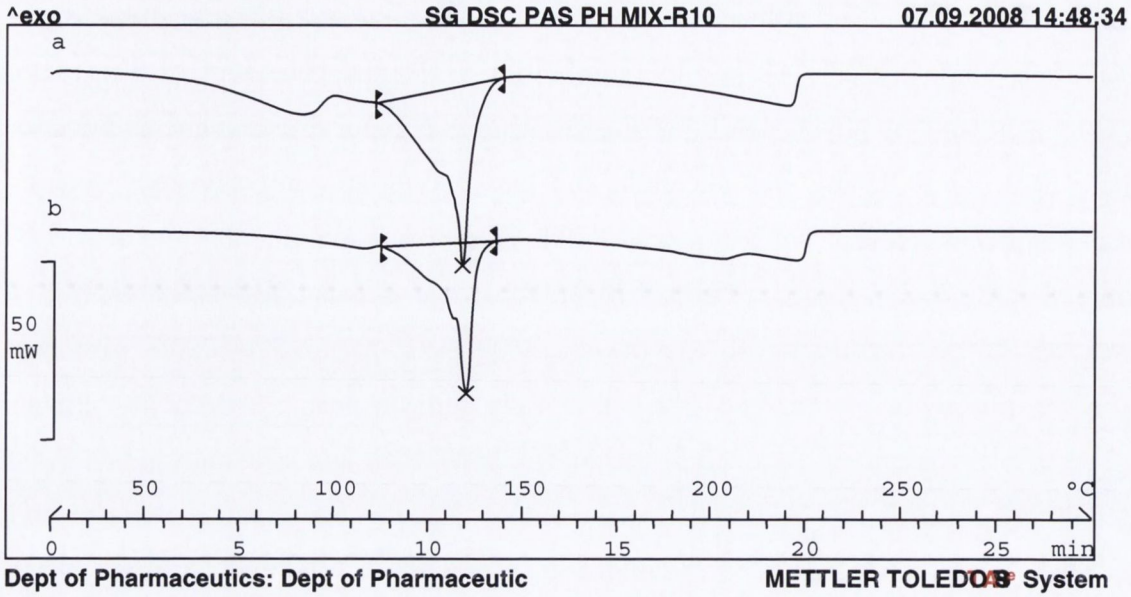

Figure 3.22- DSC scan (a) PAS/ammonium carbonate physical mix. (b) PAS/ammonium carbonate spray-dried from 90% ethanol.

The alteration of the solid state form of PAS upon spray drying with ammonium carbonate is contrasting with the results of budesonide NPMPs described by Nolan (2009). The budesonide NPMPs were obtained by spray drying from 90% (v/v) ethanol containing ammonium carbonate at an inlet temperature of 78 °C. As the spray drying process operated above the decomposition temperature of ammonium carbonate, it was expected that the ammonium carbonate was evaporated from the spray dried system with the exhaust gases, therefore producing essentially excipient-free NPMPs. The sample were analysed and it was reported that the amount of ammonia in the spray dried budesonide/ammonium carbonate samples was below the limit of detection of the assay (1% w/w).

The molecular weights, chemical structures, pKa values and solubility of budesonide and p-aminosalicylic acid are listed in Table 3.3. Budesonide is a glucocorticoid, which has no acidic group; therefore, it has no potential to react with ammonia, consequently, ammonium carbonate will behave during spray drying as a free molecule and hence the decomposition and removal of ammonium carbonate during spray drying process is likely. In contrast, p-aminosalicylic acid is an acidic compound, according to Merck Index, it has a pK_a value of 3.25 and the pH of 0.1% aqueous solution of p-aminosalicylic acid is 3.5. Therefore, p-aminosalicylic acid may react with ammonia. Serajuddin, (2007) reported that the concept of the pH of maximum solubility of certain compound (pH_{max}) plays a major role in determining whether a salt would be formed or not, and, in case it is formed, whether it would remain 'as is' or would convert to the corresponding free acidic form. The author depicted the influence of pK_a of the acid on pH_{max}, and consequently on salt

formation, where a decreases in pK_a of the acidic drug will decrease pH_{max} and, therefore, favour salt formation. Therefore, budesonide did not react with ammonium carbonate upon spray drying; on the other hand, PAS has the potential to react with ammonia, which could be the reason behind alteration of the solid state form of PAS upon spray drying with ammonium carbonate.

The ammonium salt of PAS was prepared (refer to section 3.3) and the physicochemical properties of the salt was compared to that of the spray-dried composites. Figure 3.23 shows DSC scans of ammonium salt of PAS and the spray-dried sample. DSC scans indicate that the thermal behaviour of the spray-dried sample is different from the ammonium salt of PAS. The shape of the endothermic peaks was different, endothermic peak positions was different and were at ~136°C for starting material and 130°C for spray-dried sample. The onset of the endothermic peak was ~127 °C for ammonium salt of PAS and ~130°C for the spray-dried sample.

It could be concluded from the DSC scans that the thermal behaviour of the spray dried composites was different from that of PAS unprocessed material, ammonium salt and physical mixture of PAS with ammonium carbonate.

Table 3.3- list of molecular weights, structures, pKa values and solubility of PAS and budesonide.

Drug	Mol Wt.	Structure	pKa	Solubility
PAS	153.14	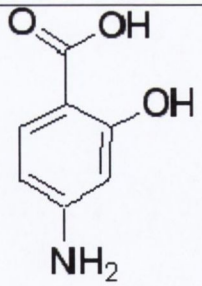	3.25	1 in 500 of water
Budesonide	430.54	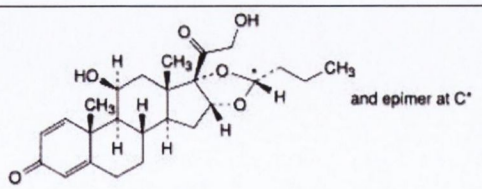	-	practically insoluble in water

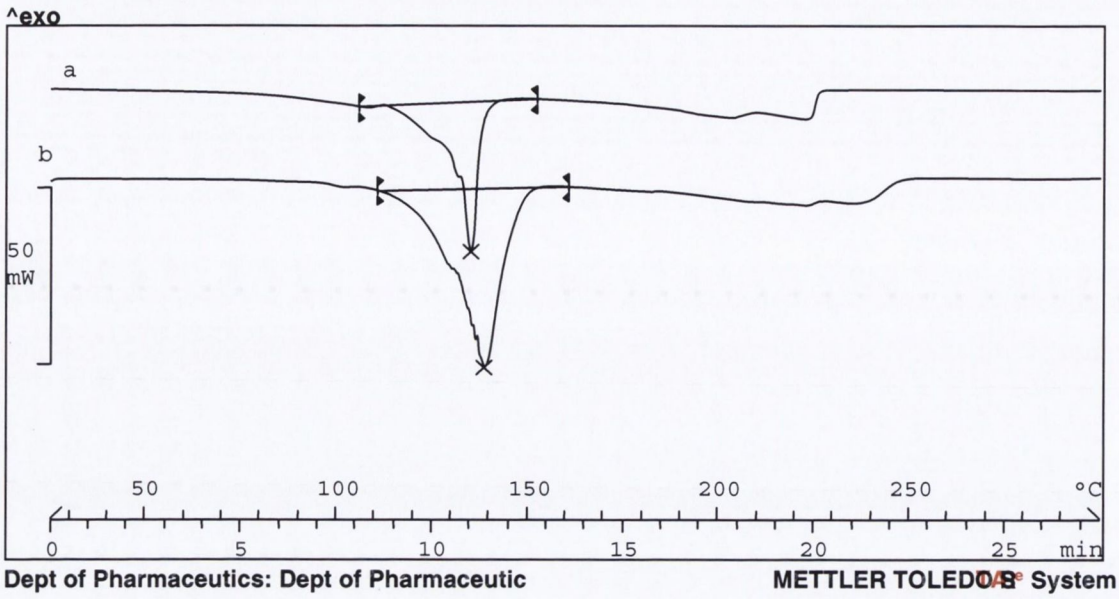

Figure 3.23- DSC scans of (a) PAS/ammonium carbonate 80:20 spray-dried from 90% ethanol (b) ammonium salt of PAS.

TGA scans of PAS starting material, PAS/ammonium carbonate physical mixture and spray-dried PAS/ammonium carbonate are shown in Figure 3.24. TG analysis revealed that the weight loss between 25˚C and 100˚C was approximately 16.3, 7.6 and 0.67% for the PAS/ammonium carbonate physical mixture, spray-dried PAS/ammonium carbonate and PAS starting material, respectively. There was an 11-fold increase in the volatile contents of the spray-dried sample in comparison to the unprocessed PAS, while the weight loss between 25˚C and 100˚C for the spray-dried sample was about half the weight loss shown in TGA scan of the physical mixture of PAS/ammonium carbonate.

The physical mixture contains 20% ammonium carbonate (ammonium carbonate decomposes into ammonia, carbon dioxide and water at temperatures over 59 ºC), therefore, it was expected that a mass loss of 20% would be registered by TGA of the physical mixture, however, the weight loss for the mixture up to 100˚C was 16.3% only. The difference between amount of ammonium carbonate added (20% of the total solid in the mixture) and the calculated mass loss between 25˚C and 100˚C could be attributed to an interaction between PAS and ammonium carbonate, this could be confirmed by the change of colour of PAS and ammonium carbonate upon mixing.

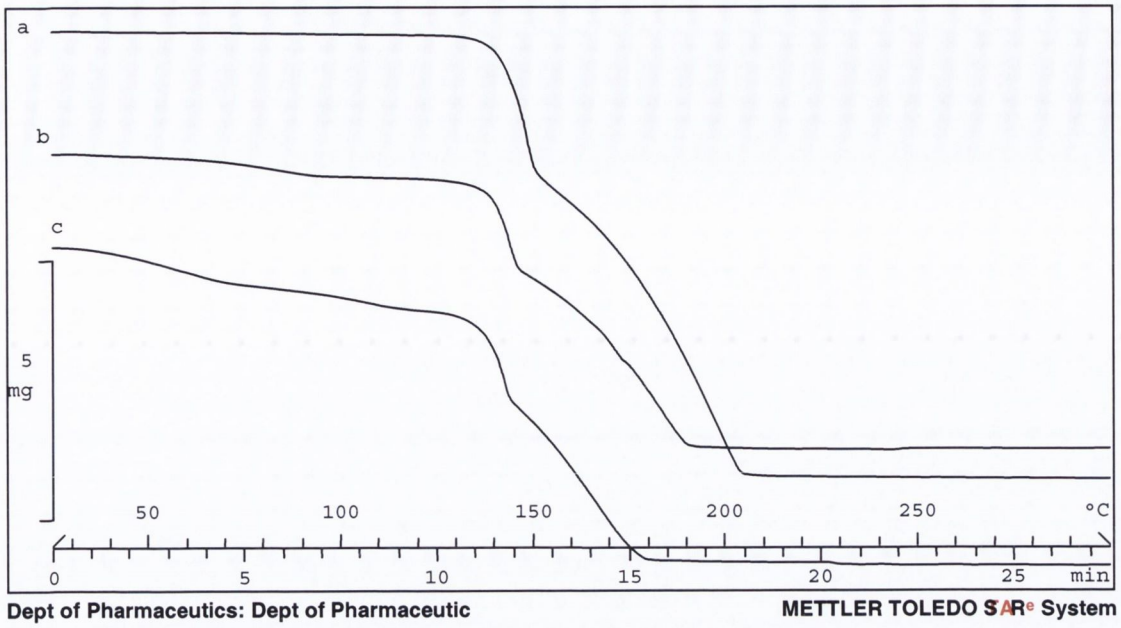

Figure 3.24- TGA scans of (a) PAS starting material (b) spray-dried PAS/ammonium carbonate 80:20 (c) physical mixture PAS/ammonium carbonate 80:20.

3.4.2.2 X-ray powder diffraction studies

X-ray diffractograms of PAS co-spray-dried PAS/ammonium carbonate are shown in Figure 3.25. The peak positions in the scan of PAS unprocessed material were consistent with the XRD scan presented by Rotich et al., (2003a) for PAS unprocessed material. Although the pattern for the spray dried sample is still crystalline and shows some of the features of the pattern of the pure PAS, it is obvious that the XRD pattern of the spray dried sample differs considerably in comparison to that of unprocessed PAS. The arrows in the XRD scans indicate positions where peaks differ between the unprocessed and spray-dried PAS.

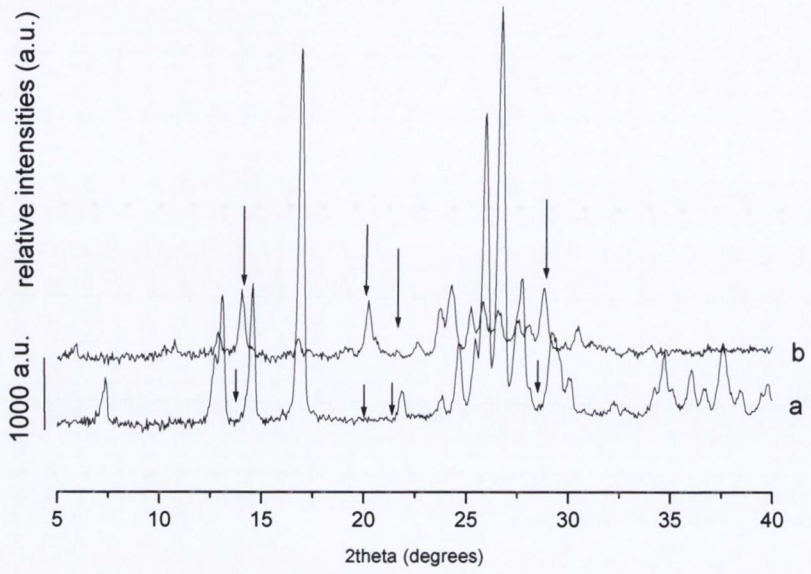

Figure 3.25- XRD scans of (a) PAS raw material (b) PAS/ammonium carbonate spray-dried from 90% v/v ethanol. The arrows in the XRD scans indicate positions where peaks differ between the unprocessed and spray-dried PAS.

Powder X-ray diffraction measurements were made on ammonium salt of PAS and compared to both unprocessed PAS and p-aminosalicylic/ammonium carbonate spray-dried system.

The XRD scan of the spray-dried sample provided further evidence of a difference between the spray-dried sample, the starting material and the prepared salt of PAS, as the spray-dried sample had different peak positions than that of ammonium salt of PAS, the arrows in the graph show where peaks of the spray-dried sample were different from the salt (Figure 3.26).

Figure 3.27 shows the XRD scan of spray-dried PAS/ammonium carbonate and 3-aminophenol (main degradation product of PAS). It is clear that the XRD pattern of spray dried sample was completely different from that of the degradation product, in addition, the additional peaks (in spray-dried sample) cannot be attributed to the breakdown product as seen from XRD of 3-aminophenol.

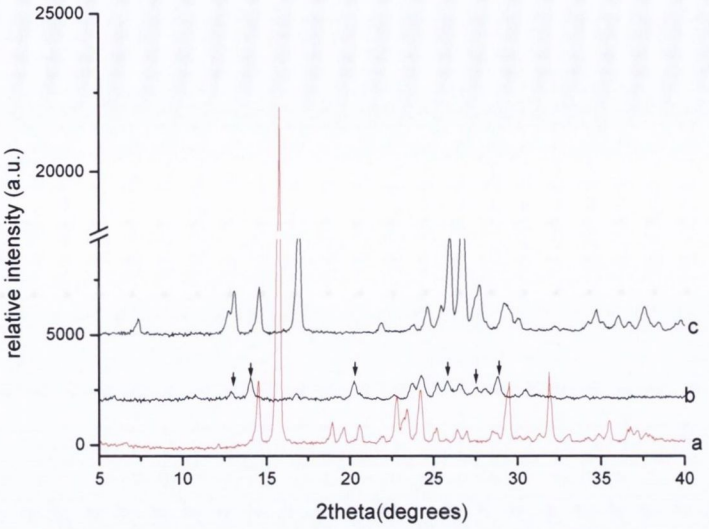

Figure 3.26- XRD scans of (a) ammonium salt of *p*-aminosalicylic (b) PAS/ammonium carbonate spray-dried from 90% ethanol (c) PAS starting material. The arrows in the graph show where peaks of the spray-dried sample were different from the salt.

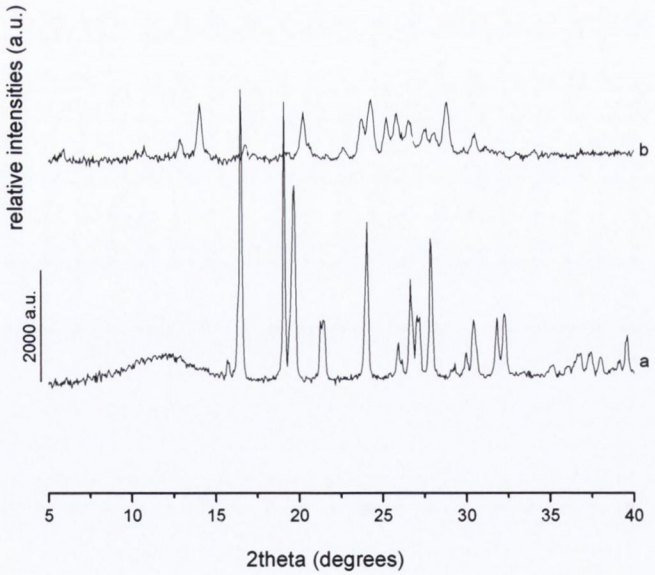

Figure 3.27- XRD scans of (a) 3-aminophenol (b) PAS/ammonium carbonate spray-dried from 90% ethanol.

XRD scan of a physical mix of PAS/ammonium carbonate was run to be compared to the scan of spray dried composites (Figure 3.28). Peaks due to PAS and ammonium carbonate were clearly present and easily detected in XRD diffractogram of the physical mix. It would appear therefore that both PAS and ammonium carbonate could be detected in the scans of the physical mix. On the other hand, XRD scan spray-dried *p*-aminosalicylic/ammonium carbonate show that some peaks in the spray-dried sample

could be attributed to the physical mixture of PAS and ammonium carbonate (black arrows). However, investigation of XRD scans shows that some of the peaks found in XRD scan of the spray-dried sample could not be attributed to physical mixture (red arrows). This may be attributable to formation of a new solid state.

A further point of interest illustrated in Figure 3.29 is that the XRD scans of spray-dried PAS/ammonium carbonate systems showed that XRD pattern of the recovered particles were different from that of unprocessed PAS, which may confirm that spray drying of PAS/ammonium carbonate resulted in a new solid state form regardless of the amount of ammonium carbonate used in spray drying process.

It could be concluded that the recovered particles from spray drying of PAS/ammonium carbonate was different from PAS starting material, ammonium salt of PAS and from 3-aminophenol (the main degradation product of PAS). Furthermore, the recovered new solid state form was obtained regardless the amount of ammonium carbonate used in the spray drying process.

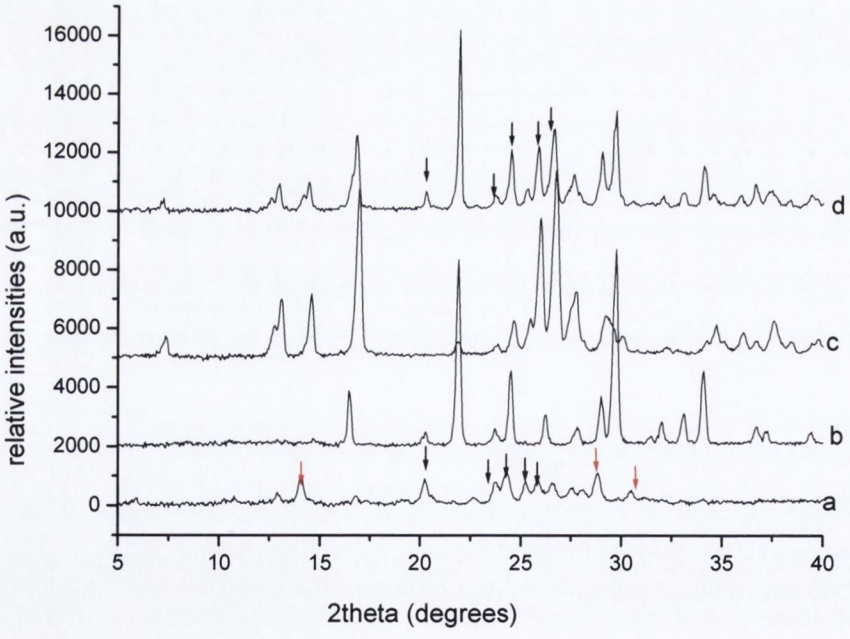

Figure 3.28- XRD scans of (a) PAS/ammonium carbonate spray-dried from 90% ethanol (b) ammonium carbonate (c) PAS raw material (d) physical mixture of PAS/ammonium carbonate. The black arrows show where peaks in spray dried sample are attributable to the physical mixture, the red arrows show where peaks in the spray dried sample could not be attributed to the physical mixture.

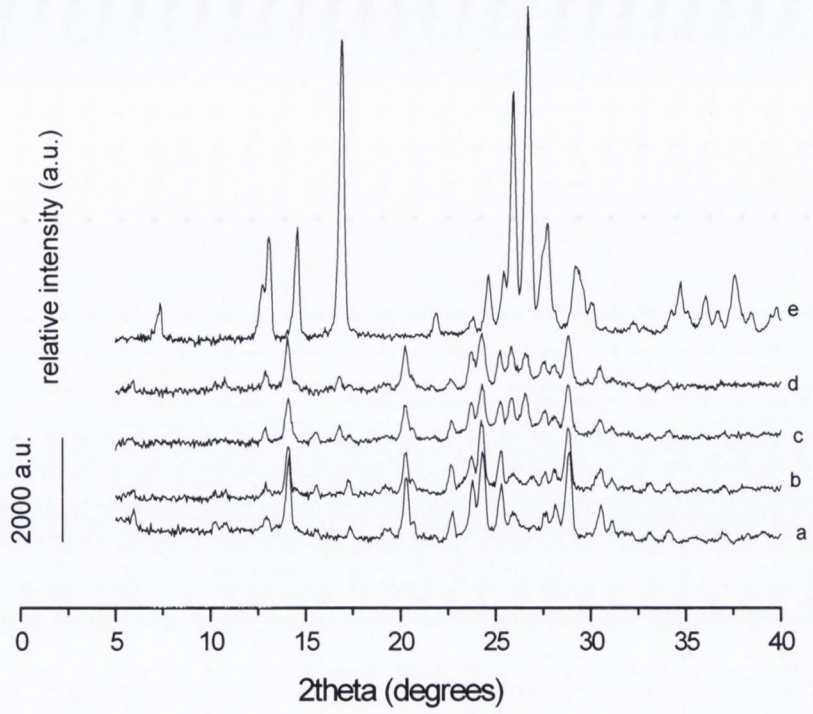

Figure 3.29- XRD scans of PAS/ammonium carbonate (a) 50:50 (b) 62:38 (c) 73:27(d) 80:20 spray-dried from 90% ethanol and (e) PAS raw material.

3.4.2.3 Infrared spectra

In the solid phase, PAS has a band in the infrared spectrum due to their NH_2 vibrations at 3520 cm^{-1}, and another absorption band at 3400 cm^{-1} due to the NH_2 and OH groups. PAS has a strong, characteristic band at 1630 cm^{-1} due to the vibration of C=O (Hassan et al, 1981).

The spectrum of pure PAS presented these characteristic signals at 3495 cm^{-1} for the NH_2 vibration, signals at 3387 cm^{-1} for the NH_2 and OH groups and a band at 1652 cm^{-1} for C=O group. Although FTIR scans of spray-dried PAS/ammonium carbonate showed the same characteristic peaks at the same wavenumbers as PAS starting material (signals at 3495 cm^{-1} and 3387 cm^{-1} for the NH_2 group and a band at 1652 cm^{-1} for C=O group), it was noticed that there were differences in the fingerprint region between the PAS unprocessed and spray-dried composite, which indicates the difference in solid state of the spray-dried sample from the starting material. FTIR spectra of PAS and spray-dried PAS/ammonium carbonate are shown in Figure 3.30. The spectrum of PAS ammonium salt is also presented in the same figure to be compared with the scans of spray-dried

sample. FTIR scans of the salt form of PAS showed that the broad signal at 3005 cm^{-1}, which may be assigned to hydrogen bonded OH group in the spectrum of PAS raw material was not found in the scans of the salt form. In addition, two signals at 3220 cm^{-1} and 1375 cm^{-1} which were not found in the scans of PAS unprocessed material, these signals perhaps attributed to ammonia (Ramis et al., 1996). The spectrum of spray dried sample also showed signals at 3220 cm^{-1} and 1375 cm^{-1} which were found in the scans of the ammonium salt of PAS, these signals may be assigned to ammonia (Ramis et al., 1996). But again investigation of the finger print region showed that the pattern in the fingerprint region of the scans of the spray dried sample and the salt are completely different.

It could be concluded that FTIR provided another evidence of the difference between spray-dried PAS/ammonium carbonate, the unprocessed material and the prepared ammonium salt, and spray drying under these conditions altered PAS chemically.

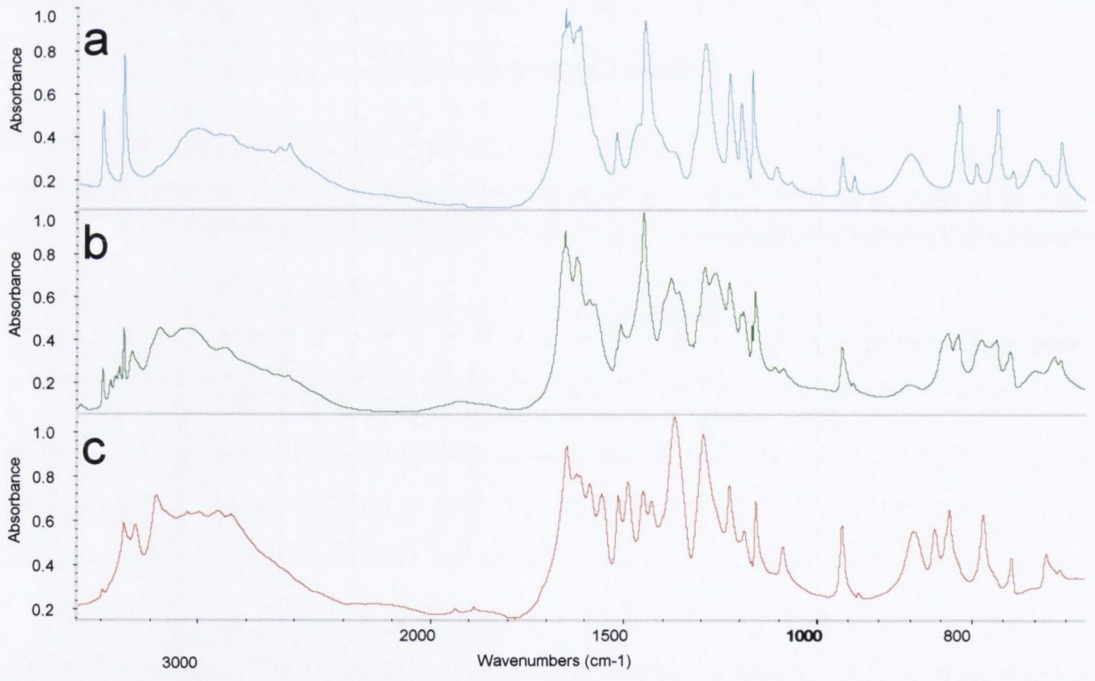

Figure 3.30- FTIR scans of (a) PAS raw material (b) PAS/ammonium carbonate spray-dried from 90% ethanol (c) PAS ammonium salt.

3.4.2.4 ^{1}HNMR spectral assignments

The structures of PAS and PAS ammonium salt are presented in Figure 3.31. The assignments of ^{1}H NMR chemical shifts of the compounds are listed in Table 3.4. The obvious signal assignments were made from ^{1}H NMR spectra according to the chemical shifts and multiplicities.

Figure 3.32 shows ^{1}H NMR spectrum of PAS starting material, it is clear that only peaks corresponding to the hydrogen of the benzene ring were recorded either for PAS unprocessed material or the spray-dried sample (Figures 3.32 and 3.33). It should be noted that the same peaks of H-1, H-2 and H-3 were recorded for both PAS unprocessed material and spray-dried sample, perhaps due to the similarity in electronic environment between unprocessed and spray dried sample. The peak at 11.36 ppm in the PAS scan (which might correspond to the carboxylic hydrogen) was not found in the scan of spray-dried sample. This could be attributed to the low intensity of the peak in the spectrum of the spray-dried sample. In contrast, extra peak was found at 7.0 ppm in the spectrum of PAS ammonium salt (Figure 3.34); this peak may be attributed to ammonium. Nuclear magnetic resonance spectroscopy results give a clear evidence of the similarity in chemical structure of the spray-dried sample and the starting material.

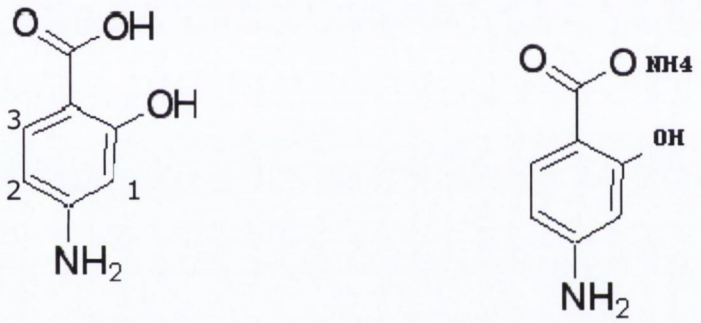

a **b**

Figure 3.31– Structure of (a) *p*- aminosalicylic acid (b) ammonium salt of p-aminosalicylic acid

Table 3.4- ^{1}H NMR data of PAS systems in DMSO

H	PAS	Spray dried composite	Ammonium salt of PAS
1	6.1	6.1	6.1
2	6.2	6.2	6.2
3	7.7	7.7	7.7
Carboxylic hydrogen	11.3	-	-
ammonium	-	-	7.0

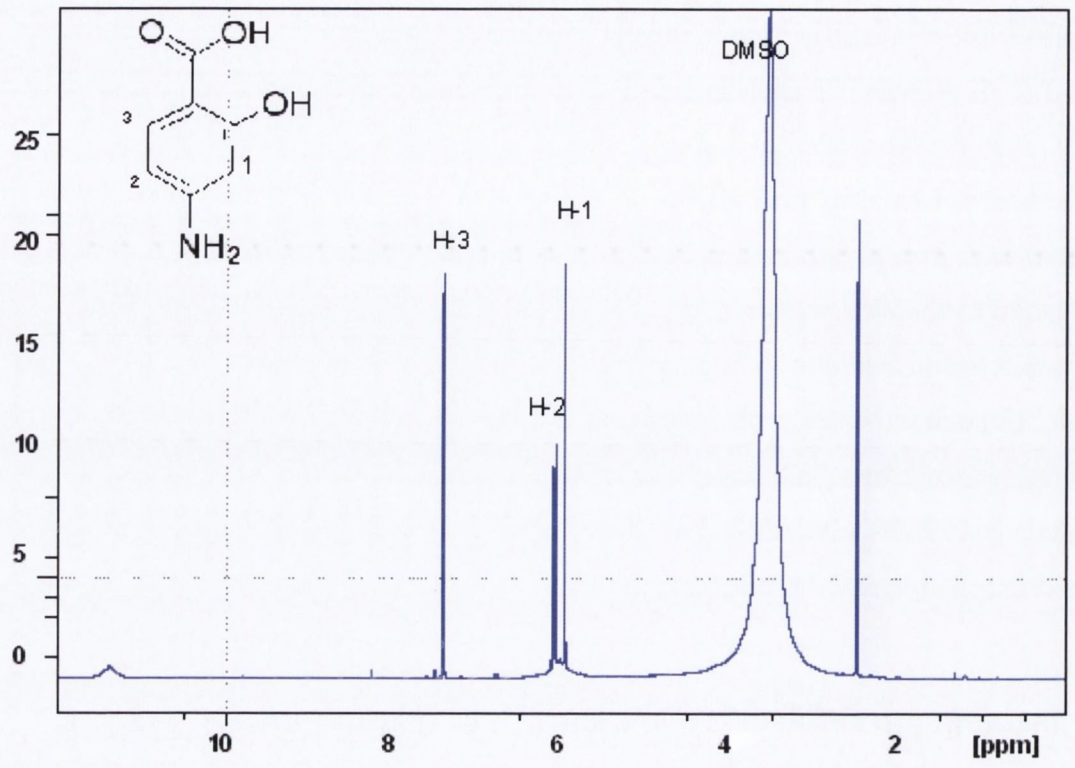

Figure 3.32- The ^{1}H NMR of PAS starting material.

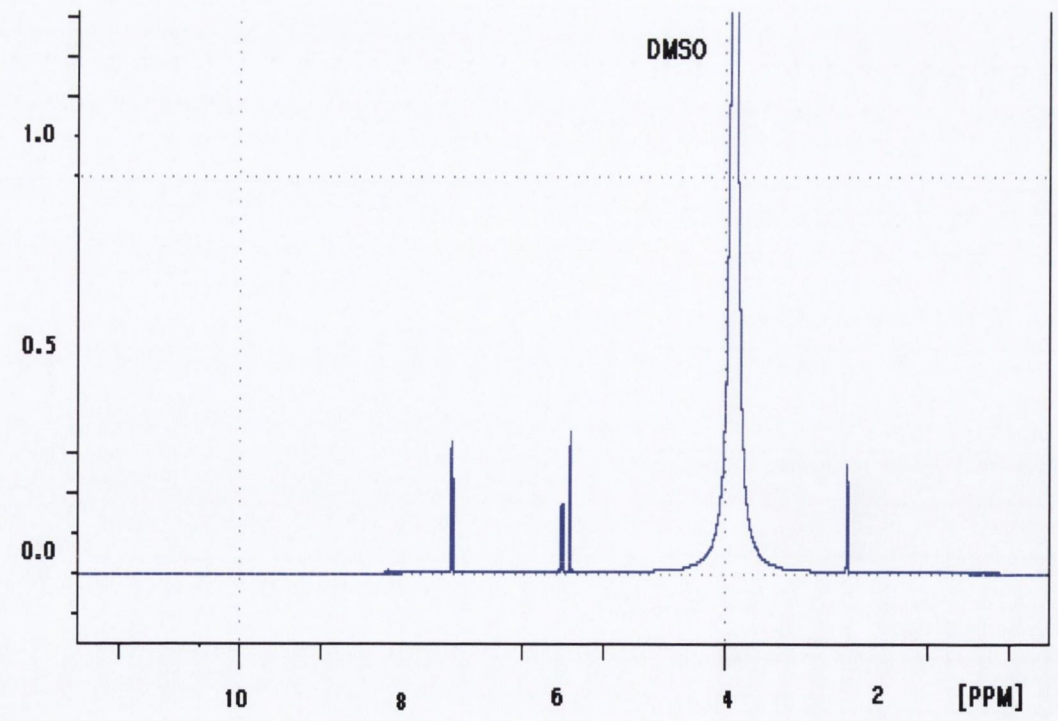

Figure 3.33- The ^{1}H NMR of PAS/ammonium carbonate spray-dried from 90% ethanol.

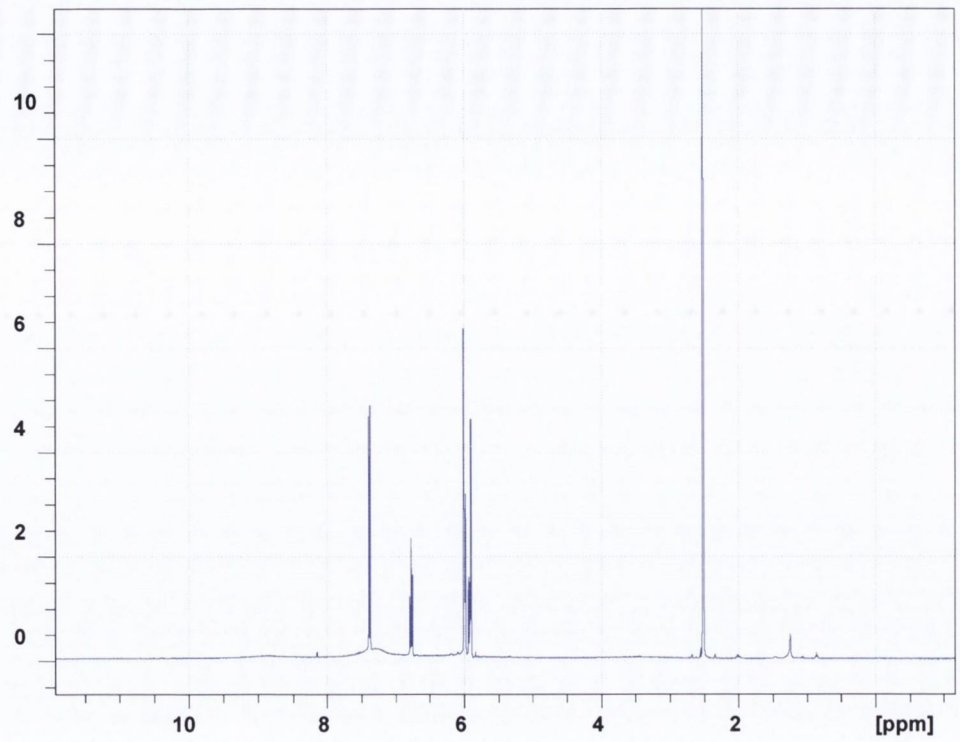

Figure 3.34- The ^{1}H NMR of PAS ammonium salt.

3.4.2.5 High performance liquid chromatography

Figure 3.35 shows HPLC chromatogram obtained for the separation of 3-aminophenol (the main degradation product of PAS) in presence of the drug. The retention time of 3-aminophenol was 1.37 min while the retention time of PAS was 5.32 min.

This HPLC method was used to determine the presence of degradation product in the spray-dried sample (3% w/v solution of PAS/ammonium carbonate spray-dried from 90% v/v ethanol) in comparison with the starting material. The results showed that the impurities measured for both spray dried and unprocessed material were less than 1%. This is in a good agreement with the purity data of the starting material (according to the specification sheet provided by the supplier). The results of HPLC reveal that the spray drying process did not degrade the spray-dried sample and these results were confirmed by XRD scans and NMR results, which showed that the X-ray diffractogram of the spray-dried sample was different from X-ray diffractogram of the main degradation product of PAS.

The stability of PAS under the spray drying conditions was consistent with the thermal degradation profile of PAS presented by Verreck et al. (2006) for PAS. Verreck et al. (2006) investigated the thermal degradation profile of PAS; the authors stored the drug at

various temperatures in a DSC pan under open conditions. This was done up to 10 min. The authors reported that HPLC results showed that PAS is thermally stable for at least 10 min when stored below100–110 °C. Bearing in mind that the drug exposed to inlet temperature of 78 °C for very short period of time, therefore, it is unlikely to decompose during spray drying.

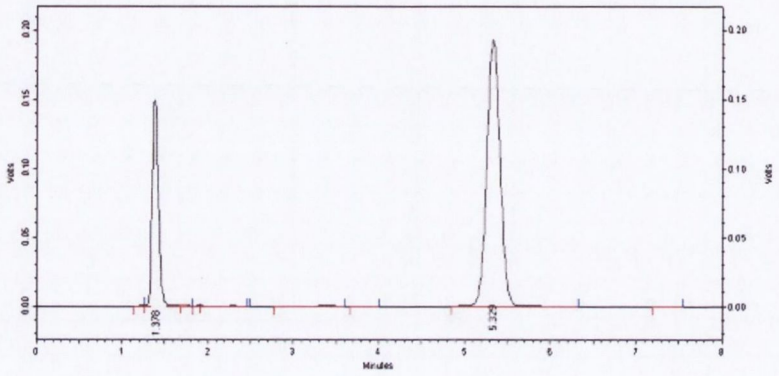

Figure 3.35- HPLC chromatogram obtained for mixture of 3-aminophenol and PAS (50:50)

3.4.3 Stoichiometry of spray dried PAS/ammonium carbonate systems

For the purpose of estimation of the stoichiometry of the spray dried PAS/ammonium carbonate, several analyses were undertaken. For example, ammonia assay for determination of ammonia contents, determination of water contents by Karl Fischer titration and the results from these analyses were interpreted in the light of TGA results. Elemental analysis was also undertaken to determine carbon, nitrogen and hydrogen contents of the spray dried samples.

Elemental analysis (CHN) was carried out for PAS, ammonium salt of PAS and different spray dried PAS/ammonium carbonate systems. The results of elemental analysis are presented in Table 3.5. CHN analysis showed that the chemical composition of the spray-dried sample differed from that of PAS starting material and of the ammonium salt of PAS. Elemental analysis also showed that the carbon content of spray-dried sample was lower than carbon content of the starting material. However, this is higher than carbon content of ammonium salt of PAS, while the nitrogen content of the spray-dried sample was higher than nitrogen content of the starting material but lower than ammonium salt of PAS, which may suggest that the spray-dried sample is not the 1:1 ammonium salt.

Estimation of the possible stoichiometry of the recovered particles based on elemental analysis showed that the stoichiometry of the spray dried samples may be p-aminosalicylic acid: ammonia: water 2:1:0.5.

An ammonia assay was undertaken for p-aminosalicylic acid raw material and the spray dried p-aminosalicylic acid/ammonium carbonate. In case of the unprocessed material, the amount of ammonia was below the limit of detection of the assay (1%). On the other hand, the amount of ammonia determined in the spray dried samples was approximately 5.18±0.92%, which confirmed the stoichiometric ratio of the particles. Water contents were also determined by Karl Fischer titration. The amount of water detected was approximately 2.08±0.14%. This was consistent with the amount of water in the proposed stoichiometric ratio of the recovered particles when determined on a molecular weight basis. Another confirmation of the stoichiometry of spray dried samples is TG analysis; TG analysis revealed that the weight loss between 25°C and 100°C was approximately 7.6% for the spray-dried composite. The loss of one ammonia molecule and half water molecule corresponds to a loss of ~7.8% by weight of p-aminosalicylic acid: ammonia: water 2:1:0.5 when determined on a molecular weight basis. Therefore, the weight loss registered in spray dried composites is consistent with the loss of one molecule of ammonia and half molecule of water.

Table 3.5- Elemental analysis of different PAS systems. Key: PAS = p-aminosalicylic acid, C = Carbon, N = nitrogen, H = hydrogen, Calculated= results of calculation and Found= results of analysis.

Sample		Analysis		
		C	H	N
PAS	Calculated	54.90	4.61	9.15
Spray dried PAS/ammonium carbonate 80:20	Found	50.75±0.17	5.30±0.02	12.46±0.19
Spray dried PAS/ammonium carbonate 73:27	Found	50.61±0.02	5.31±0.02	12.71±0.16
Spray dried PAS/ammonium carbonate 62:38	Found	50.73±0.20	5.32±0.07	12.58±0.35
Acid: ammonia: water 2:1:0.5	Calculated	50.60	5.49	12.60

3.4.4 Conclusion

It could be concluded that spray drying of p-aminosalicylic acid with ammonium carbonate resulted in alteration of the solid state form of PAS, as confirmed by several analyses. This may be attributed to the acidic nature of PAS. In addition, the stoichiometry of the spray dried composites could be 2:1:0.5 p-aminosalicylic acid: ammonia: water. This was estimated from elemental analysis of the recovered particles from spray drying process and was confirmed by ammonia assay, Karl Fisher titration and TGA. These results were in contrast to the results reported by Nolan et al., (2009), who used ammonium carbonate to produce excipient free particles of budesonide by spray drying and proved that ammonium carbonate was totally evaporated upon spray drying. The removal of ammonium carbonate reported by Nolan et al., (2009) may be attributed to the fact that budesonide has no potential to react with ammonium carbonate.

3.5 PARTICLE CHARACTERISATION OF SPRAY-DRIED PAS

PAS spray-dried from 70% ethanol, 3% and 4% PAS/ammonium carbonate 80:20 spray-dried from 90% ethanol as well as micronised PAS were selected for further characterisation in terms of laser diffraction particle sizing, surface area, bulk and tapped density. These particular spray-drying conditions were chosen to cover wide range of morphological characteristics of powder produced by spray drying of PAS under different spray drying conditions. A mixture of rod shape crystals and porous particles (Figure 3.2a), which were produced upon spray drying of PAS from 70% ethanol, compared to the aggregates of microcrystalline particles (Figure 3.15d) produced from spray drying of 4% p-aminosalicylic/ammonium carbonate 80:20 from 90% ethanol, and the mixture of porous particles and agglomerates of microcrystalline particles (Figure 3.17a) produced from spray drying of 3% p-aminosalicylic/ammonium carbonate 80:20 from 90% ethanol. All these spray-dried systems were also compared to micronised PAS. It should be noted that particle size of PAS starting material was very high in comparison to spray-dried systems so it was micronised to be compared with spray-dried systems.

Particle size distribution was determined using laser diffraction particle sizing at the standard operational settings of 2-bar air pressure and 60% vibration feed rate. Both micronised and spray-dried PAS systems with or without ammonium carbonate showed a mono-modal, highly reproducible size distribution (Figure 3.36). The narrowest size distribution was found for the 3% and 4% PAS /ammonium carbonate spray-dried systems, with a span of 1.064 compared to 1.13 for the micronised p-aminosalicylic and 1.67 for

PAS spray-dried without ammonium carbonate. Micronised PAS had an average median particle size of volume distribution d(0.5) of 2.9 ± 0.026 μm, which was slightly larger than the spray-dried PAS without ammonium carbonate, which had an average d(0.5) of 2.41 ± 0.071 μm. That was significantly smaller than the particle size of spray dried sample with ammonium carbonate. The median particle size of volume distribution (d (0.5)) for the 3% PAS /ammonium carbonate spray-dried system was 3.38 ± 0.078 μm, while for the 4% PAS/ammonium carbonate spray-dried system it was 3.67 ± 0.004 μm.

It should be noted that Labris and Dolovich, (2003) reported that particles ranging from 1-5 μm are deposited in the small airways and alveoli. Therefore, PAS systems have particles within the accepted particle size range for inhalation therapy.

The surface areas determined for the different PAS samples are given in Table 3.6. A surface area of 2.833 ± 0.218 m^2/g was measured for micronised PAS. The presence of nanoporous microparticles in the spray-dried PAS (Figure 3.2a) increased the surface area. On average, a 2.2-fold (6.192 ± 0.263 m^2/g) increase in the surface area was measured for powder recovered from spray drying of PAS without ammonium carbonate. The increase in surface area may be used as a confirmation of decrease in crystal size which was estimated from XRD scans of spray dried samples. This is based on the common principle that as the size of the crystal for same quantity of the sample decreases, the total external surface area increases. It should be noted that a strong correlation was observed between the surface area and crystal size has been given by Song et al. (2004).

A surface area of 3.427 ± 0.323m^2/g was measured for 3% PAS /ammonium carbonate 80:20 spray-dried system, higher than that measured for the micronised PAS. The higher surface area of PAS /ammonium carbonate 80:20 spray-dried system in comparison to the micronised PAS can be explained by the morphological characteristics of the spay dried particles which include porous particles and spherical aggregates of microcrystalline particles structures (Figure 3.17a). The lower surface area of spray-dried samples with ammonium carbonate in comparison to spray-dried sample without ammonium carbonate could be attributed to the difference in particle size.

Bosquillon (2004) suggested that lower powder density is associated with better aerosolisation properties. The bulk ($b\rho$) and tap ($t\rho$) densities of PAS systems also showed variation in accordance with the differences seen in the surface area measurements. Bulk ($b\rho$) and tap ($t\rho$) densities of 0.23± 0.024 g/cm^3 and 0.31 ± 0.022g/cm^3 were measured for micronised PAS. For PAS spray-dried without ammonium carbonate, the *bp* was 0.104± 0.002 g/cm^3 and the *tp* was 0.17 ± 0.009 g/cm^3, the latter representing a 2.3-fold decrease

in bulk density and 1.8-fold decrease in tap density in comparison to the micronised material. The decrease in bulk and tap densities of spray-dried PAS could be explained by the presence of porous particles in the powder recovered from spray drying of PAS. No statistically significant difference ($p > 0.05$) in the bulk and tap densities of spray-dried 3% compared to 4% PAS /ammonium carbonate 80:20 systems was measured. Carr's compressibility index values were calculated for different spray-dried PAS systems. Carr's Index values may be used as an indication of powder flow properties with a Carr's Index value greater than 40% being characteristic of powders of extremely poor flowability, a value between 32 and 38% is characteristic of very poor flowability while a value between 25 and 32% is characteristic of poor flowability. The calculated Carr's index for spray-dried without ammonium carbonate was 38.4% indicative of very poor flowing powders, values for spray-dried 3 or 4% PAS /ammonium carbonate 80:20 systems were 26.8% and 28.4% indicative of improvement of powder flowability in comparison with spray-dried system without ammonium carbonate.

Table 3.6– Particle sizing (n = 3; mean ± standard deviation), surface area (n = 3; mean ± standard deviation) and bulk and tapped densities (n = 3; mean ± standard deviation) for different PAS systems

Sample No.	**System**	**Surface area** (m^2/g)	**Particle size** (μm)			**Bulk density** (g/cm^3)	**Tapped density** (g/cm^3)
			d(0.1)	d(0.5)	d(0.9)		
	Micronised PAS	2.83 ± 0.21	1.66±0.022	2.9±0.026	4.97± 0.131	0.230±0.024	0.313±0.022
R6	SD PAS	6.19 ± 0.26	1.14±0.004	2.41±0.071	5.17± 0.274	0.104±0.002	0.168±0.009
R10	3% PAS /AC 80:20 spray-dried system	3.42 ± 0.32	1.93±0.054	3.38±0.078	5.42± 0.137	0.122±0.003	0.167±0.008
R13	4% PAS /AC spray-dried system	3.29± 0.65	2.17±0.046	3.67±0.004	6.08± 0.105	0.115±0.003	0.161±0.008

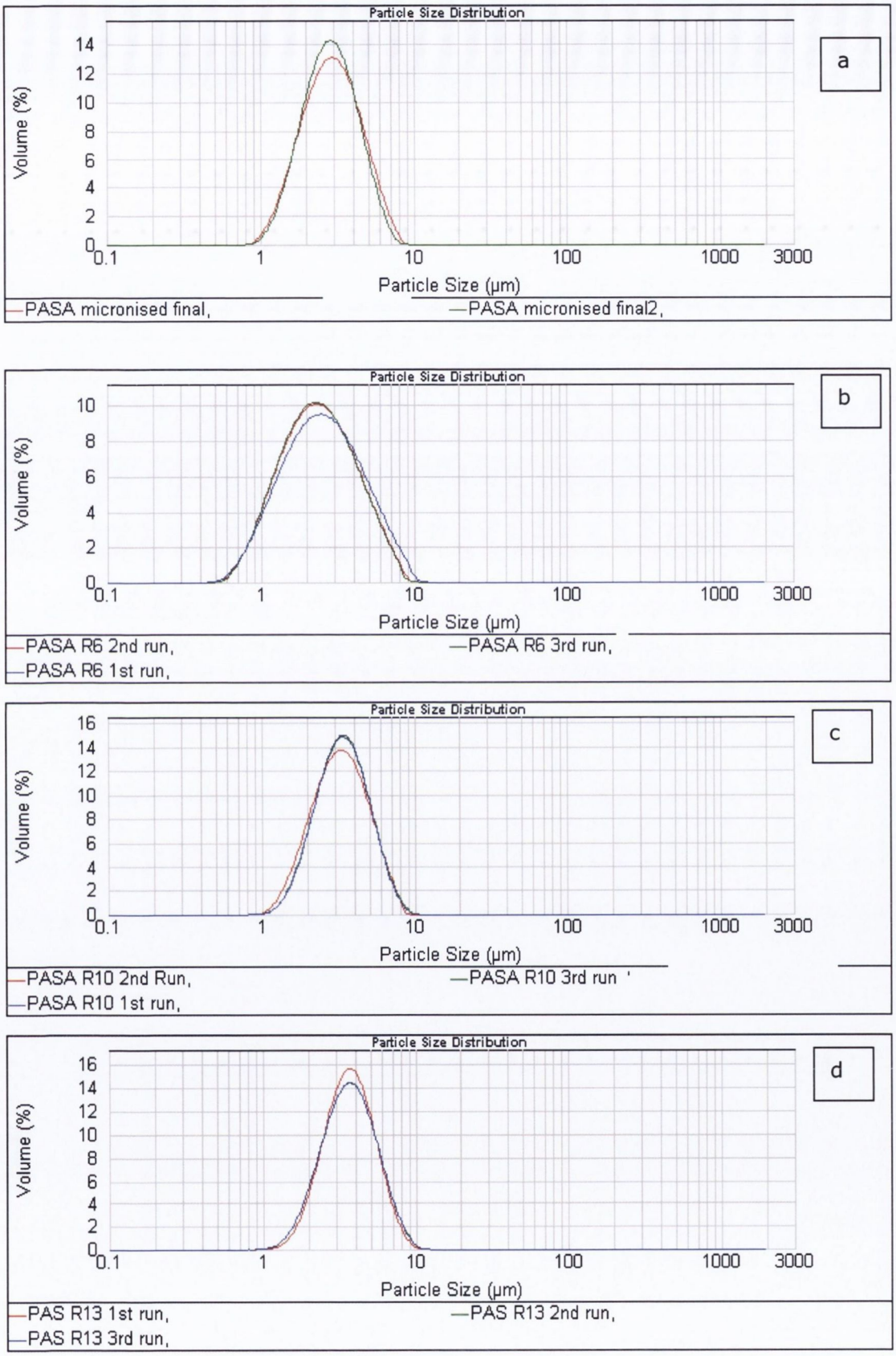

Figure 3.36 Particle size distributions of (a) micronised PAS (b) spray-dried PAS without ammonium carbonate (c) 3% and (d) 4% PAS /ammonium carbonate spray-dried system (different colour traces represent different runs).

3.6 PAS/AMMONIUM BICARBONATE SYSTEMS SPRAY-DRIED FROM ETHANOL

Straub et al., (2005) produced porous particles of paclitaxel by spray drying a solution (water/ethanol) containing the drug, a water-soluble excipient such as a sugar (mannitol) and a pore-forming agent, ammonium bicarbonate (volatile salt). The water-soluble excipient facilitates wetting of the drug particles during reconstitution, provides proper osmolality to the dosage form, and improves the storage stability of the dry powder. Similarly, the pore-forming agent is volatilised and removed during processing, however a porous particle comprised of drug and excipient is produced.

A 4% solution of PAS/ammonium bicarbonate was prepared in 90% (v/v) ethanol and spray-dried, using air as a drying gas. The concentration of ammonium bicarbonate was 20% (weight of solids). For this system, the inlet temperature was set at 78 °C. SEM micrographs (Figure 3.37) of the spray-dried material showed that the sample produced from spray drying of solution of PAS/ammonium bicarbonate 80:20 spray-dried from 90% v/v ethanol consisted of spherical particles and aggregates of microcrystalline particles.

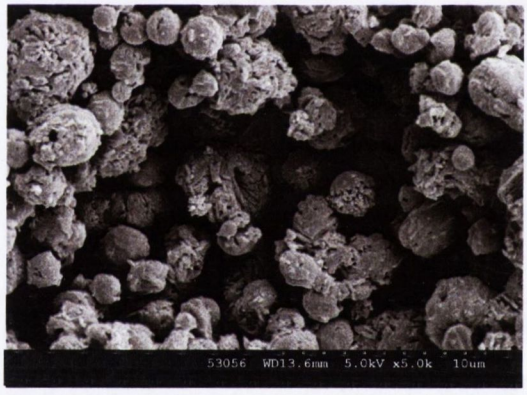

Figure 3.37- SEM micrograph of PAS/ammonium bicarbonate 80: 20 system spray-dried from 90% v/v ethanol.

X-ray diffractograms gave evidence of a difference in solid-state form between PAS/ammonium bicarbonate 80:20 spray-dried from 90% v/v ethanol and the starting material (Figure 3.38) the arrows in the XRD scans indicate positions where peaks differ between the spray dried and the unprocessed material.

Figure 3.38 also shows XRD scans of spray-dried PAS/ammonium carbonate. It is obvious that the extra peaks found in diffractograms of the spray dried samples in comparison to that of starting material (black arrows) were identical in terms of peak positions; the similarities between the scans indicate that a similar solid state is produced by spray drying of PAS/ammonium carbonate or PAS /ammonium bicarbonate.

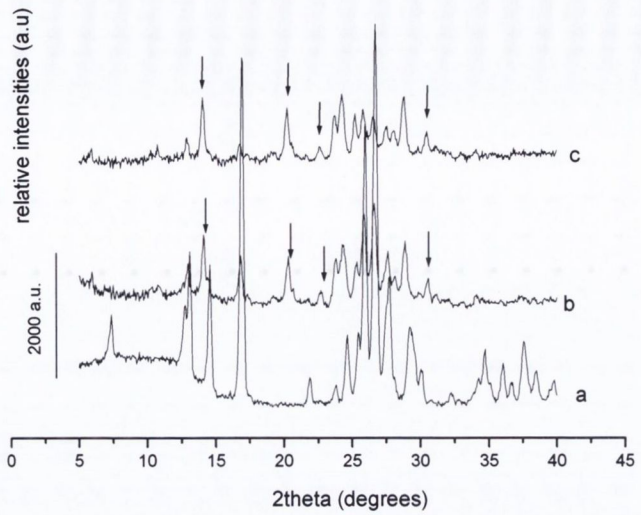

Figure 3.38 XRD scans of (a) PAS starting material (b) PAS/ammonium bicarbonate spray-dried from 90% v/v ethanol (c) PAS/ammonium carbonate spray-dried from 90% v/v ethanol. The arrows in the XRD scans indicate positions where peaks differ between the spray dried samples and the starting material.

Figure 3.39 shows DSC scans of PAS starting material and PAS/ammonium bicarbonate 80:20 spray-dried from 90% v/v ethanol. Examination of the thermograms showed that the peak position of spray-dried sample shifted compared to the starting material, the peak became irregular in shape and asymmetric, and there were differences in the onset temperature, The onset temperature was ~140°C for starting material (this is in agreement with the findings reported by Rotich et al., (2001) for unprocessed PAS) and 133°C for spray-dried sample, it is clear that the solid state form of the recovered particles was different from PAS starting material. DSC TGA scans of this system are shown in Figure 3.40. A broad endotherm at 114 °C with the onset at ~99 °C was observed. The broad endothermic peak was accompanied with weight loss of ~7% as seen in TGA scan Figure 3.40.

DSC indicated that the thermal behaviour of the spray dried sample was different from that of unprocessed material.

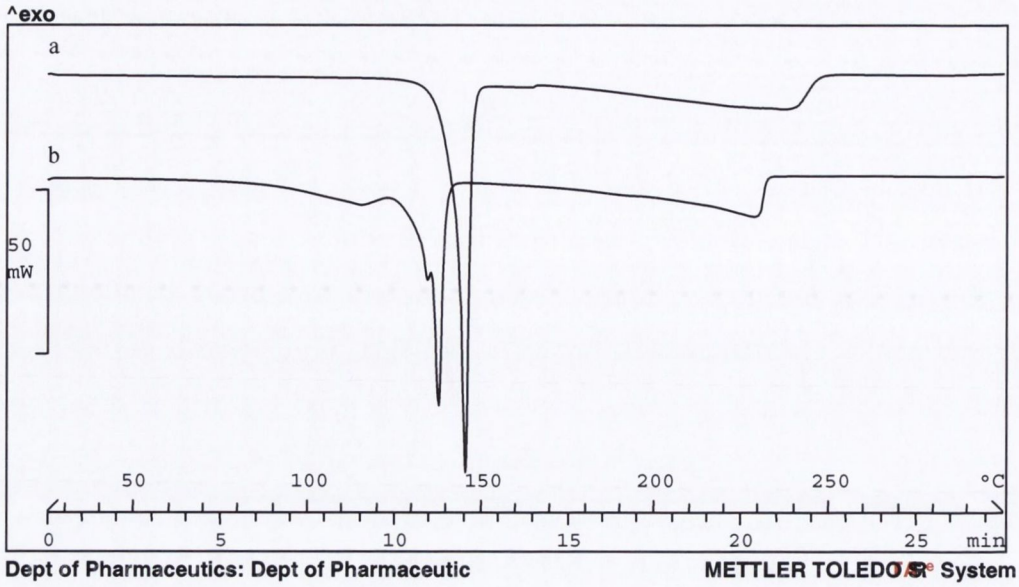

Figure 3.39- DSC scans of (a) PAS starting material (b) PAS/ammonium bicarbonate 80:20 spray-dried from 90% v/v ethanol.

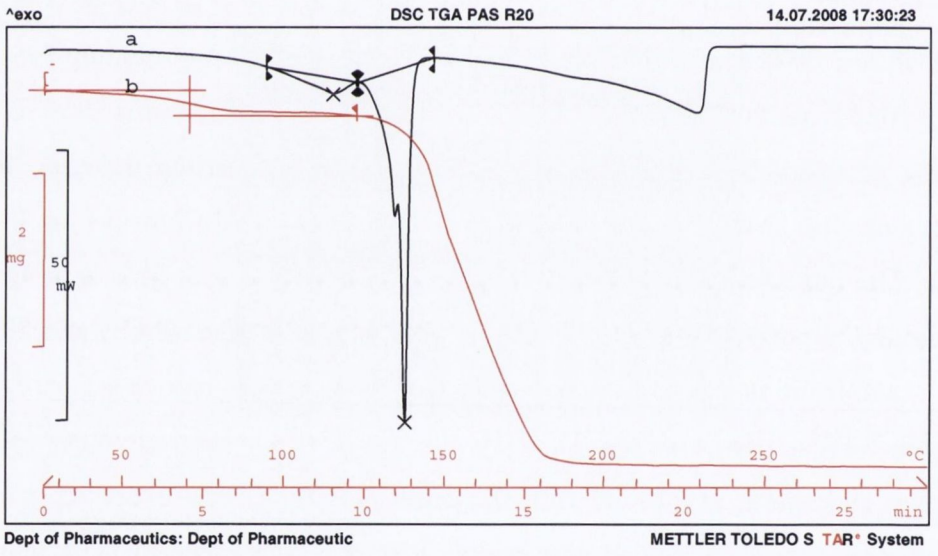

Figure 3.40- (a) DSC (b) TGA scans of PAS/ammonium bicarbonate 80:20 spray-dried from 90% v/v ethanol.

Elemental analysis of the spray dried PAS/ammonium bicarbonate is shown in Table 3.7. Calculation of the stoichiometry of the recovered particles showed that the stoichiometry of the spray dried sample could be PAS: ammonia: water 2:1:0.5. This was consistent with the results obtained by estimation of stoichiometry of spray dried PAS/ammonium carbonate. In addition, this stoichiometry was confirmed by TG analysis; TG analysis revealed that the weight loss between 25°C and 100°C was approximately 7% for the spray-dried sample. The loss of one ammonia molecule and half water molecule

corresponds to a loss of ~7% by weight of p-aminosalicylic acid: ammonia: water 2:1:0.5 when determined on a molecular weight basis. Therefore, the weight loss registered in spray dried sample is consistent with the loss of one molecule of ammonia and half molecule of water.

Table 3.7- Elemental analysis of different PAS systems. Key: PAS = p-aminosalicylic acid, C = Carbon, N = nitrogen, H = hydrogen, Calculated= results of calculation and Found= results of analysis.

Sample		Analysis		
		C	H	N
PAS	Calculated	54.90	4.61	9.15
ammonium salt of PAS	Calculated	49.41	5.92	16.46
	Found	49.80±0.17	5.79±0.07	15.99±0.49
Spray dried PAS/ammonium carbonate	Found	50.75±0.17	5.30±0.02	12.46±0.19
Spray dried PAS/ammonium bicarbonate	Found	50.74±0.15	5.12±0.24	12.60±0.007
Acid: ammonia: water 2:1:0.5	Calculated	50.60	5.45	12.64

3.7 PAS/AMMONIUM CARBONATE SYSTEMS SPRAY-DRIED FROM METHANOL

As shown in section 3.4, spray drying of PAS ammonium carbonate resulted in alteration of PAS and the stoichiometry of the resulted particles was PAS: ammonia: water 2:1:0.5. In a continuation of these results, different solutions of PAS/ammonium carbonate were prepared and spray-dried from methanol as outlined in Appendix I Table 1. It should be noted that the inlet temperature of spray drying process was 78˚C, this was the inlet temperature used for spray drying of PAS/ammonium carbonate from ethanolic solutions. After spray drying the resultant powders were viewed by SEM. SEM micrographs of spray-dried samples showed that production of spherical microparticles was dependant on methanol/water ratio as the best results in terms of morphological characteristics were obtained using either 80% or 90% methanol (Figure 3.41).

Figure 3.42 shows the DSC scans of the PAS/ammonium carbonate 80:20 spray-dried from 80% v/v methanol and PAS raw material. DSC results indicated that the thermal behaviour of PAS/ammonium carbonate spray-dried from methanol differed from that of the starting material: peak position shifted, the peak broadened and became irregular in shape and asymmetric, and there were differences in the onset temperature. The onset temperature was ~140˚C for starting material and ~130˚C for spray-dried sample. TGA registered

weight loss of ~7% over the temperature range of 25 to 100 °C for the spray dried sample, which may attributed to loss of ammonia and water.

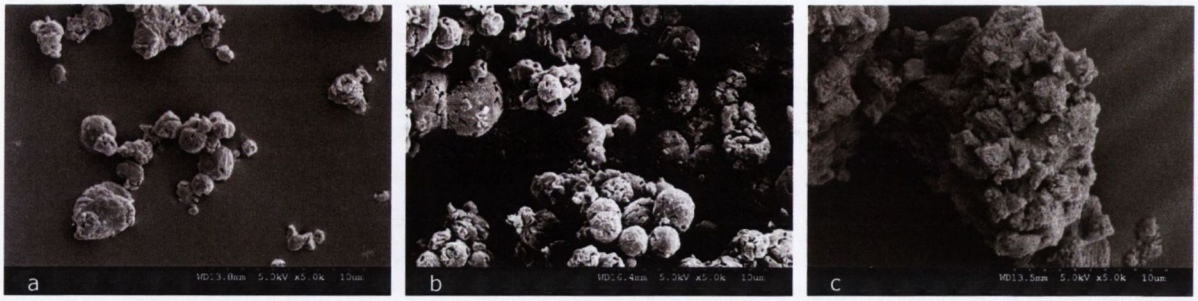

Figure 3.41- SEM micrographs of PAS/ammonium carbonate 80: 20 system spray-dried from (a) 90% v/v methanol (b) spray-dried from 80% v/v methanol (c) spray-dried from 70% v/v methanol.

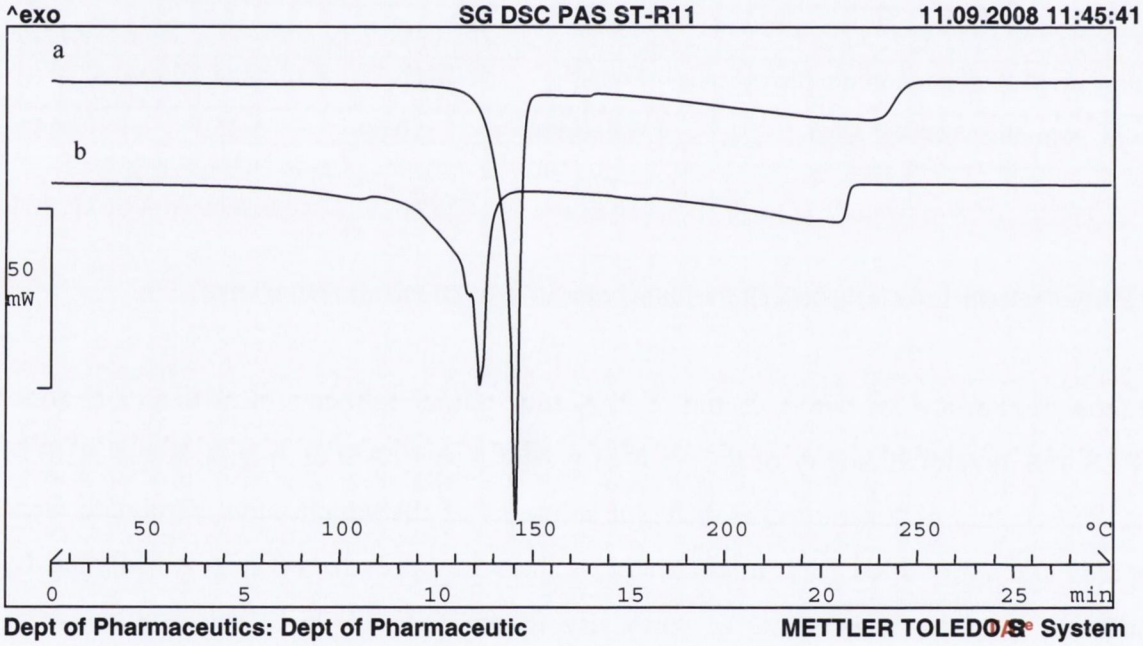

Figure 3.42- (a) DSC scan of PAS starting material (b) DSC scan of PAS/ammonium carbonate 80:20 spray-dried from 80% v/v methanol.

DSC scans of the recovered particles from spray drying of PAS/ammonium carbonate from either ethanol or methanol are shown in Figure 3.43. It is clear that the thermal behaviour of spray-dried samples was different from the starting material, which indicates that spray drying of PAS/ammonium carbonate changed the solid state of the starting material regardless of the solvent used.

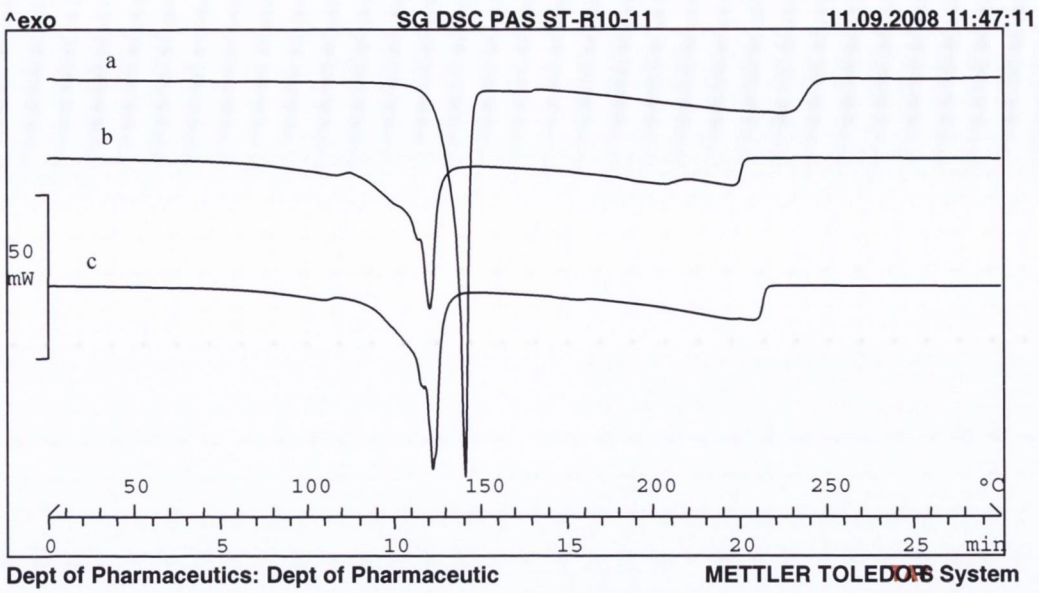

Figure 3.43- DSC scans of (a) PAS starting material and PAS/ammonium carbonate 80:20 spray-dried from (b) 90% v/v ethanol (R10) (c) 80% v/v methanol (R11)

XRD scan showed the presence of crystallinity in the spray-dried system, evident from the presence of peaks. XRD scan of PAS/ammonium carbonate spray dried from 80% v/v methanol was further evidence of the solid-state form change of the spray-dried sample compared to the starting material. The arrows in the XRD scans indicate positions where peaks differ between PAS staring material and the spray-dried sample (Figure 3.44).

Figure 3.45 shows X-ray diffractograms of PAS/ammonium carbonate spray-dried either from 90% ethanol or 80% methanol. The similarity of XRD pattern suggest that spray drying of PAS/ammonium carbonate leads to changing the solid state of p- aminosalicylic acid regardless of the solvent used.

Elemental analysis of the spray dried PAS/ammonium carbonate from methanolic solution is shown in Table 3.8. Calculation of the stoichiometry of the recovered particles showed that the stoichiometry of the spray dried sample could be PAS: ammonia: water 2:1:0.5. This was consistent with the results obtained by estimation of stoichiometry of spray dried PAS/ammonium carbonate. Moreover, this stoichiometry was confirmed by TG analysis; TG analysis revealed that the weight loss between 25˚C and 100˚C was approximately 7% for the spray-dried sample. The loss of one ammonia molecule and half water molecule corresponds to a loss of ~7% by weight of p-aminosalicylic acid: ammonia: water 2:1:0.5 when determined on a molecular weight basis. Therefore, the weight loss registered in spray dried sample is consistent with the loss of one molecule of ammonia and half molecule of water.

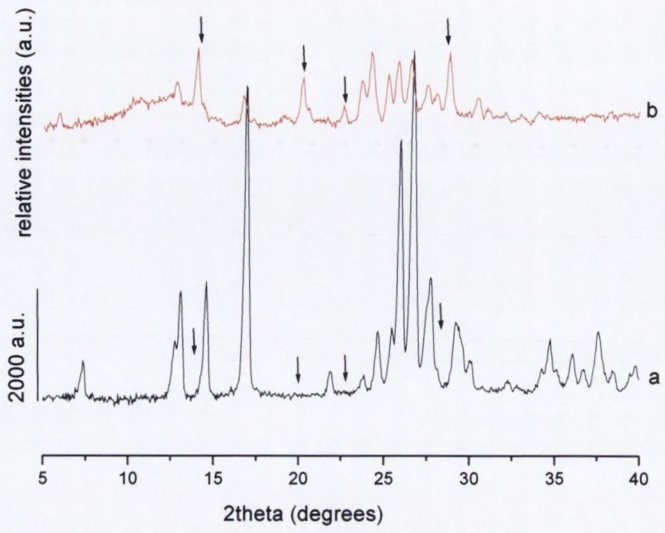

Figure 3.44 XRD scans of (a) PAS starting material (b) PAS/ammonium carbonate 80:20 spray-dried from 80% v/v methanol.

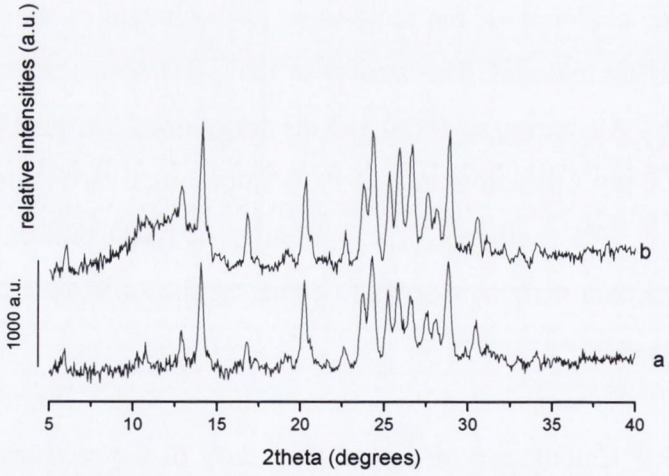

Figure 3.45 XRD scans of PAS/ammonium carbonate 80:20 (a) spray-dried from 90% v/v ethanol (b) spray-dried from 80% v/v methanol.

Table 3.8- Elemental analysis of different PAS systems. Key: PAS = p-aminosalicylic acid, C = Carbon, N = nitrogen, H = hydrogen, Calculated= results of calculation and Found= results of analysis.

Sample		Analysis		
		C	H	N
PAS	Calculated	54.90	4.61	9.15
ammonium salt of PAS	Calculated	49.41	5.92	16.46
	Found	49.80±0.17	5.79±0.07	15.99±0.49
Spray dried PAS/ammonium carbonate from ethanolic solution	Found	50.75±0.17	5.30±0.02	12.46±0.19
Spray dried PAS/ammonium carbonate from methanolic solution	Found	50.44±0.21	5.12±0.28	12.78±0.06
Acid: ammonia: water 2:1:0.5	Calculated	50.60	5.45	12.64

3.8 Spray dried PAS at elevated inlet temperature

Addition of either ammonium carbonate or ammonium bicarbonate to PAS solution may result in formation of ammonium salt of PAS as shown in the following equations:

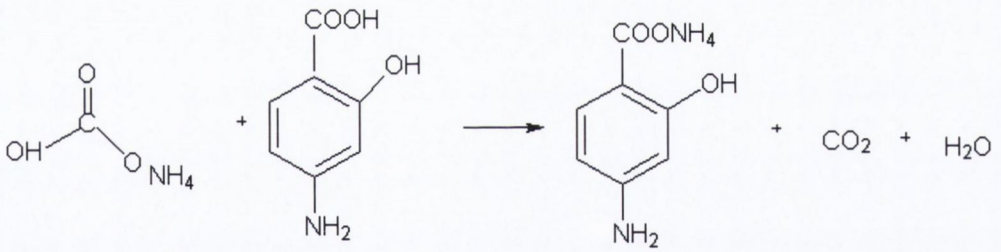

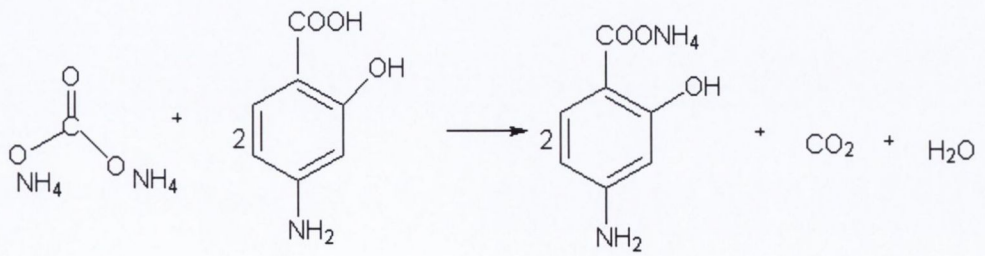

In addition, ammonium salts undergo thermal decomposition with the formation of gaseous ammonia (Frenkel et al., 1995). Furthermore, Chuck and Zacher (2000) have shown that an aqueous solution of ammonium nicotinate can be converted to nicotinic acid by spray drying. In that process, ammonium nicotinate decomposes and ammonia, together with the solvent, escape in the exhaust gas of the spray dryer. However, this conversion occurs at a reasonably high temperature (170-250˚C). The inlet temperature used for spray

drying of either PAS/ammonium carbonate or PAS/ammonium bicarbonate was relatively lower; therefore, the pure PAS was not recovered from spray drying process. This might explain the reason behind incomplete removal of ammonia upon spray drying of PAS with ammonium carbonate or ammonium bicarbonate.

Based on this discussion it was decided to spray dry PAS/ammonium carbonate and PAS/ammonium bicarbonate at higher inlet temperature, the objective of this work was to study the possibility of production of pure PAS upon spray drying of PAS with the process enhancers, this will offer better understanding of the reasons behind the change of solid state of spray-dried PAS/ammonium carbonate upon spray drying.

3% PAS/ammonium carbonate 50:50 was sprayed from 90% ethanol, the inlet temperature for this process was set at 130°C. Closed cycle was used for this sample; this layout was chosen due to the use of high inlet temperature. Nitrogen was used as the drying gas.

XRD of the spray-dried sample shows similarity to the starting material. The effect of inlet temperature is obvious; there were differences in peak positions and relative intensities between unprocessed PAS and spray dried PAS/ammonium carbonate 50:50 at 78 °C (Figure 3.46 (c) and (d)). On the other hand, all peaks found in XRD scan of the same system spray dried at 130 °C (Figure 3.46 (a)) are attributable to unprocessed PAS, except the peaks at 14.2 and 20.2 degrees (black arrow) which could be attributed to the physical mix of PAS and ammonium carbonate.

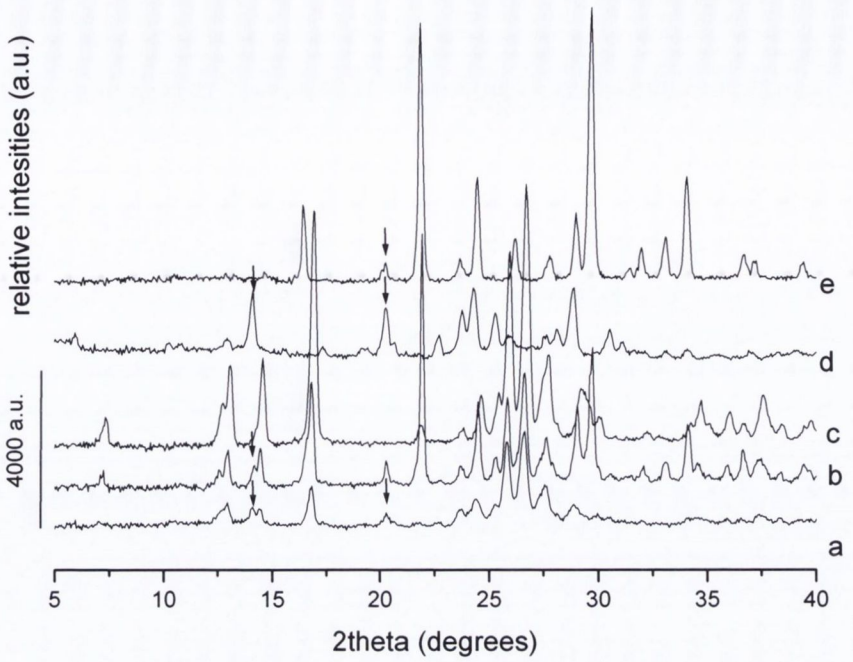

Figure 3.46- XRD scans of (a) PAS/ammonium carbonate 50:50 spray-dried at 130 °C (b) physical mixture of PAS/ammonium carbonate (c) PAS starting material (d) PAS/ammonium carbonate 50:50 spray-dried at 78 °C (e) ammonium carbonate. The arrow shows where the peak in spray dried sample could be attributed to the physical mixture.

Figure 3.47 shows DSC scan of the spray-dried sample. DSC thermogram of the spray-dried sample showed two endothermic peaks; broad endotherm peaking at ~114 °C with its onset at ~101 °C, partially comprising volatile components loss, TG analysis of this sample showed a loss of approximately 8.2% of total solid mass in the same temperature region as this endotherm. This endotherm is followed by a sharp endothermic peak at ~135 °C. This was ascribed to the melting process of PAS as confirmed by the DSC trace reported by Rotich et al., (2001) for PAS, who reported that the melting range of PAS is 131-136 °C.
The TG curve for the spray-dried sample heated in flowing nitrogen at 10 °C/min. (Figure 3.48) gives a two-stage mass loss with the discontinuity after about 35% mass loss at close to the reported melting point of the spray-dried sample (135 °C).

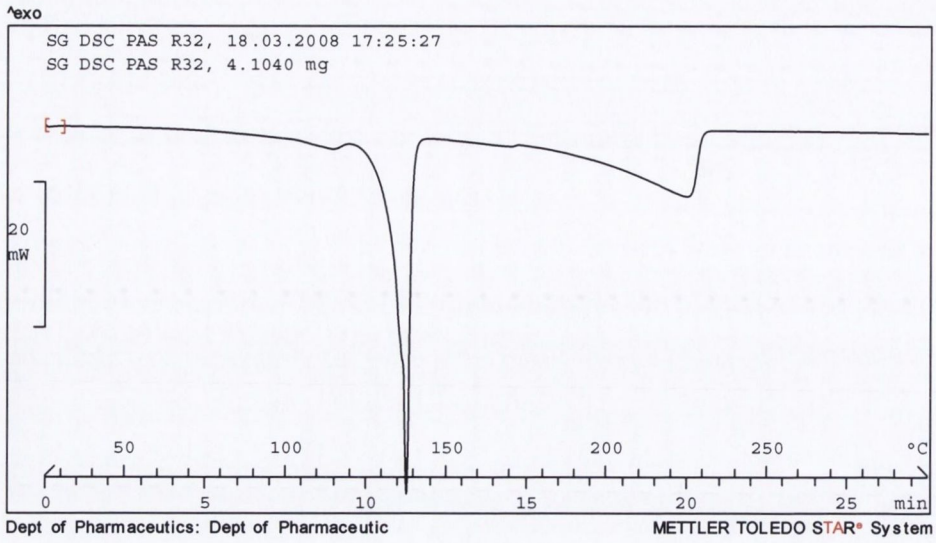

Figure 3.47- DSC scans of the PAS/ammonium carbonate 50:50 spray-dried from 90% v/v ethanol at inlet temperature of 130°C (R32).

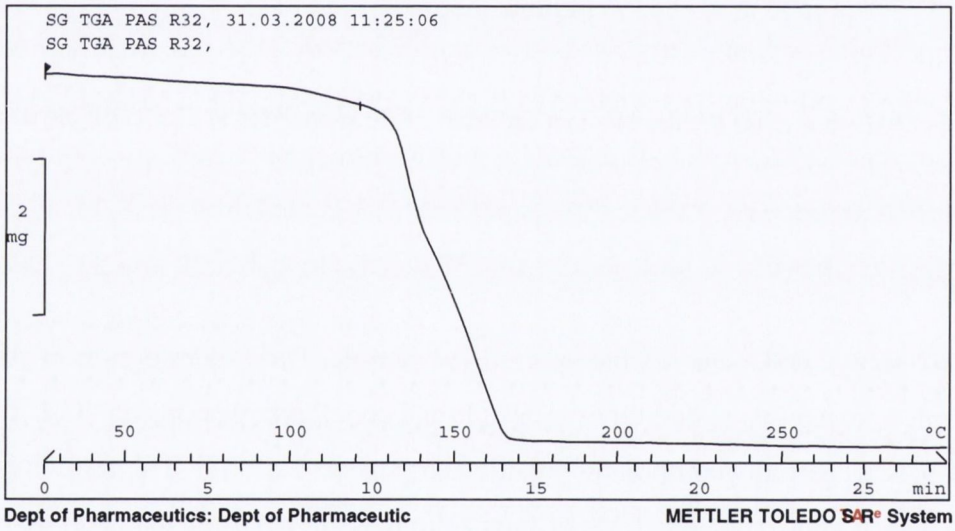

Figure 3.48- TGA scans of the PAS/ammonium carbonate 50:50 spray-dried from 90% v/v ethanol at inlet temperature of 130°C (R32).

Chuck and Zacher (2000) suggested post-treatment of spray-dried sample (as the recovered powder from spray drying of ammonium nicotinate was mainly the acid form accompanied by some impurities from the chemical reaction); PAS/ammonium carbonate 50:50 spray-dried from 90% v/v ethanol was subjected to vacuum drying (at ambient temperature and pressure of 600 mbar) overnight (hereafter referred to as System I).

Figure 3.49 shows the DSC thermograms obtained for System I and PAS unprocessed material analysed over the heating range of 25 to 300 °C. The spray-dried sample showed an endothermic process, which is similar in shape to the endothermic peak of the starting material. DSC scan of System I showed one endotherm peaking at ~141 °C, attributed to

melting (Figure 3.49 (a)), as confirmed by the literature value of 139-151 °C (Rotich et al., 2001) . An endothermic peak due to PAS melting was detected at ~140 °C on investigation of DSC thermogram of PAS starting material (Figure 3.49 (b)).

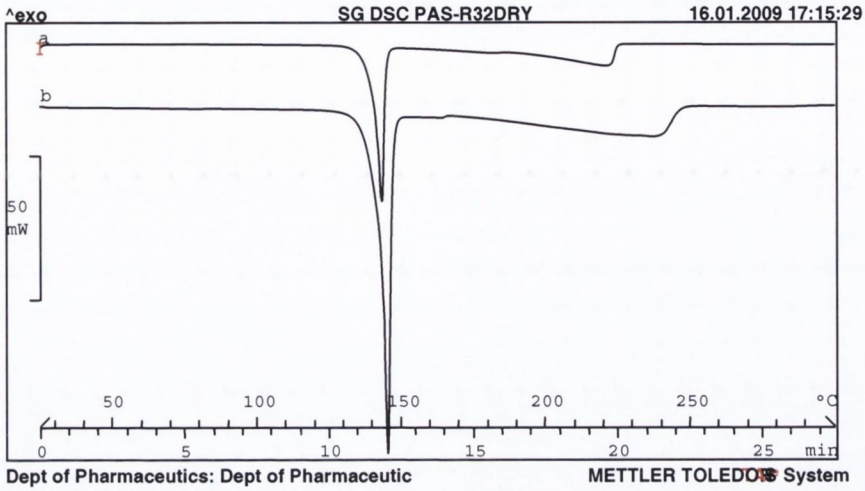

Figure 3.49- DSC scans of (a) System I (b) PAS unprocessed material

Figure 3.50 shows XRD scans of unprocessed PAS, System I spray dried PAS/ammonium carbonate at 78 °C and at 130°C. XRD analysis was carried out for System I to be compared with XRD diffractogram of unprocessed PAS. System I was XRD crystalline with peaks attributable to the starting material. There were no changes in peak positions between the unprocessed PAS and System I, but the peak intensities of the spray-dried sample were decreased in comparison to the starting material indicative of reduction of crystallinity upon spray drying. X-ray diffractograms of spray-dried PAS/ammonium carbonate at different inlet temperatures are also shown in Figure 3.50. It is obvious that spray dried sample at high inlet temperature showed one peaks at approximately 14.2 and 20.27 degrees, which was not attributable to PAS raw material, in contrast, X-ray diffractogram of spray dried sample at lower temperature was different from that of the unprocessed material; peak positions and relative intensities were different.

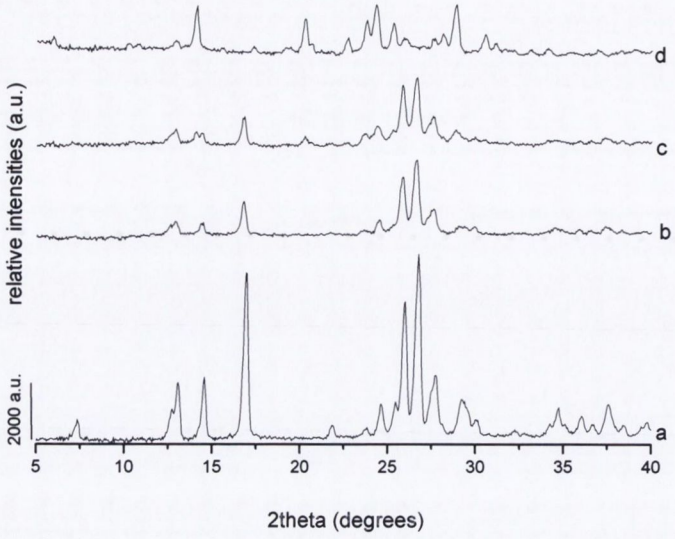

Figure 3.50- XRD scans of (a) PAS starting material (b) System I and spray-dried PAS/ammonium carbonate 50:50 at inlet temperature of (c) 130 °C (d) 78 °C.

Akkaya (2006) reported that PAS have bands in the FTIR spectrum due to their N–H asymmetric and symmetric stretching modes of the primary amine at 3494 and 3387cm^{-1} respectively, and an absorption band at 1659 cm^{-1} due to C=O group.

The spectrum of System I presented these characteristic signals at 3495 cm^{-1} and 3387 cm^{-1} for the NH_2 vibration and a band at 1652 cm^{-1} for C=O group. This was compared favourably with the FTIR data of the unprocessed material, indicating the similarity of vibration in bonding energies of the sample and that processing did not alter the chemical structure of the compound (Figure 3.51).

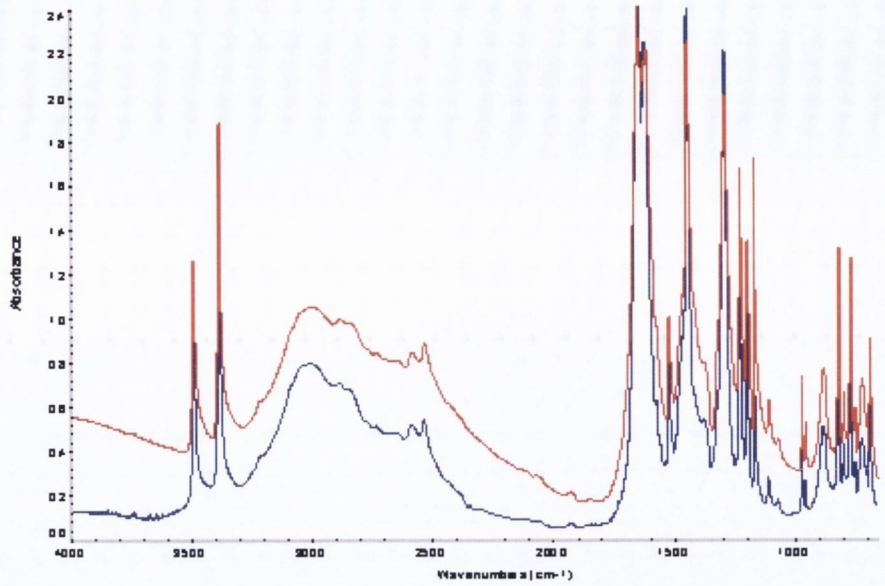

Figure 3.51- FTIR scans of PAS (blue line) System I (red line).

Elemental analysis was another evidence of the chemical nature of System I where the CHN results showed that there was no significant difference between starting material and the recovered particles, where the carbon, hydrogen and nitrogen percentage of the recovered particles compared favourably with the starting material as shown in Table 3.9.

DSC, XRD, FTIR and elemental analysis of System I showed that there were no distinct difference between the starting material and the spray-dried sample stored under vacuum overnight as seen in Figures 3.49, 3.50 and 3.51.

It could be concluded that the inlet temperature was important for production of the new solid state obtained by spray drying of PAS/ammonium carbonate, and high inlet temperature may be required for complete decomposition and removal of the process enhancers.

Table 3.9- Elemental analysis of different PAS systems

Sample		Analysis% w/w		
		C	H	N
PAS	Calculated	54.90	4.61	9.15
	Found	54.78±0.06	4.58±0.04	8.98±0.07
PAS ammonium salt	Calculated	49.41	5.92	16.46
	Found	49.80±0.17	5.79±0.07	15.99±0.49
System I	Found	54.72±0.02	4.58±0.04	9.00±0.03

Spherical aggregates of particles and crystalline particles were recovered from spray drying of PAS/ammonium carbonate 50:50 from 90% ethanol either before or after storage of the spray-dried sample under vacuum. SEM micrographs of the recovered particles are shown in Figure 3.52.

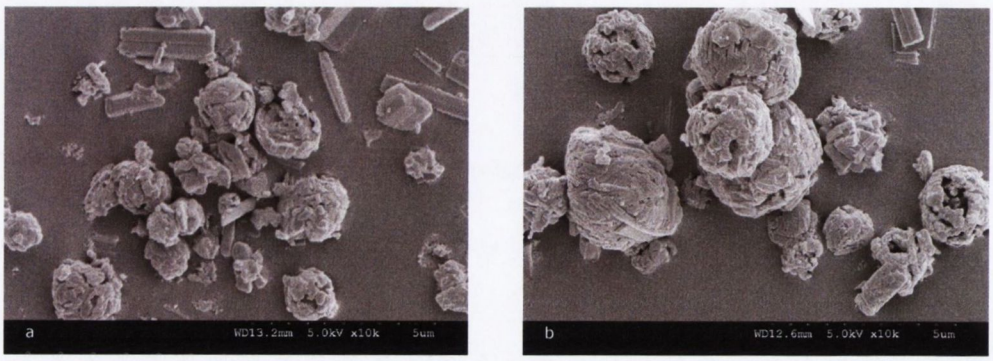

Figure 3.52- SEM micrographs of PAS/ammonium carbonate 50:50 spray-dried from 90% ethanol (a) before (b) after storage under vacuum overnight.

To ascertain if the similar results could be obtained using ammonium bicarbonate instead of ammonium carbonate 3% PAS/ammonium bicarbonate (50:50) was spray-dried from 90% ethanol at an inlet temperature of 130°C. Closed cycle was used for this sample; this layout was chosen due to the use of high inlet temperature. Nitrogen was used as the drying gas.

DSC scan of the spray-dried sample showed a broad, irregular in shape and asymmetric endothermic peak (Figure 3.53). The scan was repeated where the sample was heated to 120°C, cooled to 25°C then heated to 300°C where one sharp endothermic peak was detected, with measured enthalpy of melting at 263 J/g, which means that the recovered particles from spray drying were impure material, evidence from the broad endothermic peak found on investigation of DSC scans and these impurities are volatile evidence from the sharp peak detected in DSC scan (Figure 3.54).

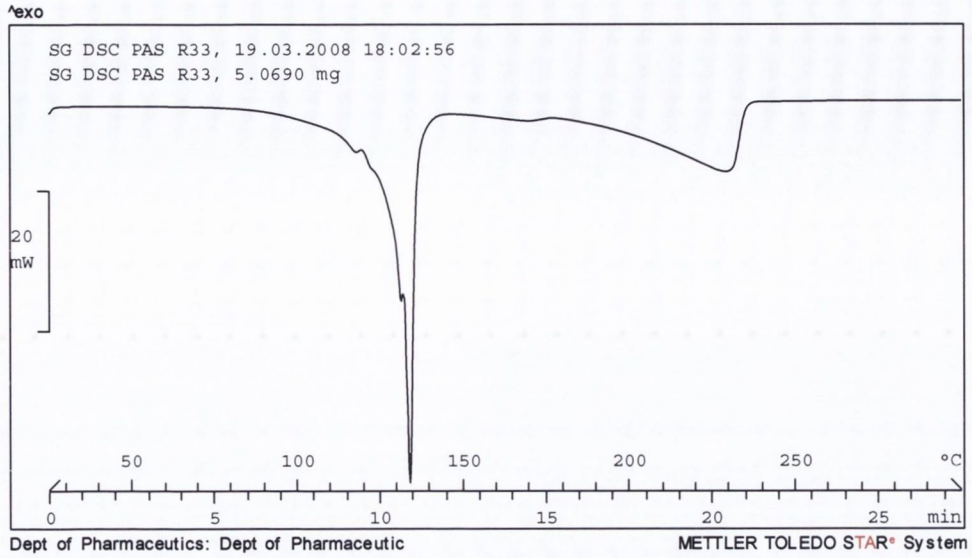

Figure 3.53- DSC scans of the PAS/ammonium bicarbonate 50:50 spray-dried from 90% v/v ethanol at inlet temperature of 130°C (R33).

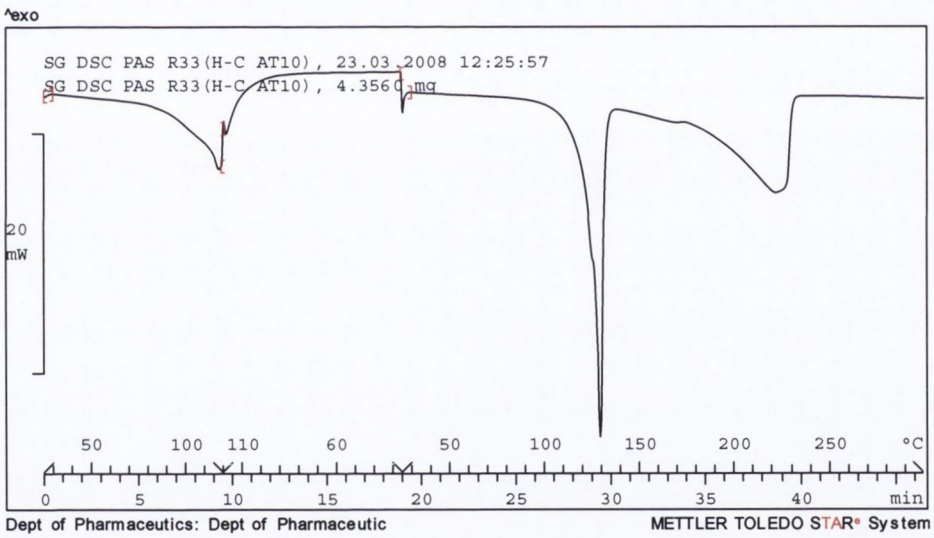

Figure 3.54- DSC scans of spray dried PAS/ammonium bicarbonate 50:50 heated to 120°C, cooled and reheated to 300°C.

The recovered particles from spray drying process was stored overnight under vacuum (hereafter referred to as System II), the DSC of these particles showed a similar pattern to unprocessed material with an endothermic peak at ~140 °C with measured enthalpy of 371 J/g, similar to the melting endotherm found in DSC scan of unprocessed material peaking at ~ 140 °C with measured enthalpy of melting at 369 J/g (Figure 3.55 (a), (b)) and to DSC trace reported by Rotich *et al.*, (2001) for PAS unprocessed material. The spray drying process and overnight storage under vacuum did not alter the solid-state characteristics of PAS, analysed by thermal analysis as seen in Figure 3.55.

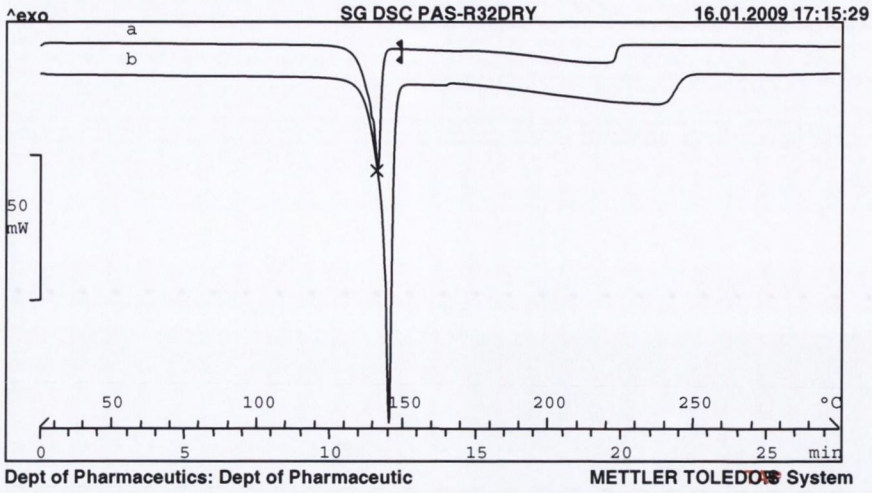

Figure 3.55- DSC scans of (a) System II (b) PAS starting material.

XRD analysis of System II showed a pattern typical of a crystalline material, as confirmed by the numerous diffraction peaks on the X-ray diffractogram. XRD patterns of System II and unprocessed material show that there was no difference in peak positions between the two samples, however, the intensities of the peaks of System II was greatly reduced in comparison to the unprocessed material (Figure 3.56).

FTIR was another evidence of the similarity between System II and the starting material as shown in Figure 3.57.

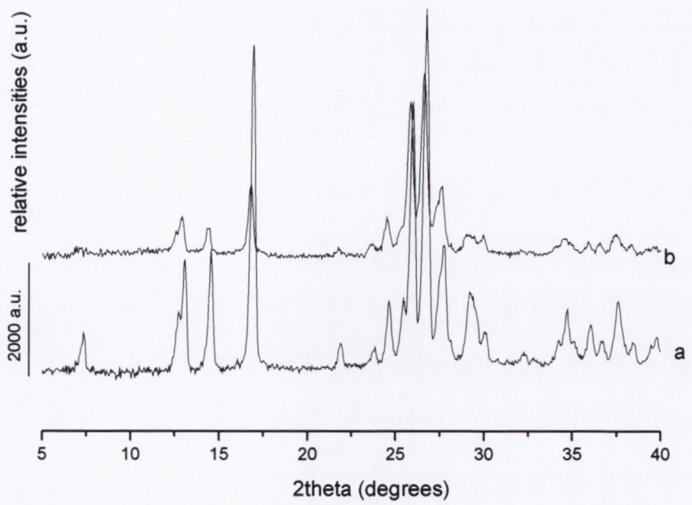

Figure 3.56- XRD scans of (a) PAS starting material (b) System II

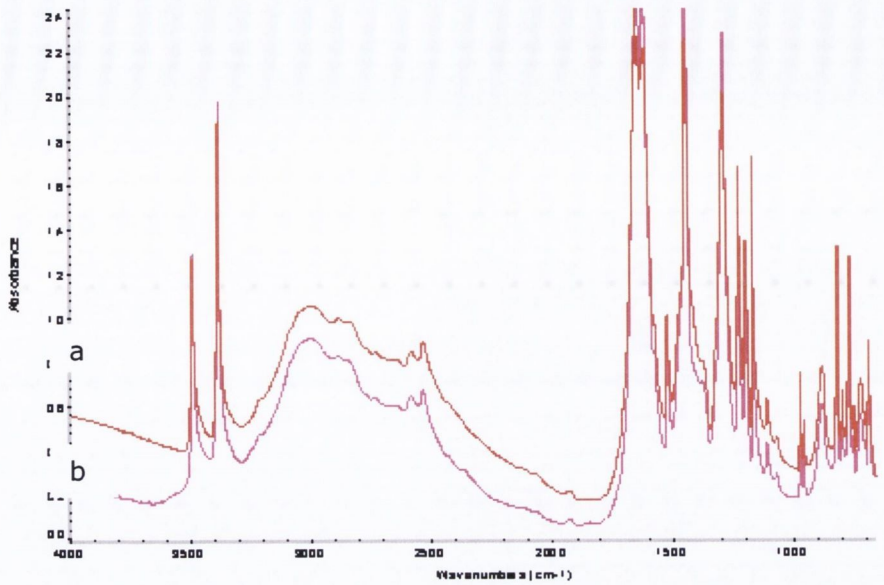

Figure 3.57- FTIR scans of (a) PAS (b) System II.

Elemental analysis of System II showed that the chemical composition of the recovered particles was the same as chemical composition of the starting material (table 3.10). This was in agreement with the results obtained by spray drying of PAS/ammonium carbonate SEM micrographs of the recovered particles before and after storage under vacuum are shown in Figure 3.58, where spherical particles as well as crystalline aggregates were recovered either before or after storage under vacuum, but the vacuum dried samples showed visible hole (red box)

Table 3.10- Elemental analysis of different PAS systems

Sample		Analysis% w/w		
		C	H	N
PAS	Calculated	54.90	4.61	9.15
	Found	54.78±0.06	4.58±0.04	8.98±0.07
PAS ammonium salt	Calculated	49.41	5.92	16.46
	Found	49.80±0.17	5.79±0.07	15.99±0.49
System II	Found	54.67±0.05	4.53±0.12	9.01±0.02

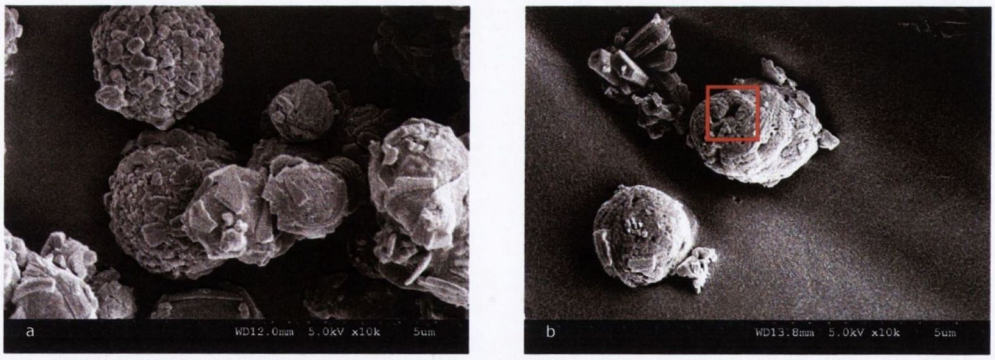

Figure 3.58- SEM micrographs of PAS/ammonium carbonate 50:50 spray-dried from 90% ethanol at an inlet temperature of 120 °C (a) before (b) after storage under vacuum overnight. The red box shows the visible hole in the particles.

Another 3% PAS/ammonium carbonate was spray-dried from 90% ethanol at an inlet temperature of 120 °C. DSC scan of the recovered particles shows an irregular broad endothermic peak (Figure 3.59). The broad irregular peak indicates that the recovered powder from the spray drying process could be impure material.

Slower heating rate was used for DSC scan of the spray-dried sample where two endothermic events were detected; broad endothermic peak at 109 °C with the onset at ~96 °C was recorded which could be attributed to volatile impurities loss. TG analysis of this sample showed a loss of approximately 8.2% of total solid mass in the same temperature region as this endotherm. Another endothermic peak was also recorded; this endothermic event was sharp and peaking at ~ 131 °C, which could be attributed to the melting process (Figure 3.60).

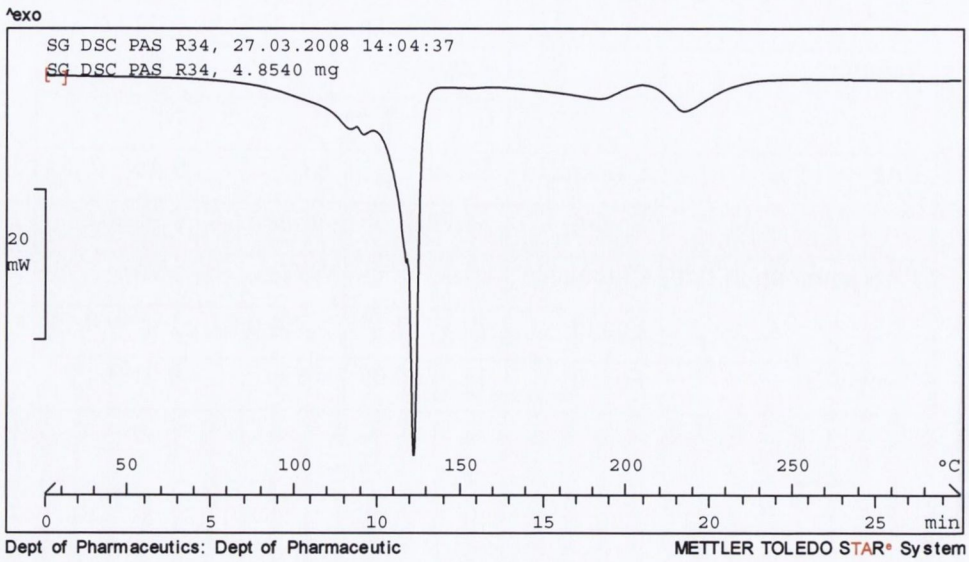

Figure 3.59- DSC scan of the PAS/ammonium carbonate 50:50 spray-dried from 90% v/v ethanol at inlet temperature of 120°C (R34).

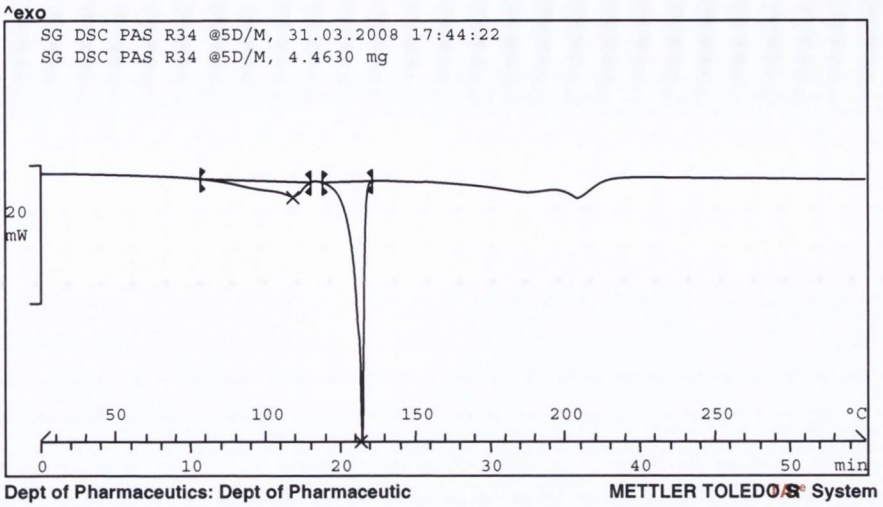

Figure 3.60- DSC scan of the PAS/ammonium carbonate 50:50 spray-dried from 90% v/v ethanol at inlet temperature of 120°C (R34) at heating rate of 5°C/min.

DSC of spray-dried sample stored under vacuum overnight (hereafter referred to as System III) showed a similar pattern to unprocessed material with an endothermic peak at ~141°C with the onset at ~140 °C with a measured enthalpy of fusion of ~372 J/g, indicative of the melting process, and similar to unprocessed material at ~ 141 °C with a measured enthalpy of fusion of ~369 J/g. The spray drying process and storage under vacuum did not alter the solid-state characteristics of PAS, analysed by these methods (Figure 3.61).

X-ray diffractogram of System III indicates the results of DSC analysis that the recovered particles were similar to the starting material. The peaks found in the XRD scan of system III could be attributed to the starting material while the intensities of peaks were reduced in comparison to the starting material (Figure 3.62).

Figure 3.63 shows SEM micrograph of the produced powder. SEM micrographs of the recovered powder showed that spray drying and post-treatment of this system resulted in hollow spherical particles.

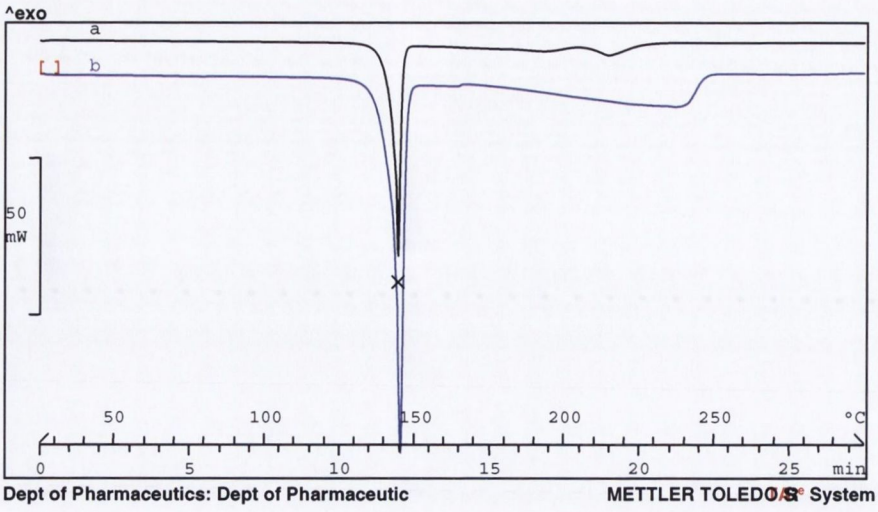

Figure 3.61- DSC scans of (a) system III (b) PAS starting material.

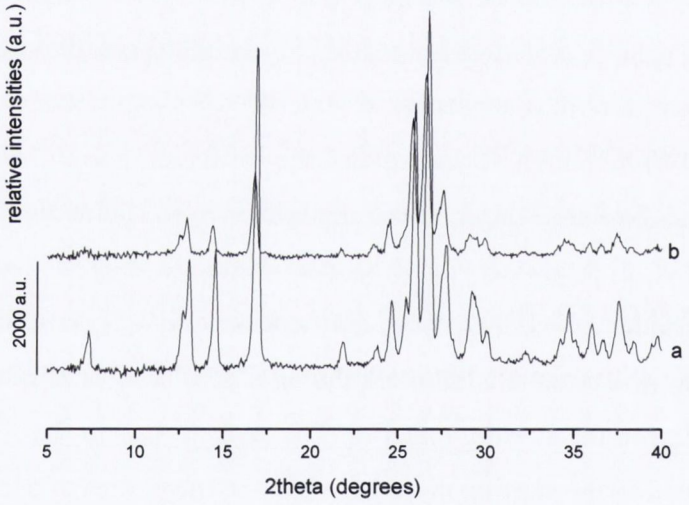

Figure 3.62- XRD scans of (a) PAS starting material (b) System III

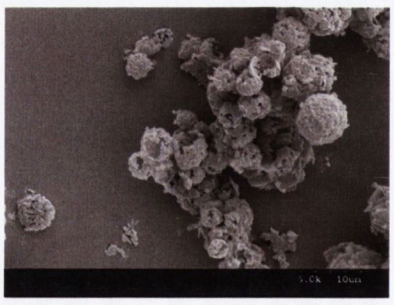

Figure 3.63- SEM micrograph of System III

3.9 PAS/ PVP SPRAY-DRIED SYSTEM

Tajber, (2005) has previously used PVP to inhibit crystallisation and promote production of an amorphous composite. A 3% w/v solution of PAS/PVP 9:1 was prepared in 90% v/v ethanol to investigate the possibility of production of amorphous form of PAS. After spray drying the resultant powder was viewed by SEM. SEM micrographs of spray-dried sample showed that the particles were rough dimpled spheres (non-porous) (Figure 3.64). XRD analysis demonstrated that PAS/PVP spray-dried sample from 90% ethanol was crystalline evident from the presence of peaks (Figure 3.65). Spray-drying PAS with PVP from these conditions did not appear promising, due to the solid-state characteristics of the composite. Further characterisation of this system was thus not undertaken.

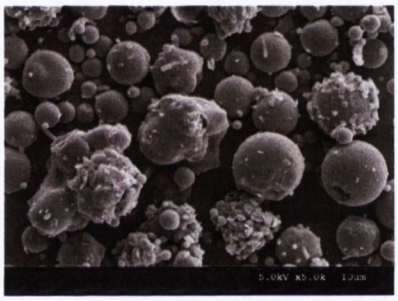

Figure 3.64- SEM micrograph of PAS/PVP 90: 10 system spray-dried from 90% v/v ethanol using compressed air as the drying gas.

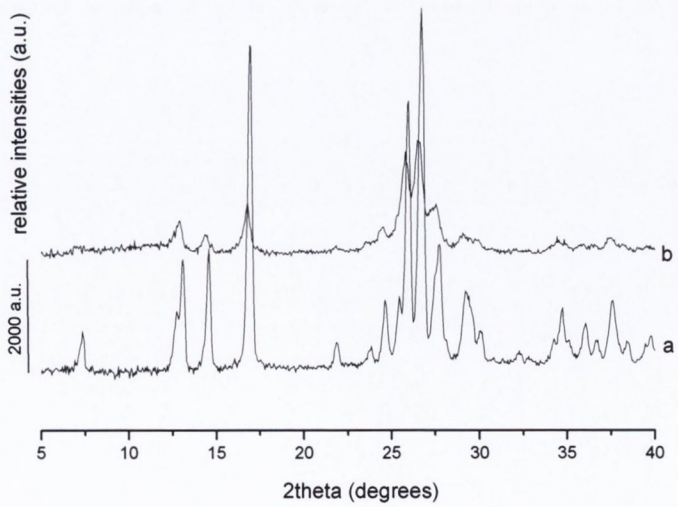

Figure 3.65 XRD scans of (a) PAS unprocessed material (b) spray-dried PAS/PVP 90: 10 from 90% v/v ethanol

3.10 *IN VITRO* DEPOSITION PROPERTIES OF SYSTEMS FOR INHALATION PURPOSES

Spray-dried 1% PAS from 70% ethanol (hereafter referred to as R6), 3% PAS/ammonium carbonate 80:20 (hereafter referred to as R10) and 73:27 (hereafter referred to as R27) spray-dried from 90% ethanol as well as micronised PAS (hereafter referred to as mic PAS) were selected for further characterisation in terms of twin impinger analysis.

These particular spray drying conditions were chosen to cover wide range of morphological characteristics of powder produced by spray drying of PAS under different spray drying conditions. A mixture of rod shape crystals and porous particles; which was seen in SEM micrographs of 1% PAS system spray-dried from 70% ethanol (R6) (Figure 3.2a). Compared to the mixture of porous particles and agglomerate of microcrystalline particles and crystalline particles which were shown in SEM micrographs of 3% PAS/ammonium carbonate 80:20 spray dried from 90% ethanol (R10) (Figure 3.17a) and spherical aggregates of microcrystalline particles, which were shown in SEM micrographs of 3% PAS/ammonium carbonate 80:20 spray dried from 90% ethanol (R27) (Figure 3.17b). All these spray-dried systems were also compared to micronised PAS.

The analysis was carried out in triplicate for each sample and the average was calculated. The results of twin impinger analysis are presented in Figure 3.66.

Figure 3.66 indicates that the percentage of the non-respirable dose is high. However, there was a difference in the ratio of dose retained in the device to that deposited in stage I of the impinger. The highest ratio is for mic PAS and is 2.7 (60.1% device/21.8% stage I) and the lowest is for R10 and is 0.7 (31.4% device/43.9% stage I).

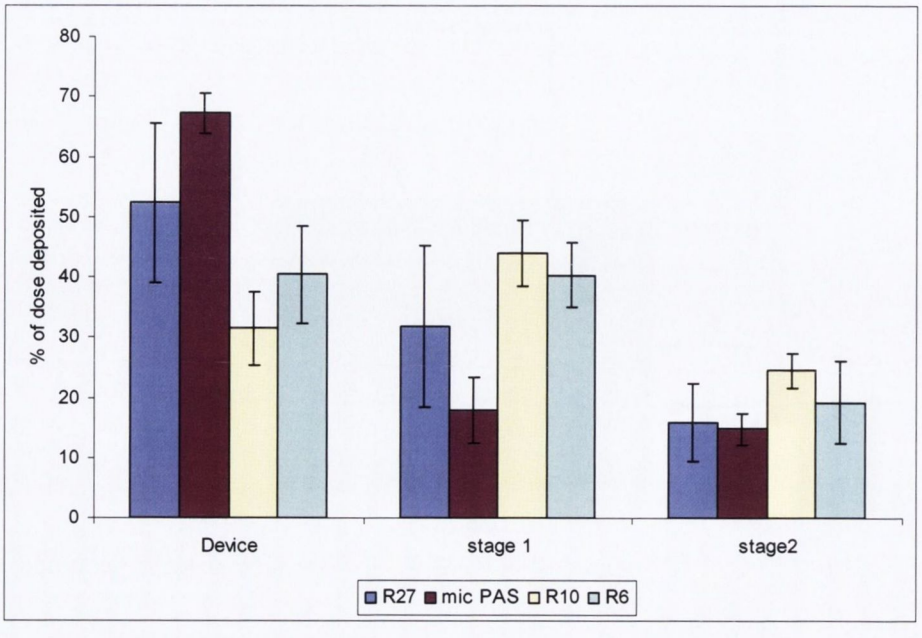

Figure 3.66- Twin impinger analysis of the micronised and spray-dried PAS samples.

Emitted dose was defined as the total quantity of the drug recovered from the upper and lower stages of the impinger and expressed as percent of the total dose loaded into the capsule. Figure 3.67 shows the emitted dose calculated for the micronised and spray-dried PAS; there is a difference in the ratio of dose retained in the device to that emitted. The greatest ratio is for mic PAS and is 1.51 (60.1 ± 3.6% device/39.8 ± 3.6% emitted) and the lowest is for R10 and is 0.45 (31.46 ± 6% device/68.54 ± 6% emitted).

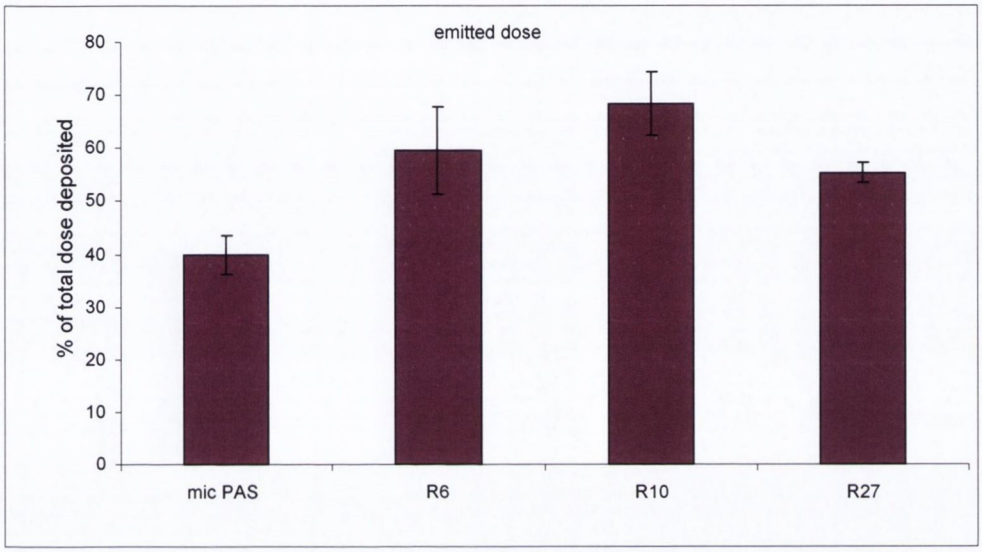

Figure 3.67- The emitted dose (i.e. deposited on stage 1 and 2 of twin impinger) of the micronised and spray-dried PAS samples.

Figure 3.68 shows the percentage of dose deposited in stage 2 of the twin impinger i.e. respirable fraction. The sample with the best deposition on stage 2 of twin impinger was R10. A statistically significant ($p < 0.05$) increase in respirable fraction was measured for R10 relative to mic PAS, with measured respirable fractions of 24.54±2.86% and 14.8±2.5%, for R10 and mic PAS respectively. No statistically significant difference ($p > 0.05$) in respirable fraction between R6, R27 and mic PAS was calculated. Generally, the large error bars for PAS/ammonium carbonate 80:20 spray-dried from 90% ethanol and PAS spray-dried from 70% ethanol indicate large standard deviations and inconsistency of the dosing.

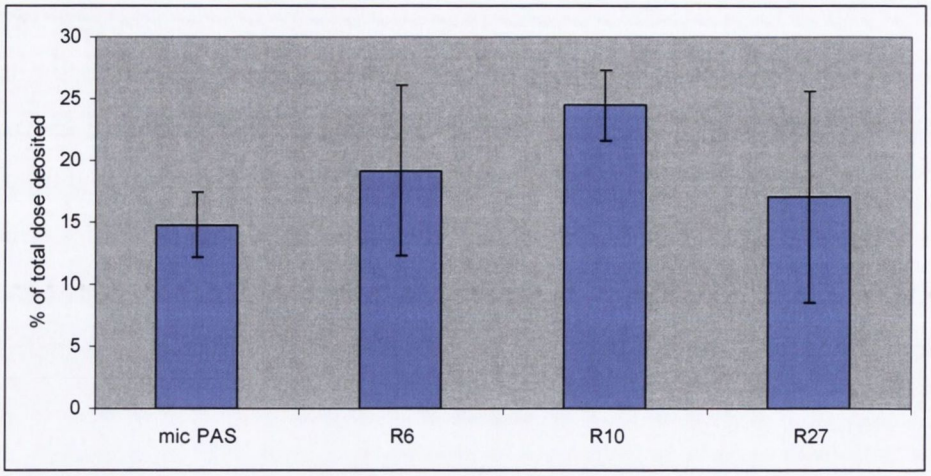

Figure 3.68 The respirable dose (i.e. deposited on stage 2 of twin impinger) of the micronised and spray-dried PAS samples.

3.11 Ammonium salt of PAS spray-dried systems

3.11.1 Physicochemical properties of spray dried salt from ethanol

As shown earlier, spray drying of PAS/ammonium carbonate resulted in alteration of the solid state of PAS unprocessed material, ammonium salt of PAS was prepared and spray dried to follow the changes observed upon spray drying of PAS/ ammonium carbonate.

A 3% (w/v) solution of ammonium salt of PAS system was spray-dried from 90% (v/v) ethanol, at an inlet temperature of 78 °C as outlined in Appendix I Table 2. DSC thermogram of the spray-dried sample showed an endothermic event with an onset temperature of melting at ~120°C. Another small endothermic peak was visible at approximately ~ 86°C (Figure 3.69). TGA analysis of the sample showed a loss of approximately 11% of total solid mass in the same temperature region as this endotherm. This weight loss is consistent with the loss of ammonia molecule (the loss of one ammonia molecule corresponds to a loss of ~10% by weight of ammonium salt of PAS when determined on a molecular weight basis). This endothermic peak was removed on examination of the DSC scan of the spray-dried sample after heating to 100°C and cooling, which might be referred to evaporation of ammonia (Figure 3.70).

The XRD scan for PAS ammonium salt spray-dried from 90% ethanol (Figure 3.71) showed different pattern in comparison with the starting material; peak positions were different and extra peaks were found on examination of XRD of the spray-dried sample, the black arrows in the scan show where peaks could be attributed to the unprocessed salt, the red arrows show where peaks could be attributed to the acid from. The results of XRD analysis may suggest that the salt was partially converted to the acidic form upon spray drying. This hypothesis may be supported by different studies found in the literature about thermal decomposition of ammonium salts and recovery of the parent acid by heating of ammonium salts (Guseinov et al., 1981; Frenkel et al., 1995; Chuck and Zacher, 2000).

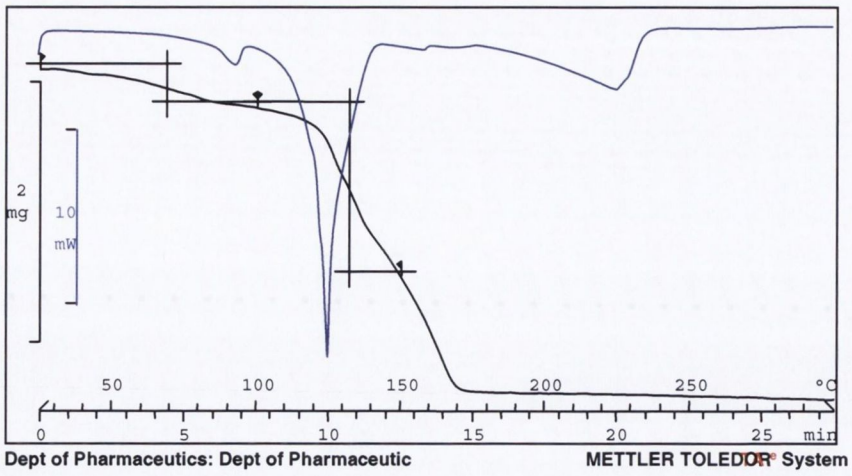

Figure 3.69- DSC and TGA scans of 3% ammonium salt of PAS system spray-dried from 90% v/v ethanol.

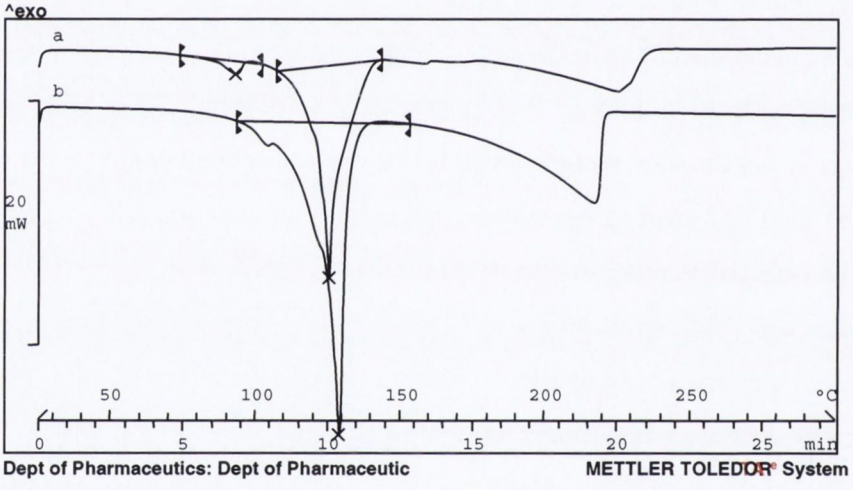

Figure 3.70- DSC scans of (a) ammonium salt of PAS system spray-dried from ethanol (b) ammonium salt of PAS system spray-dried from ethanol after heating to 100°C and cooling.

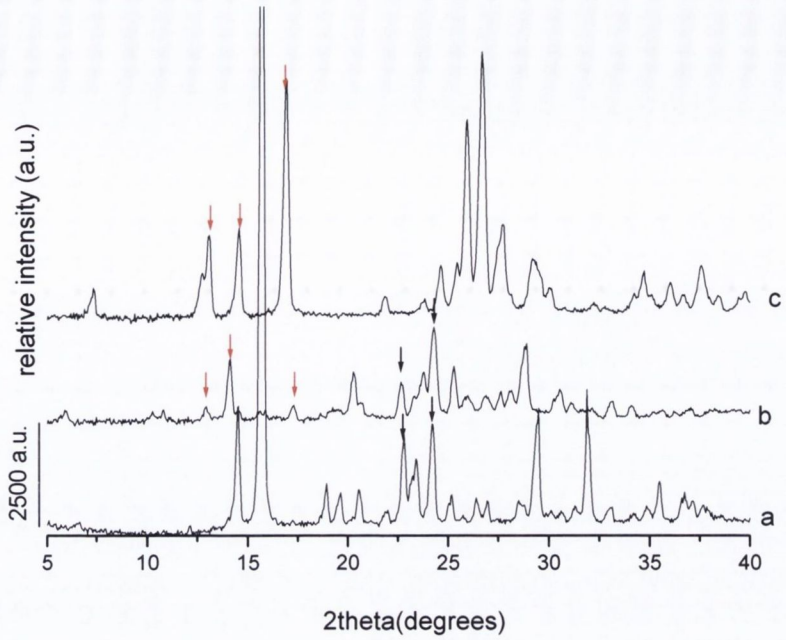

Figure 3.71- XRD scans of (a) PAS ammonium salt starting material (b) 3% ammonium salt of PAS system spray-dried from 90% v/v ethanol (c) PAS unprocessed material. The black arrows in the scan show where peaks could be attributed to the unprocessed salt; the red arrows show where peaks could be attributed to the acid from.

Guseinov et al., (1981) reported that the ability of ammonium salts to undergo thermal decomposition with the formation of gaseous ammonia and free acid is well known. In addition, thermal decomposition of ammonium salts can proceed both in the solid phase by the heating of the dry salt in a stream of inert gas (Guseinov et al., 1981), and in the liquid phase by heating the aqueous solution of the salt (Frenkel et al., 1995). Furthermore, Chuck and Zacher (2000) reported that an aqueous solution of ammonium nicotinate was converted to nicotinic acid by spray drying solution of ammonium nicotinate; the authors reported that ammonium nicotinate decomposes during spray drying process and ammonia, together with the solvent, escape in the exhaust gas of the spray dryer. But, the inlet temperature used by Chuck and Zacher (2000) was relatively high temperature (170-250°C). Therefore, it is not surprising that the solid state of ammonium salt of PAS was altered upon spray drying. Furthermore, the changes in thermal behaviour and XRD pattern of the salt upon spray drying perhaps due to partial decomposition of the salt during spray drying process, this decomposition was not complete and the parent acid was not recovered perhaps due to the low inlet temperature.

Elemental analysis of the spray dried sample is shown in Table 3.11. It is obvious from comparing the elemental analysis of the spray dried sample to that of p-aminosalicylic acid

that this inlet temperature was not sufficient for complete conversion of the salt to the equivalent acid form.

Figure 3.72 show XRD diffractograms of spray dried salt and spray dried PAS/ ammonium carbonate, it is obvious that the two XRD patterns are not the same; there are peaks found in the XRD scan of PAS/ammonium carbonate spray dried sample (black arrows), but were not found in the XRD diffractogram of spray dried salt. The difference between the two samples was confirmed by elemental analysis, where nitrogen contents of the spray dried salt was significantly different from that of spray dried PAS/ammonium carbonate.

Table 3.11- Elemental analysis of different PAS systems

Sample		Analysis% w/w		
		C	H	N
PAS	Calculated	54.90	4.61	9.15
	Found	54.78±0.06	4.58±0.04	8.98±0.07
PAS ammonium salt	Calculated	49.41	5.92	16.46
	Found	49.80±0.17	5.79±0.07	15.99±0.49
Spray dried ammonium salt	Found	50.29±0.16	5.42±0.05	15.30±0.42
Spray dried PAS/ammonium carbonate	Found	50.75±0.17	5.30±0.02	12.46±0.19
Spray dried PAS/ammonium bicarbonate	Found	50.74±0.15	5.12±0.24	12.60±0.007

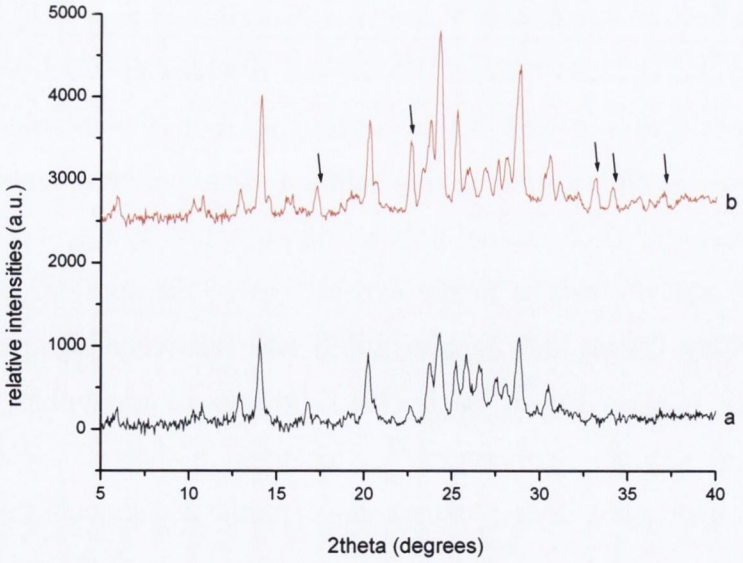

Figure 3.72- XRD scans of (a) ammonium salt of PAS system spray-dried from 90% v/v ethanol (b) PAS/ammonium carbonate spray dried system. The black arrows in the scan show where peaks are different between the two samples.

A bulk and tap densities of 0.423±0.022 g/cm^3 and 0.669±0.024 g/cm^3 were measured for ammonium salt of PAS raw material. A bulk and tap densities of 0.093±0.002 g/cm^3 and 0.133±0.008 g/cm^3 were measured for ammonium salt of PAS spray-dried from an ethanolic solution, significantly lower than that measured for the raw material. Low-density particles have been shown to have increased aerosolisation efficiency (Edwards et al., 1997).

Particle size analysis of the PAS ammonium salt system was performed and compared to the particle size of micronised PAS and PAS ammonium salt. The median particle size of volume distribution (d (0.5)) for the PAS ammonium salt spray-dried system was 3.673 µm. The median particle size of volume distribution (d (0.5)) for the micronised PAS was 2.9052± 0.026 µm, while it was 92.476 µm for PAS ammonium salt starting material. The particle size distribution was monomodal for both micronised PAS and spray dried PAS ammonium salt, but it was bimodal for the PAS ammonium salt starting material. SEM micrographs of the spray-dried material showed that the spray drying of this system resulted in spherical agglomerates of particles. The SEM micrograph of the produced powder is shown in Figure 3.73.

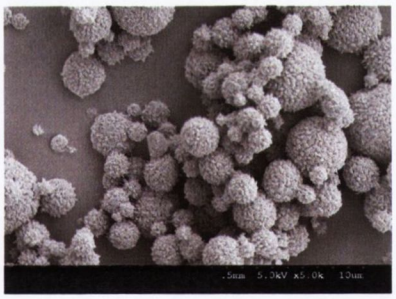

Figure 3.73- SEM micrograph of 3% ammonium salt of PAS system spray-dried from 90% v/v ethanol

3.11.2 *In vitro* deposition properties of spray dried ammonium salt.

Twin impinger analysis was carried out on the spray-dried PAS ammonium salt (AS1) and compared to results of twin impinger analysis of micronised PAS (mic PAS). The results of twin impinger analysis of spray-dried PAS ammonium salt was compared to micronised PAS and not to PAS ammonium salt starting material due to the huge difference in particle sizes between PAS ammonium salt starting material and spray-dried sample. The analysis was done at least in triplicate for each sample and the average was calculated. The results of twin impinger analysis are presented in Figure 3.74.

Figure 3.74 indicates that the percentage of the non-respirable dose is high. However, there was a difference in the ratio of dose retained in the device to that deposited in stage I of the impinger. A higher ratio was reported for micronised PAS and is 2.7 (60.1% device/21.8% stage I) while lower ratio was found for 3% (w/v) PAS ammonium salt spray-dried from 90% v/v ethanol and is 0.79 (36.29% device/45.74% stage I). However, no statistical difference in respirable fraction between spray dried salt and micronised PAS was noted.

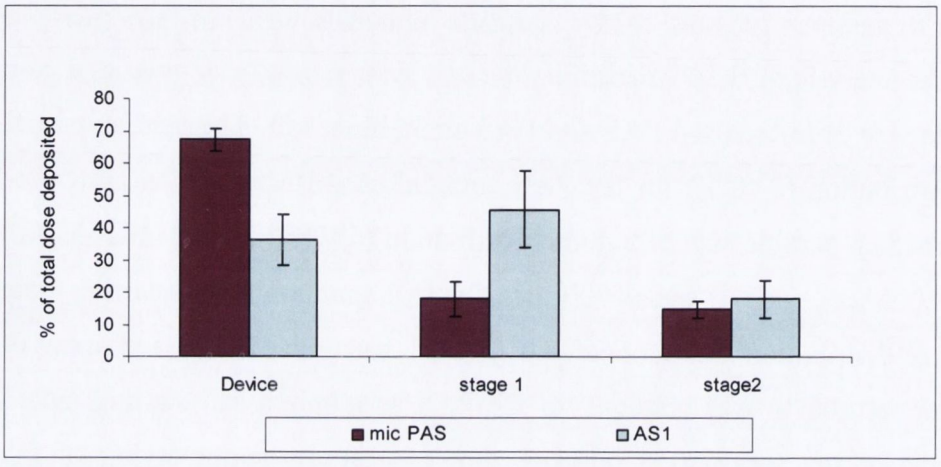

Figure 3.74- Twin impinger analysis of the micronised and spray-dried PAS samples.

Figure 3.75 shows the emitted dose acquired with the micronised PAS and spray-dried PAS ammonium salt; there is difference in the ratio of dose retained in the device to that emitted. The ratio for micronised PAS and is 1.51 (60.1 device/39.8 emitted) and the ratio for PAS ammonium salt spray-dried from 90% v/v ethanol and is 0.56 (36.29 device/63.7emitted).

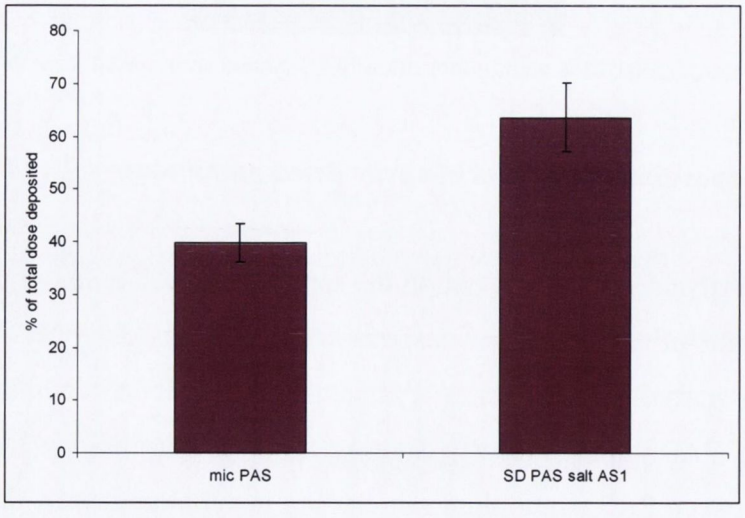

Figure 3.75- The emitted dose (i.e. deposited on stage 1 and 2 of twin impinger) of the micronised and spray-dried PAS ammonium salt samples.

Respirable fractions of different spray dried PAS systems as well as spray dried ammonium salt of PAS were compared, no statistically significant difference ($p > 0.05$) in the respirable fractions of different samples as shown in Table 3.12.

Table 3.12- Respirable fractions of different PAS spray dried systems

System	**Respirable fraction (%)**
SD PAS	19.2±6.92
SD PAS /AC80:20	24.5±2.86
SD PAS /AC 73:27	17.03±8.55
SD PAS salt	17.9±5.83

3.11.3 Ammonium salt of PAS spray-dried from water

Ammonium salt of PAS was spray dried from water to follow the alteration of solid state of PAS upon spray drying with ammonium carbonate (Corrigan, 2006). A 1% (w/v) solution of ammonium salt of PAS system was spray-dried from water, at an inlet temperature of 120°C. DSC thermogram of 1% ammonium salt of PAS system spray-dried from water showed a broad endotherm with onset temperature of ~ 103°C (Figure 3.76). TG analysis of this sample showed a loss of approximately 12% of total solid mass in the same temperature region as this endotherm. This weight loss may be due to the loss of ammonia (the loss of one ammonia molecule corresponds to a loss of 10% by weight of ammonium salt of PAS when determined on a molecular weight basis). This was followed by sharp endotherm at 133 °C, with onset temperature of ~130°C, attributed to the melting process of the sample.

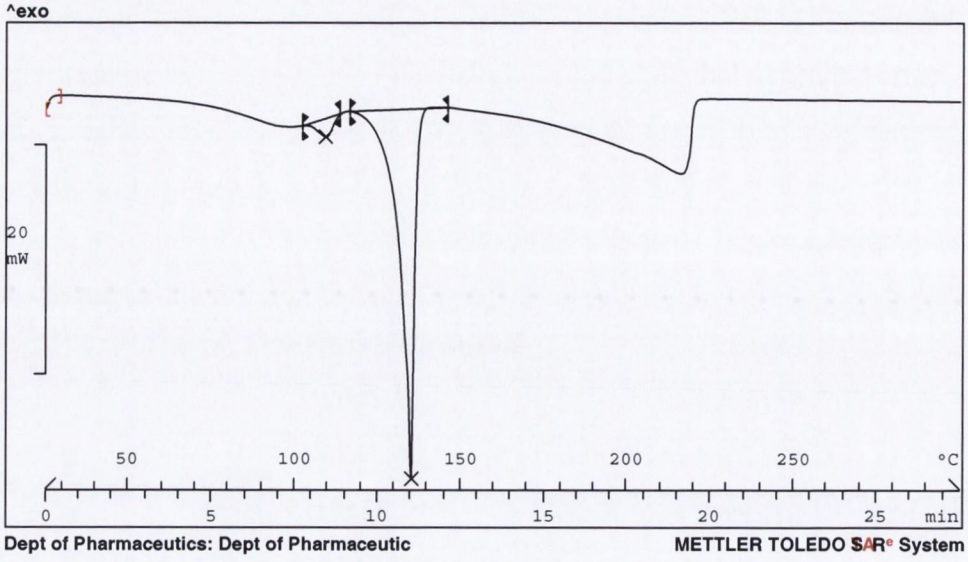

Figure 3.76- DSC scans of 3% ammonium salt of PAS system spray-dried from water.

Figure 3.77 shows XRD scan for PAS ammonium salt spray-dried from both aqueous and ethanolic solutions. The spray-dried samples were crystalline evident from the presence of peaks. The spray-dried samples showed different XRD patterns in comparison with the starting material; peak positions were different and extra peaks were found on examination of XRD scan of the spray-dried sample. Although both spray dried samples showed that peaks attributable to the unprocessed salt (black arrows), but it is obvious from the diffractograms that the scan of spray dried salt from water showed peaks attributable to the unprocessed acid (red arrows) which perhaps due to difference in inlet temperature or due to the solvent effect; it should be noted that the dielectric constant of water is 80, while that of ethanol is 24 (Scott, et al., 2000). The use of solvent with greater dielectric constant results in greater dissociation. Therefore, the difference in solid state of spray dried salt from either water or ethanolic solutions perhaps due to the lower dissociation of salt in ethanol. But none of the spray dried salt was completely converted to the equivalent acid as confirmed by elemental analysis shown in Table 3.13.

SEM micrographs showed that spray drying of this system resulted in spherical aggregates of microcrystalline particles. The SEM micrograph of the produced powder is shown in Figure 3.78.

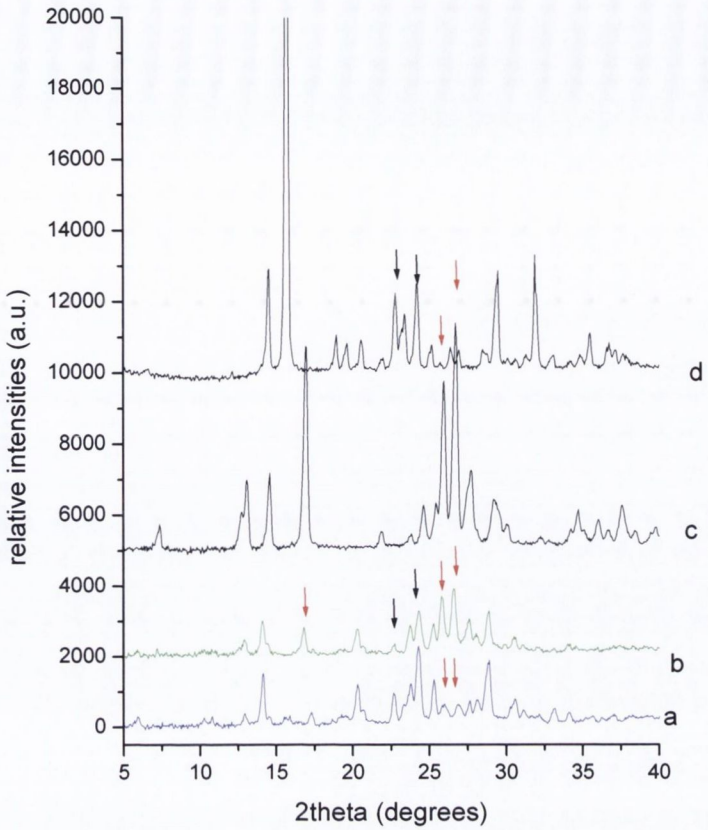

Figure 3.77- XRD scans of (a) ammonium salt of PAS system spray-dried from 90% ethanol at 78°C (b) ammonium salt of PAS system spray-dried from water at 120°C (c) PAS raw material (d) PAS ammonium salt. The red arrows show where the peaks are attributable to the acid, the black arrows show where peaks are attributable to the salt.

Table 3.13- Elemental analysis of PAS and PAS salt systems

Sample		Analysis% w/w		
		C	H	N
PAS	Calculated	54.90	4.61	9.15
PAS ammonium salt	Calculated	49.41	5.92	16.46
Spray dried ammonium salt at 78°C	Found	50.34±0.07	5.57±0.21	15.53±0.32
PAS ammonium salt spray-dried 120°C	Found	52.91±0.77	5.39±0.48	11.09±0.4

Figure 3.78 - SEM micrograph of 1% ammonium salt of PAS system spray-dried from water

3.11.4 Spray drying of ammonium salt of PAS at higher temperature

The inlet temperature of spray dried salt affected the solid state of the recovered particles as shown by XRD and elemental analysis of spray dried salt. Therefore, higher inlet temperature was used to study the possibility of production of PAS from the ammonium salt.

A 3% ammonium salt of PAS solution was spray-dried from 90% ethanol, the inlet temperature for this system was set at 130°C and nitrogen was used as the drying gas. Closed cycle was used for this sample due to the use of high inlet temperature. The spray-dried sample was stored under vacuum (at ambient temperature and pressure of 600 mbar) overnight to ascertain if similar results to those obtained from PAS/ammonium carbonate and PAS/ammonium bicarbonate could be obtained.

DSC thermogram of the processed sample shows one endothermic event, which compared favourably with the DSC scan of PAS starting material, which indicate that the spray-dried salt was converted to the acid form (Figure 3.79).

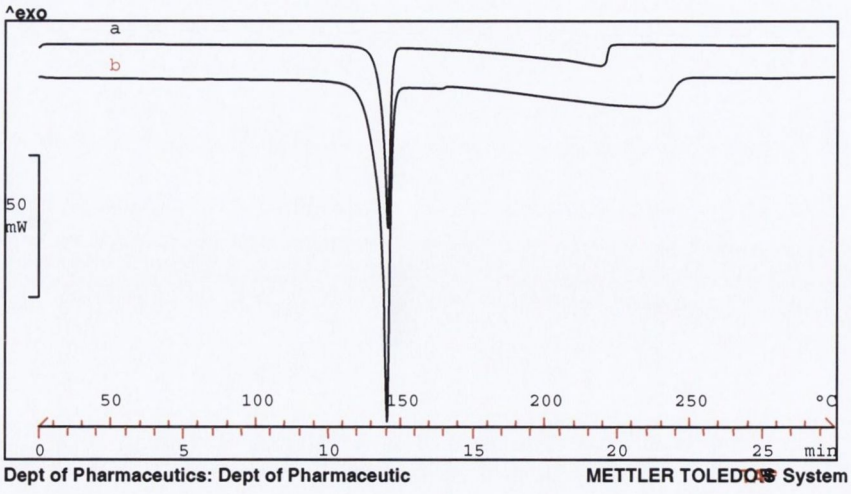

Figure 3.79- DSC scans of (a) PAS ammonium salt spray-dried from 90% v/v ethanol at inlet temperature of 130°C (AS6) stored under vacuum overnight (b) PAS starting material

XRD scan of the spray-dried sample stored under vacuum is shown in Figure 3.80. It is clear that there was no difference between PAS unprocessed material and ammonium salt of PAS spray-dried sample.

SEM micrograph of the recovered particles shows spherical porous particles and aggregates of microcrystalline particles. SEM of the produced powder is shown in Figure 3.81.

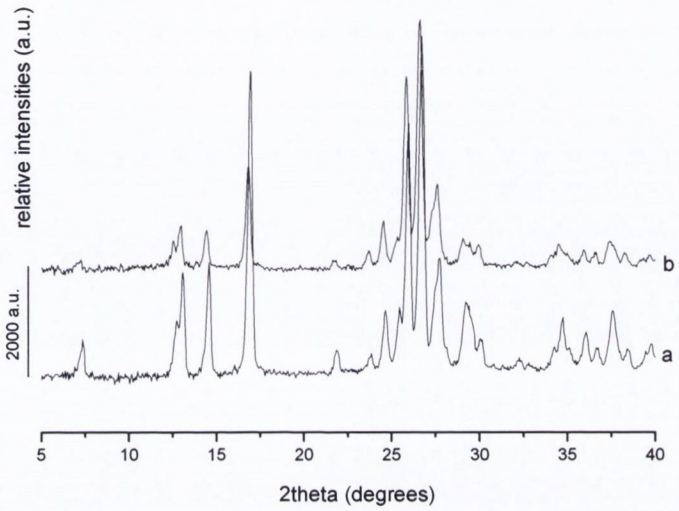

Figure 3.80- XRD scans of (a) PAS starting material (b) PAS ammonium salt spray-dried from 90% v/v ethanol at inlet temperature of 130°C (AS6) stored under vacuum overnight

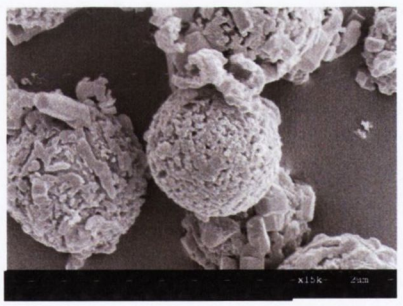

Figure 3.81- SEM micrograph of PAS ammonium salt spray-dried from 90% v/v ethanol at inlet temperature of 130°C (AS6) stored under vacuum overnight

It could be concluded that ammonium salt of PAS decomposes and ammonia, together with the solvent, escape in the exhaust gas of the spray dryer. High inlet temperature and post-treatment were required for the release of ammonia. This is in good agreement with the observation of Chuck and Zacher (2000), who stated that ammonium nicotinate, decomposes by spray drying and ammonia, together with the solvent, escape in the exhaust gas of the spray dryer.

Conclusion

A novel spray drying method was used to produce particles of PAS suitable for inhalation. The drug was spray dried in solution from a range of co-solvent system, the composition of the co-solvent employed in the spray drying process had a significant effect on the morphology of the spray dried particles.

Spray drying of PAS, at concentrations of 1, 3 and 4% w/v from different ethanolic solvents, results in crystalline particles. The particle morphology of PAS spray-dried systems varied depending on the systems spray-dried. Physicochemical characterisation of the spray dried samples demonstrated that each powder was crystalline in nature, contained low residual solvent content (≤1%) and was comprised of particles with acceptable range of particle sizes for pulmonary administration.

Spray drying of PAS/ammonium carbonate, results in crystalline particles. Ammonium carbonate concentration employed in the spray drying process is important to the successful production of uniform spherical particles. The solid state of PAS/ammonium carbonate was changed by spray drying from either methanol or ethanol. However, spray drying of PAS/ammonium carbonate did not result in production of the main degradation product of PAS (3-aminophenol), alternatively, the change may be correlated to the acidic nature of PAS. In addition, similar changes were also shown by using ammonium bicarbonate as a process additive instead of ammonium carbonate. The stoichiometry of the recovered particles could be 2:1:0.5 PAS: ammonia: water as confirmed by elemental analysis, ammonia assay, Karl Fischer titration and TGA.

Spray dried PAS systems show good potential for pulmonary delivery as indicated by the increase in emitted dose relative to the micronised PAS. In addition, Spray drying proved a successful method of producing microspherical particles, which deposited in the lower region of the twin stage impinger indicating that they were in the respirable range.

Spray drying PAS ammonium salt resulted in microcrystalline aggregates; the alteration of solid state of the salt by spray drying was confirmed by XRD, DSC and elemental analysis. In contrast, Spray drying of ammonium salt of PAS at high inlet temperature resulted in production of the acid form of PAS which could be due to decomposition of the salt upon spray drying as confirmed by thermal and elemental analysis, therefore, the alteration of ammonium salt upon spray drying at lower temperature is perhaps due to incomplete decomposition of the salt at these low inlet temperatures. Decomposition of ammonium salt of PAS upon exposure to heating during spray drying process was consistent with

Guseinov et al., (1981) who reported that thermal decomposition of ammonium salts can proceed by the heating of the salt in a stream of inert gas.

In vitro characterization of the spray dried salt showed an increase in emitted dose relative to the micronised PAS, suggesting the potential for high *in vivo* lung deposition.

CHAPTER 4- SPRAY DRYING OF ACIDIC COMPOUNDS

4.1 Introduction

As previously discussed (Chapters 3), spray drying p-aminosalicylic acid/ammonium carbonate resulted in a new solid state. This was in contrast to the results reported by other researchers in our research group who used ammonium carbonate and produced excipient-free NPMPs (Tajber, 2005, McDonald, 2005, Nolan and 2008, Nolan et al., 2009). Ammonium carbonate did not evaporate completely upon spray drying of PAS/ammonium carbonate, which was attributed to the acidic nature of PAS. In a continuation of the results obtained by spray drying of different PAS/ammonium carbonate systems, different acidic compounds (benzoic acid, salicylic acid, sulfacetamide and sulfamethizole) and their ammonium salts were selected as model drug compounds to investigate the production and physicochemical properties of the solid-state produced using a spray drying method.

To the best of our knowledge, no study on the production of porous particles by spray drying of ammonium salts is published in the literature yet. Therefore, the present study aims to give a description of the spray drying process, physicochemical properties and morphological observations from SEM of the recovered powder from spray drying of different ammonium salts.

In the current work, detailed descriptions of spray drying of different acidic compounds either with or without ammonium carbonate, as well as spray drying process of different ammonium salts are presented. The solid-state natures of particles recovered from the spray drying process are characterised in terms of their physicochemical properties. Comparisons between spray-dried and physical mixtures of different acidic compounds/ammonium carbonate are also undertaken.

4.2 SPRAY-DRIED BENZOIC ACID SYSTEMS

4.2.1 INTRODUCTION

Benzoic acid is the simplest aromatic carboxylic acid containing a carboxyl group bonded directly to a benzene ring. It is a white, crystalline powder or colourless crystals, odourless or with a very slight characteristic odour. It is soluble 1 in 300 of water, 1 in 3 of alcohol, 1 in 5 of chloroform, and 1 in 3 of ether; freely volatile in steam (Reynolds et al., 1996). The melting point of benzoic acid is between 121 °C and 124 °C (B.P. 2008). It has a pKa value of 4.19 (Indrayanto, et al., 1999). Benzoic acid was used as one of the model drugs for investigating this spray drying process, despite the fact that it is not used in inhalation therapy, due to similarity in structure between p-aminosalicylic acid and benzoic acid.

4.2.2 ETHANOL: WATER: AMMONIUM CARBONATE SPRAY-DRIED SYSTEMS

The spray drying conditions of 90% ethanol, inlet temperature 78 °C were selected for spray drying benzoic acid/ammonium carbonate composites, taking into consideration that similar spray drying conditions were used for spray drying of different solutions of p-aminosalicylic acid/ammonium carbonate. The ammonium carbonate concentration was 20%, 34% and 50% (weight of solids) as outlined in Appendix I. The choice of 20% ammonium carbonate was based on the morphological characteristics of p-aminosalicylic acid/ ammonium carbonate 80:20. The solution of benzoic acid/ ammonium carbonate 66:34 was used as it represents benzoic acid: ammonium carbonate (1:1 molar ratio) according to the ammonia contents reported by the supplier in the product specification sheet, where ammonia contents in ammonium carbonate is 30% of its weight. 50% ammonium carbonate was also used to study the effect of using ammonium carbonate higher than 1:1 benzoic acid: ammonium carbonate. A total solid concentration in solution of 3% w/v was used in all cases.

4.2.2.1 X-ray powder diffraction studies

X-ray diffractograms of benzoic acid, ammonium benzoate and spray dried benzoic acid/ammonium carbonate are shown in Figure 4.1. The peak positions in the scan of benzoic acid unprocessed material were consistent with the XRD scan presented by Rotich et al., (2003b) for benzoic acid. However, the pattern for the spray dried samples is different, which may be due to possible interaction between benzoic acid and ammonium carbonate. This was consistent with the results of XRD of spray dried PAS/ammonium

carbonate (Chapter 3), which gave evidence of alteration of the solid state of PAS upon spray drying with ammonium carbonate.

The black arrows in the XRD scans indicate positions where peaks were attributable to those of ammonium benzoate, while the red arrows indicate positions where peaks are attributable to those of benzoic acid. However, hundred percent relative intensity peak in X-ray diffractogram of benzoic acid was at approximately 8.12 degrees, this peak was not found in the scans of spray-dried systems. It was also noticed that some peaks found in X-ray diffractograms of all spray-dried composites (blue arrows) could not be attributed to either benzoic acid or ammonium benzoate, which indicates the formation of a new solid state upon spray drying of benzoic acid/ammonium carbonate regardless of the amount of ammonium carbonate used in the spray drying process.

It could be concluded that spray drying of benzoic acid under these conditions resulted in alteration of the solid stat of benzoic acid; this was compared favourably with the results of analyses of spray dried PAS/ammonium carbonate (Chapter 3).

X-ray diffractograms of spray-dried and physical mixture of benzoic acid/ammonium carbonate are presented in Figure 4.2. The black arrows indicate peaks in the X-ray diffractogram of the physical mixture, which could not be attributed to any of the individual components. Therefore, the XRD pattern of a physical mixture of benzoic acid with ammonium carbonate was not a superimposition of individual patterns, which may be attributed to interaction between benzoic acid and ammonium carbonate upon mixing. The green arrows indicate where peaks are different between the spray-dried and physical mixture of benzoic acid/ammonium carbonate. The differences between the spray-dried sample and the physical mixture exclude the assumption that the new solid state obtained by spray drying was due to presence of mixture of benzoic acid and ammonium carbonate. These results were confirmed by spray drying of ammonium carbonate from 90% ethanol at an inlet temperature of 78 °C, where ammonium carbonate was completely evaporated during spray drying process and no yield was collected.

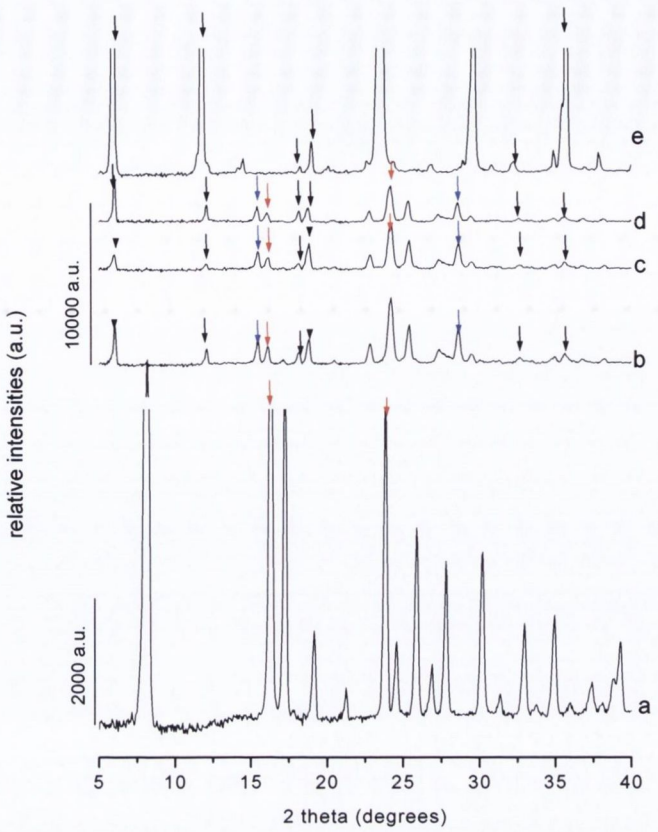

Figure 4.1- X-ray powder diffraction patterns of (a) benzoic acid unprocessed material and benzoic acid/ammonium carbonate (b) 80:20 (c) 66:34 (d) 50:50 spray-dried systems (e) ammonium benzoate starting material. The black arrows show where peaks on the scans of spray dried samples are attributable to ammonium benzoate, the red arrows show where peaks are attributable to benzoic acid, the blue arrows show where peaks in the scans of spray dried samples could not be attributed to either the acid or salt form of benzoic acid.

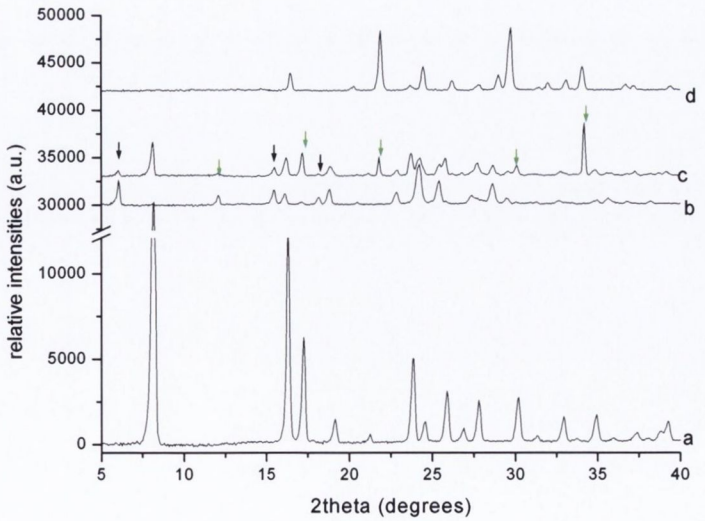

Figure 4.2- XRD scans of (a) benzoic acid unprocessed material (b) spray-dried benzoic acid/ammonium carbonate (c) physical mixture of benzoic acid/ammonium carbonate (d) ammonium carbonate. The black arrows indicate peaks in the XRD scan of the physical mixture, which could not be attributed to any of the individual components. The green arrows indicate where peaks are different between the spray-dried and physical mixture of benzoic acid/ammonium carbonate.

4.2.2.2 Thermal behaviour of spray dried composites

Figure 4.3 shows the DSC scans of benzoic acid, ammonium benzoate and various spray dried benzoic acid/ammonium carbonate systems. In the DSC thermogram of benzoic acid only one endotherm peaking at ~122 °C was observed with its onset at ~121°C, consistent with the literature values of 121°C -124°C for the melting temperature (B. P., 2008), with measured enthalpy of fusion of 141 J/g. Rotich et al., (2003b) reported that benzoic acid exhibited endothermic peak when melting took place at 122 °C. The DSC curve for the spray-dried benzoic acid/ammonium carbonate 80:20 system shows very small endotherm onset 122°C (melting point of benzoic acid), with measured enthalpy of fusion of 3.74 J/g. The decrease in the endotherm associated with the melting of benzoic acid is an indication of an interaction between benzoic acid and ammonium carbonate. This endotherm was followed by a broad endotherm peaking at 162°C. None of the other spray-dried composites shows an endotherm indicative of melting of benzoic acid, broad endotherms peaking at 162 and 158 °C were shown in DSC thermograms of spray-dried benzoic acid/ammonium carbonate 66:34 and 50:50, respectively, which indicate the change of solid state of the spray-dried systems.

In contrast to the spray-dried samples, there was an endothermic peak visible on examination of DSC thermograms of different physical mixtures of benzoic acid/ammonium carbonate attributable to melting of benzoic acid (Figure 4.4), which confirm the formation of new solid state upon spray drying of benzoic acid/ammonium carbonate.

Figure 4.5 illustrates TG curves of unprocessed benzoic acid and various benzoic acid/ammonium carbonate spray-dried systems. The TG curve gave single stage mass loss for unprocessed benzoic acid. The onset of the mass loss for benzoic acid is at about 85 °C and, at 158°C, 98% of the original mass was lost. The TG scans of spray-dried samples showed one stage mass loss. However, the onset of the mass loss was similar to that of benzoic acid starting material, but 98% of the original mass was lost by ~ 130 °C, 138 °C and 142 °C as shown in TGA scans of spray-dried benzoic acid/ammonium carbonate 50:50, 66:34 and 80:20, respectively.

In general thermal analysis (DSC and TGA) of the spray dried samples showed that the mass loss of spray dried samples started at lower temperature in comparison to the starting material and even at lower temperature than that shown by DSC endotherms, this could be explained in the light of the findings reported by Rotich et al., (2001) who reported that benzoic acid derivatives begin to sublime well before melting points. Therefore, this

thermal behaviour of spray dried sample perhaps due to sublimation of the samples. TG-FTIR studies of these systems will be useful for explanation of thermal behaviour of the spray dried systems, but these studies were not made as these techniques were not available, however, this may be an area worth investigating in future studies of thermal behaviour of spray dried benzoic acid.

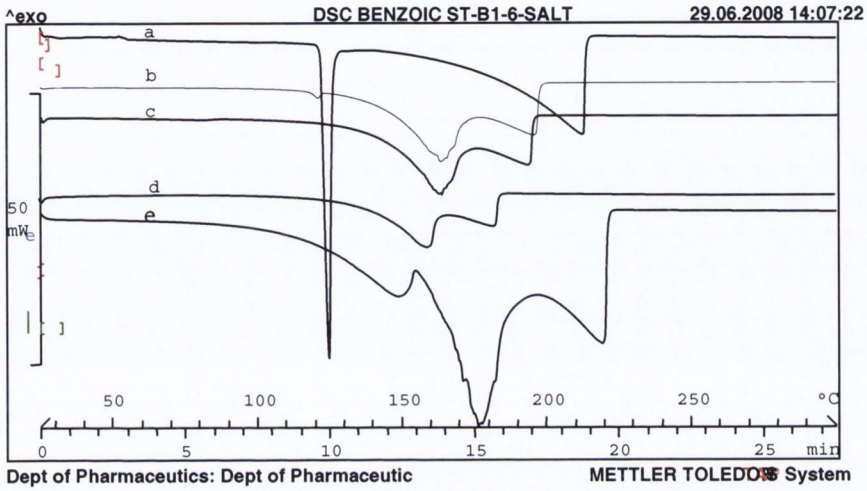

Figure 4.3- DSC scans of (a) benzoic acid raw material and spray-dried benzoic acid/ammonium carbonate (b) 80:20 (c) 66:34 (d) 50:50 (e) ammonium benzoate

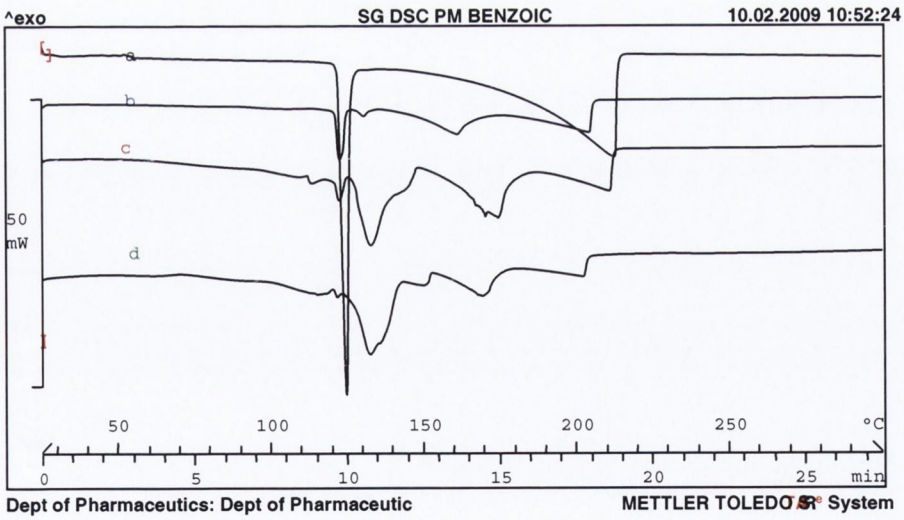

Figure 4.4- DSC scans of (a) benzoic acid raw material and physical mixtures of benzoic acid/ammonium carbonate (b) 80:20(c) 66:34 (d) 50:50

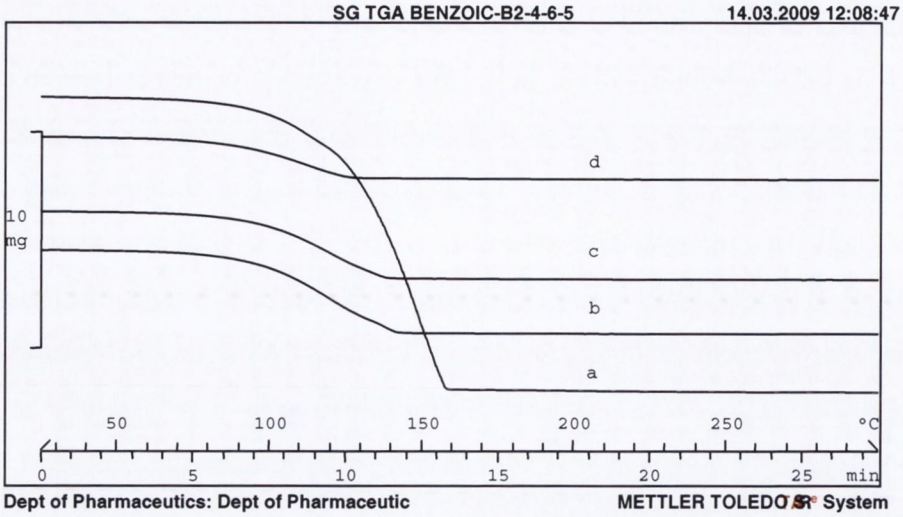

Figure 4.5- TGA scans of (a) benzoic acid raw material and spray-dried benzoic acid/ammonium carbonate (b) 80:20 (c) 66:34 (d) 50:50

4.2.2.3 Infrared spectroscopic studies

The analysis of the IR spectra of benzoic acid, as well the spectra of benzoic acid/ammonium carbonate spray-dried samples were carried out to compare the processed samples to the starting material. FTIR spectrum of unprocessed benzoic acid shows a broad feather in the 3300-2500 cm^{-1} region, which could be assigned to bonded OH stretching vibration (Figure 4.6). The spectrum also showed a signal at 1686 cm^{-1}, which was assigned to the asymmetric C=O stretching vibration, this was favourably compared to the infrared spectrum of benzoic acid reported by Indrayanto et al., (1999). The C=O absorption signal was shifted in the spectrum of spray-dried composites to 1700 cm^{-1}, which was different from that of the starting material and perhaps due to interaction of benzoic acid and the process enhancer, meanwhile, an extra band appeared at 1397 cm^{-1}, not found in the scan of the benzoic acid unprocessed material, perhaps of ammonia. However, FTIR scan of ammonium benzoate has the signal due to the carbonyl group at 1535 cm^{-1} (Oxton et al., 1977). Therefore, the recovered particles are not of the 1:1 ammonium salt of benzoic acid.

It is obvious that FTIR scans indicate that spray drying under these conditions alters benzoic acid chemically; this was confirmed by comparing the fingerprint region of unprocessed and spray-dried benzoic acid, which was different. In addition spray drying did not result in production of the 1:1 ammonium salt of benzoic acid.

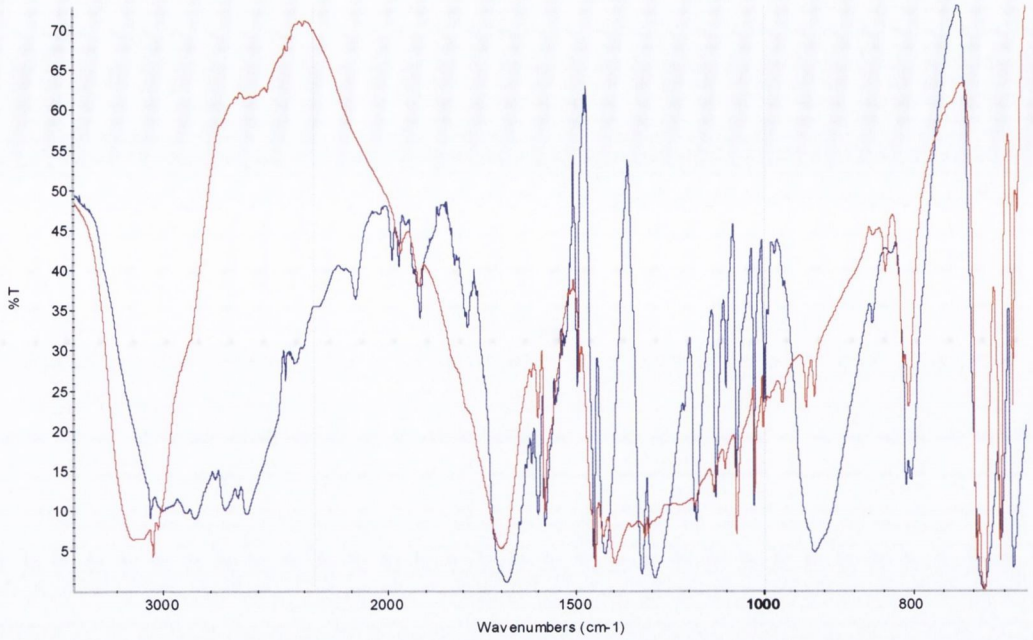

Figure 4.6- FTIR scans of benzoic acid (blue line) and spray-dried benzoic acid/ammonium carbonate (red line).

SEM micrographs of unprocessed benzoic acid and spray-dried composites are shown in Figure 4.7. The fused particles shown in the micrographs could be due to the use of vacuum during the coating and visualisation process as benzoic acid is sublimable material.

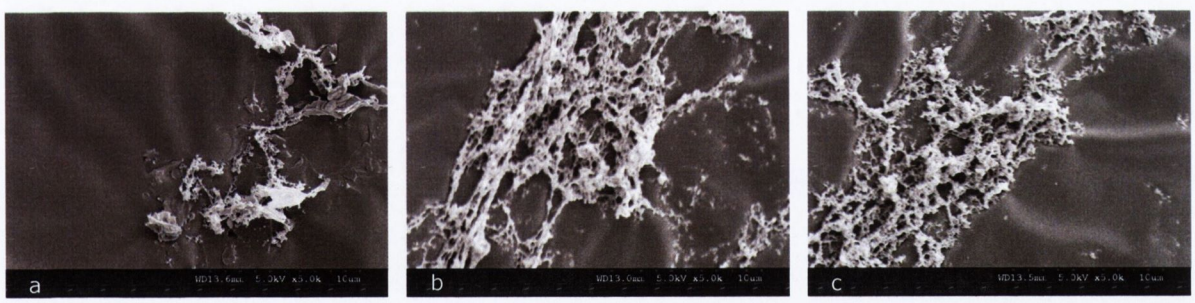

Figure 4.7- SEM micrographs of (a) unprocessed benzoic acid and spray-dried benzoic acid/ammonium carbonate (b) 80:20 (c) 66:34.

4.2.2.4 Stoichiometry of spray dried benzoic acid/ammonium carbonate

Elemental analysis (CHN) was carried out for benzoic acid starting material and benzoic acid/ammonium carbonate spray-dried system; the results are presented in Table 4.1. The results of CHN contents of spray dried composites were not consistent with the results reported by Indrayanto et al., (1999) for benzoic acid raw material. In addition, the analysis confirmed that the chemical composition of the spray-dried samples differed from that of

benzoic acid starting material; It is obvious that while there was no nitrogen in benzoic acid unprocessed material, the analysis of the spray-dried samples showed that it contains more than 5% nitrogen, which indicate alteration of benzoic acid upon spray drying of the composites.

For the purpose of estimation of the stoichiometry of the spray dried benzoic acid/ammonium carbonate, in addition of elemental analysis, determination of water contents by Karl Fischer titration was also undertaken. Unfortunately, TGA could not be used for interpretation of the results due to the sublimable nature of benzoic acid.

The stoichiometry of the spray dried composites could be 2:1 benzoic acid: ammonia. This was confirmed by elemental analysis of the recovered particles from spray drying process, which gave elemental analysis consistent with this stoichiometric ratio as shown in Table 4.1. This was different from the stoichiometry of recovered particles from spray dried p-aminosalicylic acid/ ammonium carbonate, therefore, determination of water contents in spray dried samples was important. The results of Karl Fischer titration of all spray dried composites was below the limit of detection (1%).

Table 4.1- Elemental analysis of different benzoic acid systems. Key: SD= spray dried, BOC = benzoic acid, AC= ammonium carbonate, C = Carbon, N = nitrogen, H = hydrogen, Calculated= results of calculation and Found= results of analysis.

Sample		Analysis		
		C	H	N
BOC	Calculated	68.84	4.95	0
SD BOC/AC 80:20	Found	64.43±0.03	5.89±0.07	5.23±0.16
SD BOC/AC 71:29	Found	64.23±0.25	5.96±0.02	5.51±0.23
SD BOC/AC 66:34	Found	64.19±0.20	5.95±0.04	5.47±0.28
SD BOC/AC 50:50	Found	64.22±0.16	5.93±0.01	5.38±0.15
Acid: ammonia 2:1	Calculated	64.60	5.42	5.38

4.2.3 Ethanol: water spray-dried systems

Benzoic acid was spray-dried to study the effect of spray drying process on its solid state and to compare with benzoic acid/ammonium carbonate spray-dried systems. A 3% (w/v) solution of benzoic acid was spray-dried from 90% ethanol (Appendix I). To allow for comparisons, the spray drying conditions selected were identical to the benzoic acid/ammonium carbonate systems, with the exception of the use of ammonium carbonate.

The FTIR spectrum of spray dried benzoic acid shows a broad feather in the 2500–3000 cm^{-1} region. The spectrum also showed a signal at 1686 cm^{-1}, which was assigned to the asymmetric C=O stretching vibration, this was favourably compared to the infrared characteristics of benzoic acid reported by Wang et al., (2007). In addition, the spectra of both unprocessed and spray dried samples show the characteristic peaks at the same wavenumbers. This indicates the similarity of vibration in bonding energies of the spray dried sample and that processing did not alter the chemical structure of the compound (Figure 4.8).

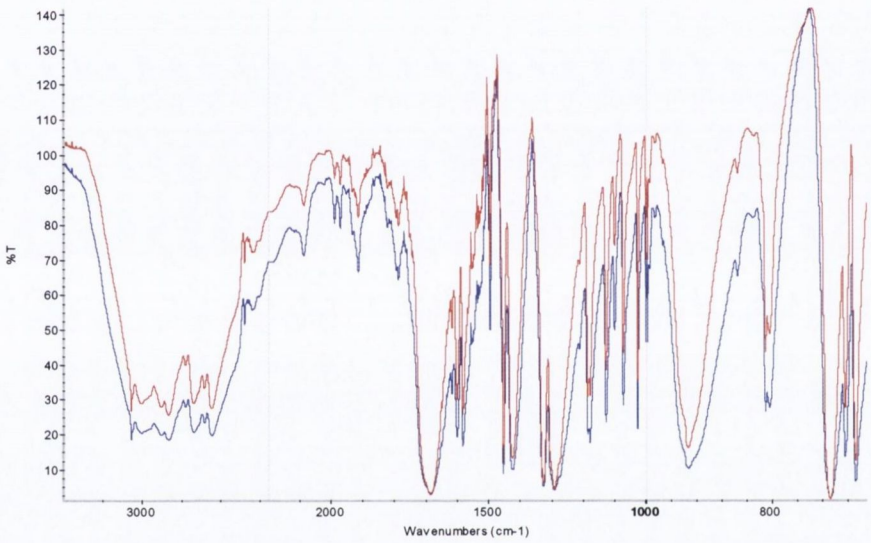

Figure 4.8- FTIR scans of benzoic acid starting material (blue line) and benzoic acid spray-dried from 90% ethanol (red line).

Figure 4.9 shows the X-ray diffractograms of unprocessed and spray-dried benzoic acid. The powder X-ray diffractogram of spray dried sample was typical of a crystalline material. The peak positions and their relative intensities were consistent with the XRD spectrum presented by Rotich et al., (2003b) for unprocessed benzoic acid. In addition, spray dried sample displayed a diffraction pattern similar to benzoic acid raw material, however with reduced peak intensities. XRD analysis demonstrated that the degree of crystallinity of benzoic acid unprocessed material was greatly reduced by spray drying. The percentage content of the crystalline form was calculated from XRD experiments, with the crystallinity of unprocessed benzoic acid assumed 100%. The combined integrated area under the three sharp peaks positioned at approximately 8.2, 16.3 and 17.3 degrees was taken for calculation. The combined area under the peaks of 3% benzoic acid spray-dried from 90% v/v ethanol showed a reduction in crystallinity of 65%.

Figure 4.10 compares the DSC thermograms of spray-dried sample of benzoic acid from 90% ethanol system with that of the starting material. In the DSC thermogram of the unprocessed starting material, only one endotherm peaking at 122 °C was observed, with its onset at 121 °C. The DSC scan of benzoic acid spray-dried from 90% (v/v) confirmed the crystallinity of the spray dried sample as the thermogram displayed only one thermal event, an endotherm peaking at 122 °C, attributed to benzoic acid melting as confirmed by the literature value of 121 °C to 124 °C for benzoic acid melting (B.P. 2008). This is in good agreement with thermal behaviour of benzoic acid as reported by Rotich et al., (2001). It could be concluded that spray drying did not result in significant alteration of thermal behaviour of unprocessed benzoic acid.

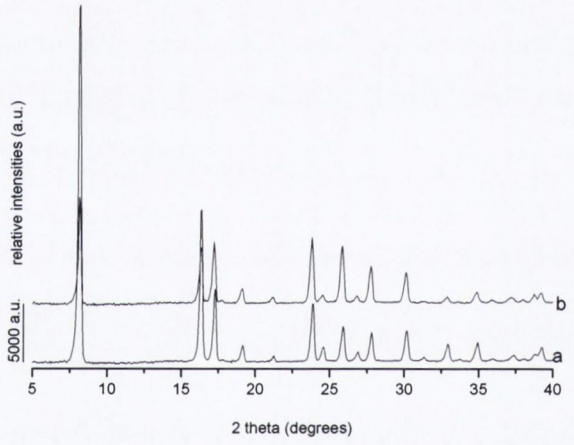

Figure 4.9- XRD scans of (a) benzoic acid unprocessed material (b) benzoic acid spray-dried from 90% ethanol.

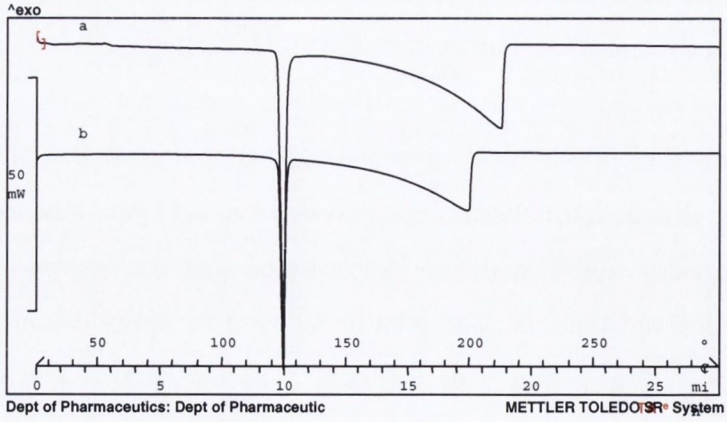

Figure 4.10- DSC scans of (a) benzoic acid starting material (b) benzoic acid spray-dried from 90% ethanol.

4.2.4 AMMONIUM BENZOATE SPRAY-DRIED SYSTEMS

As shown in Chapter 3, spray drying of ammonium salt of PAS resulted in partial decomposition of the salt and production of a new solid state form. In a continuation of these findings, ammonium benzoate was selected as a model drug compound to investigate the physicochemical properties of spray dried ammonium salts. A 3% (w/v) solution of ammonium benzoate was prepared and spray-dried from 90% (v/v) ethanol, at an inlet temperature 78 °C. XRD scan of the spray-dried sample provided evidence of differences between the spray-dried sample, ammonium benzoate starting material and benzoic acid, as the spray-dried sample had different peak positions than that of either ammonium benzoate or benzoic acid (Figure 4.11). It was also noticed that XRD pattern of spray-dried salt was similar to the pattern of spray-dried benzoic acid/ammonium carbonate (Figure 4.11 b and c). Similar results were obtained when the X-ray diffractograms of spray-dried ammonium salt of p-aminosalicylic acid were compared to spray-dried p-aminosalicylic acid/ammonium carbonate. XRD scans of spray-dried ammonium benzoate and spray-dried benzoic acid/ammonium carbonate showed peaks attributable to the salt form (black arrows), peaks attributable to the acid form (red arrows) and new peaks which could not be attributed to either the acid or the salt forms of benzoic acid (blue arrows).

Elemental analysis was carried out for spray-dried ammonium benzoate; the results are presented in Table 4.2. The analysis showed that the chemical composition of the spray-dried sample differed from that of benzoic acid and of the ammonium benzoate starting materials. Elemental analysis showed that the nitrogen content of spray-dried sample was lower than the nitrogen content of ammonium benzoate starting material, while carbon contents of spray-dried sample was higher than that of ammonium benzoate (Table 4.2). This difference in nitrogen and carbon contents between unprocessed and spray-dried sample is perhaps due to partial decomposition of ammonium benzoate upon spray drying. It should be noted that Chuck and Zacher (2000) reported decomposition of ammonium salt upon spray drying; they showed that ammonium nicotinate decomposes and ammonia, together with the solvent, escape in the exhaust gas of the spray dryer.

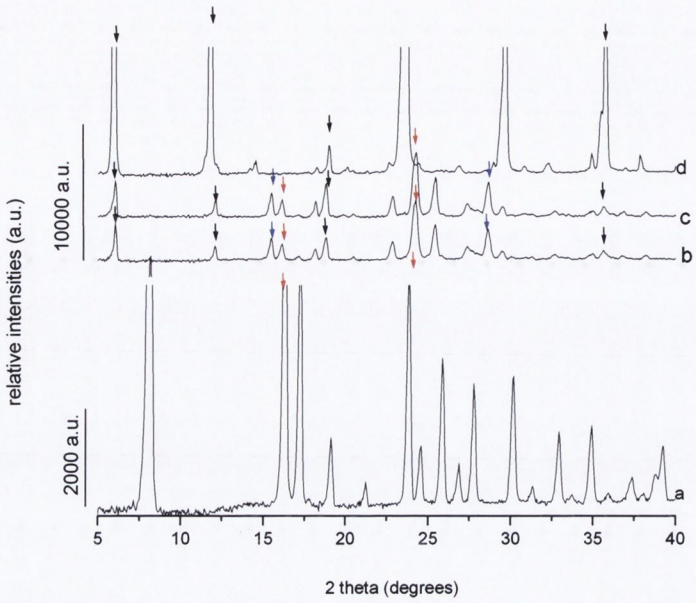

Figure 4.11- XRD scans of (a) benzoic acid starting material (b) benzoic acid/ammonium carbonate spray-dried from ethanol (c) ammonium benzoate spray-dried from ethanol (d) ammonium benzoate starting material. Key: peaks in XRD scans of processed samples attributable to the salt form (black arrows), peaks attributable to the acid form (red arrows) and new peaks which could not be attributed to either the acid or the salt forms of benzoic acid (blue arrows).

Table 4.2- Elemental analysis of different benzoic acid systems

	%C	%H	%N
Benzoic acid	68.84	4.95	0
Spray dried ammonium benzoate	63.96±0.12	5.93±0.07	5.63±0.06
Ammonium benzoate	60.42	6.51	10.06

DSC scan of benzoic acid showed a sharp endotherm peaking at 122 °C attributable to benzoic acid melting. This is in good agreement with the observation of Rotich et al., (2001), who stated that the melting point of crystalline benzoic acid was 122 °C. DSC trace of ammonium benzoate, in contrast showed broad endothermic events that could be due to decomposition on melting. According to the manufacturer's specification sheet, ammonium benzoate melts at 192-198 °C with decomposition (Figure 4.12). The DSC scan of spray-dried ammonium benzoate showed a different pattern from unprocessed material with a broad endothermic peak at ~163 °C. The DSC thermogram of spray-dried benzoic acid/ammonium carbonate is comparable with that of spray-dried ammonium benzoate with a broad endothermic peak at ~162 °C.

It could be concluded from XRD scans and thermal analysis that a similar solid state is recovered upon spray drying of either ammonium benzoate or benzoic acid/ammonium carbonate.

Figure 4.13 illustrates TG curves of unprocessed and spray-dried ammonium benzoate. The TG curve gave single stage mass loss for both samples. 98% of the original mass of ammonium benzoate was lost by 161 °C; similar percentage mass loss occurred by 134 °C in the spray-dried sample. Generally TG showed that the mass loss of spray dried samples started at lower temperature in comparison to the starting material and even at lower temperature than that shown by DSC endotherms, this could be explained in the light of the findings reported by Rotich et al., (2001) who reported that benzoic acid derivatives begin to sublime well before melting point. Therefore, this thermal behaviour perhaps due to sublimation of the samples

SEM micrographs of unprocessed and spray-dried ammonium benzoate are shown in Figure 4.14. While the unprocessed particles were large irregular shape crystals, the spray-dried sample showed fused particles, which perhaps due to partial conversion of spray-dried ammonium benzoate to benzoic acid. As shown earlier benzoic acid is sublimable, so the use of vacuum during the coating and visualisation process may affect the morphological characters seen by SEM.

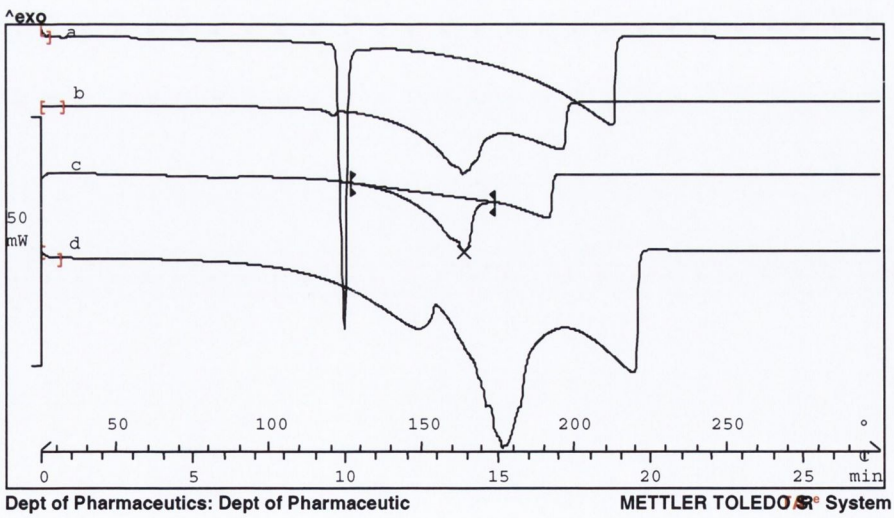

Figure 4.12- DSC scans of (a) benzoic acid starting material (b) spray-dried benzoic acid/ammonium carbonate (80:20) (c) spray-dried ammonium benzoate (d) ammonium benzoate starting material

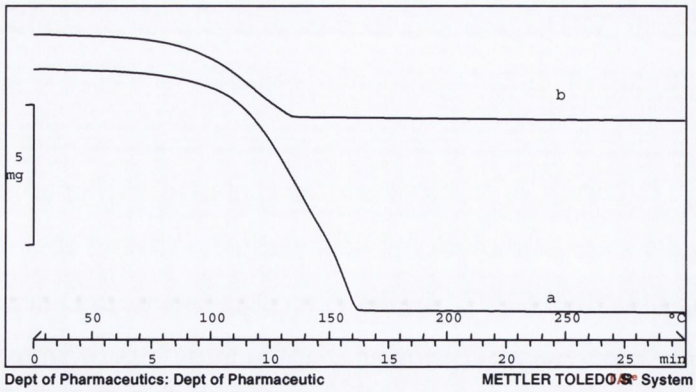

Figure 4.13- TGA scans of ammonium benzoate (a) unprocessed material (b) spray-dried from 90% ethanol.

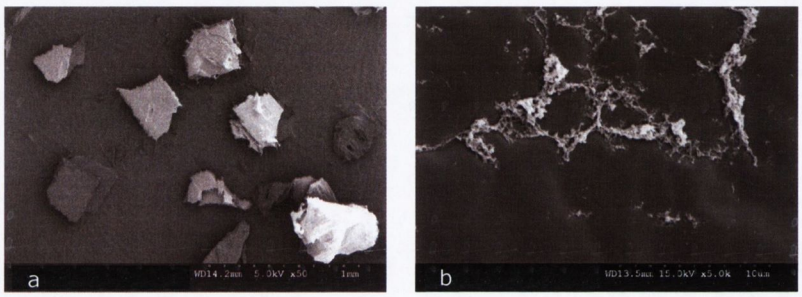

Figure 4.14- SEM micrographs of (a) unprocessed (b) spray-dried ammonium benzoate

4.3 Spray-dried salicylic acid systems

4.3.1 Introduction

Salicylic acid is an aromatic carboxylic acid. It is a white, crystalline powder or colourless crystals, odourless or with a very slight characteristic odour. Soluble 1 in 460 of water, 1 in 15 of boiling water, 1 in 3 of alcohol, 1 in 45 of chloroform, 1 in 3 of ether, and 1 in 135 of benzene (Reynolds et al., 1996). The melting point of salicylic acid is between 158 °C and 161 °C (B.P. 2008). It has a pKa value of 4.19 (Indrayanto, et al., 1999). Salicylic acid was selected for investigation due to its structural similarity with p-aminosalicylic acid to follow the findings of alteration of the solid state forms of acidic compounds upon spray drying with process enhancers. The structure of salicylic acid is shown in Figure 4.15.

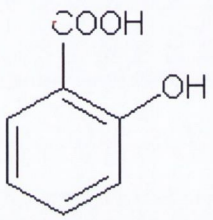

Figure 4.15-structure of salicylic acid

4.3.2 Spray-dried salicylic acid with ammonium carbonate

As previously reported (Chapter 3), using ammonium carbonate in spray drying process of p-aminosalicylic acid resulted in formation of uniform spherical agglomerates of microcrystalline particles. The solid state of recovered particles was different from either starting acid or prepared ammonium salt. The objective of this work was to spray dry salicylic acid systems to ascertain if similar results to those obtained by spray drying p-aminosalicylic acid/ ammonium carbonate could be obtained. A 3% solution of salicylic acid/ammonium carbonate was prepared in 90% (v/v) ethanol and spray-dried, using air as a drying gas. The ammonium carbonate concentration was 20%, 30%, 42% and 50% (weight of solids) as outlined in Appendix I. The choice of 20% ammonium carbonate was based on the morphological characteristics of 3% p-aminosalicylic acid/ ammonium carbonate 80:20 which showed spherical aggregates of microcrystalline particles. The solution of salicylic acid/ ammonium carbonate 70:30 was used as it represents salicylic acid: ammonium carbonate (1:1 molar ratio) molar ratio according to the ammonia contents reported by the supplier in the product specification sheet, where ammonia

contents in ammonium carbonate is 30% of its weight. On the other hand, 42% ammonium carbonate represents salicylic acid: ammonium carbonate 1:1 molar ratio according to the molecular weights of PAS and ammonium carbonate. 50% ammonium carbonate was also used to study the effect of using ammonium carbonate higher than 1:1 salicylic acid: ammonium carbonate. For these systems, the inlet temperature was set at 78°C.

4.3.2.1 X-ray powder diffraction studies

Figure 4.16 shows XRD scans of salicylic acid unprocessed material, different spray-dried salicylic acid/ ammonium carbonate systems and ammonium salicylate.

The XRD pattern of salicylic acid unprocessed material was consistent with the XRD scan presented by Rotich et al., (2003b) for salicylic acid. On the other hand, the XRD pattern of the Spray dried samples is different in comparison to that of starting material; peak positions shifted, the diffractograms showed peaks which could not attributed to the starting material, and there were differences in the relative peak intensities, which may be due to possible interaction between salicylic acid and ammonium carbonate. This was consistent with the results of XRD of spray dried benzoic acid/ammonium carbonate (Chapter 4.1), which gave evidence of alteration of the solid state of benzoic acid upon spray drying with ammonium carbonate.

The black arrows in the XRD scans indicate positions where peaks were attributable to those of ammonium salt, while the red arrows in the XRD scans indicate positions where peaks were attributable to those of the salicylic acid. Investigation of the XRD scans shows a gradual disappearance of the peaks attributable to salicylic acid from spray-dried salicylic acid/ammonium carbonate by increasing ammonium carbonate contents. It should be noted that peaks at approximately 14.8, 16.7 and 26.4 degrees, which could be attributed to ammonium salicylate were found in all spray-dried salicylic acid/ ammonium carbonate systems. While the peak at approximately 8.7 degrees was not found in the X-ray diffractogram of salicylic acid/ ammonium carbonate 80:20 spray-dried system, but was found in X-ray diffractograms of other spray-dried samples where higher concentrations of ammonium carbonate was used. It was also noticed that some peaks found in X-ray diffractograms of all spray-dried composites (blue arrows) could not be attributed to either salicylic acid or ammonium salicylate, which indicates the formation of a new solid state form upon spray drying of salicylic acid/ammonium carbonate regardless of the amount of ammonium carbonate used in the spray drying process.

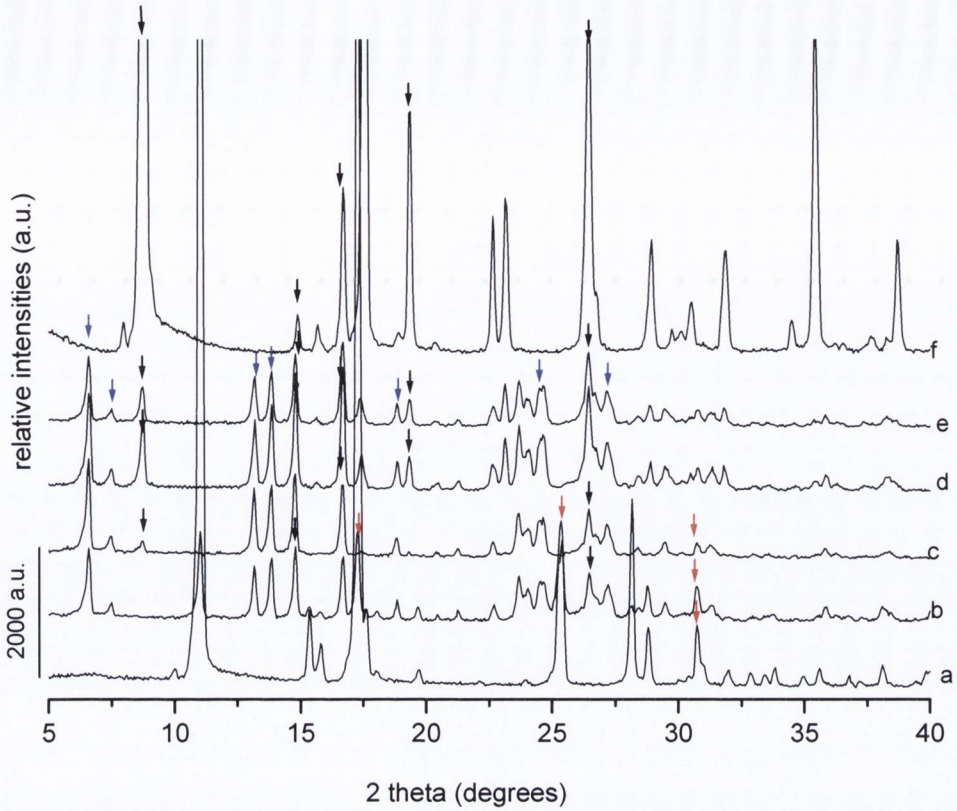

Figure 4.16- XRD scans of (a) salicylic acid unprocessed material and salicylic acid/ammonium carbonate (b) 80:20 (c) 70:30 (d) 58:42 (e) 50:50 spray-dried systems (f) ammonium salicylate. The black arrows in the XRD scans indicate positions where peaks are attributable to those of ammonium salt; the red arrows indicate positions where peaks are attributable to those of the salicylic acid, the blue arrows show where peaks could not be attributed to the acid or the salt.

X-ray diffractograms of spray-dried and physical mixture of salicylic acid/ammonium carbonate are presented in Figure 4.17. The XRD pattern for the physical mixture contains mainly superimposed features of the pure components. However, the X-ray diffractogram of the physical mixture showed peaks (black arrows) that could not be attributed to any of the individual components, the presence of these peaks confirm interaction between salicylic acid and ammonium carbonate upon mixing. The green arrows indicate where peaks are different between the spray-dried and physical mixture of salicylic acid/ammonium carbonate. The differences between the spray-dried sample and the physical mixture exclude the assumption that the new solid state obtained by spray drying was due to presence of mixture of salicylic acid and ammonium carbonate.

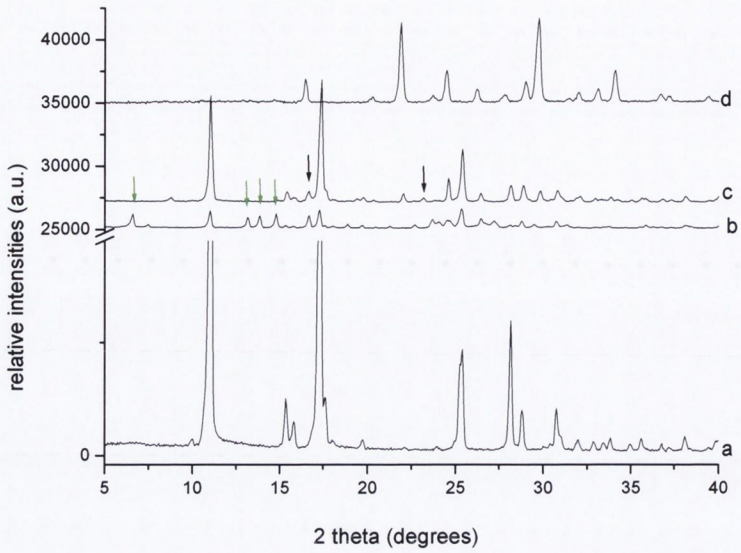

Figure 4.17- XRD scans of (a) salicylic acid unprocessed material (b) spray-dried salicylic acid/ammonium carbonate (c) physical mixture of salicylic acid/ammonium carbonate (d) ammonium carbonate. The black arrows indicate peaks in XRD scan of the physical mixture which could not be attributed to any of the individual components, the green arrows indicate where peaks are different between the spray-dried and physical mixture of salicylic acid/ammonium carbonate.

4.3.2.2 Thermal behaviour of spray dried samples

DSC scans of salicylic acid/ammonium carbonate spray-dried systems are shown in Figure 4.18. The DSC curve of salicylic acid starting material show sharp melting endotherm with its onset temperature of 158 °C, Rotich et al., (2001) reported that salicylic acid exhibited endothermic peak when melting took place at 158-162 °C. On the other hand, DSC results indicated that the thermal behaviour of salicylic acid/ammonium carbonate spray-dried systems differed from that of the starting material: endothermic peak position shifted, the peak became irregular in shape, and there were differences in the onset temperatures. The onset temperature was ~158°C for starting material and ~143°C, ~143°C and ~145°C for spray-dried salicylic acid/ammonium carbonate 70:30, 50:50 and 58:42, respectively. DSC thermogram of ammonium salicylate is also presented in Figure 4.18, where broad endothermic events were observed in the scan.

TGA registered weight loss of ~3% and ~10% from 25-100°C for unprocessed salicylic acid and salicylic acid/ammonium carbonate spray-dried systems, respectively (Figure 4.19).

This further loss is less than the expected value for almost complete evaporation/decomposition of 30, 42 and 50% by mass of ammonium carbonate in the

system, which confirm that the recovered particles are not simple physical mixtures, this was consistent with the XRD results of different salicylic acid systems which showed that the recovered particles were different from the physical mix.

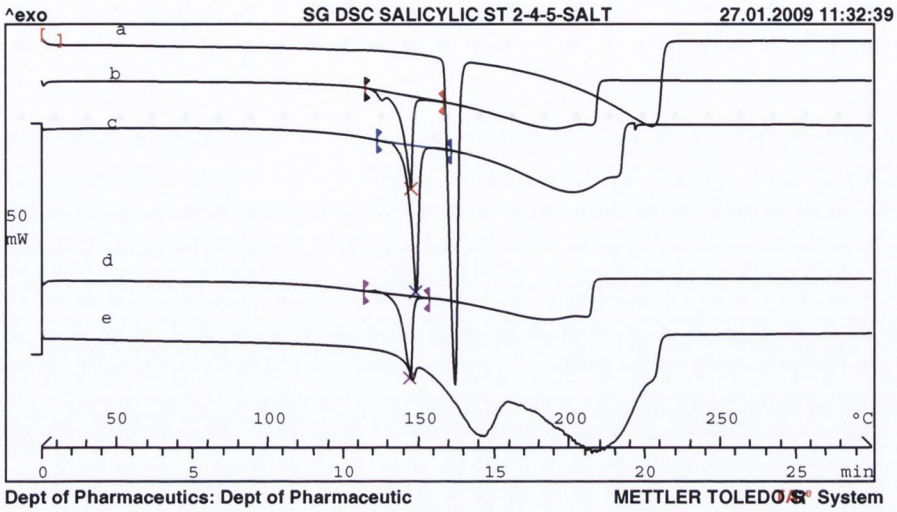

Figure 4.18- DSC scans of (a) salicylic acid unprocessed material and salicylic acid/ammonium carbonate (b) 70:30 (c) 58:42 (d) 50:50 spray-dried samples (e) ammonium salicylate.

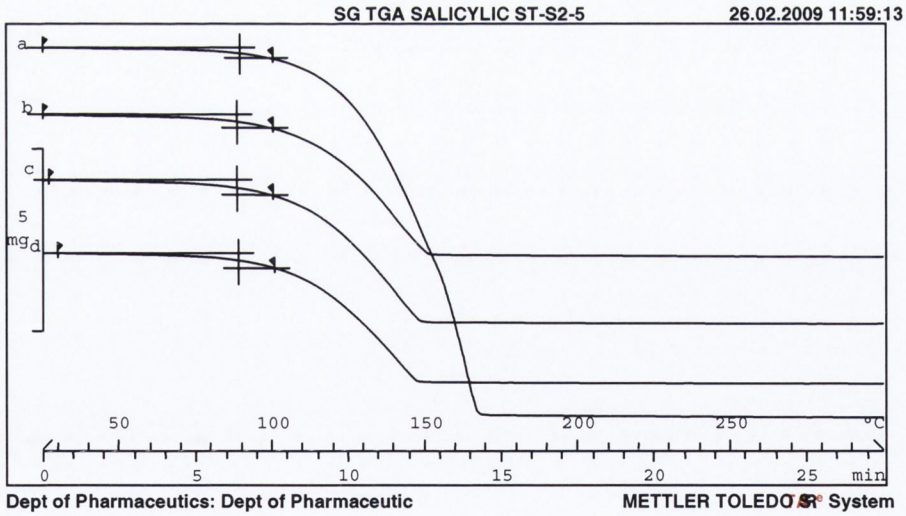

Figure 4.19- TGA scans of (a) salicylic acid unprocessed material and salicylic acid/ammonium carbonate ((b) 80:20 (c) 70:30 (d) 58:42 spray-dried systems.

4.3.2.3 Infrared spectroscopic studies

FTIR spectra of unprocessed salicylic acid showed signal at 1657 cm^{-1} due to the carboxylic carbonyl group and a signal at 3238 cm^{-1} due to the OH group, this was favourably compared to the reported infrared characteristics of salicylic acid reported by

Abounassif et al., (2001). The C=O absorption signal was shifted in the spectrum of spray-dried composites to 1676 cm^{-1}. The signal due to OH group in the spectra of the spray-dried samples was also shifted to 3216 cm^{-1}. The spectra of spray dried samples also showed a signal at 1388 cm^{-1}, this was not found in the scan of salicylic acid unprocessed material. This signal could be attributed to ammonia. On the other hand, FTIR scan of ammonium salicylate has a signal at 1620 cm^{-1} due to the carbonyl group. Therefore, the recovered particles are not of the 1:1 ammonium salt of salicylic acid.

The changes shown in fingerprint region of this spectrum in comparison to the spectrum of salicylic acid starting material suggest that spray drying under these conditions alter salicylic acid chemically (Figure 4.20). In addition, the resulted particles were not comparable to the parent acid or to ammonium salicylate.

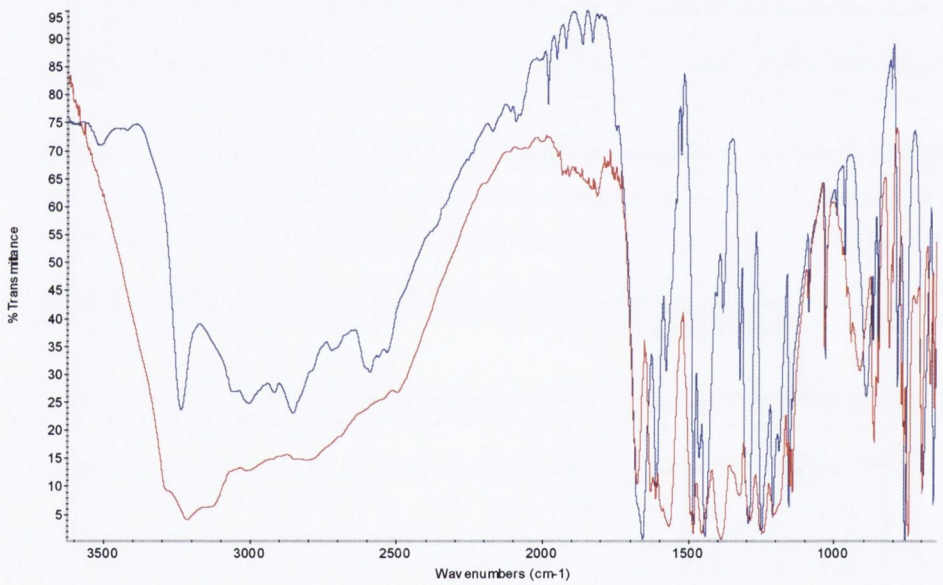

Figure 4.20- FTIR spectra of salicylic acid raw material (blue line) spray-dried salicylic acid/ammonium carbonate (red line).

SEM micrographs of salicylic acid/ammonium carbonate spray-dried systems are shown in Figure 4.21. Fused and collapsed particles were recovered; this may be due to application of vacuum during sample preparation and visualisation process.

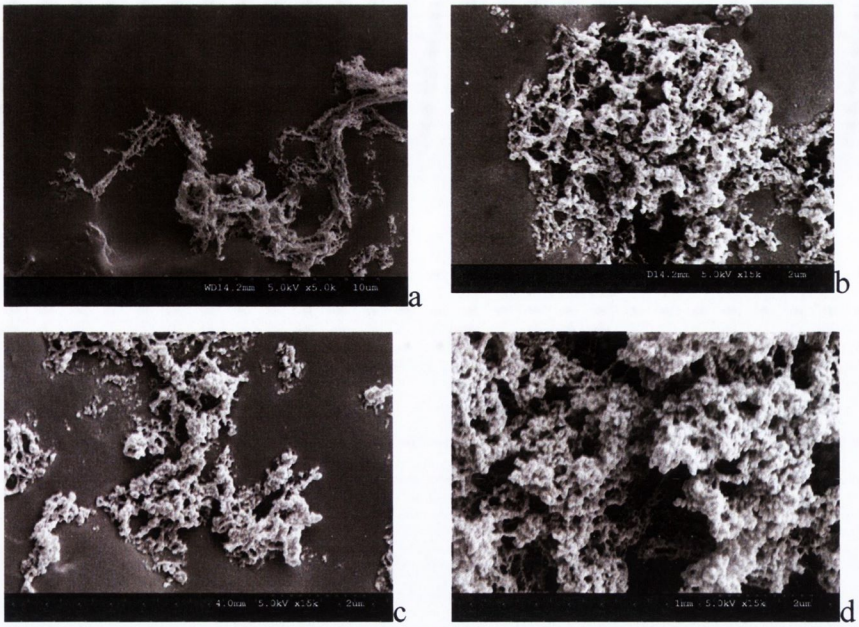

Figure 4.21- SEM scans of (a) salicylic acid unprocessed material and salicylic acid/ammonium carbonate (b) 70:30 (c) 58:42 (d) 50:50 spray-dried samples.

4.3.2.4 Stoichiometry of the salicylic acid systems

Elemental analysis (CHN) was carried out for different salicylic acid/ammonium carbonate spray-dried systems; the results are presented in Table 4.3. The analysis confirmed that the chemical composition of the spray-dried samples differed from that of salicylic acid starting material. It was also noticed that while there was no nitrogen in salicylic acid unprocessed material, the analysis of the spray-dried samples showed that it contains more than 4% nitrogen, regardless of amount of ammonium carbonate used in spray drying process, which indicate formation of a new solid state upon spray drying of the composites. The stoichiometry of the spray dried composites could be 2:1 salicylic acid: ammonia. This was estimated from elemental analysis of the recovered particles from spray drying process, which gave elemental analysis consistent with this stoichiometric ratio as shown in Table 4.3. This was different from the stoichiometry of recovered particles from spray dried p-aminosalicylic acid/ ammonium carbonate, therefore, determination of the water content in the spray dried samples was important. The results of the Karl-Fischer titration of the spray dried samples revealed that the water content was below the limit of detection (1%).

Another confirmation of the stoichiometry of spray dried samples is TG analysis; TG analysis revealed that the weight loss between 25˚C and 100˚C was approximately 3% and 10% for salicylic acid unprocessed material and the spray-dried composite. The difference in mass loss between the stating material and spray dried sample is 7%, this. In addition,

the loss of one ammonia molecule corresponds to a loss of ~7% by weight of salicylic acid: ammonia 2:1 when determined on a molecular weight basis. Therefore, the weight loss registered in spray dried composites is consistent with the loss of one molecule of ammonia.

This stoichiometry is consistent with the stoichiometry of recovered particles from spray dried benzoic acid/ ammonium carbonate (Chapter 4.1).

Table 4.3- Elemental analysis of different salicylic acid systems. Key: SD= spray dried, SAC = salicylic acid, AC= ammonium carbonate, C = Carbon, N = nitrogen, H = hydrogen.

Sample	Analysis		
	C	H	N
SAC	60.87	4.37	0
SD SAC/AC 80:20	57.36±1.56	5.02±0.33	5.03±0.40
SD SAC/AC 70:30	57.30±0.82	4.91±0.20	4.83±0.56
Acid: ammonia 2:1	57.53	4.82	4.79

4.3.3 Spray-dried salicylic acid without ammonium carbonate

As previously shown, spray drying of salicylic acid with ammonium carbonate had a significant effect on the physicochemical properties of spray dried composites. Therefore, it was important to study the effect of spray drying on the physicochemical characteristics of salicylic acid.

A 3% solution of salicylic acid was prepared in 90% (v/v) ethanol at an inlet temperature of 78°C, open cycle was used for this sample. Air was used as the drying gas. These spray drying conditions were selected to allow for comparison with the physicochemical properties of spray dried salicylic acid ammonium carbonate.

X-ray diffractograms of unprocessed and spray-dried salicylic acid are shown in Figure 4.22. The powder X-ray diffractogram of spray dried salicylic acid was typical of a crystalline material. The peak positions were consistent with the XRD scan presented by Rotich et al., (2001) for salicylic acid. In addition, spray-dried sample displayed a diffraction pattern similar to salicylic acid raw material, however with reduced peak intensities. XRD analysis demonstrated that the degree of crystallinity of salicylic acid raw material was greatly reduced by spray drying. The percentage content of the crystalline

form was calculated from XRD experiments, with the crystallinity of unprocessed salicylic acid assumed 100%. The combined integrated area under the three sharp peaks positioned at approximately 11.04, 17.3 and 28.15 degrees was taken for calculation. The combined area under the peaks of 3% salicylic acid spray-dried from 90% v/v ethanol showed a reduction in crystallinity of 67%.

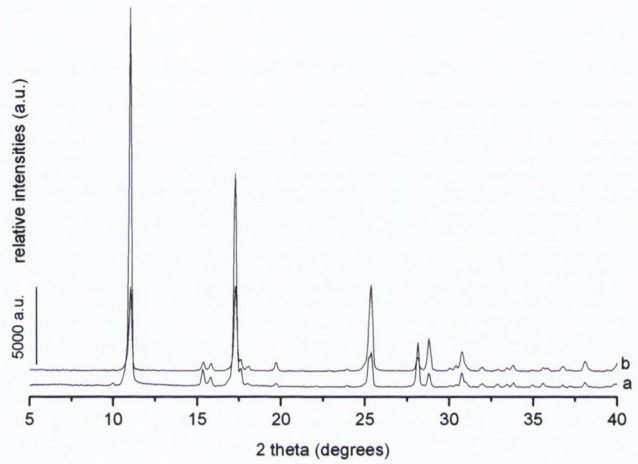

Figure 4.22- XRD scans of (a) salicylic acid unprocessed material (b) salicylic acid spray-dried from 90% ethanol.

Figure 4.23 compares the DSC thermograms of spray-dried sample of salicylic acid from 90% ethanol system with that of the starting material. In the DSC thermogram of the unprocessed starting material, only one endotherm peaking at 158 °C was observed, with measured enthalpy of fusion of 164.32 J/g. The DSC scan of salicylic acid spray-dried from 90% (v/v) displayed only one thermal event, an endotherm peaking at 158 °C, attributed to salicylic acid melting. This is in good agreement with the literature value of 158 °C to 161 °C for salicylic acid (B.P. 2008), with measured enthalpy of fusion of 164.3 J/g.

The shapes of TGA scans were similar for salicylic acid unprocessed and spray-dried powders (Figure 4.24). The TG curve for salicylic acid starting material heated in flowing nitrogen at 10 °C/min gives a one-stage mass loss. TGA registered weight loss of 3.11% and 3.72% over the temperature range of 25 to 100 °C for salicylic acid starting material and spray-dried salicylic acid from 90% (v/v) ethanol, respectively. The difference in weight loss over the temperature range of 25 to 100 °C between starting material and spray-dried sample could be attributed to residual solvent content in the spray-dried samples.

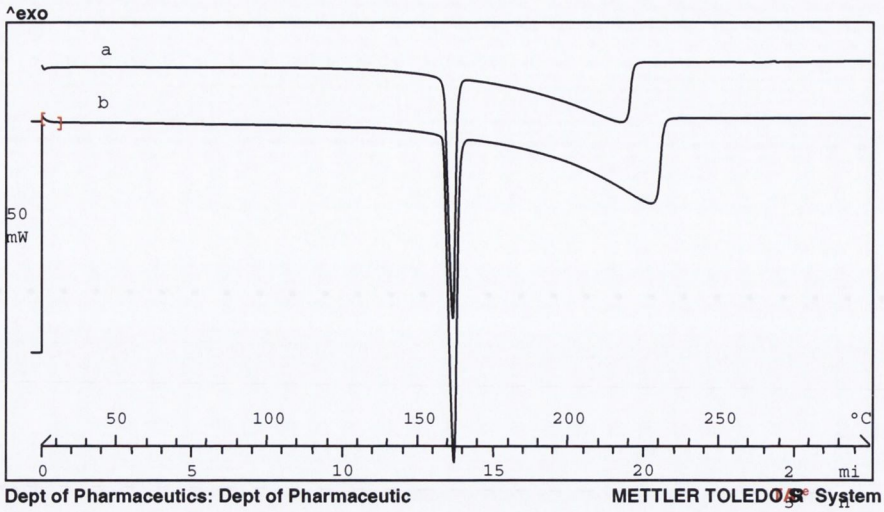

Figure 4.23- DSC scans of salicylic acid (a) spray-dried from 90% ethanol (b) unprocessed material

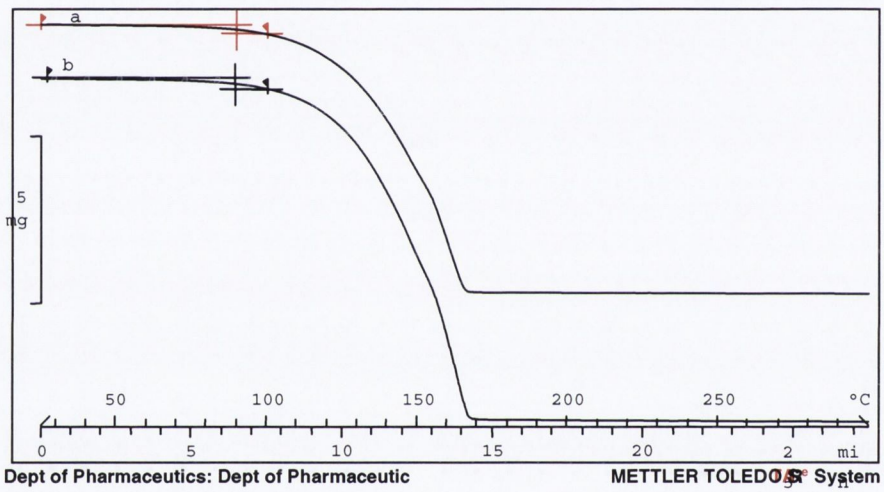

Figure 4.24- TGA scans of salicylic acid (a) spray-dried from 90% ethanol (b) unprocessed material

Infrared spectra of salicylic acid raw material and spray-dried salicylic acid system are shown in Figure 4.25. Abounassif et al. (2001) reported that salicylic acid has bands in the IR spectrum due to OH group at 3220 cm^{-1} and an absorption band at 1650 cm^{-1} due to carboxylic C=O group. The spectrum of salicylic acid raw material presented these characteristic signals at 3238 cm^{-1} for the OH group. The signal of OH group was observed at 3238 cm^{-1} for spray-dried salicylic acid. The spectra of both unprocessed and spray-dried salicylic acid showed signal at 1657 cm^{-1} due to carboxylic carbonyl group. The infrared spectrum of the spray-dried sample was nearly identical to that of the unprocessed material, indicating the similarity of vibration in bonding energies of the sample and that processing did not alter the chemical structure of the compound.

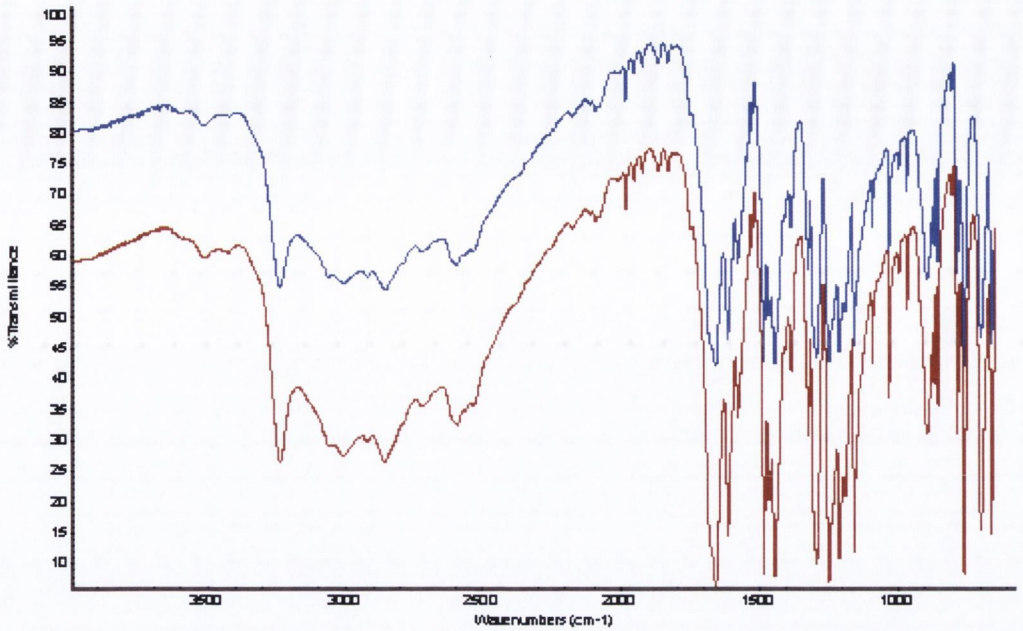

Figure 4.25- FTIR spectra of salicylic acid raw material (blue line) spray-dried salicylic acid (red line).

4.3.4 AMMONIUM SALICYLATE SPRAY-DRIED SYSTEMS

4.3.4.1 INTRODUCTION

A previous attempt at spray drying ammonium salt produced a new solid state, which was different from either the acid or salt form of p-aminosalicylic acid (refer to Chapter 3), ammonium salicylate was selected as model drug compound to investigate the physicochemical properties of spray-dried sample.

4.3.4.2 ETHANOL: WATER SPRAY-DRIED SYSTEM

A 3% (w/v) solution of ammonium salicylate was prepared and spray-dried from 90% (v/v) ethanol, at an inlet temperature 78 °C. These spray drying conditions, were selected based on previous work on spray-drying of ammonium salt of PAS (Chapter 3).

XRD scan of the spray-dried sample provided evidence of a difference between the spray-dried sample, ammonium salicylate starting material and salicylic acid unprocessed material, as the spray-dried sample had different peak positions than that of either ammonium salicylate or salicylic acid (Figure 4.26). It was also noticed that XRD pattern of spray-dried salt was similar to the pattern of spray-dried salicylic acid/ammonium carbonate (Figure 4.26 b and c). Similar results were obtained when the X-ray diffractograms of spray-dried ammonium salt of benzoic acid were compared to spray-dried benzoic acid/ammonium carbonate. XRD scans of spray-dried ammonium salicylate and spray-dried salicylic acid/ammonium carbonate showed peaks attributable to the salt

form (black arrows), peaks attributable to the acid form (red arrows) and new peaks which could not be attributed to either the acid or the salt forms of benzoic acid (blue arrows).

DSC scan of the spray-dried sample confirmed the differences between the spray-dried sample and ammonium salicylate starting material (Figure 4.27). DSC thermogram of spray-dried sample showed sharp endotherm peaking at ~148 °C with its onset at ~145 °C, while DSC scan of unprocessed ammonium salicylate showed broad endotherm. DSC scan of spray-dried sample was also different from the scan of salicylic acid raw material; peak position shifted, and there were differences in the onset temperatures (Figure 4.27). The onset temperature was ~158°C for salicylic acid starting material and ~145°C for spray-dried sample.

SEM micrographs showed that spray drying of this system resulted in fused particles as shown in Figure 4.28.

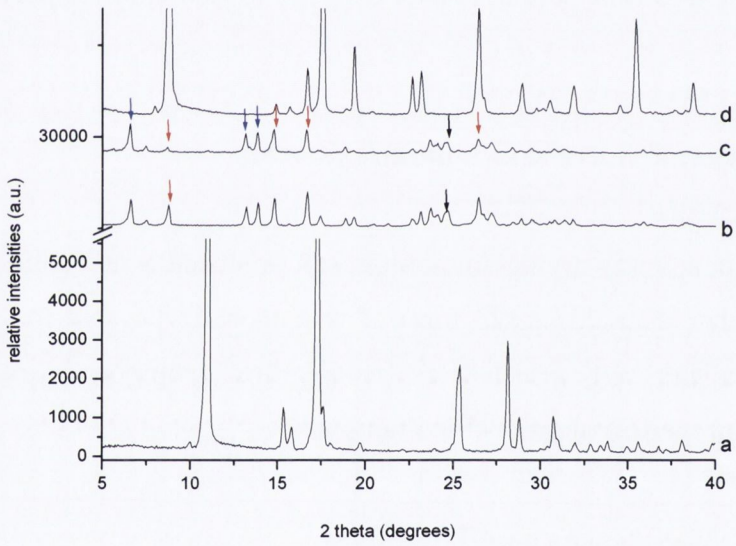

Figure 4.26- XRD scans of (a) salicylic acid starting material (b) spray-dried salicylic acid/ammonium carbonate (c) spray-dried ammonium salicylate (d) ammonium salicylate starting material. The red arrows in the XRD scans indicate positions where peaks could be attributed to ammonium salicylate, while black arrow indicates position where peak could be attributed to salicylic acid; the blue arrows indicate where peaks could not be attributed to any of the starting materials.

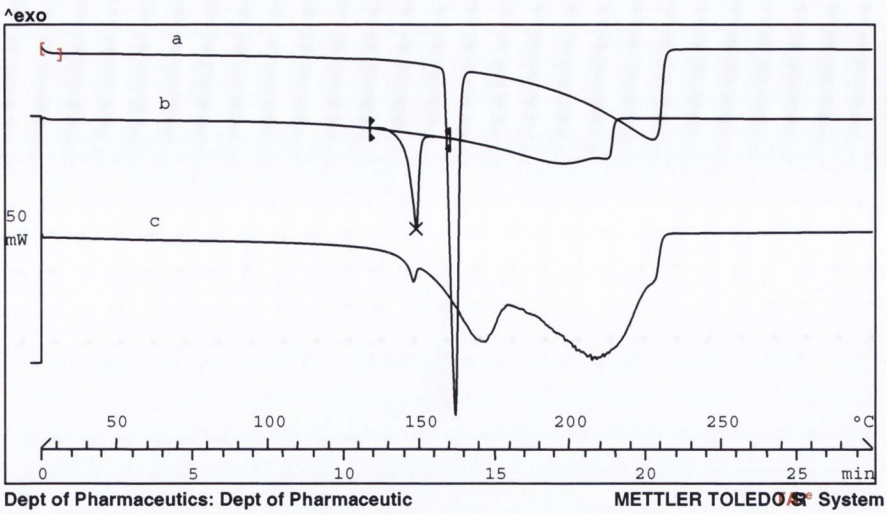

Figure 4.27- DSC scans of (a) salicylic acid starting material (b) spray-dried ammonium salicylate (c) ammonium salicylate starting material

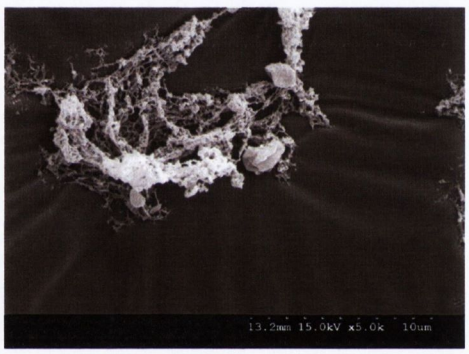

Figure 4.28 - SEM micrograph of ammonium salicylate system spray-dried from 90% ethanol

Figure 4.29 and 4.30 display spectra of salicylic acid raw material, spray-dried and unprocessed ammonium salicylate. In solid phase salicylic acid has bands in the IR spectrum due to OH group at 3220 cm^{-1} and an absorption band at 1650 cm^{-1} due to carboxylic C=O group (Abounassif et al. 2001). The spectrum of salicylic acid raw material presented these characteristic signals at 3238 cm^{-1} for the OH group. The spectra of both unprocessed and spray-dried salicylic acid showed signal at 1657 cm^{-1} due to carboxylic carbonyl group. On the other hand, FTIR scan of ammonium salicylate has signal at 1620 due to carbonyl group. Investigation of the IR spectrum of spray-dried ammonium salicylate showed a signal at 1677 cm^{-1} for the C=0 group. These characteristic bands are different from either salicylic acid or ammonium salicylate. In addition, the finger print region of the spectrum of spray-dried ammonium salicylate was different from both spectra of salicylic acid and the ammonium salt as shown in Figures 4.29 and 4.30. It could be concluded that the solid state form of the salt was altered chemically upon spray drying.

The change of ammonium salicylate upon spray drying was not surprising in the light of the published data about thermal decomposition of ammonium salts which can proceed in the solid phase by the heating of the dry salt in a stream of inert gas (Guseinov et al., 1981). Therefore, salicylic acid content of the spray dried ammonium salicylate was determined according to B.P (2008); the results showed that ammonium salicylate spray dried from 90% ethanol contained 56.01±1.33% salicylic acid. It should be noted that no salicylic acid was detected in ammonium salicylate unprocessed material when subjected to the same test which confirm that ammonium salicylate was partially converted to the acid form upon spray drying. This compares favourably with the results of spray dried ammonium nicotinate by Chuck and Zacher, (2000), who showed that ammonium nicotinate was decomposed by spray drying to produce the parent acid.

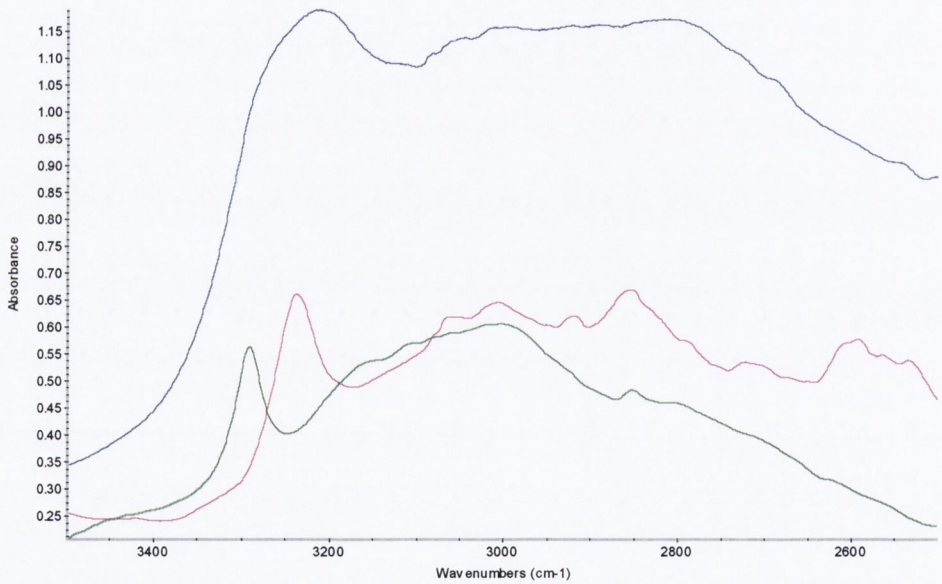

Figure 4.29- FTIR spectra in the region 2500–3500 $cm^{-1}$of salicylic acid raw material (red line), ammonium salicylate (green line) and spray-dried ammonium salicylate (blue line).

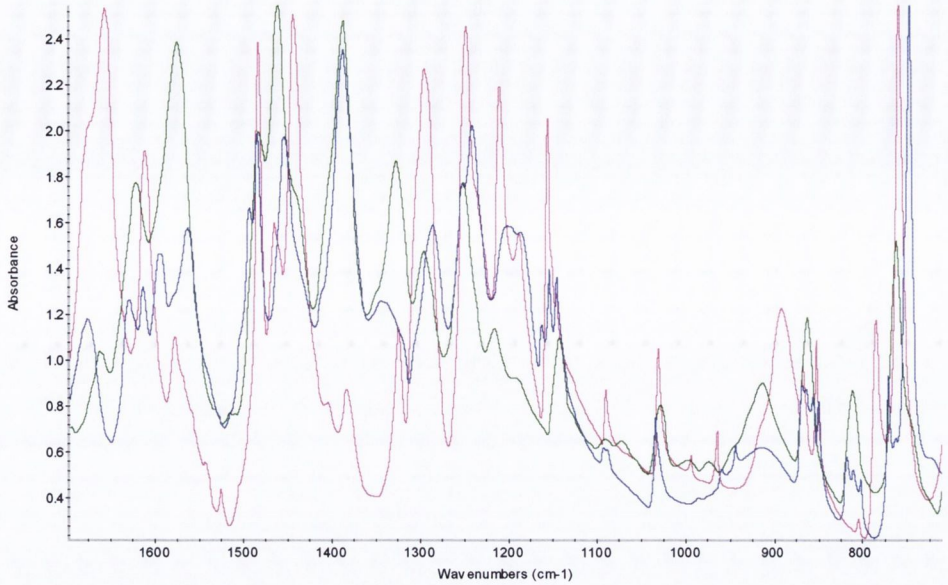

Figure 4.30- FTIR spectra in the region 700–1700 $cm^{-1}$of salicylic acid raw material (red line), ammonium salicylate (green line) and spray-dried ammonium salicylate (blue line).

4.3.4.3 WATER SPRAY-DRIED SYSTEM

In order to follow the alteration of ammonium salicylate upon spray drying, a 3% (w/v) solution of ammonium salicylate system was spray-dried from water, at an inlet temperature of 120°C. DSC thermogram of 3% ammonium salicylate system spray-dried from water is shown in Figure 4.31. DSC scan of the spray-dried salt showed that the solid state form of the spray-dried sample was different from ammonium salicylate; the scan of the spray-dried sample showed sharp endotherm peaking at ~147 °C in contrast to a broad endotherm shown in the DSC scan of unprocessed ammonium salicylate. This indicates the alteration of thermal behaviour of ammonium salicylate upon spray drying.

DSC thermogram of the spray-dried sample was also different from salicylic acid; peak position was shifted and there was difference in onset temperature, the onset temperature was ~158°C for salicylic acid and ~146 °C for spray-dried ammonium salicylate. This may be attributed to incomplete decomposition of the salt under these conditions.

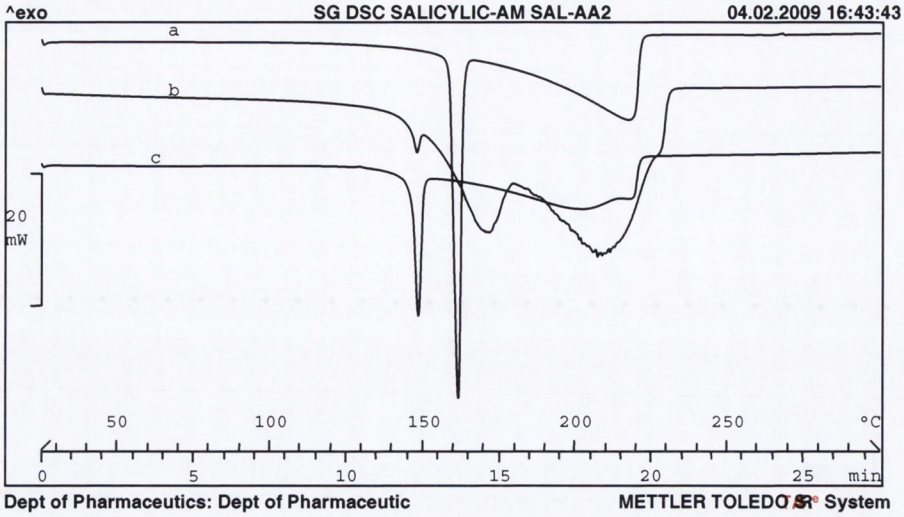

Figure 4.31- DSC scans of (a) salicylic acid unprocessed material (b) ammonium salicylate unprocessed material (c) ammonium salicylate system spray-dried from water.

SEM micrographs showed that spray drying of this system resulted in fused particles. The SEM micrograph of the produced powder is shown in Figure 4.32.

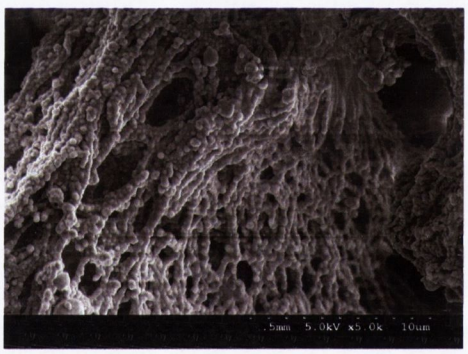

Figure 4.32- SEM micrograph of ammonium salicylate system spray-dried from water

Figure 4.33 shows XRD scan for ammonium salicylate spray-dried from water. The spray-dried sample was crystalline (presence of peaks). It was also noticed that the spray-dried sample showed different XRD pattern in comparison to the starting material; peak positions were different and extra peaks were found on examination of XRD scan of the spray-dried sample, which may suggest that a new solid-state form was recovered from spray drying. The black arrows show where peaks in X-ray diffractogram of spray-dried ammonium salicylate could be attributed to salicylic acid, while red arrows show peaks in X-ray diffractogram of spray-dried ammonium salicylate could be attributed to ammonium salicylate, which may suggest that the spray-dried salt could be partially converted to salicylic acid.

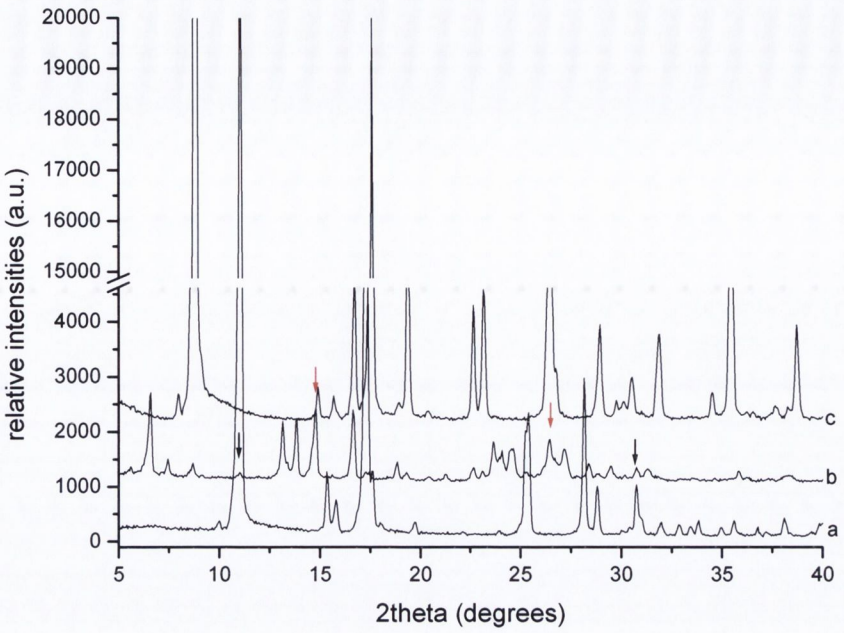

Figure 4.33- XRD scans of (a) salicylic acid starting material (b) ammonium salicylate spray-dried from water (c) ammonium salicylate starting material. The black arrow show where peaks in XRD scan of spray-dried ammonium salicylate could be attributed to salicylic acid, the red arrows show peaks in XRD scan of spray-dried ammonium salicylate could be attributed to ammonium salicylate.

4.3.4.4 Elemental analysis of spray dried ammonium salicylate

Elemental analysis (CHN) was carried out for different spray dried ammonium salicylate; the results are presented in Table 4.4. The analysis showed that the chemical composition of the spray-dried samples differed from that of ammonium salicylate starting material. In particular the nitrogen contents of the spray dried samples was lower than that of the unprocessed material, this may be attributed to the decomposition of the salt upon spray drying and partial release of ammonia.

These results could be explained on the light of the findings of Chuck and Zacher (2000), who produced nicotinic acid from aqueous solutions of ammonium nicotinate by spray drying, the authors showed that the recovered particles contained residual ammonium nicotinate, in addition recovered nicotinic acid particles were freed from residual ammonium nicotinate by a thermal post-treatment in a fluidized dryer or under reduced pressure.

In the current work the inlet temperature was quite low (78 °C) in comparison to that used by Chuck and Zacher (2000) which was 160-250 °C, therefore, it was not surprising that

pure salicylic acid was not produced by spray drying method used in this work due to the low inlet temperature.

Table 4.4- Elemental analysis of different salicylic acid and ammonium salicylate systems.

Sample	Analysis		
	C	H	N
Salicylic acid unprocessed material	60.87	4.37	0
Ammonium salicylate unprocessed material	54.18	58.47	9.02
Spray dried ammonium salicylate from water	56.47±0.62	5.21±0.13	5.64±0.43
Spray dried ammonium salicylate from ethanol	56.60±0.53	5.19±0.12	5.35±0.22

XRD diffractograms of unprocessed salicylic acid, spray-dried salicylic acid/ ammonium carbonate, ammonium salicylate spray-dried from either 90% ethanol or water and ammonium salicylate starting material are shown in Figure 4.34. It is obvious that the scans of spray dried salt from water and from ethanol have same peak positions; therefore, same solid state form was produced upon spray drying of the salt regardless of the solvent. Moreover, the peak positions in XRD scans of spray dried salts were similar to that of spray dried salicylic acid/ammonium carbonate except the peak at ~8.7 degrees which was found in the scan of the spray dried composites, and attributable to the unprocessed salt, this peak was not found in the scans of the spray dried salt. This could be attributed to the decomposition of the salt upon spray drying.

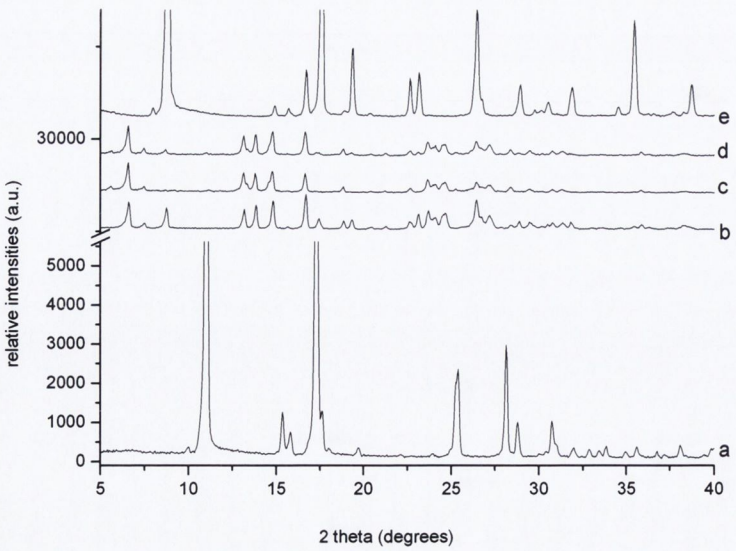

Figure 4.34- XRD scans of (a) salicylic acid starting material (b) spray-dried salicylic acid/ ammonium carbonate system (c) ammonium salicylate spray-dried from 90% ethanol (d) ammonium salicylate spray-dried from water (e) ammonium salicylate starting material

4.4- SPRAY DRIED PYRAZINOIC ACID

4.4.1 INTRODUCTION

Pyrazinoic acid is the active derivative of pyrazinamide (Schaller et al, 2002). Heifets et al (1989) showed that pyrazinoic acid possesses specific antimicrobial activity. The mechanism of action of pyrazinamide is based on the assumption that pyrazinamide-susceptible *Mycobacterium tuberculosis* strains produce pyrazinamidase, which hydrolyses pyrazinamide to the antibacterial moiety pyrazinoic acid. It is a clear to off-white crystalline powder, soluble in cold water; the melting point is between 222 °C and 225 °C. It has a pKa value of 2.92. Pyrazinoic acid was selected for investigation due to its acidic nature; the structure of pyrazinoic acid is shown in Figure 4.35.

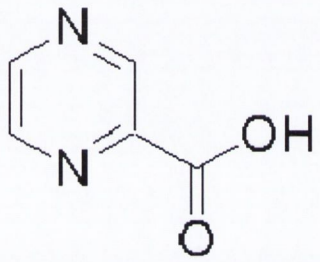

Figure 4.35- structure of pyrazinoic acid

4.4.2 PYRAZINOIC ACID: AMMONIUM CARBONATE SPRAY DRIED SYSTEMS

In Chapter 3, it was shown that a new solid state form of p-aminosalicylic acid was produced. Pyrazinoic acid was used as one of the model drugs for investigating this spray drying process, due to similarity in structure between p-aminosalicylic acid and pyrazinoic acid.

The spray drying conditions of 90% ethanol, inlet temperature 78 °C were selected for spray drying pyrazinoic acid/ammonium carbonate composites. It should be noted that pyrazinoic acid/ammonia 66:34 represents a (1:1 molar ratio) molar ratio according to ammonia content in ammonium carbonate reported by the supplier, so 20, 27, 34 and 50% ammonium carbonate were selected to represent a range of ammonium carbonate below and above pyrazinoic acid/ammonium carbonate 1:1 molar ratio.

Figure 4.36 shows X-ray diffractograms of co-spray dried pyrazinoic acid/ammonium carbonate. The black arrows in the XRD scans indicate positions where peaks were attributable to those of pyrazinoic acid, while the red arrows indicate positions where peaks are attributable to those of ammonium salt of pyrazinoic acid. It was also noticed that some peaks found in X-ray diffractograms of spray dried composites (blue arrows) could not be attributed to either pyrazinoic acid or ammonium salt of pyrazinoic acid, which indicates the formation of new solid state form upon spray drying of pyrazinoic

acid/ammonium carbonate regardless of the amount of ammonium carbonate used in spray drying process. It should be noted that the hundred percent relative intensity peak in XRD scan of ammonium salt of pyrazinoic acid which was at 12.85 degrees was found only in XRD scan of spray dried pyrazinoic acid/ammonium carbonate 50:50, while it was not found in any the scans of other spray dried composites. On the other hand, the hundred percent relative intensity peak in XRD scan of pyrazinoic acid which was at 27.65 degrees was found only in the XRD scan of spray dried pyrazinoic acid/ammonium carbonate 80:20 and 73:27. This indicates the alteration of the solid state form of the recovered particles, which is in good agreement with the results obtained from analysis of spray dried acidic compounds (p-aminosalicylic acid, benzoic acid and salicylic acid) with ammonium carbonate.

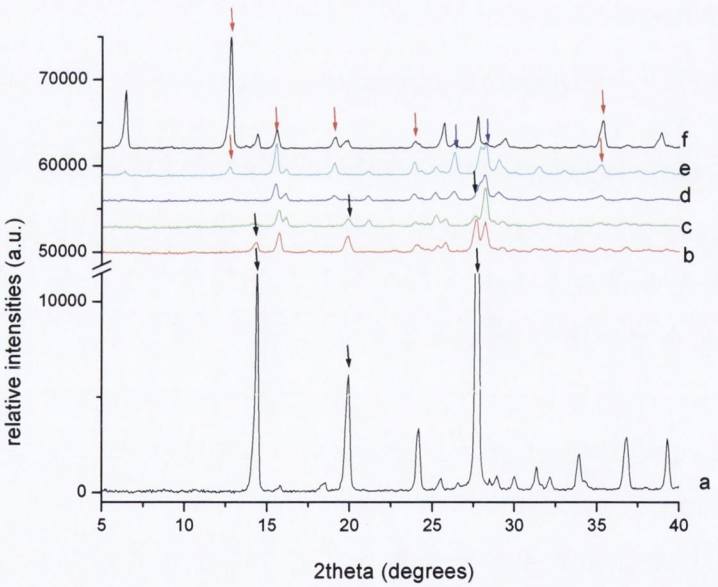

Figure 4.36- XRD scans of (a) pyrazinoic acid ammonium carbonate and spray dried pyrazinoic acid/ammonium carbonate (b) 80:20 (c) 73:27 (d) 66:34 (e) 50:50 and (f) ammonium salt of pyrazinoic acid. The black arrows in the XRD scans indicate positions where peaks were attributable to those of pyrazinoic acid, the red arrows indicate positions where peaks are attributable to those of ammonium salt of pyrazinoic acid, the blue arrows indicate positions where peaks could not be attributed to either pyrazinoic acid or ammonium salt of pyrazinoic acid.

Figure 4.37 compares the DSC thermograms of all spray-dried samples of pyrazinoic acid/ammonium carbonate with that of the starting material. Only one thermal event on the DSC scan of pyrazinoic acid raw material was recorded, an endotherm, peaking at ~223 °C,

with measured enthalpy of 649 J/g, characteristic of pyrazinoic acid melting, confirmed by the literature values of 222-225 °C for the melting temperature and enthalpy of fusion (according to specification sheet supplied by the manufacturer). In contrast, DSC scans of spray dried composites showed an endothermic peak at 184°C, 179°C, 186 °C and 186°C with measured enthalpy of ~81 J/g, ~60 J/g, ~174 J/g and ~179 J/g for spray dried pyrazinoic acid with 20%, 27% 34% and 50% ammonium carbonate, respectively. TGA registered weight loss of 65, 100, 100 and 100% from 25-190°C for unprocessed pyrazinoic acid and pyrazinoic acid/ammonium carbonate 80:20, 73:27, 66:34 and 50:50 spray dried systems, respectively.

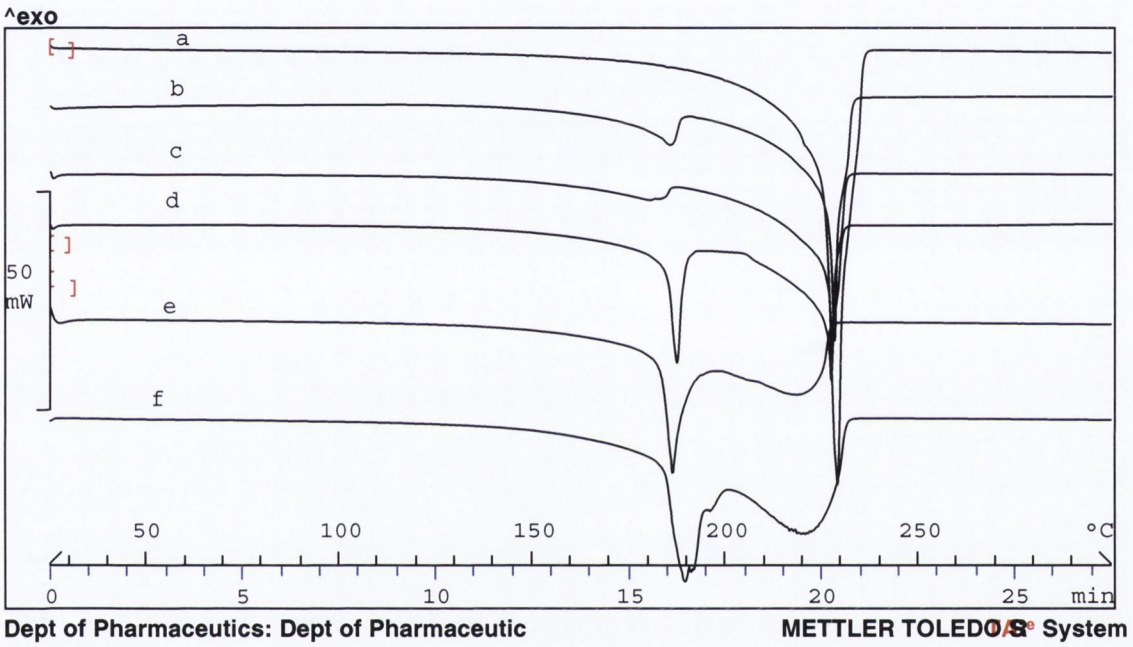

Figure 4.37- DSC scans of (a) pyrazinoic acid and spray dried pyrazinoic acid/ammonium carbonate (b) 80:20 (c) 73:27 (d) 66:34 (e) 50:50 and (f) ammonium salt of pyrazinoic acid.

SEM micrographs of pyrazinoic acid unprocessed material and spray dried pyrazinoic acid/ammonium carbonate systems are shown in Figure 4.38. It can be seen that the particles of the pyrazinoic acid starting material are large and non-uniform in shape. In contrast, the particles of spray-dried samples were smaller. Spray dried samples were mixtures of smooth and rough surface particles (Figure 4.38).

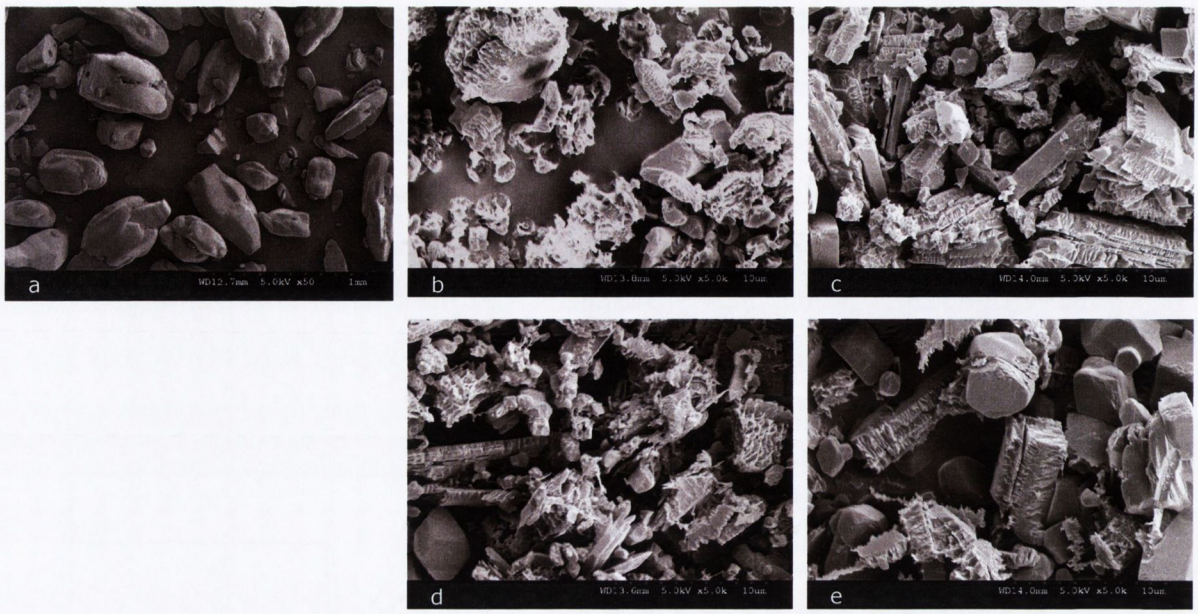

Figure 4.38- SEM micrographs of (a) pyrazinoic acid and spray dried pyrazinoic acid/ammonium carbonate (b) 80:20 (c) 73:27 (d) 66:34 (e) 50:50.

4.4.2.1 Stoichiometry of spray dried pyrazinoic acid systems

Elemental analysis (CHN) was carried out for different pyrazinoic acid/ammonium carbonate spray-dried systems; the results are presented in Table 4.5. The analysis showed that the chemical composition of the spray-dried samples differed from that of pyrazinoic acid starting material.

The stoichiometry of the spray dried composites could be 2:1 pyrazinoic acid: ammonia. This was estimated from elemental analysis of the recovered particles from spray drying process, which gave elemental analysis consistent with this stoichiometric ratio as shown in Table 4.5. This was in agreement with the stoichiometry of recovered particles from spray dried benzoic acid/ ammonium carbonate and spray dried salicylic acid/ammonium carbonate.

Table 4.5- Elemental analysis of different salicylic acid systems. Key: SD= spray dried, AC= ammonium carbonate, C = Carbon, N = nitrogen, H = hydrogen.

Sample		Analysis		
		C	H	N
Pyrazinoic acid	Calculated	48.39	3.24	22.57
SD pyrazinoic acid/AC 80:20	Found	45.33±1.40	3.74±0.37	25.97±1.70
SD pyrazinoic acid/AC 73:27	Found	45.35±1.42	3.99±0.37	26.03±1.6
Acid: ammonia 2:1	Calculated	45.45	3.81	26.50

4.4.3 Ammonium salt of pyrazinoic acid spray dried systems

As shown in Chapter 3, a new solid state form was produced by spray drying of ammonium salts of p-aminosalicylic acid. The recovered particles were spherical aggregates of microcrystalline particles. The porous nature of the recovered particles was to arise due to volatilisation of the ammonium component of the salt. In a continuation of these findings, the ammonium salt of pyrazinoic acid was prepared and spray dried to investigate the effect of spray drying on the physicochemical properties of the salt.

The ammonium salt of pyrazinoic acid was prepared and characterised before spray drying. SEM micrographs of the prepared salt show elongated crystals and non-uniform shape particles, which vary in size as seen in Figure 4.39. XRD scans of the ammonium salt of pyrazinoic acid indicate the crystalline structure of the salt, evidence from the presence of well-defined peaks in the X-ray powder diffractogram of the unprocessed material (Figure 4.40).

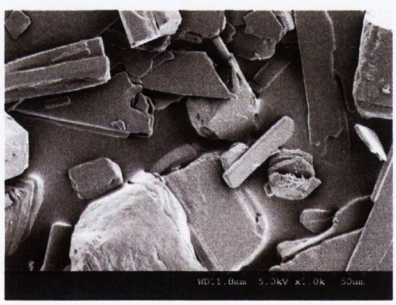

Figure 4.39- SEM micrograph of ammonium salt of pyrazinoic acid starting material

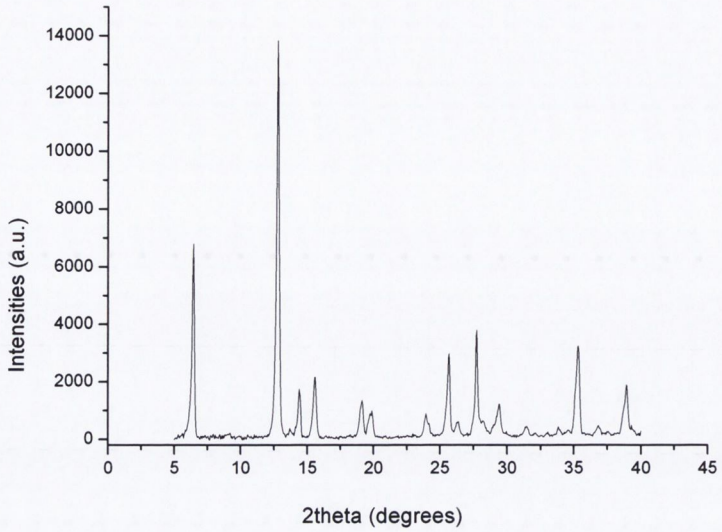

Figure 4.40- XRD scan of ammonium salt of pyrazinoic acid starting material

DSC and TGA scans of ammonium salt of pyrazinoic acid are shown in Figure 4.341. DSC scan shows an endothermic event, peaking at 187 °C, with its onset at 183 °C and measured enthalpy of 172 J/g. TG analysis of the salt showed a loss of approximately total solid mass in the same temperature region as this endotherm.

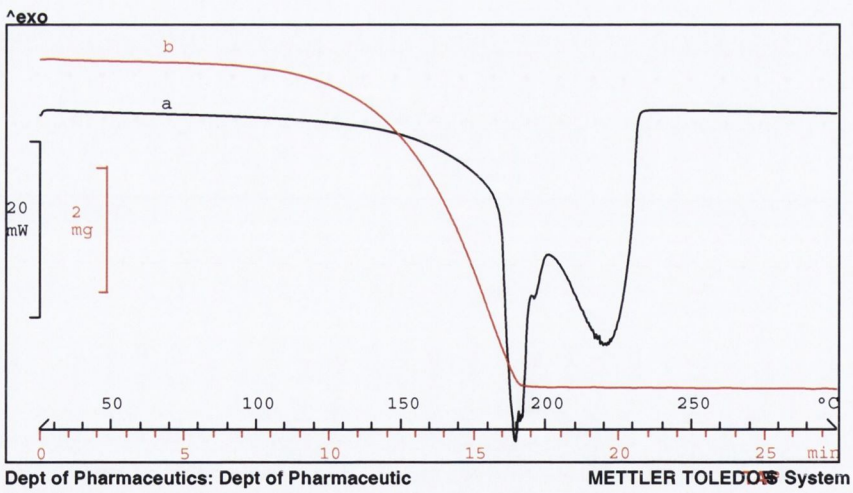

Figure 4.41- (a) DSC and (b) TGA scans of ammonium salt of pyrazinoic acid starting material

Spray drying of 3% ammonium salt of pyrazinoic acid from 90% ethanol at an inlet temperature of 78°C resulted in spherical microcrystalline aggregates and porous particles. The porosity of particles may be attributed to volatilisation of the ammonium component of the salt. This was in agreement with the result reported for ammonium salt of p-

aminosalicylic acid., for the ammonium salt of *p*-aminosalicylic acid spray dried from 90% ethanol at an inlet temperature of 78°C (Figure 4.42).

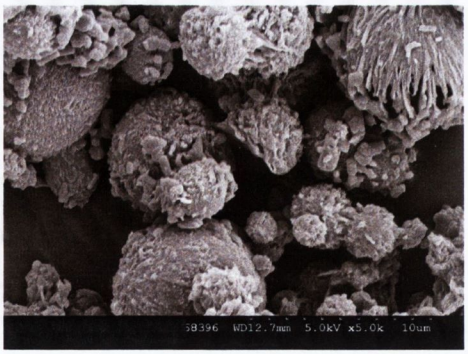

Figure 4.42- SEM micrographs of ammonium salt of pyrazinoic acid spray dried from 90% ethanol.

XRD scan of the spray-dried sample provided evidence of differences between the spray-dried sample, ammonium salt of pyrazinoic acid starting material and pyrazinoic acid, as the spray-dried sample had different peak positions than that of either the salt or acid forms (Figure 4.43). It was also noticed that XRD pattern of spray-dried salt was similar to the pattern of spray-dried pyrazinoic acid/ammonium carbonate (Figure 4.43 b and c). This was in agreement with results obtained when the X-ray diffractograms of spray-dried ammonium salt of p-aminosalicylic acid were compared to spray-dried p-aminosalicylic acid/ammonium carbonate. XRD scans of spray-dried ammonium salt of pyrazinoic acid and spray-dried pyrazinoic acid/ammonium carbonate showed peaks attributable to the salt form (red arrows), peaks attributable to the acid form (black arrows) which could be due to partial decomposition of the salt.

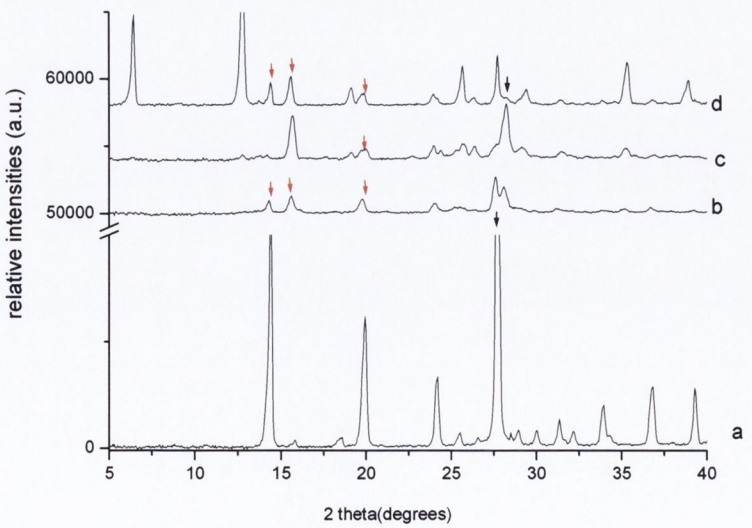

Figure 4.43- XRD scans of (a) pyrazinoic acid (b) spray dried pyrazinoic acid/ammonium carbonate (c) spray dried ammonium salt of pyrazinoic acid (d) unprocessed ammonium salt of pyrazinoic acid. The red arrows show peaks attributable to the salt form, the black arrows show peaks attributable to the acid form.

DSC scan of spray dried salt showed an endothermic peak at 186 °C with its onset at 183 °C. This was compared favourably with the unprocessed material as shown in Figure 4.44.

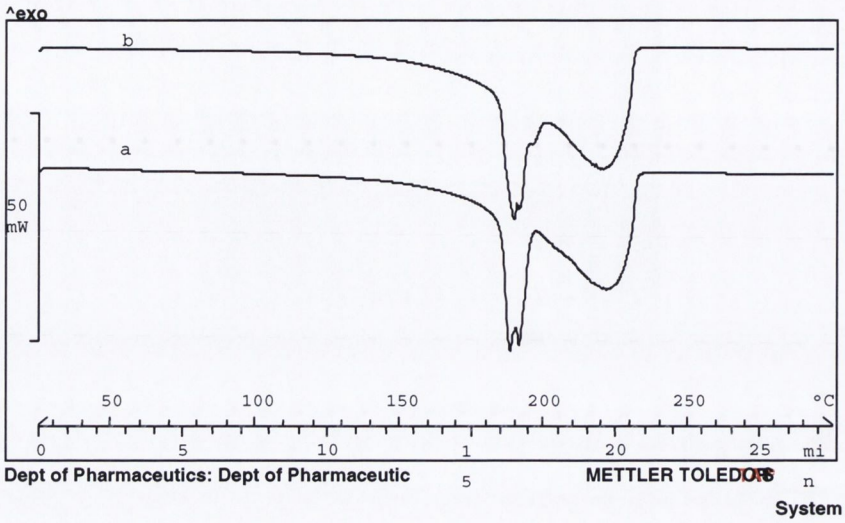

Figure 4.44- DSC scans of (a) spray dried ammonium salt of pyrazinoic acid (b) unprocessed ammonium salt of pyrazinoic acid.

4.5 SPRAY-DRIED SULFACETAMIDE SYSTEMS

4.5.1 INTRODUCTION

Sulfacetamide is a white or yellowish-white crystalline powder. It is soluble 1 in 150 of water, 1 in 15 of ethanol, and 1 in 7 of acetone; very slightly soluble in chloroform; slightly soluble in ether; soluble in mineral acids and alkali hydroxides (Moffat et al.,2004). It has pKa values of 5.4 and 2 (Cairns, 2003). It has a melting point between 182 °C and 184 °C as reported by the supplier in the product specification sheet. Although the occurrence of polymorphism in the sulfonamide group of drugs is very common, Yang and Guillory, (1972) reported that sulfacetamide is one of sulfonamides in which polymorphism was not found.

4.5.2 SPRAY-DRIED SULFACETAMIDE WITH AMMONIUM CARBONATE

In a continuation of our findings shown earlier, where new solid state forms were produced upon spray drying of acidic compounds with ammonium carbonate, sulfacetamide was selected as an acidic model drug compound to investigate the physicochemical properties of recovered particles upon spray drying with a process enhancer.

Different solutions of sulfacetamide/ammonium carbonate were spray-dried from 90% (v/v) ethanol, with the spray dryer operating in the open mode configuration using spray drying conditions given in Appendix I. It should be noted that that sulfacetamide/ammonium carbonate 80:20 represents a (1:1 molar ratio) molar ratio according to the ammonia contents reported by the supplier in the product specification sheet, where ammonia contents in ammonium carbonate is 30% of its weight. So 10, 20, 30 and 50% ammonium carbonate were selected to represent a range of ammonium carbonate below and above sulfacetamide/ammonium carbonate 1:1 molar ratio.

The FTIR spectra of sulfacetamide raw material and sulfacetamide/ ammonium carbonate spray-dried sample are shown in Figures 4.45 and 4.46. Sulfonamides have strong bands in the IR spectrum due to their N-H stretching vibrations in the region of 3390-3245 cm^{-1}, and a strong absorption band at 1360-1315 cm^{-1} due to the asymmetric stretching vibration of the SO_2 group (Socrates, 1994). The spectrum of unprocessed sulfacetamide presented these characteristic signals at 3381 cm^{-1} and 3256 cm^{-1} for the N-H stretching vibrations, and signals at 1322 cm^{-1} for the SO_2 stretching vibrations. The spray-dried sample showed the same characteristic peaks at the same wavenumbers, but also the IR spectrum of the spray dried sample showed a signal at 1500-1550 cm^{-1} (Figure 4.46), this may be attributed

to NH_3^+ deformation vibration. In addition this signal was compared favorably with FTIR spectrum of ammonium salt of sulfacetamide as shown in Figure 4.46.

It is obvious from FTIR that all bands appeared in the scan of the spray dried sample could be attributed to either the acid or the salt forms of sulfacetamide.

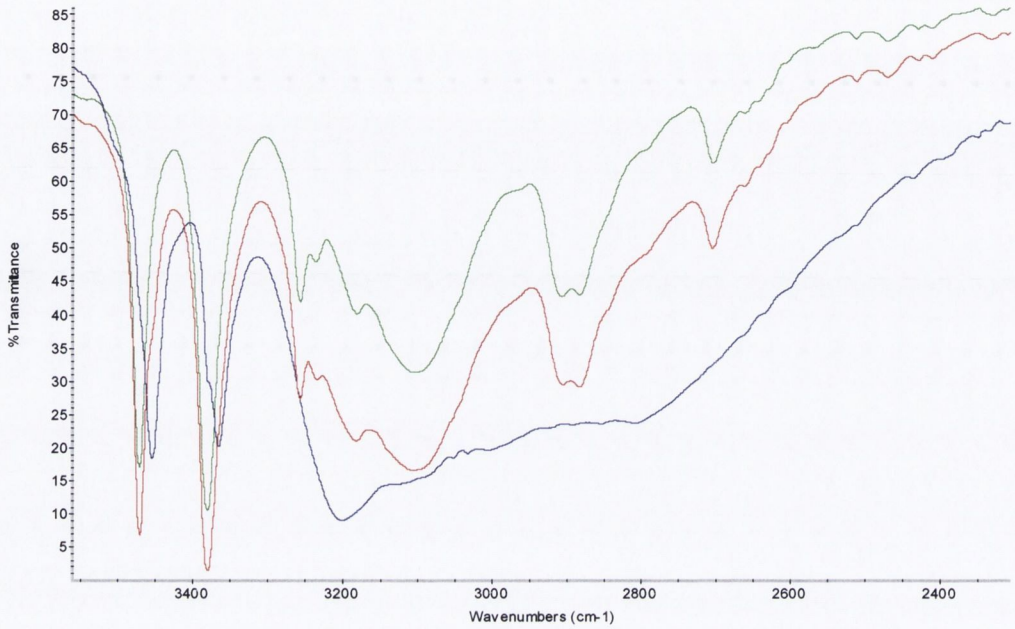

Figure 4.45- FTIR spectra in the region 2400–3500 cm^{-1} of ammonium salt of sulfacetamide-unprocessed material (blue line) sulfacetamide-unprocessed material (green line) spray-dried sulfacetamide/ammonium carbonate (red line).

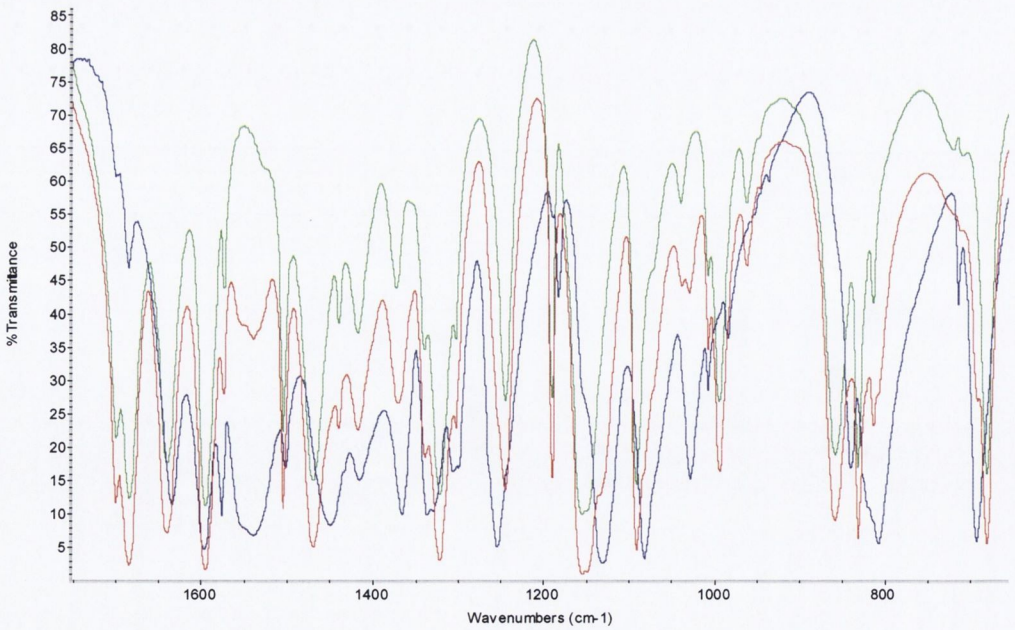

Figure 4.46- FTIR spectra in the region 750–1700 cm^{-1} of ammonium salt of sulfacetamide-unprocessed material (blue line) sulfacetamide-unprocessed material (green line) spray-dried sulfacetamide/ammonium carbonate (red line).

X-ray diffractograms of spray dried sulfacetamide/ammonium carbonate are shown in Figure 4.47. The black arrows in the XRD scans indicate positions where peaks were attributable to those of ammonium salt of sulfacetamide, while the red arrows indicate positions where peaks are attributable to those of sulfacetamide.

It is obvious that the peaks shown in XRD scan of the processed samples are mixture of peaks of the acid form and of the salt form. In addition, all peaks in XRD scans of processed samples could be attributed to either the salt or the acid forms of sulfacetamide. Therefore, the recovered particles could be a mixture of sulfacetamide and ammonium salt of sulfacetamide.

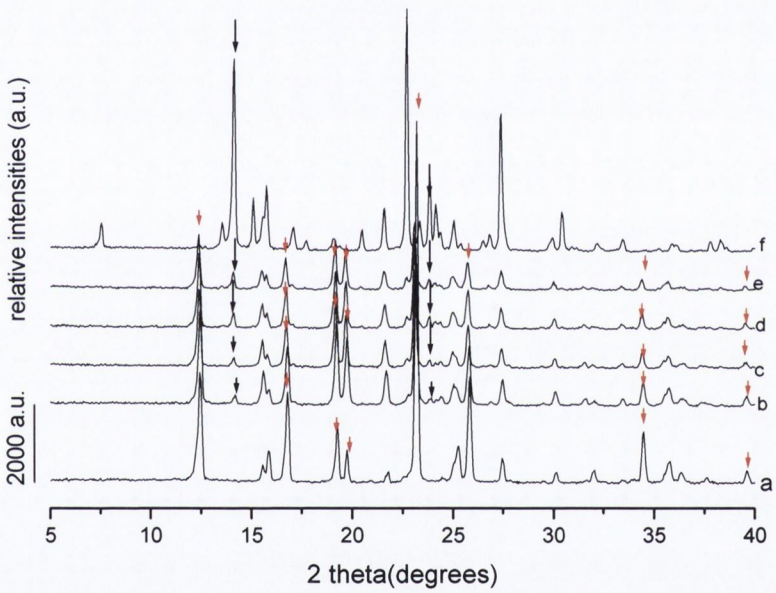

Figure 4.47- XRD scans of (a) sulfacetamide raw material and sulfacetamide/ammonium carbonate (b) 90:10 (c) 80:20 (d) 70:30 (e) 50:50 spray-dried systems (f) ammonium salt of sulfacetamide. The black arrows in the XRD scans indicate positions where peaks were attributable to those of ammonium salt of sulfacetamide; the red arrows indicate positions where peaks are attributable to those of sulfacetamide.

DSC scans of unprocessed sulfacetamide and its spray-dried systems from 90% (v/v) ethanol with different concentrations of ammonium carbonate are shown in Figure 4.48. An endothermic peak due to sulfacetamide melting was detected at ~184 °C with measured onset of ~183 °C, this result was compared favorably with the literature value of 181-184 °C (USP, 2008). Sulfacetamide/ammonium carbonate spray-dried systems, in contrast showed additional broad endothermic processes peaking at ~155, 158, 156 and 156 °C in spray dried sulfacetamide/ammonium carbonate 90:10, 80:20, 70:30 and 50:50,

respectively. This endotherm was compared to that of the salt (Figure 4.49), which confirms that the spray dried sample could be a mixture of the salt and the acid form of sulfacetamide.

TG analysis of spray dried sulfacetamide/ammonium carbonate showed a loss of ~4.6% of total solid mass in the same temperature region as these endotherms (Figure 4.50).

On the other hand, DSC of sulfacetamide/ammonium carbonate 50:50 physical mixture showed a broad endothermic peak from 55 °C to ~160 °C. TG analysis of the physical mixture showed a loss of approximately 43.7% of total solid mass in the same temperature region as this endotherm. This was followed by sharp endothermic peak at ~183 °C indicative of the melting temperature of sulfacetamide, similar to published data (USP, 2008) (Figure 4.51). These results confirm that the spray dried samples were not a simple mixture of sulfacetamide and ammonium carbonate.

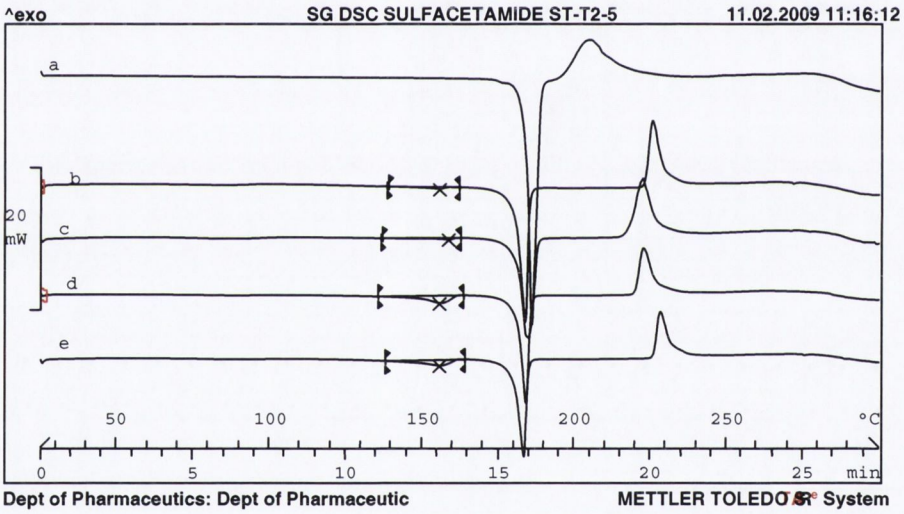

Figure 4.48- DSC scans of (a) sulfacetamide raw material and spray-dried sulfacetamide/ammonium carbonate (b) 90:10 (c) 80:20 (d) 70:30 (e) 50:50

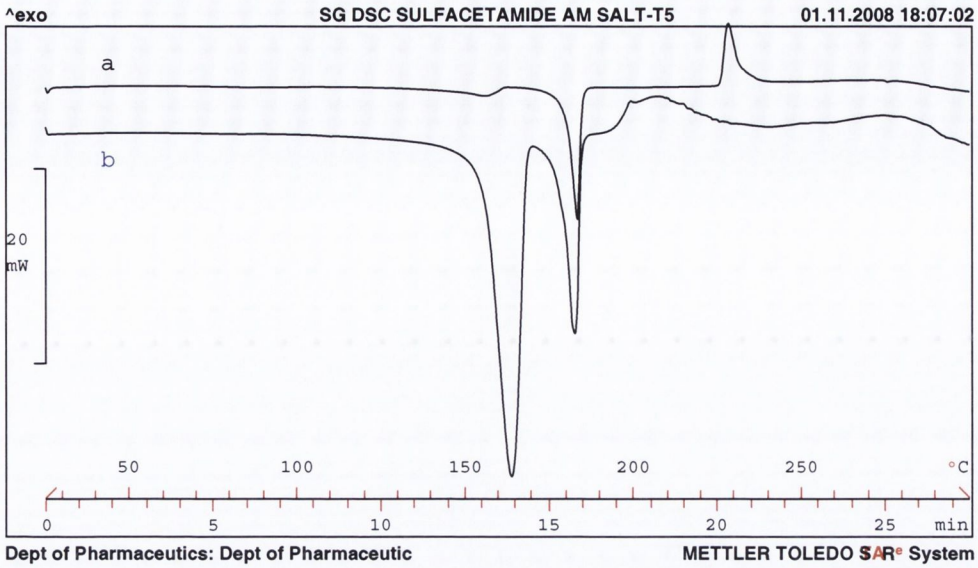

Figure 4.49- DSC scans of (a) spray-dried sulfacetamide/ammonium carbonate (b) ammonium salt of sulfacetamide.

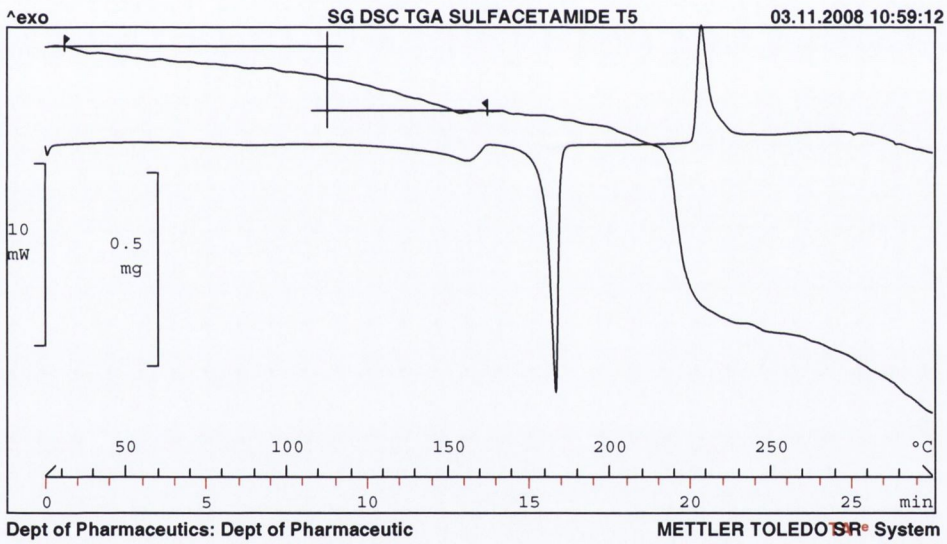

Figure 4.50- DSC and TGA scans of sulfacetamide/ammonium carbonate spray-dried system.

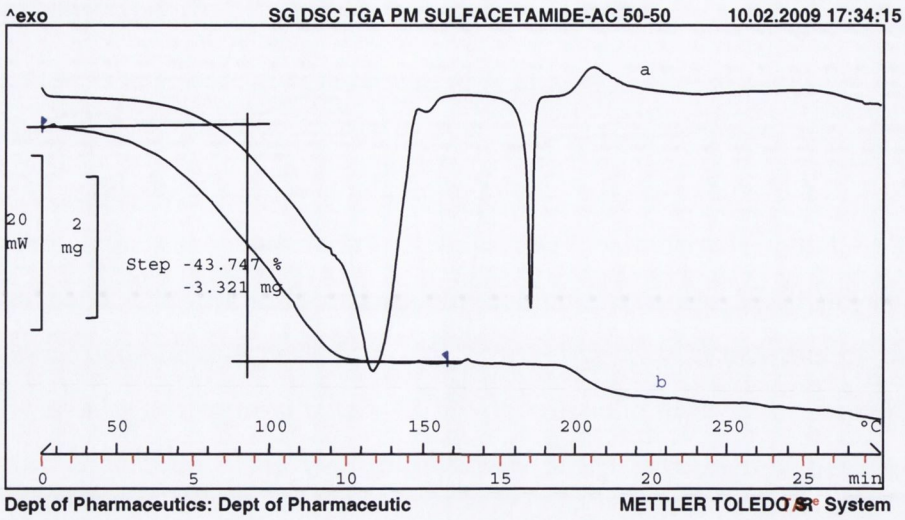

Figure 4.51-DSC and TGA scans of physical mixture of sulfacetamide-ammonium carbonate.

The spray-dried sulfacetamide/ammonium carbonate systems from 90% (v/v) ethanol produced non-porous, fused irregular and round shaped particles, as observed from SEM micrographs. This was in contrast to the rod shape morphology of sulfacetamide raw material (Figure 4.52).

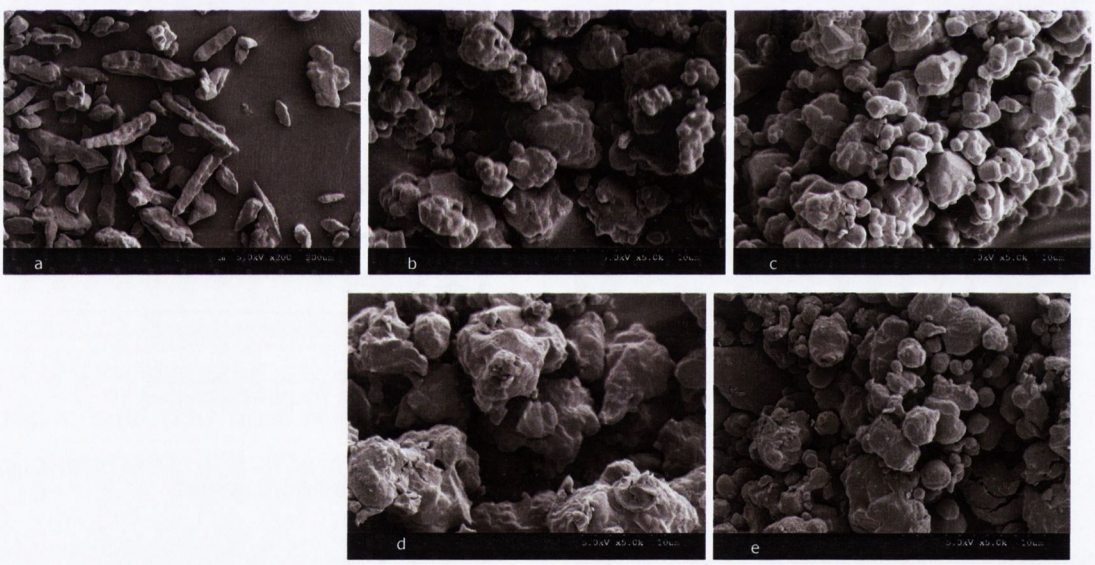

Figure 4.52- SEM micrographs of (a) sulfacetamide unprocessed material and sulfacetamide/ammonium carbonate (b) 90:10(c) 80:20(d) 70:30 (e) 50:50 systems spray-dried from 90% (v/v) ethanol.

4.5.3 Preparation of ammonium salt of sulfacetamide

Synthesis of sulfacetamide ammonium salt was confirmed by elemental analysis. The results of elemental analysis are shown in Table 4.6. Ammonium salt of sulfacetamide is a crystalline powder as shown by the presence of well-defined peaks in the X-ray powder

diffractogram of the unprocessed material (Figure 4.53a). In the DSC thermogram of the unprocessed sulfacetamide salt an endotherm, peaking at ~162 °C was observed, with a measured enthalpy of ~246 J/g (Figure 4.53b). This was followed by another endotherm peaking at ~181 °C with its onset at 178 °C, with a measured enthalpy of ~81 J/g.

Table 4.6- Elemental analysis of ammonium salt of sulfacetamide

Sample		Analysis% w/w		
		C	H	N
Sulfacetamide	Calculated	44.81	4.78	12.97
ammonium salt of sulfacetamide	Calculated	41.54	5.66	18.16
	Found	41.57±0.02	5.69±0.02	17.94±0.15

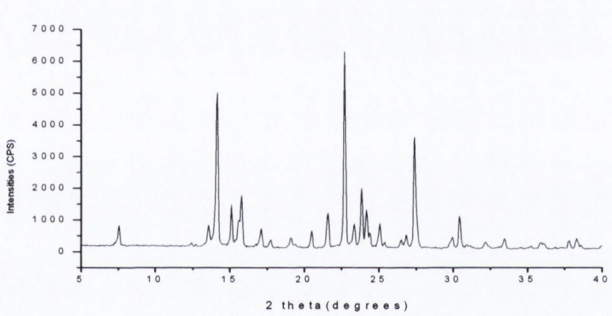

a

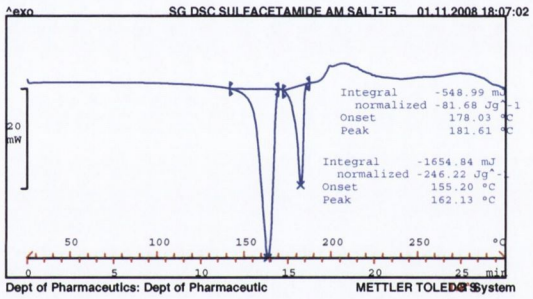

b

Figure 4.53- (a) XRD scan (b) DSC thermogram of ammonium salt of sulfacetamide

4.5.4 Solid-state and thermal properties of spray-dried ammonium salt of sulfacetamide

A 3% (w/v) solution of the ammonium salt of sulfacetamide was spray-dried from 90% (v/v) ethanol, at an inlet temperature of 78 °C and from water at an inlet temperature of 120 °C as outlined in Appendix I. Spray drying of sulfacetamide salt either from 90% ethanol or from water produced a crystalline powder, as confirmed by the numerous diffraction peaks evidenced on the X-ray pattern (Figure 4.54). The arrows in the X-ray diffractograms show where peaks could be attributed to sulfacetamide raw material, which indicate that the ammonium salt of sulfacetamide was partially decomposed upon spray drying.

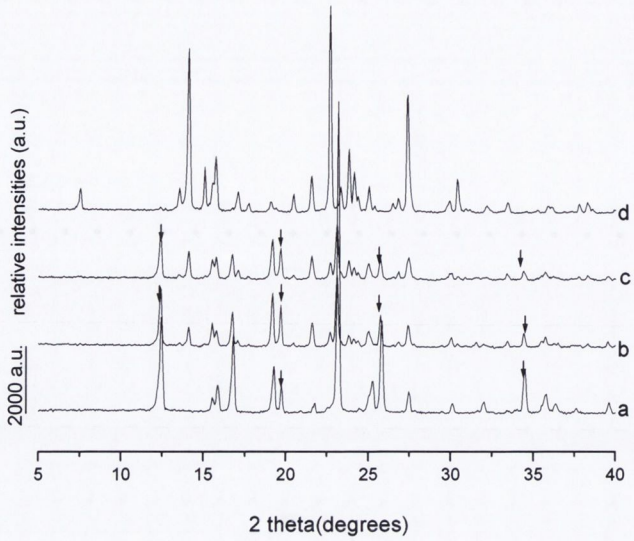

Figure 4.54- XRD diffractograms of (a) sulfacetamide raw material, (b) spray-dried sulfacetamide salt from ethanol (c) spray-dried sulfacetamide ammonium salt from water (d) sulfacetamide ammonium salt raw material. The arrows in the XRD scan show where peaks could be attributed to the sulfacetamide raw material.

SEM micrographs of spray-dried sulfacetamide ammonium salt are shown in Figure 4.55. Spray dried particles from ethanol appeared as agglomerates of irregular shape crystalline particles, with smooth surfaces, while spray-dried sample from water showed deformed spheres consisting of irregular surfaces with visible holes (red box).

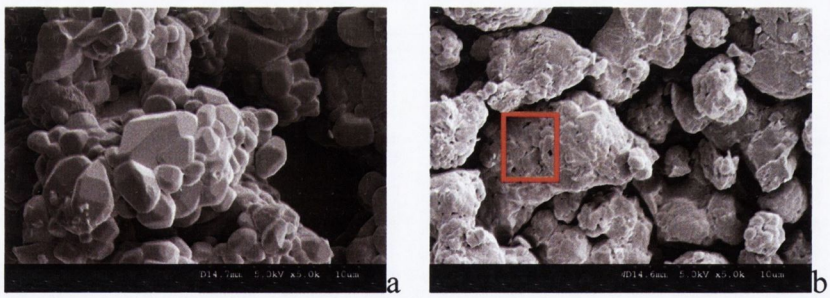

Figure 4.55- SEM micrographs of spray-dried sulfacetamide salt from (a) 90%ethanol (b) water. The red box shows the visible holes in the recovered particles.

DSC analysis of spray-dried salt showed three thermal events (Figure 4.56), a broad endotherm at 98 °C with its onset at 83 °C, partially comprising solvent loss, followed by another broad endotherm peaking at 151 °C. TG analysis of the spray-dried sample showed a loss of approximately 1.7% of total solid mass in the same temperature region as this

endotherm. The third event in the DSC scan is a sharp endotherm peaking at ~184 °C indicative of sulfacetamide melting, similar to the endothermic peak shown in DSC scan of sulfacetamide raw material. The melting endotherm was similar to published data for sulfacetamide melting (USP, 2008).

TG analysis measured weight loss of 0.7% over the temperature range of 25 to 100 °C, attributed to residual moisture and/or ethanol content Figure 4.57).

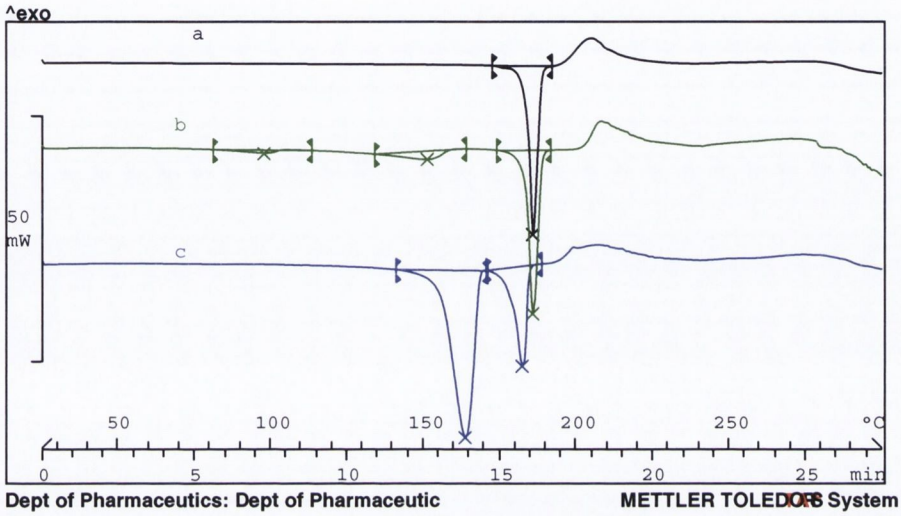

Figure 4.56 DSC scans of (a) sulfacetamide raw material (b) spray-dried ammonium salt of sulfacetamide (c) ammonium salt of sulfacetamide raw material.

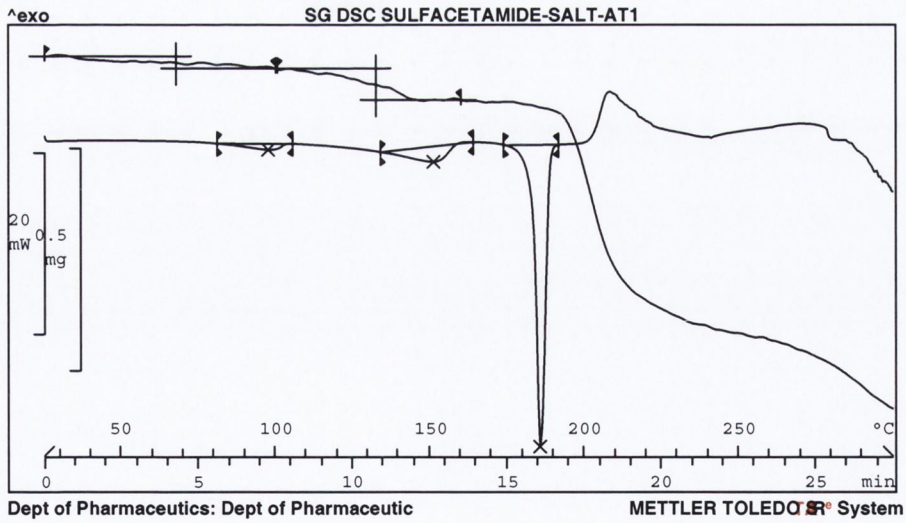

Figure 4.57 DSC and TGA scans of spray-dried ammonium salt of sulfacetamide

4.5.5 Spray-dried sulfacetamide without ammonium carbonate

Sulfacetamide was spray-dried without ammonium carbonate to study the effect of spray drying process on the solid state form of sulfacetamide and to compare with sulfacetamide/ammonium carbonate spray-dried systems. A solution of sulfacetamide was spray-dried from 90% ethanol as outlined in Appendix I. The spray drying conditions selected were identical to the sulfacetamide/ammonium carbonate systems, with the exception of the use of ammonium carbonate.

Figure 4.58 shows the X-ray diffractograms of unprocessed and spray-dried sulfacetamide. Spray-dried sample displayed a diffraction pattern similar to sulfacetamide starting material, however with reduced peak intensities. DSC scan of sulfacetamide spray-dried system shows only one endotherm peaking at ~183 °C with peak onset at ~182 °C, which was compared favorably with the literature value of sulfacetamide melting (USP, 2008), with measured enthalpy of 118 J/g (Figure 4.59).

It is obvious from XRD and thermal analysis that the solid state nature of the spray-dried sample was similar to the unprocessed sulfacetamide, and the changes found in spray-dried sulfacetamide/ammonium carbonate could be due to chemical interaction between sulfacetamide and ammonium carbonate.

Non-porous spherical fused particles and irregular particles were observed in SEM micrographs of spray-dried sulfacetamide (Figure 4.60).

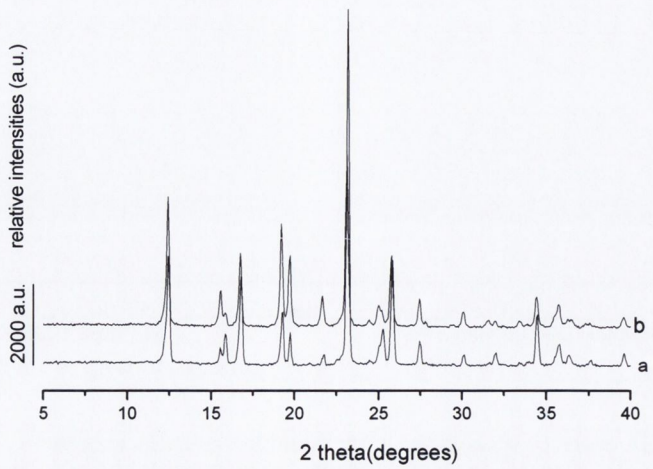

Figure 4.58- XRD diffractograms of (a) sulfacetamide raw material, (b) spray-dried sulfacetamide from ethanol.

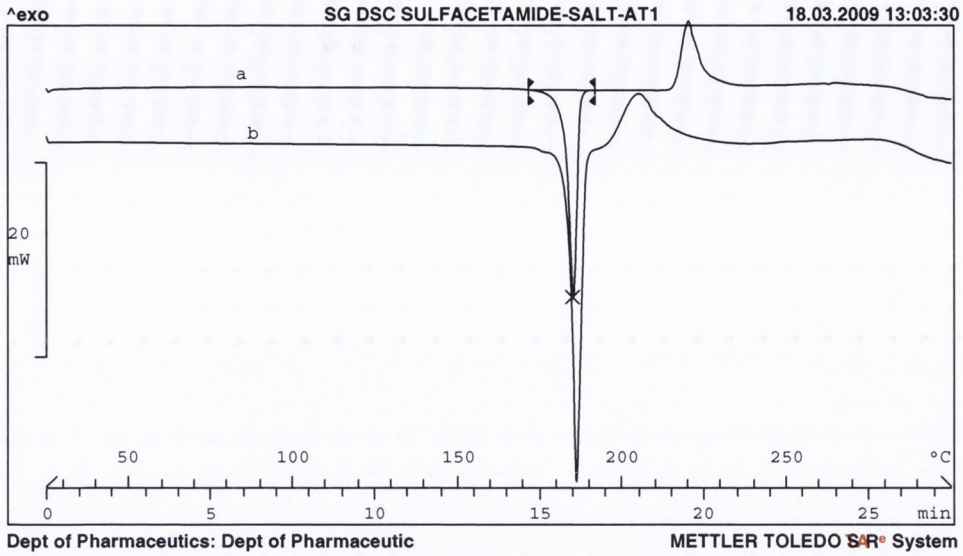

Figure 4.59- DSC scans of (a) spray-dried (b) unprocessed sulfacetamide.

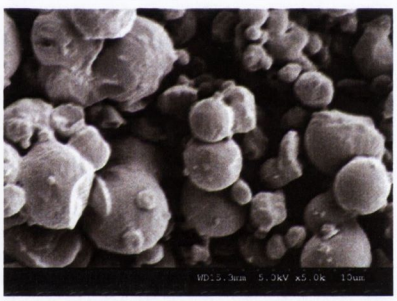

Figure 4.60- SEM micrographs of sulfacetamide system spray-dried from 90% (v/v) ethanol at 78°C.

4.6 SPRAY-DRIED SULFAMETHIZOLE SYSTEMS

4.6.1 INTRODUCTION

Sulfamethizole is either in a form of colourless crystals or a white or creamy-white crystalline powder. It is soluble 1 in 2000 of water, 1 in 30 of ethanol, 1 in 40 methanol and 1 in 13 of acetone, 1 in 2800 chloroform (Moffat et al.,2004). It has a melting point of 210°C (B. P. 2008). It has pKa values of 1.8 and 5.3 (Qiang and Adams, 2004). Sulfamethizole is not an antitubercular agent, but it is an acidic drug compound, so it was selected to investigate the production and physicochemical properties of particles.

4.6.2 SPRAY-DRIED SULFAMETHIZOLE WITH AMMONIUM CARBONATE

Initially a 0.5% (w/v) solution of sulfamethizole was spray-dried from 90% (v/v) ethanol. This concentration of ethanol was selected to allow for continuity with the successful production of spherical microcrystalline aggregates using p-aminosalicylic acid system spray-dried from 90% (v/v) ethanol (refer to Chapter 3). It should be noted that that sulfamethizole/ammonia 83:17 represents a (1:1 molar ratio) molar ratio according to ammonia content in ammonium carbonate reported by the supplier, so 5, 10 and 20% ammonium carbonate were selected to represent a range of ammonium carbonate below and above sulfamethizole/ammonium carbonate 1:1 molar ratio.

SEM micrographs of the spray-dried systems are shown in Figure 4.61. Generally, non-porous, spherical particles with a rough surface texture were produced, some visible holes were also observed in SEM micrographs of sulfamethizole/ammonium carbonate 95:5 spray-dried system.

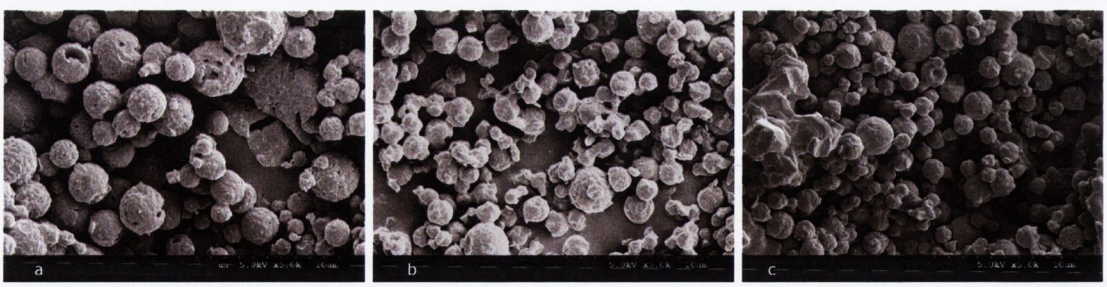

Figure 4.61 - SEM micrographs of 0.5 % sulfamethizole/ammonium carbonate (a) 95:5 (b) 90:10 (c) 80:20 systems spray-dried from 90% (v/v) ethanol at 78°C.

DSC scans of sulfamethizole starting material and its spray-dried systems from 90% (v/v) are shown in Figure 4.62. An endothermic peak due to melting was detected at ~209 °C. The literature value of melting is about 210°C (B.P. 2008). Yeo and Lee (2004) reported

that sulfamethizole exhibited endothermic event when melting took place at 212 °C. Generally, DSC thermograms of spray-dried composites showed exothermic and endothermic events. This thermal behaviour of spray dried samples was consistent with the thermal behaviour of spray dried sulfamethizole with or without ammonium carbonate reported by Nolan (2008), who showed that, DSC of all spray dried sulfamethizole systems exhibited exothermic and endothermic events.

In the DSC thermogram of sulfamethizole/ammonium carbonate 95:5 spray-dried system, a recrystallisation exotherm was observed peaking at ~101 °C with its onset at ~91 °C and exothermic enthalpy of 20 J/g. Investigation of DSC scan of sulfamethizole spray-dried with 10% (w/w) ammonium carbonate shows an exothermic peak peaking at ~100 °C with an onset temperature at approximately 90°C and with exotherm enthalpy of 13.9 J/g. The exothermic process was followed by a melting endotherm, peaking at 209 °C with an onset temperature at approximately at 208 °C. An exothermic peak was visible on DSC scan of sulfamethizole/ammonium carbonate 80:20 spray-dried system peaking at approximately 102 °C with an onset temperature at approximately 84°C and with exotherm enthalpy of 13.2 J/g. This was then followed by the melting endotherm, which had an onset temperature at approximately 208 °C. Nolan (2008) reported that spray dried sulfamethizole either with or without ammonium carbonate exhibited exothermic event followed by melting endothermic when melting took place at ~209 °C

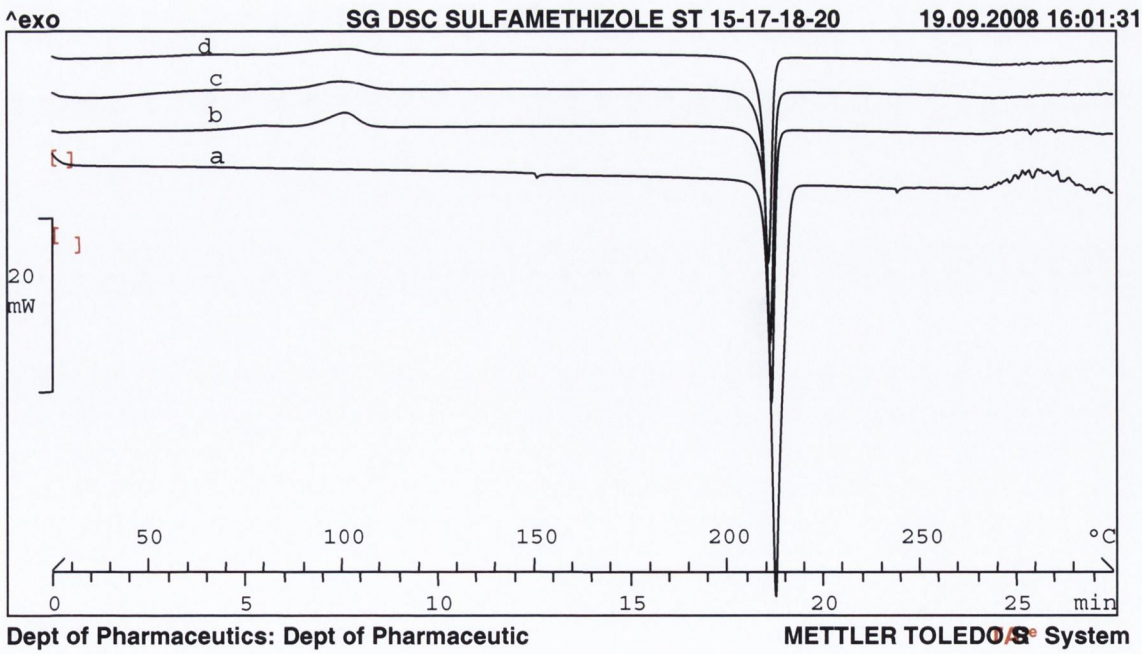

Figure 4.62- DSC scans of (a) sulfamethizole starting material and 0.5% sulfamethizole/ammonium carbonate (b) 95:5 (c) 90:10 (d) 80:20 system spray-dried from 90% v/v ethanol.

Figure 4.63 presents the X-ray powder diffractogram of sulfamethizole starting material, the numerous diffraction peaks confirming the crystalline form of the sample. Diffraction peaks of reduced intensity attributable to sulfamethizole starting material were detected in 0.5% sulfamethizole spray-dried composites. The similarity in peak positions indicates that there were no changes in the distance between atoms in the crystals but the alterations in peak intensities is perhaps due to changes of the arrangement of atoms in the crystal structure. Nolan (2008) also reported the occurrence of this alteration in peak intensities for sulfamethizole spray-dried from ethanol with or without ammonium carbonate, which was attributed to modification of the crystalline structure.

It should be noted that the spray dried systems were XRD crystalline as confirmed by powder X-ray diffraction, however DSC analysis showed exothermic recrystallisation peaks, indicative of some amorphous material having been produced on spray drying and thus intermediate degrees of crystallinity of the processed samples.

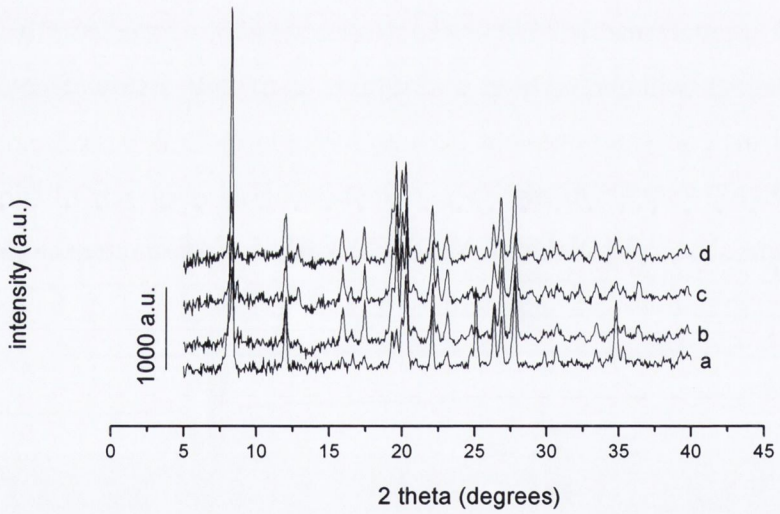

Figure 4.63- XRD scans of (a) Sulfamethizole starting material and 0.5% sulfamethizole/ammonium carbonate (b) 95:5 (c) 90:10 (d) 80:20 system spray-dried from 90% v/v ethanol.

4.6.2.1 Chemical composition of spray dried sulfamethizole/ammonium carbonate

4.6.2.1.1 Infrared spectroscopic studies

Sulfonamides have strong bands in the IR spectrum due to their N-H stretching vibrations in the region of 3390-3245 cm^{-1}, and a very strong broad absorption band at 1360-1315 cm^{-1} due to the asymmetric stretching vibration of the SO_2 group (Socrates, 1994). The

spectrum of unprocessed sulfamethizole presented these characteristic signals at 3342.4 cm^{-1} and 3253.3 cm^{-1} for the N-H stretching vibrations, and signals at 1376.6 cm^{-1} and 1326.3 cm^{-1} for the SO_2 stretching vibrations. Figure 4.64 displays spectra of sulfamethizole raw material and sulfamethizole/ ammonium carbonate spray-dried sample. There was no difference between the starting material and spray-dried composites indicating that spray drying did not affect the chemical structure of sulfamethizole.

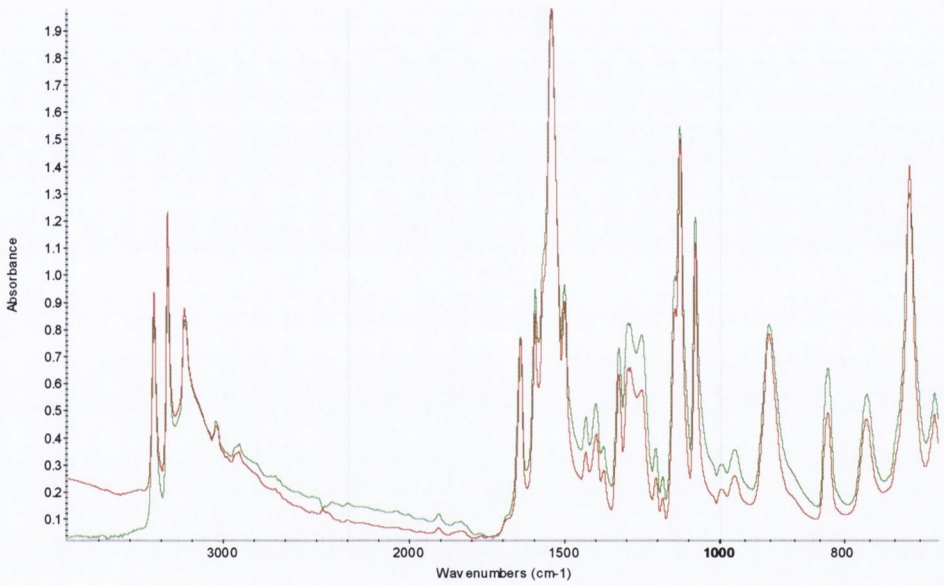

Figure 4.64- FTIR spectra of sulfamethizole-unprocessed material (green line), spray-dried sulfamethizole (red line).

4.6.2.1.2 Elemental analysis

Elemental analysis of the spray dried samples is shown in Table 4.7. It is obvious form the elemental analysis that the chemical composition of the recovered particles from spray drying of sulfamethizole /ammonium carbonate was similar to that of unprocessed sulfamethizole. In addition, there was no interaction between sulfamethizole and ammonium carbonate as indicated by XRD, DSC and FTIR. This was in contrast to the results obtained by spray drying of acidic drugs/ammonium carbonate, which showed alteration of acidic drugs upon spray drying with ammonium carbonate.

Sulfamethizole was chosen as a model drug due to it is acidic pKa to follow the finding obtained from spray drying of ammonium salt of p-aminosalicylic acid. Several trials to

prepare ammonium salt of sulfamethizole were made, using either ammonia solution or ammonium acid carbonate. However, all trials were unsuccessful.

The molecular weights, chemical structures, pKa values and solubility of sulfacetamide and sulfamethizole are listed in Table 4. 8. Although both sulfa compounds have same pKa values, but they differ by substitution on the sulfanilamide structure, sulfacetamide has acetyl group, while sulfamethizole has 5-methyl-1,3,4-thiadiazol group. It should be noted that sulfonyl group is the acidic group in the structure, so the lack of interaction between sulfamethizole and ammonium carbonate perhaps due to the presence of bulky group (methyl thiadiazol) which may hinder the interaction. In addition, aqueous solubility of sulfacetamide is much higher than that of sulfamethizole. Serajuddin, (2007) reported that the concept of the pH of maximum solubility of certain compound (pH_{max}) plays a major role in determining whether a salt would be formed or not, and, in case it is formed, whether it would remain 'as is' or would convert to the corresponding free acidic form. Serajuddin, (2007) depicted the effect of solubility of the acid and its pK_a value on pH_{max}, and consequently on salt formation, where an increase in solubility and decreases in pK_a of the acidic drug will decrease pH_{max} and, therefore, favour salt formation. Therefore, it may be assumed that the potential of salt formation of sulfacetamide is higher than that of sulfamethizole due to higher solubility of sulfacetamide in comparison to sulfamethizole.

Table 4.7- Elemental analysis of different sulfamethizole systems. Key: SD= spray dried, AC= ammonium carbonate, C = Carbon, N = nitrogen, H = hydrogen, Calculated= results of calculation and Found= results of analysis.

Sample	Analysis			
	C	H	N	S
Sulfamethizole unprocessed material	39.98	3.72	20.72	23.72
SD sulfamethizole/AC 95:5	39.86±0.16	3.70±0.02	20.60±0.16	23.61±0.15
SD sulfamethizole/AC 90:10	39.68±0.07	3.70±0.02	20.57±0.12	23.66±0.22
SD sulfamethizole/AC 80:20	39.61±0.02	3.72±0.01	20.71±0.07	23.56±0.36

Table 4.8 list of molecular weights, structures, pKa values and solubility of sulfacetamide and sulfamethizole.

Drug	Mol Wt.	Structure	pKa	Solubility
Sulfacetamide	214.24	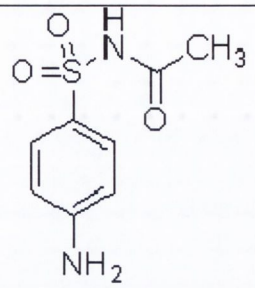	5.4	1 in 150 of water
Sulfamethizole	270.33	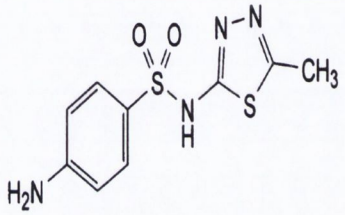	5.4	1 in 2000 of water

4.6.2.2 Effect of feed concentration

It is well known that spray drying is an expensive process; therefore, manufacturers tend to use the highest concentration for thermal economy. However, this is limited by the ability to atomise the solution effectively (Walton and Mumford, 1999). On the other hand, an increase in feed solids may lead to heavy drying chamber deposits, a general indication that maximum feed solids may have been exceeded (Masters, 1991). In the current work the solubility of sulfamethizole in 90% ethanol was the limiting factor in the drug concentrations used. At a co-solvent concentration of 90% (v/v) ethanol a solubility of 1.8 g/100 ml was measured, thus the selection of a 1.5% (w/v) feed concentration represented a close to saturated state.

Different solutions of sulfamethizole/ammonium carbonate were prepared and spray-dried from 90% ethanol; a total solid concentration in solution of 1% w/v was used in all cases. Generally, non-porous, spherical, roughened particles with visible holes were observed (Figure 4.65). Powders produced using 5% ammonium carbonate displayed signs of surface fusion between particle surfaces. This phenomenon was less apparent by using 10 and 20% ammonium carbonate in addition to the rough appearance of the particles and presence of visible pores (red box) and occasional small particles.

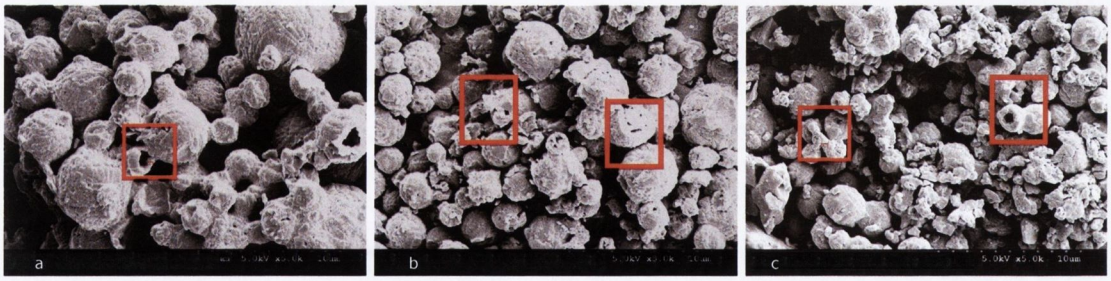

Figure 4.65- SEM micrographs of 1% sulfamethizole/ammonium carbonate (a) 95:5 (b) 90:10 (c) 80:20 systems spray-dried from 90% (v/v) ethanol at 78°C. The red boxes show the visible pores in the spray dried particles.

DSC analysis of spray-dried 1% sulfamethizole/ammonium carbonate showed only one endothermic event (Figure 4.66). This was ascribed to the melting process of sulfamethizole. The difference between unprocessed sulfamethizole and spray-dried composites in DSC scans was the presence of exothermic processes in DSC thermograms of spray-dried samples. A recrystallisation exotherm with peak onset at ~94 °C and peaking at ~101 °C with exotherm enthalpy of 34.5 J/g was found on investigation of DSC thermogram of 1% sulfamethizole/ ammonium carbonate 95:5 spray-dried system. Investigation of DSC scan of 1% sulfamethizole spray-dried with 10% (w/w) ammonium carbonate shows an exothermic process peaking at ~100 °C with an onset temperature at approximately 87°C with exotherm enthalpy of 16 J/g. An exothermic peak was also visible in the DSC thermogram of 1% sulfamethizole/ammonium carbonate 80:20 spray-dried system peaking at approximately 101 °C with an onset temperature at approximately 91°C with exotherm enthalpy of 17 J/g.

XRD pattern of sulfamethizole starting material is shown in Figure 4.67. Diffraction peaks of reduced intensity attributable to sulfamethizole starting material were detected in the spray-dried samples sulfamethizole/ammonium carbonate. The XRD results are comparable to the XRD scans of sulfamethizole spray-dried from 80% (v/v) ethanol by Nolan, (2008).

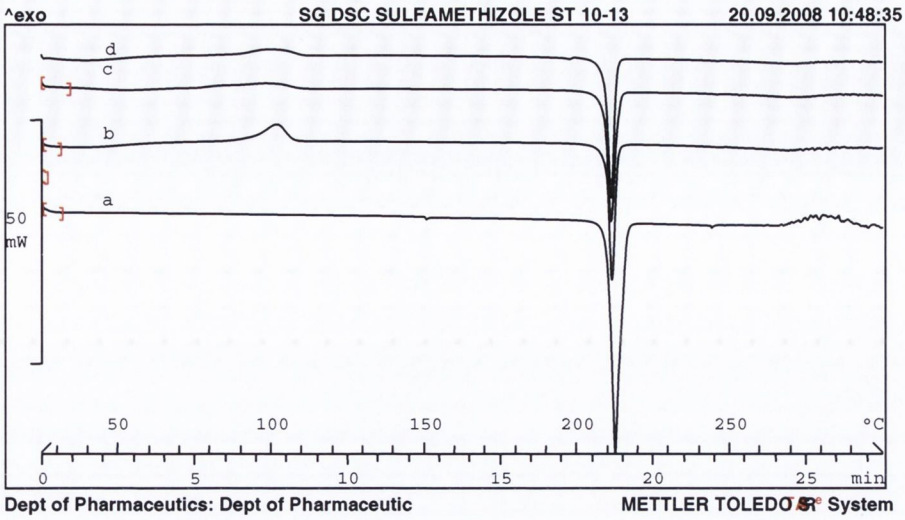

Figure 4.66- DSC scans of (a) Sulfamethizole starting material and 1% sulfamethizole/ammonium carbonate (b) 95:5 (c) 90:10 (d) 80:20 system spray-dried from 90% v/v ethanol.

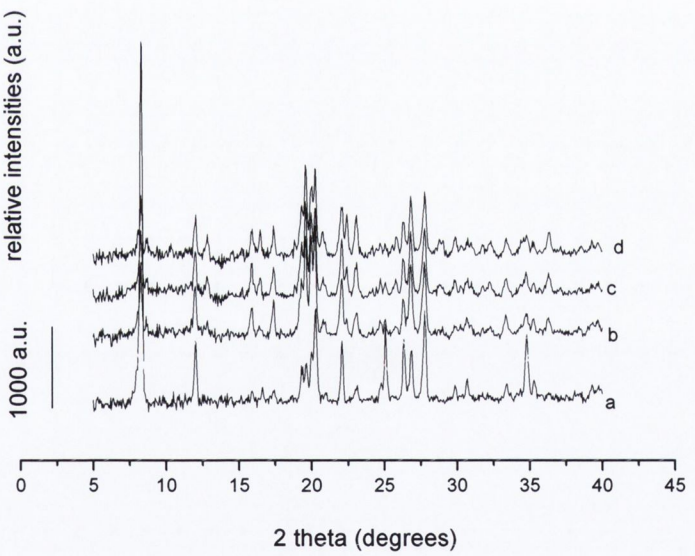

Figure 4.67- XRD scans of (a)unprocessed sulfamethizole and 1% sulfamethizole/ammonium carbonate (b) 95:5 (c) 90:10 (d) 80:20 system spray-dried systems.

The effect of total concentration was also studied; a 1.5% (w/v) solution of sulfamethizole was spray-dried from 90% (v/v) ethanol, incorporating 5, 10 and 20% by weight of solids ammonium carbonate. Figure 4.68 shows DSC scans of sulfamethizole starting material and 1.5% sulfamethizole/ammonium carbonate spray-dried samples. An endothermic event was found on investigation of DSC scan of 1.5% sulfamethizole spray-dried composites. The powder recovered from spray drying of 1.5 % sulfamethizole/ammonium carbonate

80:20 system recrystallised on heating as is evident by the exotherm in the DSC scan, which had an onset temperature at approximately 93°C, peaking at approximately 103°C, with exotherm enthalpy of 22.6 J/g . The recrystallisation exotherm was then followed by the melting endotherm, which had an onset temperature at approximately 209°C. DSC scan of spray-dried 1.5% sulfamethizole with 5% by weight of solids ammonium carbonate showed two thermal events, an exotherm peaking at ~103 °C, with exotherm enthalpy of 22.9 J/g, and endotherm, peaking at ~209 °C, recognised as melting endotherm.

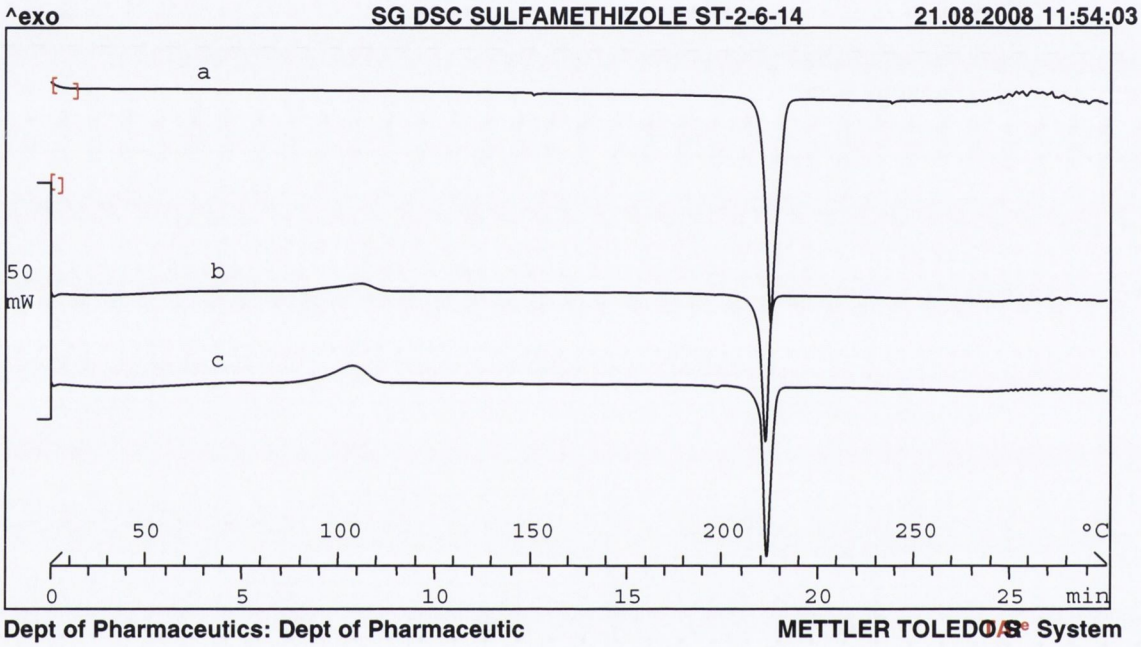

Figure 4.68- DSC scans of (a) unprocessed sulfamethizole and 1.5% sulfamethizole/ammonium carbonate (b) 80:20 (c) 95:5 systems spray-dried from 90% v/v ethanol.

X-ray diffraction studies of spray-dried 1.5 % sulfamethizole systems from 90% (v/v) ethanol (processed with ammonium carbonate) showed crystalline forms of the drugs to be present, confirmed by the numerous intense diffraction peaks observed on the X-ray diffractograms (Figure 4.69). Diffraction peaks of reduced intensity attributable to sulfamethizole starting material were detected in the spray-dried samples. These results were consistent with the XRD pattern reported for spray-dried sulfamethizole by Nolan (2008). These spray-dried systems produced spherical shaped particles with rough surfaces. Evidence of holes was clearly visible on selected particle surfaces, as observed from SEM micrographs (Figure 4.70).

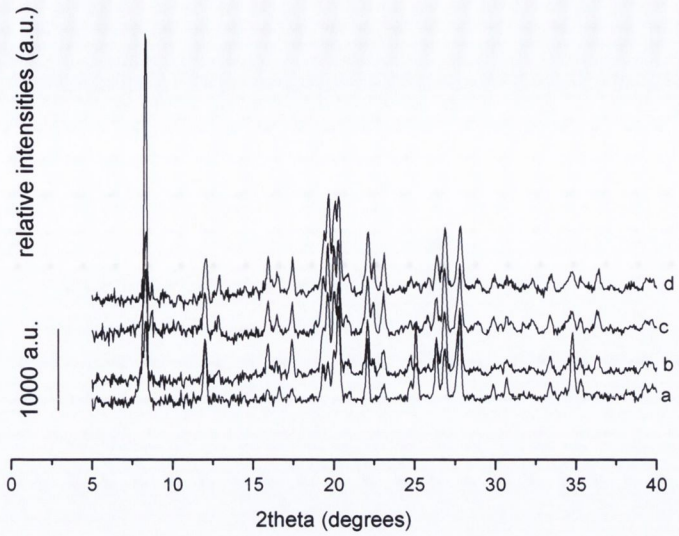

Figure 4.69- XRD scans of (a)unprocessed sulfamethizole and 1.5% sulfamethizole/ammonium carbonate (b) 90:10 (c) 80:20 (d) 95:5 system spray-dried from 90% v/v ethanol.

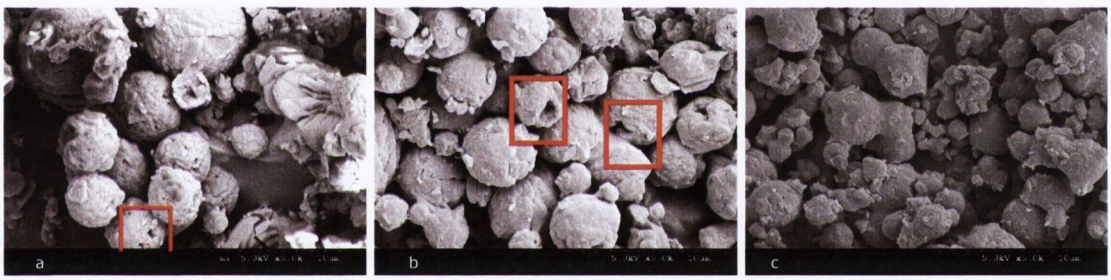

Figure 4.70- SEM micrographs of 1% sulfamethizole/ammonium carbonate (a) 95:5 (b) 90:10 (c) 80:20 systems spray-dried from 90% (v/v) ethanol at 78°C. The red boxes show the visible pores in the spray dried particles.

4.6.3 SPRAY-DRIED SULFAMETHIZOLE WITHOUT AMMONIUM CARBONATE

Sulfamethizole was spray-dried without ammonium carbonate to study the effect of the spray drying process on the physicochemical properties of spray-dried samples. 0.5, 1.0 and 1.5% (w/v) solutions of sulfamethizole were spray-dried from 90% (v/v) ethanol. Collected powder was viewed using SEM; the particles appeared as spherical formations consisting of rough surfaces with few visible holes (Figure 4.71).

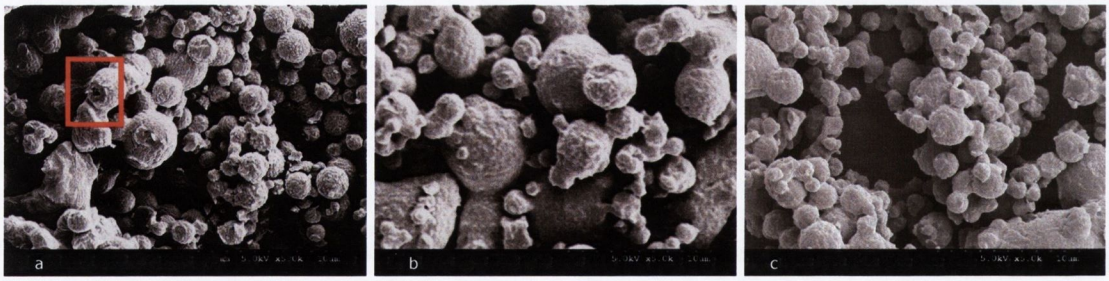

Figure 4.71- SEM micrographs of (a) 0.5% (b) 1% (c) 1.5% sulfamethizole system spray-dried from 90% (v/v) ethanol at 78°C. The red boxes show the visible pores in the spray dried particles.

DSC scan of 0.5% sulfamethizole spray-dried system shows recrystallisation exotherm was evident with peak onset at ~86°C, peaking at ~94°C with enthalpy of 27 J/g, which was followed by a melting endotherm, peaking at ~209 °C. A recrystallisation exotherm with peak onset at ~82°C, peaking at ~91°C with exotherm enthalpy of 35.3 J/g, was found on investigation of DSC scan of 1% sulfamethizole spray-dried system. Unlike the 0.5% and 1% sulfamethizole spray-dried systems, DSC scan of 1.5% sulfamethizole spray-dried from 90% ethanol did not show an exothermic peak. The spray drying process was repeated to check the repeatability of the results. DSC of the repeated spray-dried sample again did not show any exothermic event, which could be attributed to differences in crystallinity between spray-dried 0.5%, 1%, and 1.5% sulfamethizole (Figure 4.72).

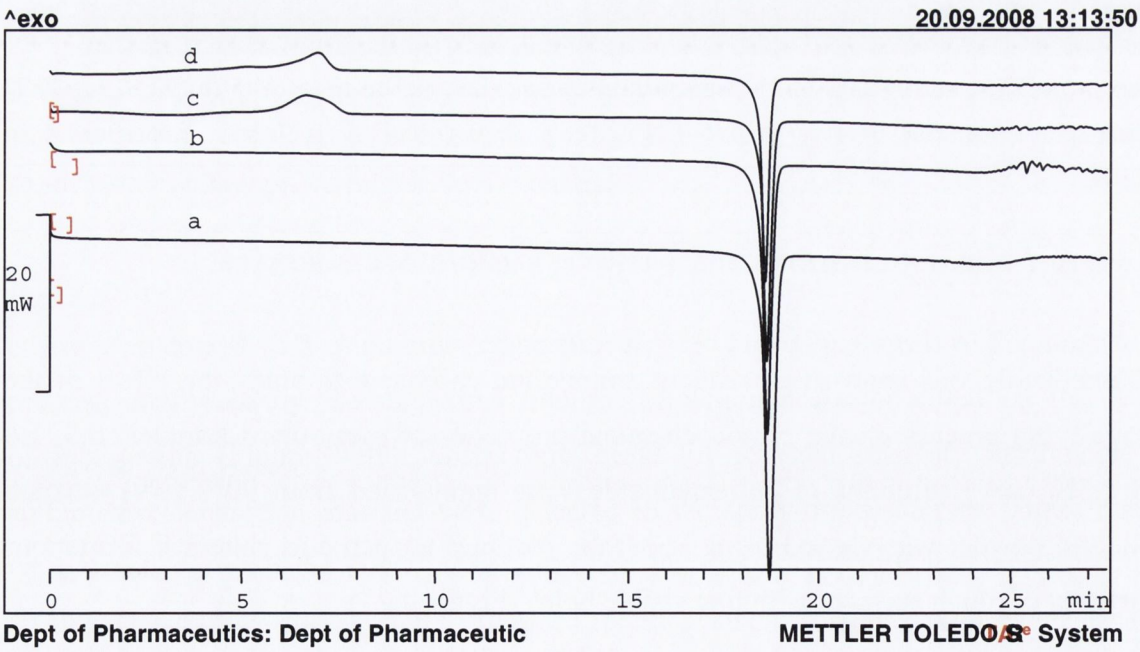

Figure 4.72- DSC scans of (a) 1.5% (b) 1.5% (2nd run) (c) 1% (d) 0.5% sulfamethizole spray-dried from 90% v/v ethanol

XRD provided further evidence of differences in crystallinity between 0.5, 1 and 1.5% sulfamethizole spray-dried systems. XRD pattern of different spray-dried sulfamethizole systems are shown in Figure 4.73. The relative intensity of the peak at 20.2 degrees is 100%. This peak was used to compare relative crystallinity of different spray-dried sulfamethizole. The height of the peak was 1113 cps for 0.5% sulfamethizole spray-dried system; 1226 cps for 1% sulfamethizole spray-dried system, while it was 1509 cps for 1.5 % sulfamethizole spray-dried system. These results suggested that the relative crystallinity of spray-dried sulfamethizole was dependant on feed concentration of spray-dried solution. This was in agreement with Chidavaenzi et al., (1997), who reported that the feed concentration have a significant effect on the properties of the spray dried materials. The authors showed that the increase in lactose content in the feed liquid in the more concentrated preparations resulted in a decrease in percentage amorphous lactose in the spray dried products.

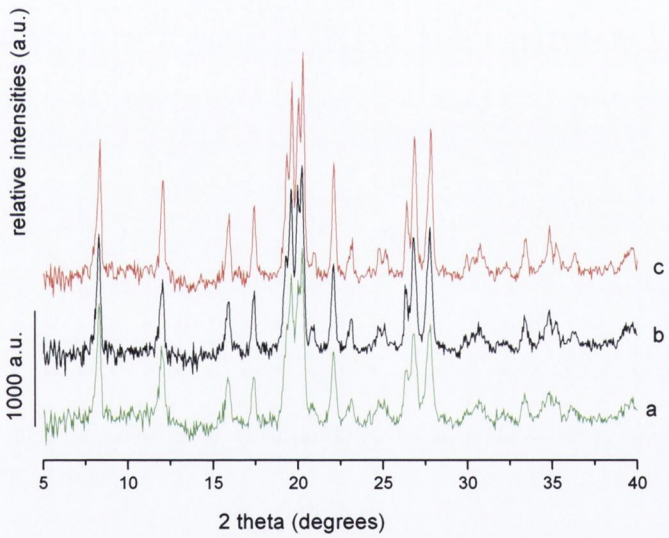

Figure 4.73- XRD scans of (a) 0.5% sulfamethizole (b) 1% sulfamethizole (c) 1.5% sulfamethizole spray-dried from 90% v/v ethanol.

Conclusion

Co-spray drying of benzoic acid/ammonium carbonate resulted in predominantly crystalline powdered products as confirmed by XRD and DSC. The solid state form of the recovered particles was changed as confirmed by XRD, DSC, FTIR and elemental analysis, the stoichiometry of the recovered particles could be 2:1 acid: ammonia. This was in contrast to the spray dried benzoic acid without ammonium carbonate which gave particles similar to the starting material. This alteration in solid state form of the acid upon spray drying with ammonium carbonate was attributed to interaction between the acid and the process additive. Ammonium benzoate was partially converted to the acid form upon spray drying. This was consistent with findings of represented by Chuck and Zacher (2000), for spray dried ammonium nicotinate. The authors showed that ammonium nicotinate was decomposed upon spray drying and ammonia, together with the solvent, escape in the exhaust gas of the spray dryer. The authors showed that the recovered particles were mainly nicotinic acid.

Spray drying of salicylic acid, with or without ammonium carbonate, results in crystalline particles. The actual particle morphology of salicylic acid spray-dried systems could not be properly seen due to the use of vacuum during the coating and visualisation process. Spray drying of salicylic acid without ammonium carbonate did not alter the starting material chemically, as confirmed by FTIR. The solid state of salicylic acid/ammonium carbonate was changed by spray drying from ethanol; the stoichiometry of the recovered particles could be 2:1 acid: ammonia as calculated from elemental analysis. Spray drying ammonium salicylate resulted in particles having new solid-state characteristics, which was partially converted to salicylic acid as indicated by analysis of the spray-dried samples.

Spray drying of pyrazinoic acid/ammonium carbonate resulted in a new solid state as confirmed by XRD and DSC, the differences in solid state was dependent on ammonia contents used in spray drying process. Spherical aggregates of microcrystalline particles and porous particles were recovered from spray drying of ammonium salt of pyrazinoic acid. This could be due to volatilisation of ammonia.

The solid state of recovered particles from spray drying of acidic sulfa compounds/ammonium carbonate was dependent on the interaction between the model drug and ammonium carbonate. The recovered particles from spray-drying of sulfacetamide/ammonium carbonate could be a mixture of the acid and salt forms of sulfacetamide and there were evidence of sulfacetamide /ammonium carbonate interactions detected by DSC and XRD analysis and FTIR. On the other hand, there was no interaction between sulfamethizole and ammonium carbonate as indicated by XRD, DSC and FTIR

analysis and the solid state of spray dried sulfamethizole/ammonium carbonate was similar to unprocessed sulfamethizole, in addition elemental analysis of the spray dried composites showed that there were no differences between spray dried sulfamethizole/ammonium carbonate and the unprocessed sulfamethizole. This confirms that the change in solid state of spray dried acidic compound/ammonium carbonate is dependent on the drug/ammonium carbonate interaction. Spray drying sulfamethizole resulted in systems of varying crystallinity, the crystallinity depending on the feed concentration of the drug.

CHAPTER 5 - SPRAY-DRIED ANTI-TUBERCULAR AGENTS SYSTEMS

5.1 INTRODUCTION

As shown in the general introduction, anti-tubercular agents needed to be administered in large amounts. The usual adult dose of rifampicin is 8 to 12 mg/kg. Isoniazid usual adult dose is 5 mg/kg, to a maximum of 300 mg, daily by mouth and pyrazinamide dose is 15 to 20 mg/kg daily (maximum 2 g daily) (Reynolds, et al., 1996). Persistent, high blood levels of anti-tubercular drugs are required for proper treatment, which currently can be achieved by prolonged oral administration, which is inconvenient to the patient. The failure of anti-tubercular chemotherapy is mainly due to patient non-compliance (Burman et al., 1997), hence the importance of reducing the drug dose. In order to solve this problem, targeted anti-tubercular drug delivery to the lung may increase local therapeutic effect and reduce systemic exposure.

Attempts by Pandey et al., (2003) at preparation of inhaled antitubercular formulation, showed that pulmonary delivery of antitubercular drugs is feasible. Briefly, the authors prepared nanoparticles containing rifampicin, isoniazid and pyrazinamide encapsulated in poly (DL-lactide-co-glycolide), by the multiple emulsion technique. The drug loading (mg drug/g polymer) was 570 ± 27 for rifampicin, 663 ± 58 for isoniazid and 680 ± 56 for pyrazinamide. A single nebulisation to guinea pigs resulted in sustained therapeutic drug levels in the plasma for 6–8 days and in the lungs for up to 11 days. The elimination half-life and mean residence time of the drugs were significantly prolonged compared to oral administration, resulting in an enhanced relative bioavailability (compared to oral administration) for encapsulated drugs (12.7, 32.8 and 14.7-fold for rifampicin, isoniazid and pyrazinamide, respectively). On nebulisation of nanoparticles containing drugs to infected guinea pigs at every 10th day, no tubercle bacilli could be detected in the lung after five doses of treatment whereas 46 daily doses of orally administered drug were required to obtain an equivalent therapeutic benefit.

In the current work, different frontline anti-tubercular agents (isoniazid, rifampicin and pyrazinamide) were spray dried using conditions outlined in Appendix I. The spray drying parameters used included inlet temperature, drying gas and solvent composition. The effects of the spray drying parameters on the morphological characteristics of isoniazid, rifampicin and pyrazinamide spray-dried systems were examined, using a range of spray drying conditions in order to study the feasibility of producing microparticles of anti-tubercular agents for pulmonary drug delivery. An *in vitro* evaluation was carried out on

selected spray dried and micronised samples. The findings from this study provided a basis for the subsequent formulation of particles suitable for inhalation by spray drying process.

5.2 Spray-dried isoniazid systems

5.2.1 Introduction

Isoniazid is a first-line anti-tubercular medication used in the prevention and treatment of tuberculosis. In the current project, the preparation and properties of spray-dried isoniazid systems with and without excipients (PVP or hydroxypropyl-β-cyclodextrin) present were investigated. The morphology of all the powders produced from the spray-dried systems were analysed using the scanning electron microscope, and subsequently some of these systems were selected for further characterisation.

The objective of this study was to spray dry isoniazid to ascertain if nanoporous microparticles could be produced and subsequently to optimise the processing parameters and spray drying conditions to produce nanoporous microparticles.

5.2.2 Isoniazid systems spray-dried from methanol/butyl acetate

Healy et al., (2007) reported that the hydrophobic/hydrophilic nature of the compound drug is an important factor in selecting the solvent system for spray drying. Ní Ógáin (2006) reported that spray drying of the hydrophilic non-reducing sugar (trehalose) from a co-solvent ratio of 80:20 (v/v) and 50:50 (v/v) methanol: butyl acetate, resulted in nanoporous microparticles. Isoniazid is freely soluble in water (USP, 2007), therefore, it was hypothesized that the methanol: butyl acetate system would offer most potential in terms of nanoporous microparticles production of isoniazid. Isoniazid was prepared in 80% methanol/ 20% butyl acetate v/v and 50% methanol /50% butyl acetate v/v and spray-dried at an inlet temperature of 78 °C. The resultant powders were viewed by SEM. SEM micrographs of these systems showed irregular fused rough particles (Figure 5.1 b & c), in contrast to the large, irregular crystals of isoniazid raw material (Figure 5.1 a). Mc Donald (2005), Nolan (2008) reported that production of NPMPs was dependant on several spray-drying parameters/conditions, including inlet drying temperature. Therefore, the effect of changing inlet drying temperature was initially considered. The inlet temperature was changed to 100 °C, maintaining all other conditions as in initial experiments. Large fused aggregates of particles were recovered as shown in SEM (Figure 5.1 d &e). It is clear that increasing inlet temperature did not improve the morphological characteristics of spray dried isoniazid under these conditions.

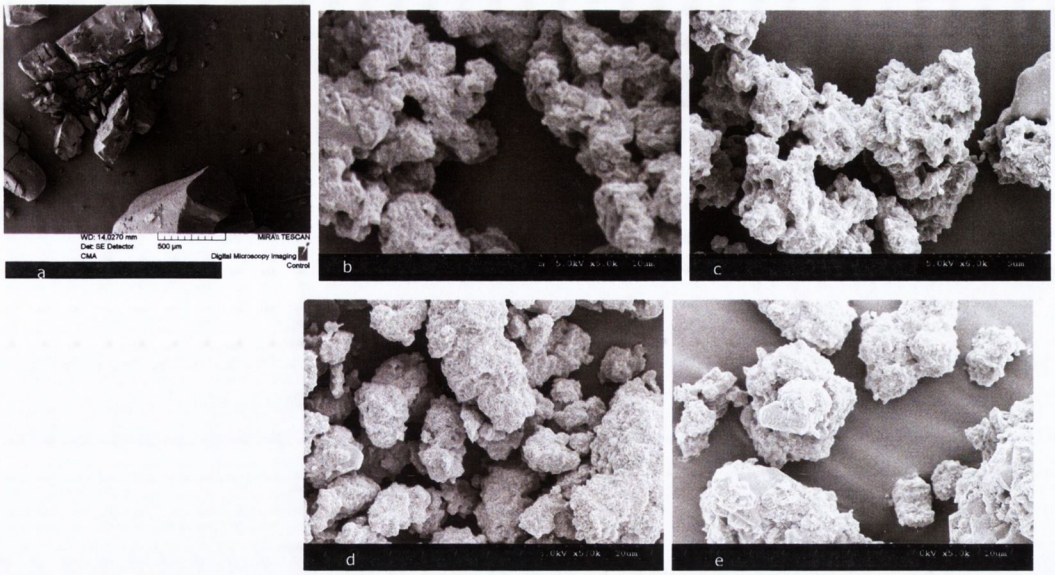

Figure 5.1- SEM micrographs of (a) isoniazid starting material and isoniazid spray-dried from methanol/butyl acetate (b)80:20 at an inlet temperature of 78°C (c) 50:50 at an inlet temperature of 78°C (d) 80:20 at an inlet temperature of 100°C (e) 50:50 at an inlet temperature of 100°C.

The X-ray powder diffractograms of spray dried isoniazid from methanol/ butyl acetate solvent systems displayed peaks, characteristic of crystalline isoniazid unprocessed material, confirming the crystalline form of the samples. The crystallinity of the spray dried samples was reduced in comparison to isoniazid raw material, indicated by the reduction in peak intensities of spray dried samples in comparison to the starting material (Figure 5.2). DSC data shown in Figure 5.3 supported the crystalline nature of the spray-dried isoniazid. DSC analysis showed only one thermal event, an endothermic peak, with its onset at ~170 °C for both unprocessed and spray dried samples, ascribed to the melting process and confirmed by the literature value of 170 to 173 °C for isoniazid (USP, 2008).

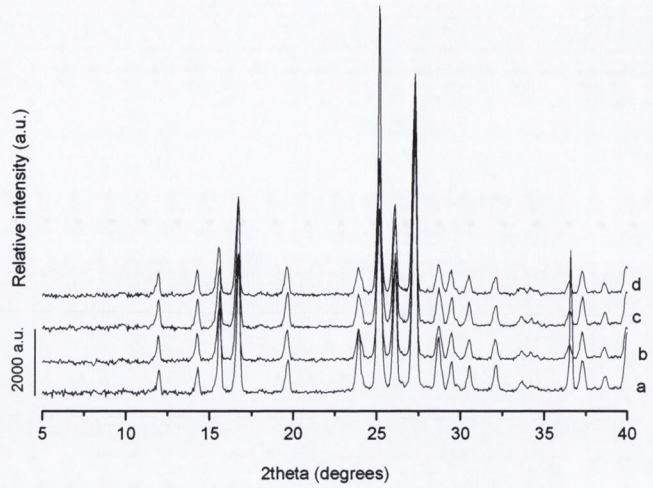

Figure 5.2 – XRD scans of isoniazid (a) starting material (b) spray-dried from methanol/butyl acetate 80:20 at 78°C (c) spray-dried from methanol/butyl acetate 80:20 at 100°C (d) spray-dried from methanol/butyl acetate 50:50 at 100°C.

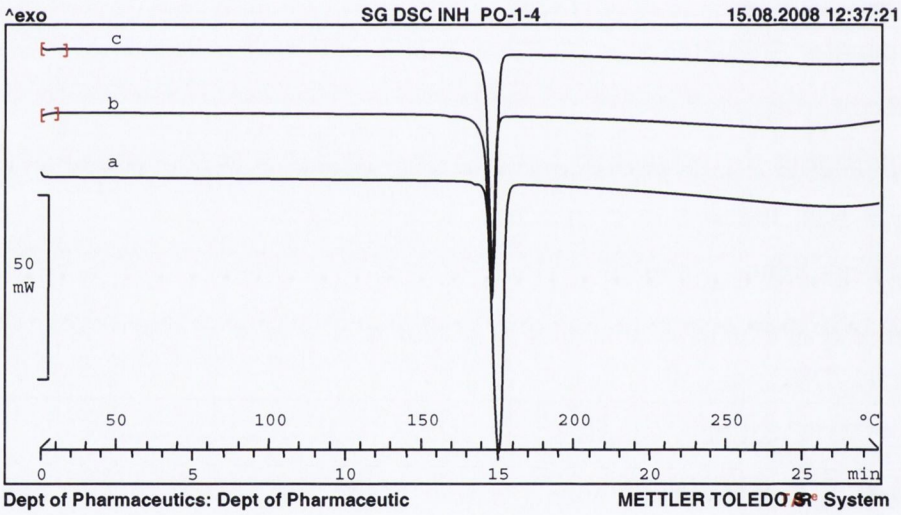

Figure 5.3 – DSC scans of (a) isoniazid starting material and isoniazid spray-dried from methanol/butyl acetate (b) 80:20 (c) 50:50

5.2.3 Water: Methanol: butyl acetate solvent systems

Spray drying of isoniazid from water: methanol: butyl acetate systems was considered based on results reported by Katheri (2007) with chitosan glutamate (water-soluble compound) from various solvent ratios of water: methanol: butyl acetate, which resulted in nanoporous microparticles.

Isoniazid spray-dried from water: methanol: butyl acetate 1: 15: 15 and 1:6:6 showed a crystalline XRD pattern as shown in Figure 5.4. The crystalline form of the spray-dried

systems was evident from the presence of peaks. It was also noticed from XRD analysis that the degree of crystallinity of spray-dried isoniazid was reduced in comparison to the raw material.

DSC scans shown in Figure 5.5 supported the crystalline nature of spray-dried isoniazid. A melting endotherm was visible on investigation of isoniazid unprocessed material, which had an onset temperature at ~171 °C and peaking at ~173 °C, which is in good agreement with the melting point reported in the literature at 170 to 173 °C (USP, 2007). The DSC thermograms of isoniazid spray-dried from water: methanol: butyl acetate 1:15:15 or 1:6:6 (Figure 5.5 b and c) showed one thermal event, an endothermic peak with onset temperature of ~ 170 °C.

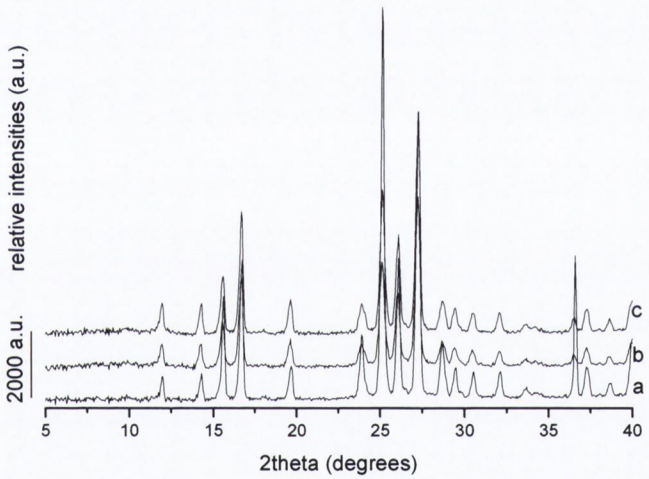

Figure 5.4- XRD scans of (a) isoniazid starting material and isoniazid spray-dried from water: methanol: butyl acetate (b) 1:15:15 (c) 1:6:6.

.

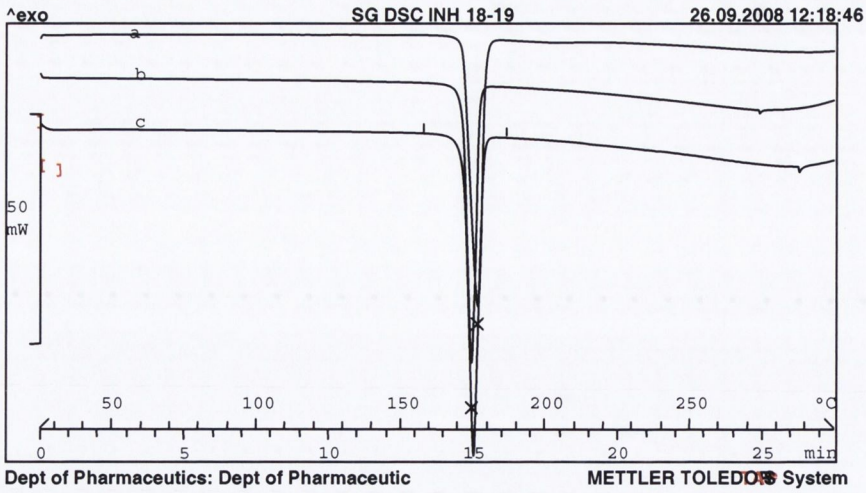

Figure 5.5- DSC scans of (a) isoniazid starting material and isoniazid spray-dried from water: methanol: butyl acetate (b) 1:15:15 (c) 1:6:6.

SEM micrographs of spray dried isoniazid from water: methanol: butyl acetate 1:15:15 showed non-porous irregular shaped, large masses of powder with rough surfaces (Figure 5.6b). The change in co-solvent to 1:6:6 water: methanol: butyl acetate resulted in non-porous, smooth and rough surface particles as shown in Figure 5.6 c.

It could be concluded that spray drying of isoniazid from different ratios of methanol: butyl acetate or water: methanol: butyl acetate produced non-porous particles. The spray dried systems resulted in predominantly crystalline powdered products as confirmed by DSC and XRD analysis.

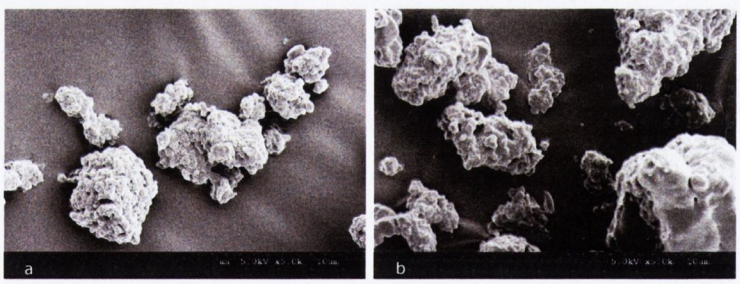

Figure 5.6- SEM micrographs of isoniazid spray-dried from water: methanol: butyl acetate (a) 1:15:15 (b) 1:6:6.

5.2.4 Spray-dried excipients systems

5.2.4.1 Introduction

A previous attempt at spray drying hydroxypropyl β-cyclodextrin (HP-β-CD) and PVP produced porous particles (Li, 2005). Generally, the apparatus used was a Büchi Mini Spray Dryer; HP-β-CD was spray dried from methanol/butyl acetate, PVP solution was prepared from a solvent composition of 50% (v/v) methanol: 50% (v/v) butyl acetate. PVP

and HP-β-CD were spray dried. The objective of this work was to spray dry the same excipients to ascertain if NPMPs could be produced and subsequently co-spray dry these excipients with isoniazid.

5.2.4.2 PVP spray-dried systems

A 2.0% (w/v) solution of PVP was spray-dried from methanol/butyl acetate 50:50 at an inlet temperature of either 100°C or 120°C, These were the inlet temperatures used by Li (2005), when solutions of PVP were spray-dried. The SEM micrographs of these systems (Figure 5.7) showed that the particles recovered were porous particles with visible holes and having different particle sizes. This was in good agreement with results of spray drying of the same systems reported by Li, (2005)

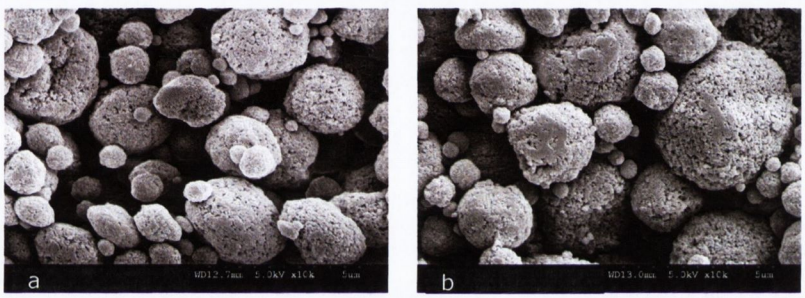

Figure 5.7- SEM micrographs: PVP system spray-dried from methanol/butyl acetate at an inlet temperature of (a) 100°C (b) 120°C.

5.2.4.3 HP- β-CD spray-dried systems

HP-β-CD was spray-dried from water/methanol/butyl acetate 1:6:6 or 1:15:15 at an inlet temperature of 100 °C. This was the inlet temperature used by Li (2005) when HP-β-CD was spray dried. The recovered particles were porous spherical particles with visible holes having different particle sizes (Figure 5.8).

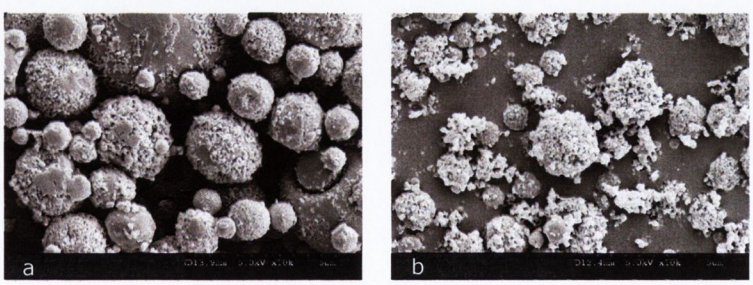

Figure 5.8-SEM micrographs of HP- β-CD system spray-dried from water/methanol/butyl acetate (a) 1:6:6 (b) 1:15:15.

5.2.5 ISONIAZID/ HP- β-CD SPRAY-DRIED SYSTEMS

As shown earlier spray drying of the hydrophilic oligosaccharide HP-β-CD using the mixed solvent system of water: methanol: butyl acetate in the ratio of 1:15:15 was successful in NPMPs production. Initial investigations using mixed solvents involved spray drying solutions of isoniazid/ HP-β-CD (1:9, 2:8 and 1:1) from the co-solvent system water: methanol: butyl acetate at solvent ratios of 1:15:15 (v/v) at an inlet temperature of 100 °C, this was the inlet temperature used when HP-β-CD spray dried from water: methanol: butyl acetate.

DSC results of spray-dried isoniazid/ HP-β-CD are shown in Figure 5.9. There was no melting process for isoniazid in DSC scans of isoniazid/ HP-β-CD 1:9 spray-dried system. The disappearance of the melting endotherm in DSC scan of isoniazid/ HP-β-CD 1: 9 spray-dried system indicate the miscibility of isoniazid and HP-β-CD and the conversion of the crystalline form of isoniazid into amorphous state. Investigation of the DSC scans shows a gradual disappearance of the melting peak of isoniazid. DSC scan of isoniazid/ HP-β-CD 1:1 spray-dried system shows that the melting peak of isoniazid was shifted towards lower temperature. Similar observation was found upon investigation of DSC scan of isoniazid/ HP-β-CD 2:8 and 3:7 spray-dried systems where the melting peak was shifted towards lower temperature and broadened.

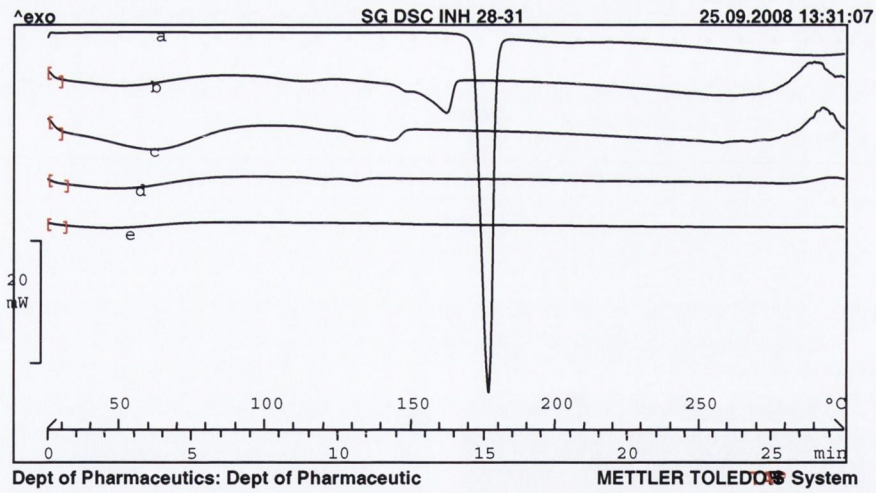

Figure 5.9- DSC scans of (a) isoniazid starting material and isoniazid/ HP-β-CD (b) 1:1 (c) 3:7(d) 2:8(e) 1:9 spray-dried systems.

The peaks of isoniazid starting material disappeared in isoniazid/ HP-β-CD 1:9 spray-dried system perhaps due to formation of complex between isoniazid and HP-β-CD (Figure 5.10). These results were favorably compared with the findings reported by Jain and

Adeyeye, (2001) who reported that the characteristic crystalline peaks of danazol disappeared when complexed with β- cyclodextrin derivative due to formation of inclusion complex. Powder X-ray diffraction analysis of isoniazid/ HP-β-CD 2:8 spray-dried system revealed that the sample was predominantly amorphous, but for the presence of very low intensity peaks at 16.8, 25.4, 26.2 and 27.3 degrees. X-ray diffractogram of isoniazid/ HP-β-CD 3:7 spray-dried system revealed that the sample was predominantly amorphous, but for the presence of small low intensity peaks at ~15.8, 16.8 25.4, 26.2 and 27.3 degrees, which corresponded to peaks of isoniazid raw material. Spray-dried isoniazid/ HP-β-CD (1:1) was a crystalline material as confirmed by the numerous diffraction peaks shown on the X-ray scan.

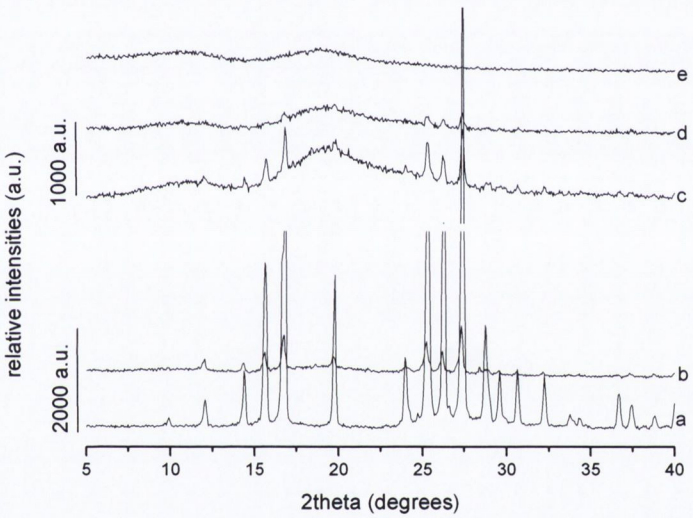

Figure 5.10- XRD scans of (a) isoniazid starting material and isoniazid/ HP-β-CD (b) 1:1 (c) 3:7 (d) 2:8 (e) 1:9 spray-dried systems.

An XRD scan of a physical mix of crystalline isoniazid in amorphous HP-β-CD was run to establish whether crystalline isoniazid mixed with amorphous HP-β-CD would be detectable by XRD. Figure 5.11 shows the X-ray diffractograms of physical mixture of crystalline isoniazid and spray dried isoniazid/ HP-β-CD 1:9. It is obvious that several peaks attributable to isoniazid were found in the scan of the physical mixture, even at this low concentration of crystalline material (10%, w/w isoniazid). On the other hand, the spray-dried sample was predominantly amorphous. Therefore, it was possible to detect isoniazid in a sample containing 90% (w/w) of HP-β-CD using XRD technique. Hence, the absence of isoniazid peaks in the diffractogram of spray-dried composite could not be

attributed to the high content of HP-β-CD or to the limit of detection by XRD. It would appear therefore that isoniazid is present in the amorphous form in the spray dried system.

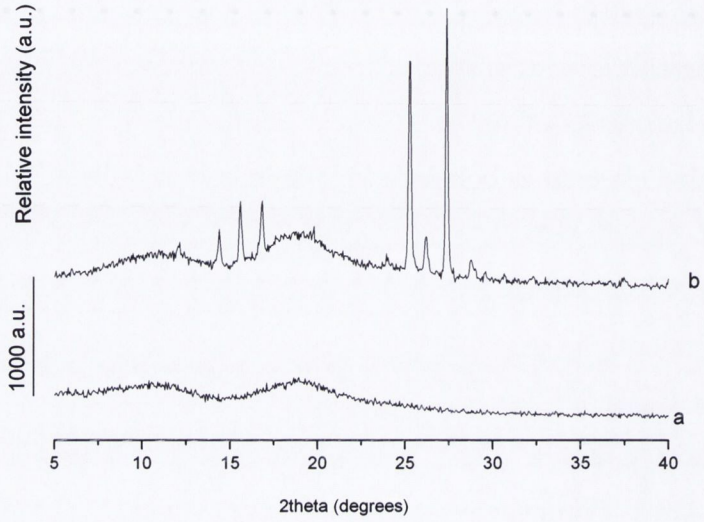

Figure 5.11- XRD scans of (a) spray –dried and (b) physical mixture of isoniazid/ HP-β-CD 1:9

It is clear that the morphology of the recovered powder was dependent on HP-β-CD content in spray-dried sample. SEM micrographs of spray-dried isoniazid/ HP-β-CD 1:9 system showed spherical porous particles, while particles of spray dried 2:8 composite were fused spherical particles, in contrast to the irregularly shaped aggregates of particles and small spherical particles observed in SEM micrographs spray dried isoniazid/ HP-β-CD 1:1 (Figure 5.12).

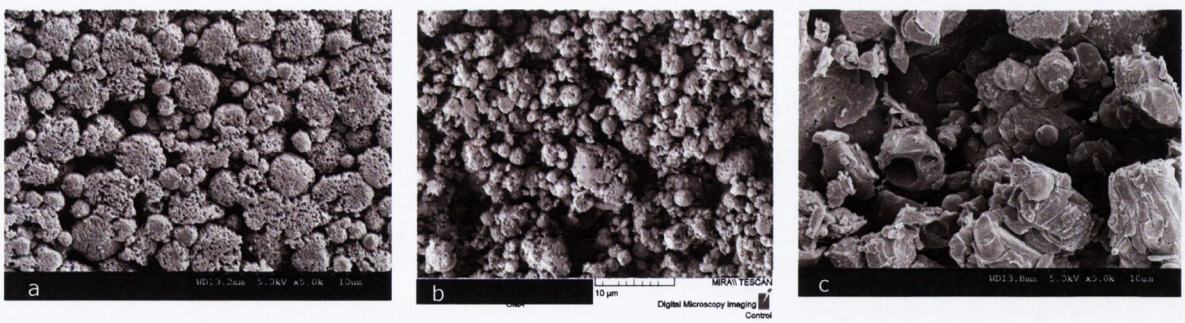

Figure 5.12- SEM micrographs of isoniazid/ HP-β-CD (a) 1:9 (b) 2:8 (c) 1:1 spray-dried systems.

FTIR spectra of unprocessed isoniazid and spray-dried isoniazid/ HP-β-CD 1:1 are shown in Figure 5.13. According to Gunasekaran et al., (2009), isoniazid in the solid phase has a strong band in the FTIR spectrum at 1667 cm^{-1} due to C=O stretching vibration, a band at 1334 cm^{-1} due to C-N stretching vibrations and a band at 3303 cm^{-1} due to N-H stretching vibration. The spectrum of unprocessed isoniazid shows a band at 1667 cm^{-1} due to C=O stretching vibration, a band at 1334 cm^{-1} due to C-N stretching vibrations and band at 3303 cm^{-1} due to N-H stretching vibration.

It was observed that IR spectrum of spray-dried isoniazid/ HP-β-CD (1:1) (crystalline isoniazid) was compared favorably with that of isoniazid starting material. It shows the characteristic bands at 3303 cm^{-1} due to N-H stretching vibration, 1668 cm^{-1} due to C=O stretching vibration and band at 1335 cm^{-1} due to C-N stretching vibrations. This was nearly identical to that of the starting material, indicating the similarity of vibration in bonding energies of the sample and that processing did not alter the chemical structure of the compound.

Figure 5.14 shows FTIR spectra of spray dried crystalline isoniazid (spray dried isoniazid/ HP-β-CD 1:1) and spray dried amorphous isoniazid (spray dried isoniazid/ HP-β-CD 1:9), FTIR spectroscopy of the amorphous isoniazid indicated that the characteristic bands of isoniazid disappeared. In addition, a broad peak of O-H stretching in the range of 3000 to 3600 cm^{-1} was found in the spectrum, this corresponds to the multiple O-H functional groups of HP-β-CD molecules. This was consistent with the results obtained from X-ray diffraction, DSC scans of spray dried isoniazid/ HP-β-CD 1:9 which suggested that isoniazid was completely miscible with HP-β-CD.

.

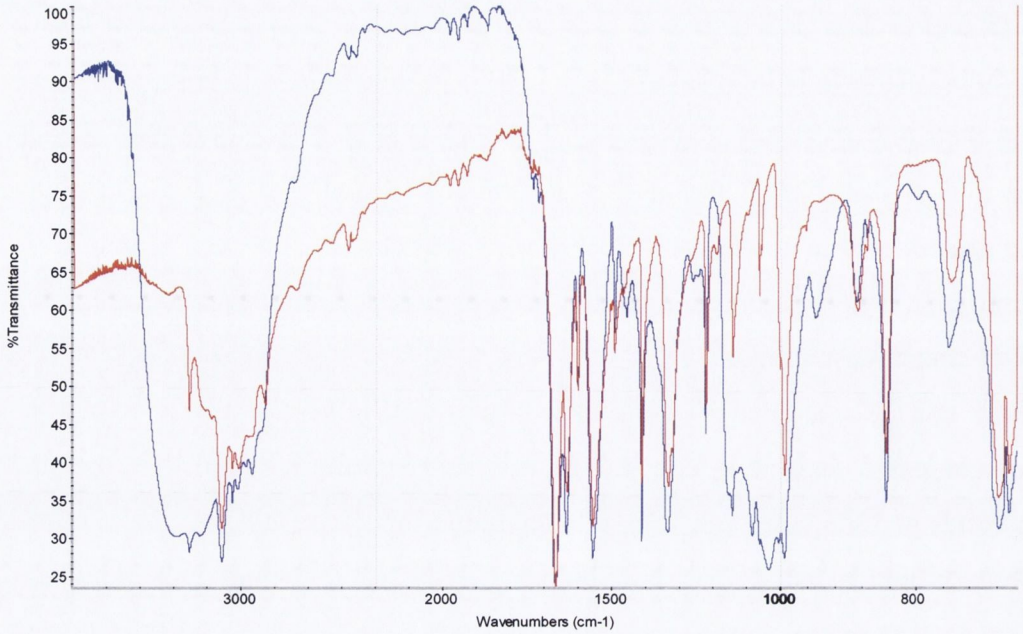

Figure 5.13- FTIR spectra of isoniazid unprocessed material (red line), spray-dried INH/ HP-β-CD 1:1(blue line).

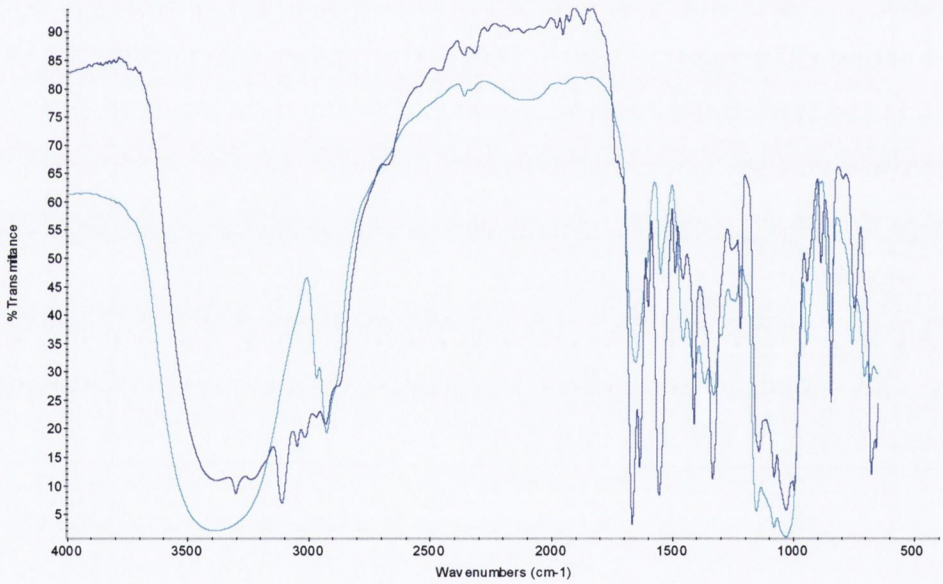

Figure 5.14- FTIR scans of spray-dried isoniazid/ HP-β-CD 1:9 (green line) and spray-dried isoniazid/HP-β-CD 1:1 (blue line).

Furthermore, Figure 5.15 is a report generated by The OMNIC E.S.P. software, by searching different libraries for the best match for the analysed material. It is obvious that FTIR spectrum of spray-dried isoniazid/ HP-β-CD 1:9 was compared favorably with the IR spectra of HP-β-CD

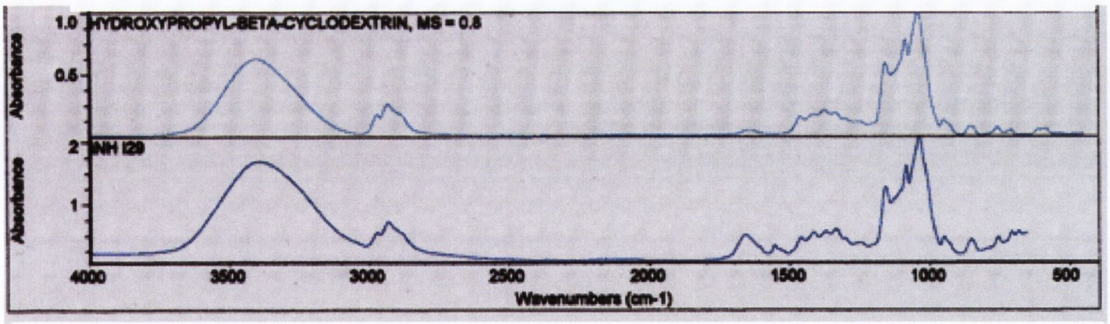

Figure 5.15- FTIR scans of spray-dried isoniazid/ HP-β-CD 1:9 (dark blue line) and HP-β-CD from Nicolet library (light blue lines).

5.2.6 Moisture sorption-desorption study for isoniazid/ HP-β-CD (1:9) spray-dried system

York, (1983) reported that the water vapor sorption properties of pharmaceutical materials such as excipients, binders, and drug formulations are recognised as critical factors in determining their storage, stability, processing and application performance. The objective of this study was to investigate the moisture sorption characteristics of isoniazid/ HP-β-CD (1:9) particles produced by co-spray drying of isoniazid/ HP-β-CD (1:9). This is useful in studying the stability of the spray dried composite. The choice of isoniazid/ HP-β-CD (1:9) spray-dried system was based on SEM and XRD results of this system, which indicated the formation of amorphous nanoporous microparticles of isoniazid.

Figure 5.16 displays the typical moisture sorption and desorption results obtained from isoniazid/ HP-β-CD (1:9) spray-dried system at 25 °C. Two complete sorption and desorption cycles were collected. The first cycle is shown in black square symbols (sorption) and white square symbols (desorption), while the second cycle is represented by the black triangle symbols (sorption) and white triangle symbols (desorption) traces. The adsorption trace displays the percentage change in mass, referenced to the dry mass, versus the target relative humidity. It should be noted that for this sample and conditions there is virtually no difference between the first and second cycle desorption isotherms. The isoniazid/ HP-β-CD (1:9) spray-dried system is very hydrophilic, as indicated by the huge percentage change in mass between 40 and 90% RH (first cycle). The isoniazid/ HP-β-CD (1:9) spray-dried system isotherm shows a drop in mass for the 70-80% RH step, which could be attributed to sample crystallisation. The crystalline phase will often have a much lower capacity and/or affinity for water vapor, resulting in a net mass loss at a critical relative humidity. For this sample, isoniazid/ HP-β-CD (1:9) spray-dried system may crystallise at 70-80% RH and 25 °C, it was not possible to make XRD to confirm the

crystallinity because the sample gave a sticky film on the sample holder as shown in Figure 5.17. Also, there is no drop in water uptake in the sorption isotherms of the second cycle which could be attributed to changes in the surface or in solid state form. Together, these results indicate that water sorption is not completely reversible.

It should be noted that the physical stability (solid-state stability) of amorphous isoniazid (spray dried isoniazid/ HP-β-CD (1:9)) under the storage conditions of 25 °C/75% relative humidity was examined. However, sticky mass was observed after storage which was not suitable for further investigation.

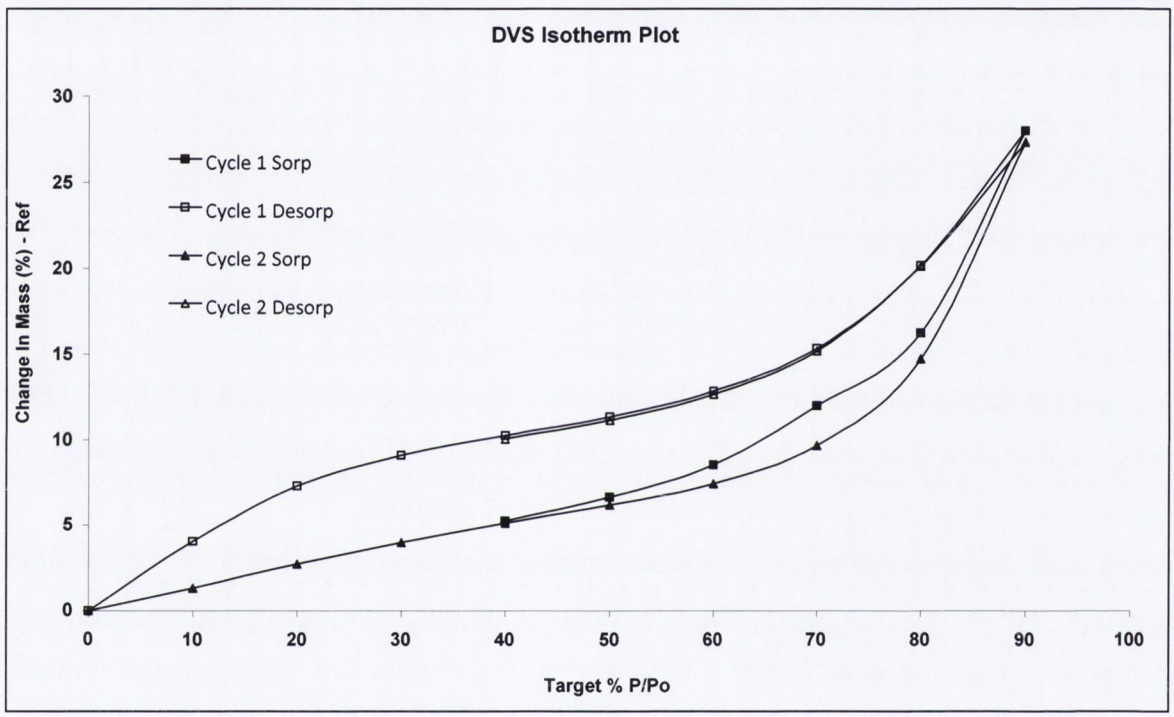

Figure 5.16- Adsorption and desorption isotherms of water on spray-dried INH/ HP-β-CD (1:9) (first cycle in black and white square symbols, second cycle in black and white triangle at 25 °C.

Figure 5.17- sticky film of spray dried INH/ HP-β-CD in the DVS sample holder

5.2.7 Isoniazid/PVP systems spray-dried from methanol/butyl acetate

Considering that, spray-dried PVP from methanol/butyl acetate produced spherical NPMPs as shown earlier and as reported by Li (2005), the same solvent was used for subsequent

spray drying of isoniazid/PVP systems. Isoniazid/PVP composite systems consisting of different PVP ratios were spray-dried at an inlet temperature of 100 °C using the spray drying parameters outlined at Appendix I. SEM micrographs of the produced powders are shown in Figure 5.18. It is clear that different PVP concentrations produced significant changes in the morphological characters of the spray-dried samples. At higher proportion of PVP (INH/PVP 1:9 and 2:8) the spray-dried particles were spherical porous particles (Figure 5.18 c and d), while in lower proportions of PVP (INH/PVP 3:7 and 1:1) it was observed that the particles were fused in both systems (Figure 5.18 (a) and (b)). It was concluded from these micrographs that significant changes in particle shape of spray-dried isoniazid is dependent on the PVP proportion.

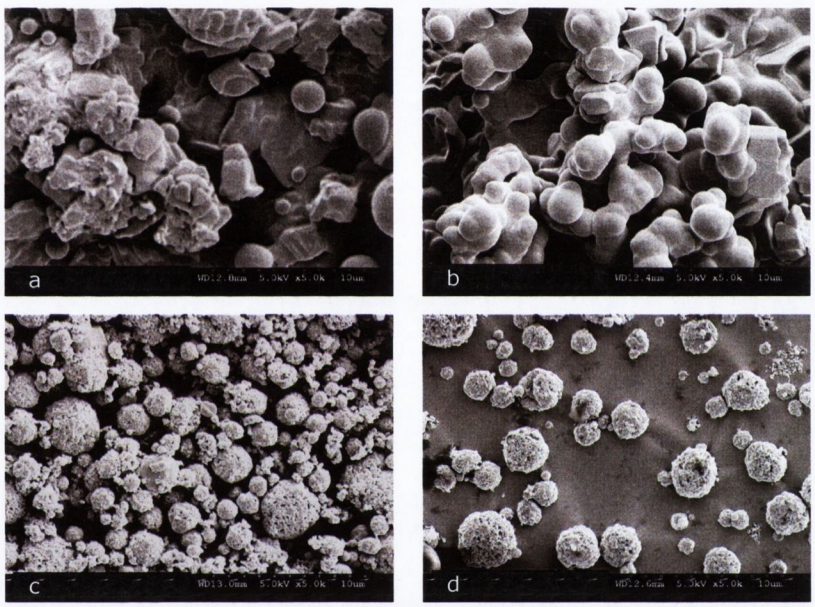

Figure 5.18 - SEM micrographs of isoniazid/PVP 40.000 (a) (1:1) (b) (3:7) (c) (2:8) (d) (1:9) systems spray-dried from methanol/butyl acetate at an inlet temperature of 100 °C.

DSC results of spray-dried isoniazid/PVP at an inlet temperature of 100 °C are shown in Figure 5.19. Investigation of the DSC scans shows a gradual disappearance of the melting peak of isoniazid. There was no melting process for isoniazid in DSC scans of isoniazid/PVP 1:9 and 2:8 spray-dried systems. DSC scan of isoniazid/PVP 1:1 spray-dried system shows that the melting peak of isoniazid was shifted towards lower temperature. Similar observation was found upon investigation of DSC scan of isoniazid/PVP 3:7 spray-dried system where the melting peak was shifted towards lower temperature and broadened. The disappearance of the melting endotherm in DSC scan of isoniazid/PVP 1:9 and 2:8

spray-dried systems indicate the miscibility of isoniazid and PVP and the conversion of the crystalline form of isoniazid into amorphous state.

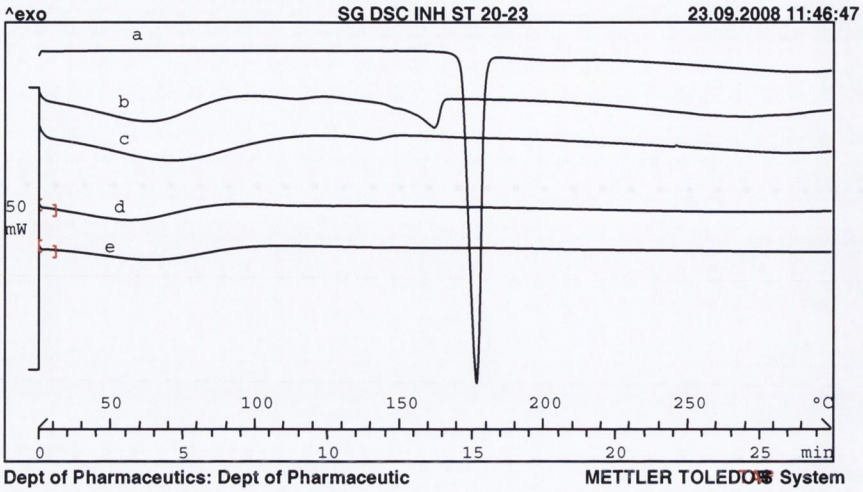

Figure 5.19- DSC scans of (a) isoniazid starting material and isoniazid/PVP 40.000 (b) (1:1) (c) (3:7) (d) (2:8) (e) (1:9) system spray-dried from methanol/butyl acetate.

X-ray diffraction analysis of spray-dried isoniazid/PVP systems showed that isoniazid/PVP 1:9 spray-dried from methanol/butyl acetate 50:50 at an inlet temperature of 100 °C were amorphous as indicated by the broad "halo" pattern with no distinct peaks as shown in Figure 5.20. X-ray diffraction analysis of isoniazid/PVP 2:8 showed very low intensity peaks at approximately 17, 26 and 27 2θ degrees, spray dried isoniazid/PVP 3:7 spray-dried system showed peaks at ~16, 17, 26 and 27 2θ degrees, these peaks were attributed to the peaks of isoniazid unprocessed material. The crystalline nature of isoniazid/PVP 1:1 spray-dried system is clear from XRD pattern of this system evidence from presence of peaks attributable to isoniazid starting material.

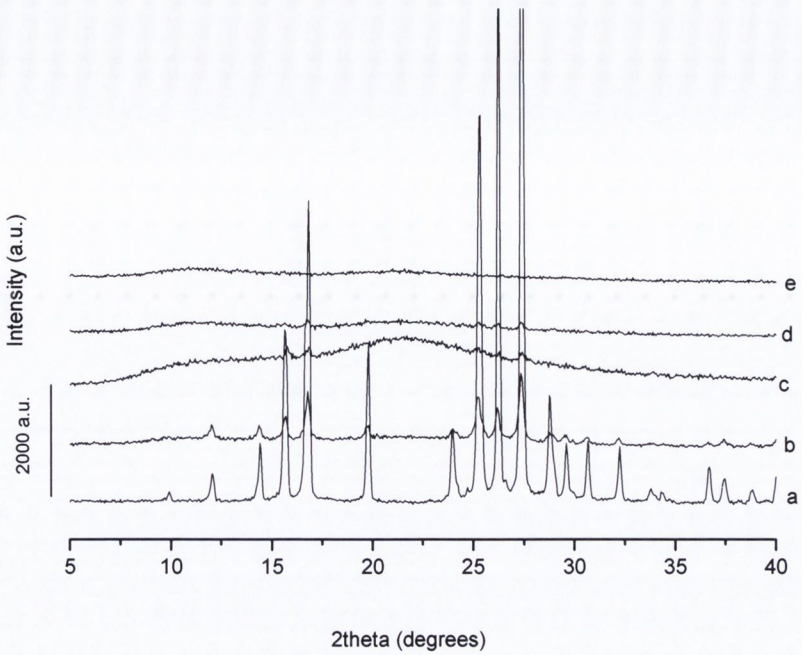

Figure 5.20- XRD scans of (a) isoniazid starting material and isoniazid/PVP (b) (1:1) (c) (3:7) (d) (2:8)(e) (1:9) system spray-dried from methanol/butyl acetate an inlet temperature of 100 °C.

Walton and Mumford, (1999) reported that increasing temperature of drying air produces a decrease in bulk and particle density due to an increase in particle size and a greater tendency for the particles to be hollow. The effect of inlet temperature was also investigated. A range of four composites consisting of isoniazid/PVP 1:9, 2:8, 3:7 and 1:1 were prepared and spray-dried at an inlet temperature of 120°C.

DSC scans of isoniazid/PVP spray-dried samples at an inlet temperature of 120°C are shown in Figure 5.21. Generally, the DSC scans show similarity to those spray-dried at an inlet temperature 100 °C, where there was no melting peak in DSC scans of isoniazid/PVP 1:9 and 2:8 spray-dried systems, which indicate miscibility of isoniazid and PVP when spray-dried at these ratios. The melting peak of isoniazid was shifted in DSC scans of isoniazid/PVP 1:1 and 3:7 spray-dried systems as shown in Figure 5.21.

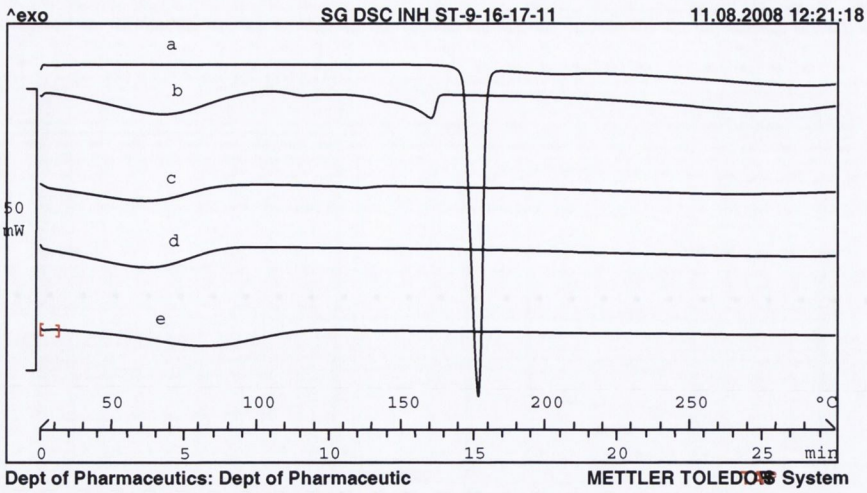

Figure 5.21- DSC scans of (a) isoniazid starting material and isoniazid/PVP 40.000 (b) (1:1) (c) (3:7) (d) (2:8) (e) (1:9) systems spray-dried from methanol/butyl acetate at an inlet temperature of 120 °C.

X-ray diffraction analysis of spray-dried isoniazid/PVP systems showed that isoniazid/PVP 1:9 and 2:8 spray-dried from methanol/butyl acetate 50:50 at an inlet temperature of 120 °C were amorphous as indicated by the broad "halo" pattern with no distinct peaks as shown in Figure 5.22. X-ray diffraction analysis of isoniazid/PVP 3:7 spray-dried system showed very low intensity peaks attributable to the peaks of isoniazid, unprocessed material. The crystalline nature of isoniazid/PVP 1:1 spray-dried system is clear from XRD pattern of this system evidence from presence of peaks attributable to isoniazid starting material.

SEM micrographs of spray-dried isoniazid/PVP at an inlet temperature of 120 °C showed the effect of PVP on the morphological properties of the recovered particles, spherical porous particles were produced upon using high concentration of PVP (90% of total solid) (Figure 5.23 d). In contrast, fused aggregations of particles were seen in SEM micrographs of spray dried isoniazid/PVP 1:1 (Figure 5.23 a)

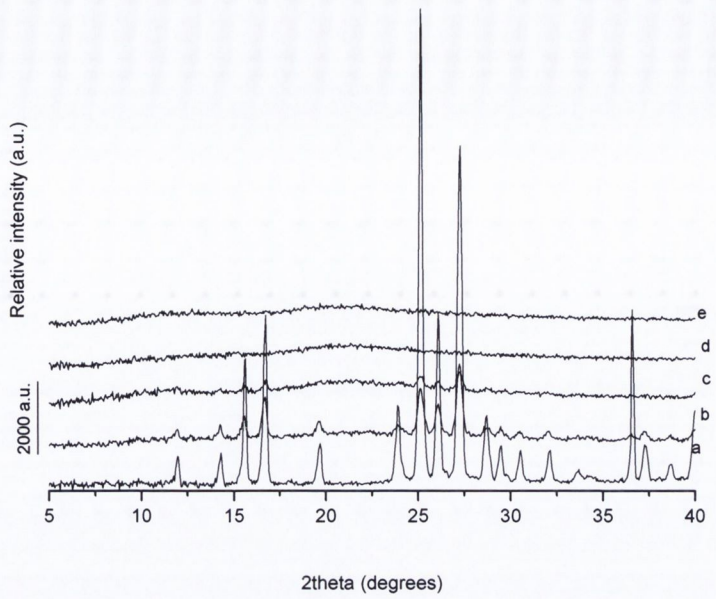

Figure 5.22- XRD scansof (a) isoniazid starting material and isoniazid/PVP (b) (1:1) (c) (3:7) (d) (2:8) (e) (1:9) systems spray-dried from methanol/butyl acetate 50:50 at inlet temperature of 120 °C.

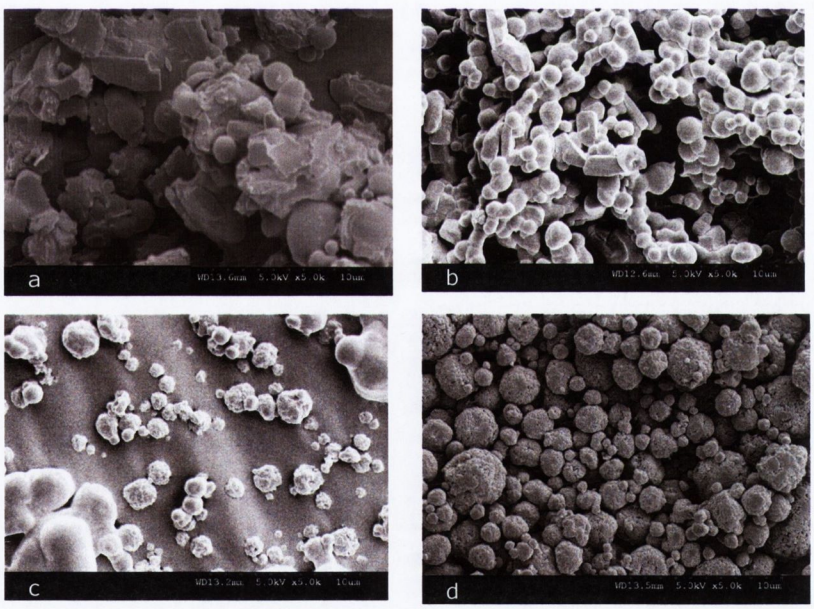

Figure 5.23- SEM micrographs of isoniazid/PVP (a) 1:1 (b) (3:7) (c) (2:8) (d) (1:9) spray-dried from methanol/butyl acetate 50:50 at inlet temperature of 120 °C.

5.2.8 PARTICLE CHARACTERISATION OF SPRAY-DRIED ISONIAZID

Isoniazid/ HP-β-CD 1:9 spray-dried system, isoniazid/PVP 1:9 spray-dried at an inlet temperature of 120 °C, isoniazid/PVP 2:8 and 1:9 spray-dried at an inlet temperature of 100 °C as well as micronised isoniazid were selected for further characterisation in terms

of particle size, surface area and twin impinger analysis. These particular spray drying conditions were chosen as they were the closest to the desired result. Ideally, uniform and porous particles within the size range of 2-5 μm are desirable. These spray-dried systems were also compared to micronised isoniazid. It should be noted that particle size of isoniazid starting material has very high in comparison to spray-dried samples so it was micronised to be compared with spray-dried systems. The analysis was carried out at least in triplicate for each sample and the average was calculated.

Particle size distribution was determined using laser diffraction particle sizing at the standard operational settings of 2-bar air pressure and 60% vibration feed rate. Both micronised and spray-dried isoniazid systems showed a mono-modal, highly reproducible particle size distribution (Figure 5.24). The narrowest size distribution was found for the isoniazid / HP-β-CD 1:9 spray-dried system, with a span averaging 1.34 compared to 1.63 for the micronised isoniazid. Micronised isoniazid had an average median particle size of volume distribution d(0.5) of 4.01 ± 0.12 μm, which was larger than the spray-dried isoniazid/ HP-β-CD 1:9, which had an average d(0.5) of 2.33 ± 0.03 μm. The difference in particle size between different isoniazid/ PVP spray dried samples was statistically non-significant.

The surface areas determined for the different isoniazid samples are given in (Table 5.1). A surface area of 1.66 ± 0.06 m^2/g was measured for micronised isoniazid. A statistically significant 27-fold increase in surface area (45.12 ± 0.29 m^2/g) was measured for spherical NPMPs of spray-dried isoniazid/ HP-β-CD relative to micronised isoniazid, which could be attributed to the porous structure of NPMPs of spray dried sample, as the open porous structure provide a large surface area for nitrogen adsorption.

The nanoporous microparticles structure of spray-dried isoniazid/PVP (Figure 5.23d) increased surface area. On average, a 6.5-fold (10.70 ± 0.09 m^2/g) increase in surface area was measured for powder recovered from spray drying of isoniazid/PVP 1:9 at an inlet temperature of 120 °C. A surface area of 23.65 ± 0.20 m^2/g and 30.82 ± 0.26 m^2/g was measured for isoniazid/PVP 2:8 and 1:9 spray-dried at an inlet temperature of 100 °C, respectively, which was 14- fold and 18-fold higher than that measured for the micronised isoniazid.

Table 5.1– Particle sizing and surface area for different isoniazid systems. Key: SD= spray-dried, INH=isoniazid

System	**Surface area** (m^2/g)	**Particle size** (μm) d(0.5)
Micronised INH	1.66 ± 0.06	4.01 ± 0.12
SD INH/PVP 1:9 at 120 °C	10.70 ± 0.09	2.91 ± 0.12
SD INH/PVP 1:9 at 100 °C	30.82 ± 0.26	3.09 ± 0.05
SD INH/PVP 2:8 at 100 °C	23.65 ± 0.20	2.97 ± 0.01
SD INH/ HP-β-CD 1:9	45.12 ± 0.29	2.33 ± 0.03

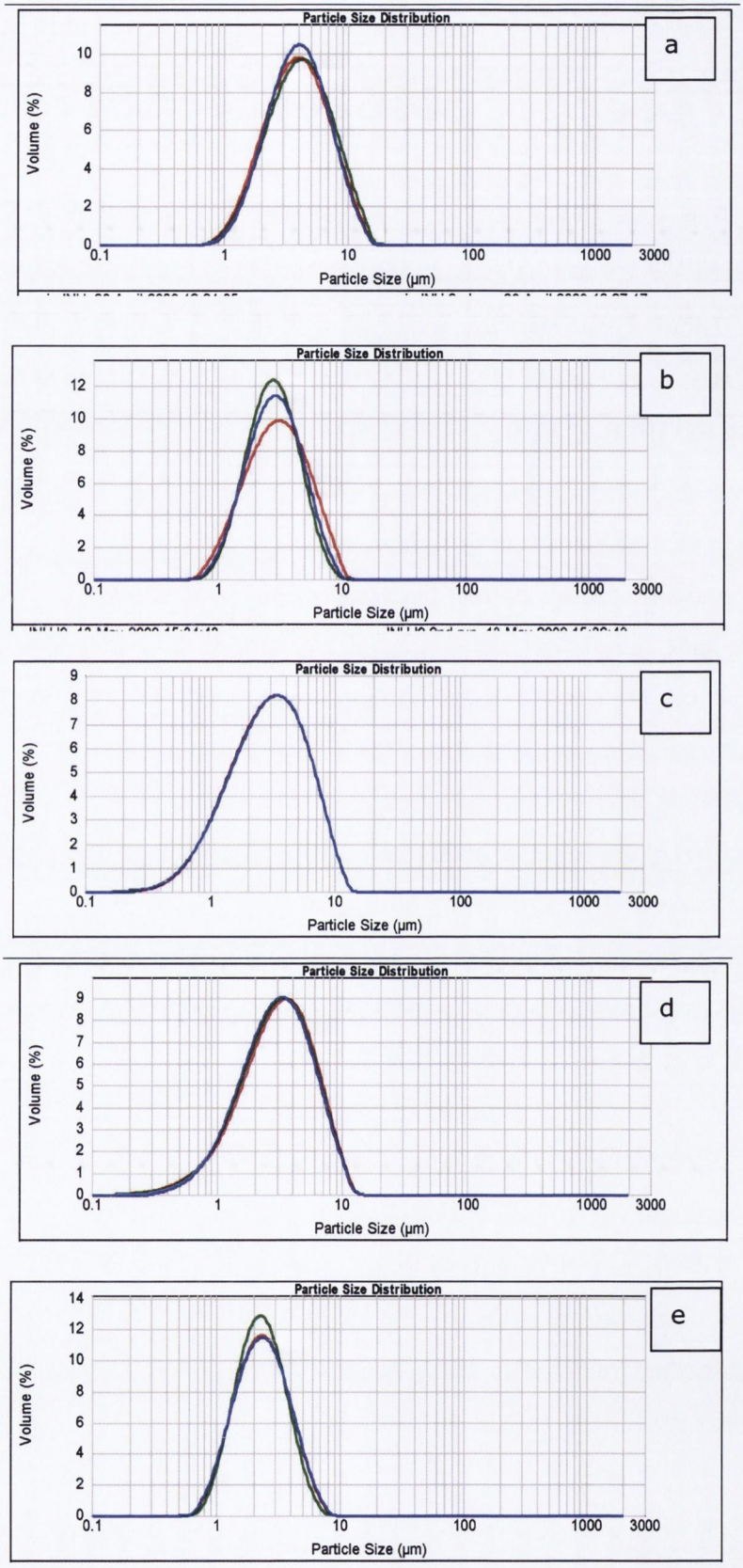

Figure 5.24 Particle size distributions of (a) micronised isoniazid (b) isoniazid/PVP 1:9 at an inlet temperature of 120 °C (c) isoniazid/PVP 2:8 spray-dried at an inlet temperature of 100 °C (d) isoniazid/PVP 1:9 spray-dried at an inlet temperature of 100 °C (e) isoniazid / HP-β-CD 1:9 spray-dried system.

5.2.9 *IN VITRO* DEPOSITION PROPERTIES OF SYSTEMS FOR INHALATION PURPOSES

As shown earlier micronised isoniazid was used instead of isoniazid raw material due to the fact that the particle size of isoniazid starting material is very high in comparison to spray-dried samples, so it was micronised to be compared with spray-dried systems. The twin impinger analysis was carried out in triplicate for each sample and the average was calculated. The results of twin impinger analysis are presented in Figure 5.25.

Figure 5.25 indicates that the percentage of dose retained in the device is high for micronised isoniazid in comparison to all spray-dried systems. Generally the dose retained in the device for all spray dried samples was less than 20%, while for micronised isoniazid the dose retained in the device was 38.6±11.7%. It was also noticed that there was a difference in the ratio of dose retained in the device to that deposited in stage I of the impinger. The highest ratio is for micronised isoniazid and is 0.9 and the lowest is for isoniazid/PVP 2:8 spray-dried at an inlet temperature of 100 °C and is 0.2. Generally, the large error bars for micronised and spray-dried samples indicate large standard deviations and inconsistency of the dosing. Two sample t-tests were used for statistical analysis of the results.

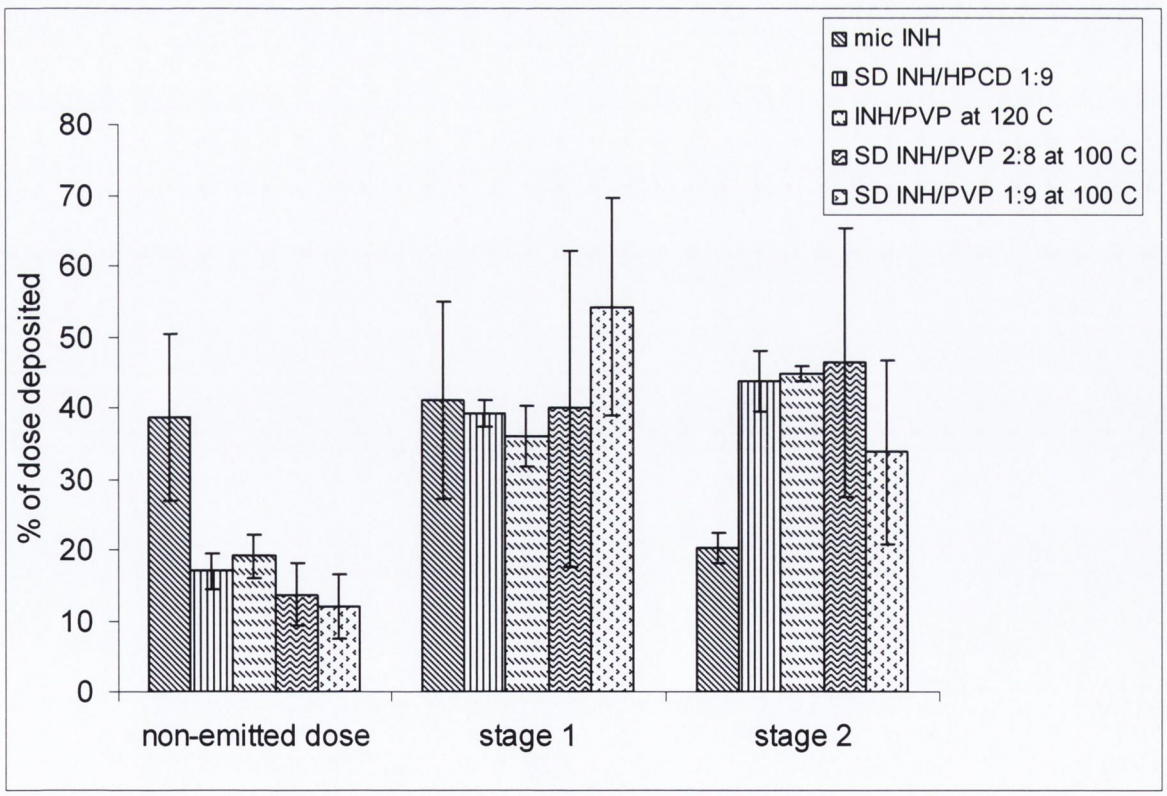

Figure 5.25- Twin impinger analysis of the micronised and spray-dried isoniazid samples.

Emitted dose was defined as the total quantity of the drug recovered from the upper and lower stages of the impinger and expressed as percent of the total dose loaded into the capsule. Figure 5.26 shows the emitted dose calculated for the micronised and spray-dried isoniazid; the emitted dose for micronised isoniazid was 61.3± 11.74, significantly lower than that calculated for NPMPs of isoniazid. There is no statistically significant difference ($p > 0.05$) in the emitted dose of spray-dried samples, measured at 82.9 ±2.54, 80.9±3.16, 87.9±4.51 and 86.3±4.39 for powders produced by spray drying of isoniazid / HPCD 1:9, isoniazid/PVP 1:9 at 120 °C, isoniazid/PVP 2:8 at 100 °C and isoniazid/PVP 1:9 at 100 °C respectively.

A further point of interest was that different spray dried systems have different particle size and different surface area, but there was no statistically significant difference in the percentage of dose deposited. This may be attributed to the fact that all spray dried samples have particle size suitable for inhalation (1-5 μm), therefore, all these particles can be deposited in the lung. Meanwhile, there is no correlation between the decrease in particle size and the extent of the percentage of dose deposited (Nolan, 2008). In other words Labris and Dolovich, 2003 reported that small size particles (1-5 μm) are deposited in the small airways and alveoli and are generally accepted to be "respirable", but the sample had the highest respirable fraction may not had the smallest particle size (Nolan, 2008) or had the highest surface area (Ní Ógáin, 2008).

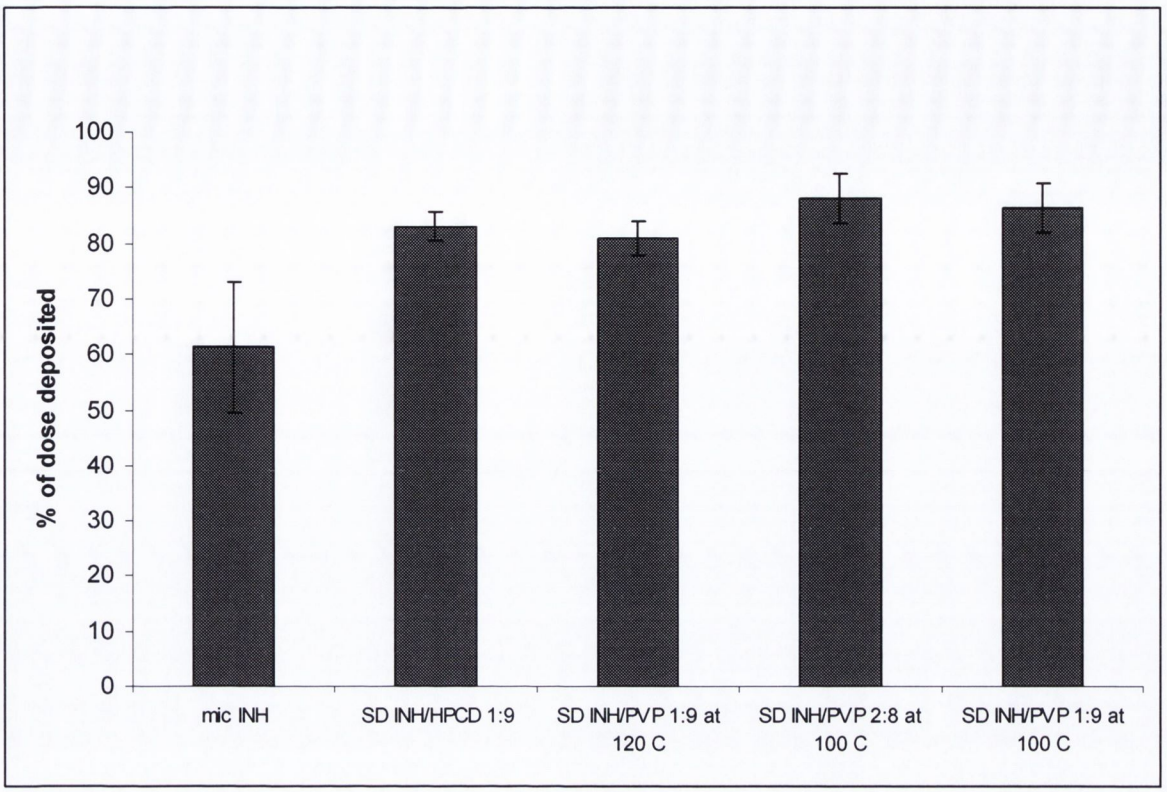

Figure 5.26- The emitted dose (i.e. deposited on stage 1 and 2 of twin impinger) of the micronised and spray-dried isoniazid samples.

Figure 5.27 shows the percentage of dose deposited in stage 2 of the twin impinger i.e. respirable fraction. Generally, the large error bars for NPMPs of isoniazid indicate large standard deviations and inconsistency of the dosing. The sample with the lowest deposition on stage 2 of twin impinger was micronised isoniazid, with measured respirable fractions of 20.32±2.20%. No statistically significant difference ($p > 0.05$) in respirable fraction between spray-dried isoniazid samples was calculated.

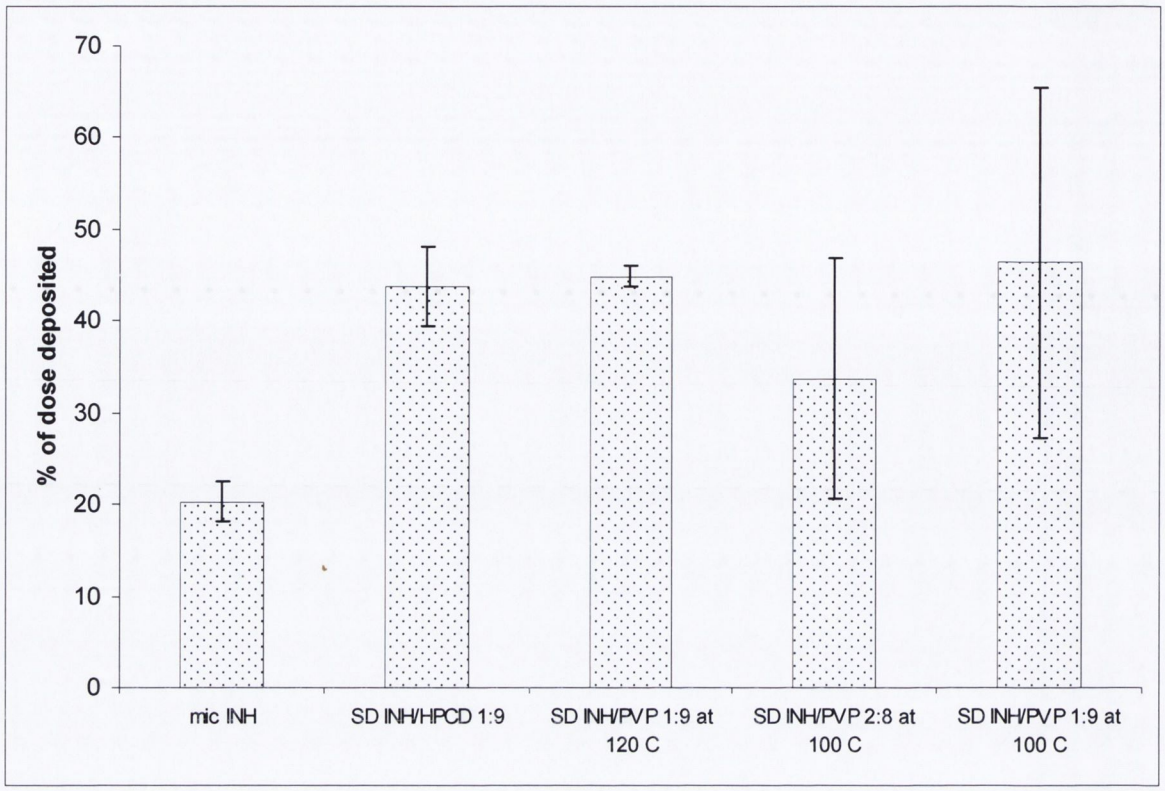

Figure 5.27 The respirable dose (i.e. deposited on stage 2 of twin impinger) of the micronised and spray-dried isoniazid samples.

Conclusion

The MeOH: BA and H_2O: MeOH: BA systems were used to spray dry isoniazid at different inlet temperatures; both systems were unsuccessful for spray-drying NPMPs and resulted in a mixed morphology of aggregates of particles. Isoniazid when processed alone gave material with a reduced degree of crystallinity as observed by XRD. Co-spray drying of isoniazid: excipient (PVP and HP-ß-CD) resulted in XRD amorphous systems in high concentration of the excipient, lower concentrations of the excipient gave predominantly amorphous phase with weak peaks of the starting isoniazid. The morphological characters of co-spray dried isoniazid: excipient systems showed that high concentration of excipient was required to produce NPMPs of composite.

5.3 Spray-dried rifampicin systems

5.3.1 Introduction

Rifampicin is an antibiotic used in the treatment of various infections due to mycobacteria and other susceptible organisms. It is used, mainly with isoniazid and pyrazinamide, as a component of multidrug regimens for the treatment of tuberculosis (Reynolds et al., 1996). The bactericidal activity of rifampicin is directly proportional to the concentration at the target site, so it is a so-called concentration-dependent antibiotic. However, rifampicin has a rather low aqueous solubility and according to the manufacturer's (Sigma) specification sheet, the solubility of rifampicin in water is 1.3 mg/ml in pH=4.3 and 2.5 mg/ml in pH=7.3 at 25°C. This low solubility limits the possibility of achieving high concentration in the broncho-alveolar epithelium-lining fluid when administered as aerosolised solution; this limited solubility also leads to poor bioavailability of drug and in turn affects the drug delivery system.

Low solubility of rifampicin is not the only aspect which should be considered during formulation process; polymorphism is another important issue that should be considered. Agrawal et al., (2004) reported that rifampicin exhibits polymorphism and exists in two crystalline forms (II and I) and an amorphous from. It should be noted that polymorphism of rifampicin is always postulated as a probable reason for its variable bioavailability (Agrawal et al., 2004).

Treatment period should be also considered during formulation of rifampicin, as it requires a high-dose treatment (the usual adult dose of rifampicin is 8 to 12 mg/kg. over a period of 4–6 months). *Mycobacterium tuberculosis* is known to develop resistance with traditional delivery systems of rifampicin as serum levels were found to vary below minimum inhibitory concentrations in clinical investigations. Rifampicin also has various side effects at dose levels administered in long-term clinical therapies, such as hepatotoxicity (Mandell and Sande, 1985). Hence, the importance of formulation of efficient stable dosage forms of rifampicin.

There are numerous reports in the literature regarding the efficiency of delivery of rifampicin. Suarez et al., (2001) used tuberculosis-infected guinea pig to screen for targeted delivery to the lungs by nebulisation, of either rifampicin alone, rifampicin within poly (lactide-co-glycolide) microspheres or polymer microparticles alone. The study supports the potential of rifampicin-loaded microspheres delivered to the lungs to treat pulmonary tuberculosis.

Recently, Sung et al., (2009) formulated rifampicin in a dry powder for pulmonary delivery. In this process, porous particles were obtained by spray drying process, the spray dried solution consisted of 1.20 g of L-leucine and 0.80 g of rifampicin in 200 ml water and 300 ml ethanol. The apparatus used was Mobile Minor spray dryer (Niro, Inc). The inlet temperature was set at 95°C and the solution feed rate at 50 ml/min. The authors reported that rifampicin content of the powder was measured to be 39.1□±□0.3%. SEM of the recovered particles showed that the spray-dried formulation produced thin-walled particle structures. The volume median diameter of the particles was 2.7□±□0.1 μm, and fine particle fraction of the total dose less than 5.8 μm, FPF_{TD}=□67.8□±□0.5%. Sung et al., (2009) performed pharmacokinetic studies with formulations delivered to guinea pigs by intratracheal insufflation and compared to oral and intravenous delivery of rifampicin. The doses administered were intravenous dose of 10 mg/kg, oral dose of 2.5 mg/kg, and pulmonary dose of the formulation of 2.5 mg/kg. The authors reported that these doses were based on the practical limitations of delivering large masses of dry powders to the guinea pigs. The pharmacokinetic study showed that the area under the curve (AUC) and the bioavailability for pulmonary administration of particle formulations was AUC~0.98 to 2.16 and F~0.53 to 0.72, which was significantly higher than that of the oral rifampicin treatment (AUC~0.21; versus F~0.17). These results reflect the feasibility of pulmonary delivery of rifampicin.

In the current study, production of dry powder of rifampicin suitable for inhalation is investigated. Recovered particles are characterised in terms of their physicochemical properties and *in vitro* aerosolisation performance by impaction studies.

5.3.2 Complexation of rifampicin

As previously discussed, the low aqueous solubility of rifampicin limits the possibility of achieving a high concentration in the broncho-alveolar epithelium-lining fluid when administered as aerosol. Therefore, it is important to use excipient(s) to enhance the solubility of rifampicin. Cyclodextrin can increase the apparent solubility of rifampicin due to the formation of water-soluble inclusion complexes in which a polar interior of the hollow, truncated cone-like cyclodextrin encapsulates hydrophobic parts of drug molecules (Tewes et al., 2008). Cyclodextrins have already been proposed for lung administration (Louey and Garcia-Contreras, 2004). Hydroxypropyl-β-cyclodextrin (HP-β-CD) is a cyclodextrin derivative, which is shown to be non-toxic after short term human exposure

(Evrard et al., 2004). Thus, forming a HP-β-CD complex with rifampicin is the focus of our efforts in this part of our study.

A known excess of rifampicin was added to a HP-β-CD solution. Sodium hydroxide or ammonium carbonate were used to adjust the pH to a value higher than 7.9 to enhance complexation of rifampicin with HP-β-CD, the complexation efficacy is enhanced when the pH value is increased above the pKa value of rifampicin (7.9) leading to an unprotonated molecule (Tewes et al., 2008). Bearing in mind that the final formula will be administered by inhalation, the pH of the complex was then adjusted to 7.4 (physiological pH) by hydrochloric acid 37% (v/v) after complexation was achieved.

Formation of complexes between rifampicin and HP-β-CD resulted in an increase in rifampicin apparent solubility. This increase was dependent on the molecule used to control the pH. When sodium hydroxide was used, the apparent solubility was 8.03 mg/ml, which is three times higher than the solubility of rifampicin raw material at this pH value according to the specification sheet for unprocessed rifampicin. When ammonium carbonate was used, the apparent rifampicin solubility was 22.61 mg/ml. This was nine times higher than the solubility of the unprocessed rifampicin, and this value was compared favorably with the data found by Tewes et al., (2008) using sodium tetraborate as a buffer.

5.3.3 Spray dried complex systems

In order to formulate dry particles made of rifampicin/HP-β-CD complex, the complex was spray dried from an aqueous solution, at an inlet temperature of 120 °C, this is the inlet temperature used for spray drying of aqueous solution of ammonium salt of p-aminosalicylic acid. Although ammonium salt of p-aminosalicylic acid is not structurally related to rifampicin, but the inlet temperature was chosen because of using the same solvent system.

The loading of the sample was defined as the mass of rifampicin divided by the mass of particles (rifampicin plus the cyclodextrin). Loading efficiency was defined as the loading of rifampicin divided by theoretical loading of rifampicin; theoretical loading of rifampicin is the amount of rifampicin in the solution of spray-dried complex divided by the total amount of rifampicin and HP-β-CD in the same solution. As the loading increases, the limits on the amount of the drug delivered increases. Loading and loading efficiency for spray-dried rifampicin complex are shown in table 5.2. For the particles made of complex in sodium hydroxide solution, the loading of the drug was 7.83 ± 1.15 wt%, while for that

in ammonium carbonate solution the loading was more than doubled to 16.12 ± 0.38 wt%. It is obvious that for spray dried complex buffered with either sodium hydroxide or ammonium carbonate there is a large amount of the HP-β-CD excipient.

Table 5.2 Loading and loading efficiency of particles formulated by spray drying two different rifampicin complex solutions.

	Complexation in sodium hydroxide solution	Complexation in ammonium carbonate solution
Loading (wt %)	7.83 ± 1.15	16.12 ± 0.38
Loading Efficiency (%)	105.30 ± 15.49	87.40 ± 2.07

Particle size distribution of spray dried complex was determined using laser diffraction particle sizing at the standard operational settings of 2 bar air pressure and 60% vibration feed rate. Particles of spray-dried rifampicin complex showed a mono-modal distribution and highly reproducible size distribution (Figure 5.28). The narrowest size distribution was found for the particles formulated by spray-drying rifampicin complex prepared in sodium hydroxide, with a span averaging 1.63 compared to 3.01 for the spray-dried rifampicin complex prepared in ammonium carbonate. Spray-dried complexes prepared in sodium hydroxide solution has an average median particle size of volume distribution d(0.5) of 3.12 ± 0.01 μm, which was slightly larger than spray-dried complex prepared in ammonium carbonate solution, which had an average d(0.5) of 2.79 ± 0.01 μm.

On average, a higher surface area was measured for particles of spray-dried rifampicin complex prepared in ammonium carbonate in comparison to recovered particles of spray-dried rifampicin complex prepared in sodium hydroxide (Table 5.3). A surface area of 2.30±0.05 m^2/g was measured for spray-dried rifampicin complex prepared in sodium hydroxide. A statistically significant 3.9-fold increase in surface area (9.06±0.08m^2/g) was measured for spray-dried rifampicin complex prepared in ammonium carbonate relative to that prepared in sodium hydroxide. The higher surface area of spray-dried rifampicin complex prepared in ammonium carbonate can be explained by the smaller particle size in comparison to spray-dried rifampicin complex prepared in sodium hydroxide.

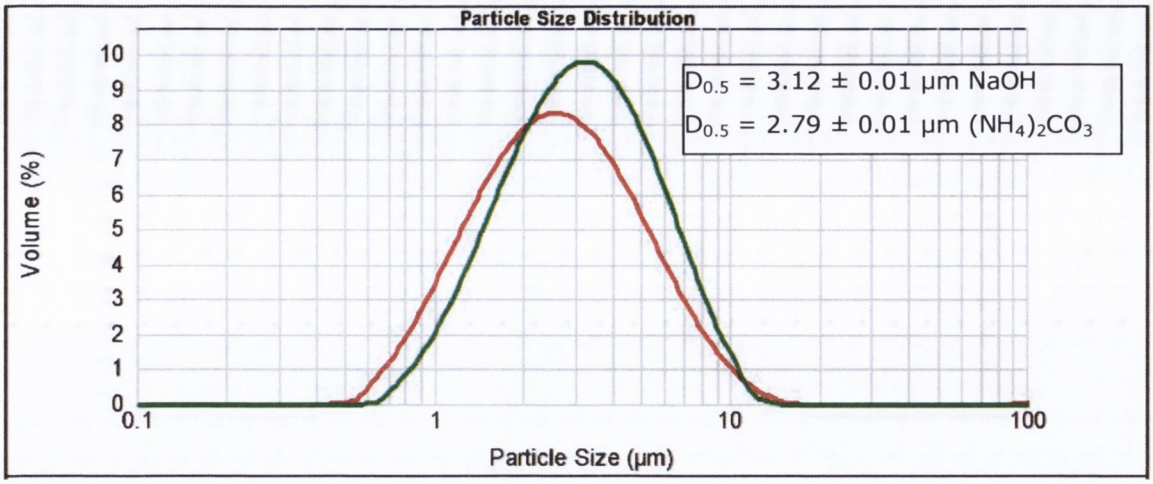

Figure 5.28- Particle size distributions of spray-dried rifampicin complex prepared in sodium hydroxide (green line), ammonium carbonate (red line).

Table 5.3– Particle sizing and surface area for different rifampicin systems.

System	Surface area (m^2/g)	Particle size (µm) d(0.5)
Spray dried rifampicin complex prepared in $(NH_4)_2CO_3$	9.06±0.08	2.79 ± 0.01
Spray dried rifampicin complex prepared in NaOH	2.30±0.05	3.12 ± 0.01

5.3.4 Other rifampicin spray dried system

Spray–drying rifampicin complex from H_2O: MeOH: BA systems was considered based on results isoniazid/ HP-β-CD (refer to section 5.1). 10 ml of aqueous solution of rifampicin complex was mixed with 50 ml of methanol and 50 ml of butyl acetate. Spray drying was carried out in the closed mode configuration (conditions detailed in Appendix I), with an inlet drying temperature of 100 °C.

The mixtures of rifampicin and HP-β-CD were spray dried to be compared to the spray-dried complex. The spray drying conditions of 100% water, inlet temperature 120 °C were selected for spray drying rifampicin/ HP-β-CD mixtures, the concentration of rifampicin was 8% and 22% (weight of solids) as outlined in Appendix I. The choice of 8% and 22% rifampicin was based on the analysis of rifampicin/ HP-β-CD complexes prepared either in sodium hydroxide or in ammonium carbonate.

5.3.5 Physicochemical and morphological characterisation of spray dried rifampicin

Characterisation of rifampicin raw material was carried out using a sample sourced from Sigma. Spray dried rifampicin systems characterised included rifampicin/HP-β-CD complex spray dried from water or water: methanol: butyl acetate. The characterisation of spray dried rifampicin/HP-β-CD mixture was carried out on the sample spray dried from water.

The powder X-ray diffractogram of rifampicin raw material (Figure 5.29 (a)) was typical of a crystalline material as confirmed by the numerous diffraction peaks. The peak positions and their relative intensities were consistent with the XRD spectrum presented by Agrawal et al., (2004) for rifampicin Form I, as the characteristic peaks of form I were found at 2 theta = 13.7 and 14.5 degrees. The hundred percent intensity peak was at 14.5 degrees. DSC scans of the unprocessed rifampicin confirmed that the starting material is Form I, as only one exotherm with its onset at ~255 °C was observed, with a measured enthalpy of fusion of ~183 J/g (Figure 5.30). This is in a good agreement with the observation of Agrawal et al., (2004), who stated that the DSC scans of form I a show sharp exotherm at 255–266 °C.

X-ray diffractograms of all spray-dried rifampicin/ HP-β-CD showed that the peaks of rifampicin disappeared, regardless of the composition of the spray dried system, which could be attributed to the presence of a high ratio of HP-β-CD or the samples were rendered amorphous upon processing.

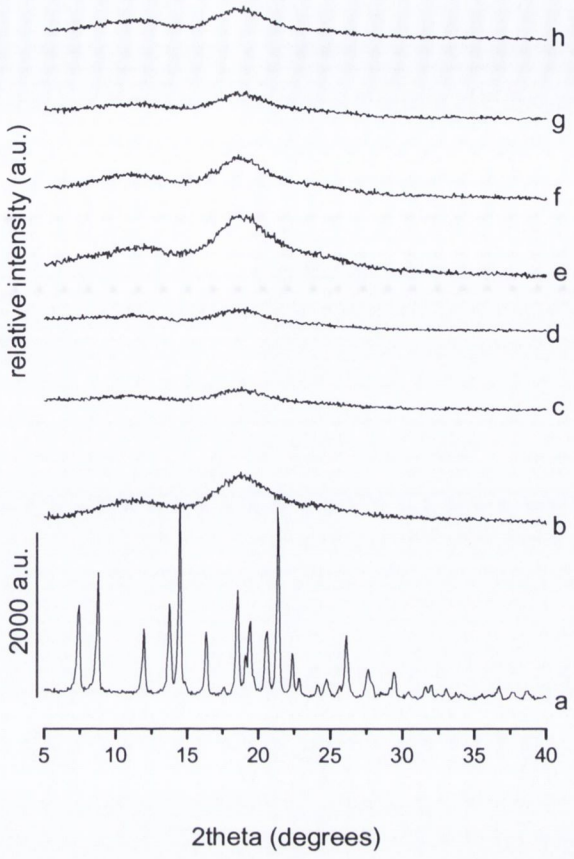

Figure 5.29- XRD scans of (a) rifampicin unprocessed material (b)rifampicin complex prepared in sodium hydroxide spray-dried from H_2O (c) rifampicin complex prepared ammonium carbonate spray-dried from H_2O (d) rifampicin/ HP-β-CD mixtures prepared in sodium hydroxide spray-dried from H_2O (e) rifampicin/ HP-β-CD mixtures prepared in ammonium carbonate spray dried from H_2O (f) rifampicin/ HP-β-CD complex prepared in sodium hydroxide spray-dried from H_2O: MeOH: BA (g) rifampicin/ HP-β-CD complex prepared in ammonium carbonate spray-dried from H_2O: MeOH: BA and (h) HP-β-CD starting material.

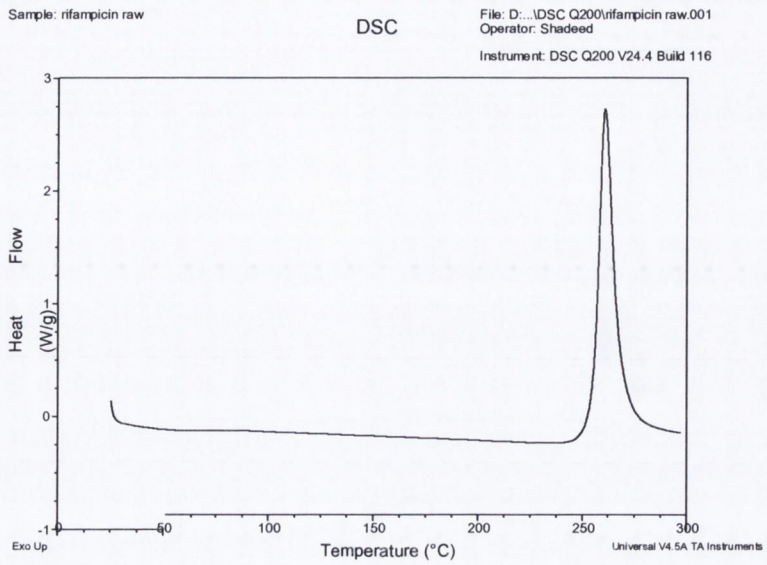

Figure 5.30- DSC scan of rifampicin raw material

An XRD scan of a physical mixture of rifampicin/ HP-β-CD was run to establish whether rifampicin suspended in HP-β-CD would be detectable by XRD. Figure 5.31 shows XRD scans of rifampicin unprocessed material as well as physical mixtures of rifampicin/ HP-β-CD. Peaks due to rifampicin were clearly seen in physical mixture scan, even at low concentration of rifampicin (8%, w/w rifampicin). Therefore, it was possible to detect rifampicin in a sample containing high contents of HP-β-CD using the XRD technique. Hence, the absence of rifampicin peaks in the diffractogram of spray-dried composite could not be attributed to the high content of HP-β-CD or to the limit of detection by XRD. These results were favorably compared with the findings reported by Jain and Adeyeye, (2001) who reported that the characteristic crystalline peaks of danazol disappeared when complexed with β- cyclodextrin derivative due to formation of inclusion complex.

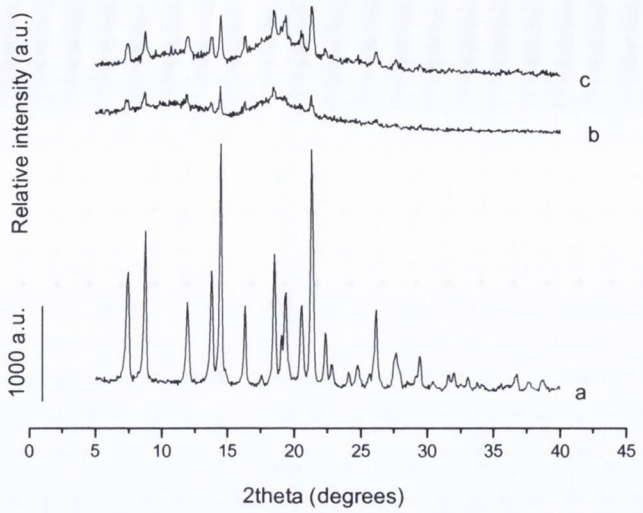

Figure 5.31- XRD scans of (a) rifampicin unprocessed material and (b) physical mixture of rifampicin/ HP-β-CD containing 8% rifampicin complex prepared in sodium hydroxide (c) physical mixture of rifampicin/ HP-β-CD containing 22% rifampicin complex prepared in ammonium carbonate.

Spray drying of aqueous solution of rifampicin complex using either sodium hydroxide or ammonium carbonate to adjust pH, resulted in the production of the more stable polymorph, Form I. For spray-dried rifampicin complex prepared in sodium hydroxide decomposition of this polymorph (Form I) occurs in the 240°C-260°C region and is shown by a single exotherm (Figure 5.32a). For spray-dried rifampicin complex prepared in ammonium carbonate decomposition occurs at a slightly lower temperature as seen in Figure 5.32b. These results indicate that complexation may protect the drug from the conversion to the less stable polymorph, form II.

DSC thermograms of the complex prepared in sodium hydroxide spray dried from H_2O: MeOH: BA showed an exothermic event starting at 214 °C, which followed by decomposition exotherm at 249 °C. A similar thermal behaviour was shown for the spray-dried complex prepared in ammonium carbonate, where DSC scan showed an exotherm at ~208 °C and finally decomposed at ~241 °C (Figure 5.32 (c) and (d)). These thermal events were characteristic of rifampicin amorphous form and in a good agreement with the finding reported by Agrawal et al., (2004) for the thermal behaviour of amorphous form of rifampicin. It is obvious that spray drying of rifampicin complex from H_2O: MeOH: BA solutions showed conversion of rifampicin from Form I to the amorphous form.

DSC thermograms of the spray-dried rifampicin- HP-β-CD mixture prepared in sodium hydroxide showed only one exothermic peak at ~250 °C. While the thermal behaviour of

spray-dried mixture prepared in ammonium carbonate was different, where DSC scan showed an exotherm at ~211 °C and finally decomposed at ~251 °C. These thermal events were characteristic of rifampicin amorphous form and in a good agreement with the finding reported by Agrawal et al., (2004).

A further point of interest was the absence of distinct glass transition in DSC scans of amorphous form of rifampicin. This was in agreement with the thermal behaviour of the amorphous form of rifampicin presented by Agrawal et al., (2004). Furthermore, the absence of indication of glass transition in DSC suggest that rifampicin is a good glass former and may require more sensitive method to determine its glass transition (Hancock and Zografi, 1997). It should be noted that Agrawal et al., (2004) reported that no crystallisation was observed after storage of amorphous form of rifampicin up to eighteen months indicating that glass transition is well above the ambient temperature.

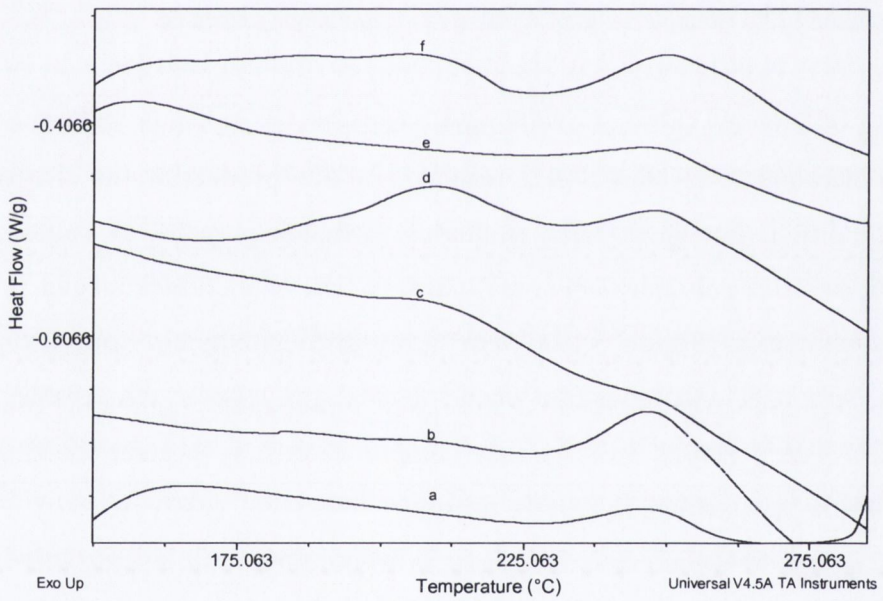

Figure 5.32- DSC scans of (a) rifampicin complex prepared in sodium hydroxide spray-dried from H2O (b) rifampicin complex prepared ammonium carbonate spray-dried from H2O (c) rifampicin/ HP-β-CD complex prepared in sodium hydroxide spray-dried from H2O: MeOH: BA (d) rifampicin/ HP-β-CD complex prepared in ammonium carbonate spray-dried from H2O: MeOH: BA (e) rifampicin/ HP-β-CD mixture prepared in sodium hydroxide spray-dried from H2O (f) rifampicin/ HP-β-CD mixtures prepared in ammonium carbonate spray dried from H2O.

The morphology of the different samples was studied using SEM. The particles of the rifampicin-unprocessed material are seen in Figure 5.33 (a) and are uniform rod like particles as expected. These particles are relatively big in size, so have a smaller surface

area, and therefore will have poor dissolution properties. It is clear that the particles of rifampicin have been reduced in size after the process of complexation with HP-β-CD followed by spray drying. A reduction in particle size will increase the specific surface area and in turn may increase the solubility and dissolution rate of the particles.

The particles of spray-dried rifampicin complex prepared in sodium hydroxide are roughly spherical in shape. They are not of a uniform size but all particles have a relatively large surface area (Figure 5.33 (b)). Spray-dried complex prepared in ammonium carbonate had more flattened particles and the surface appears to be more folded leading to an overall increase in surface area (Figure 5.33 (c)). It should be noted that a surface area of 2.30±0.05 m^2/g was measured for spray-dried rifampicin complex prepared in sodium hydroxide. A statistically significant 3.9-fold increase in surface area (9.06±0.08m^2/g) was measured for spray-dried rifampicin complex prepared in ammonium carbonate relative to that prepared in sodium hydroxide.

Porous particles were not produced by spray drying rifampicin complex from water: methanol: butyl acetate, but the particles were mainly spherical with different particle size and had a smooth surface morphology (Figure 5.33 (d) and (e)).

The particles recovered from spray drying of rifampicin/ HP-β-CD mixtures were generally irregularly shaped and uneven particles with different particle sizes as shown in SEM micrographs of the spray dried samples (Figure 5.33 (f) and (g)).

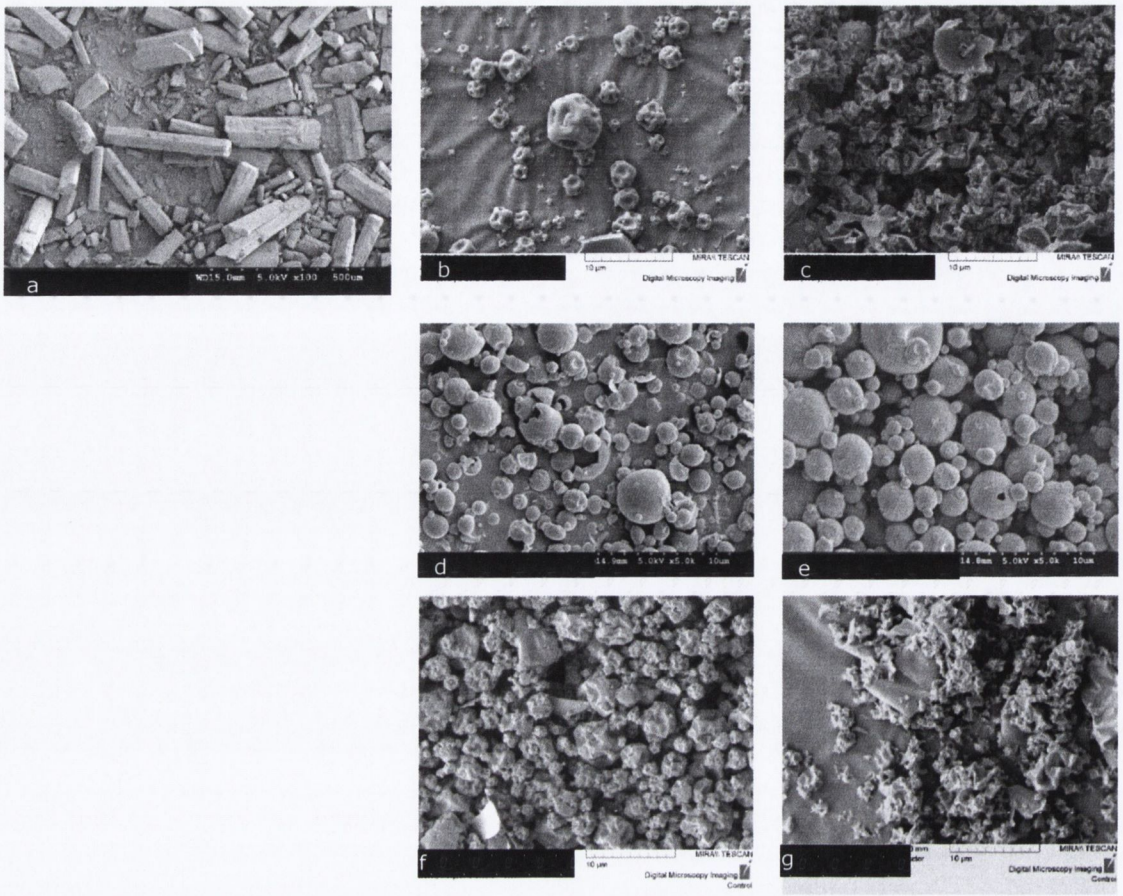

Figure 5.33- SEM micrographs of (a) rifampicin unprocessed material, (b) rifampicin complex prepared in sodium hydroxide spray-dried from H2O (c) rifampicin complex prepared ammonium carbonate spray-dried from H2O (d) rifampicin/ HP-β-CD complex prepared in sodium hydroxide spray-dried from H2O: MeOH: BA (e) rifampicin/ HP-β-CD complex prepared in ammonium carbonate spray-dried from H2O: MeOH: BA (f) rifampicin/ HP-β-CD mixture prepared in sodium hydroxide spray-dried from H2O (g) rifampicin/ HP-β-CD mixtures prepared in ammonium carbonate spray dried from H2O.

5.3.6 Dissolution study

Dissolution is a process by which a solid substance enters into a solvent to yield a solution (Davies and Feddah, 2003). This study was carried out bearing in mind that the rate of dissolution of an inhaled drug is linked to its onset and duration of therapeutic activity. The dissolution profiles of different samples of rifampicin are presented in Figure 5.34. It should be noted that solubility of rifampicin at pH 7.4 is 2.5 mg/ml, so the amount equivalent to 5 mg rifampicin was used in 20 ml dissolution medium to maintaining a volume of dissolution media that is 10 times greater than the volume at the saturation point of the drug.

The dissolution process was described in the form of a dissolution profile of the ratio of the sample dissolved over time. The spray-dried particles dissolved faster compared to the unprocessed material. At pH 7.40, the amount dissolved measured for spray dried complex prepared in sodium hydroxide particles at the first time point (5 min) was ~100%; while for unprocessed rifampicin, it was 22.9 ± 5%, and it was 84.3± 2.8% for the spray dried complex prepared in ammonium carbonate. In fact, processing of rifampicin resulted in an increase of rifampicin dissolution rate. Dissolution at physiological pH (7.4) is very fast for both spray-dried complexes either prepared in sodium hydroxide or ammonium carbonate which could be attributed to smaller particle size and higher solubility of the processed samples in comparison to the starting material.

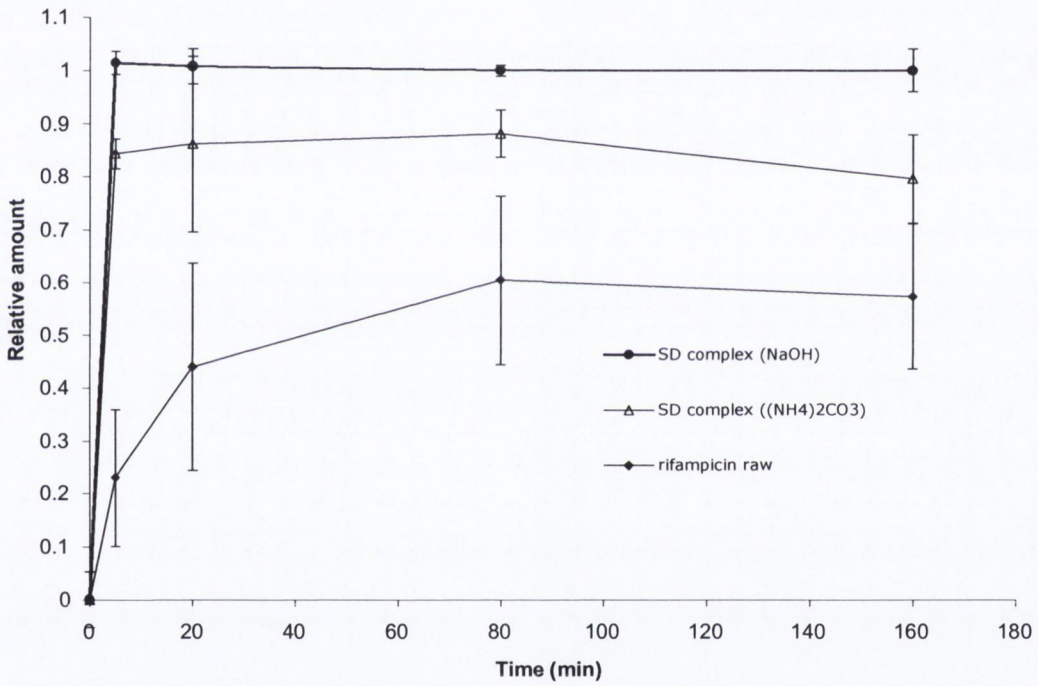

Figure 5.34- Relative amounts of dissolved per unit time of spray-dried rifampicin complex prepared in sodium hydroxide, ammonium carbonate and rifampicin raw material at physiological pH.

5.3.7 *In vitro* drug deposition of spray dried complex

In order to reach the lower respiratory tract and optimise drug absorption, dry powder aerosols need to present aerodynamic diameters between 1 and 5 μm (Bosquillon et al., 2004). Larger particles influence in the oro-pharynx while sub-micron particles remain suspended in air and are exhaled.

In order to examine these and to assess aerodynamic properties, *in vitro* drug deposition using a next generation impactor (NGI) was undertaken. NGI results are shown in Figure 5.35. The *in vitro* deposition profile showed a high deposition in the mouthpiece and throat,

and within the stages of the impactor, deposition in the mid stages – particularly stages 2, 3, 4, and 5 (Figure 5.35).

The fine particle fraction percentage, Mass Median Aerodynamic Diameter (MMAD) and Geometric standard deviation (GSD) of spray dried rifampicin complexes are presented in Table 5.4. NGI data showed that spray-dried rifampicin complex prepared in ammonium carbonate particles had a statistically significant ($p < 0.05$) higher fine particle fraction (51.5% ± 2.5) than spray-dried complex prepared in sodium hydroxide particles (39.7% ± 3.53). Mass median aerodynamic diameters for spray-dried complex prepared in either sodium hydroxide or ammonium carbonate were almost identical. However, the average emitted dose (expressed as percentage of nominal dose emitted from the inhaler) calculated for the aerosolised samples varied; the emitted dose for spray-dried complex prepared in sodium hydroxide was 65.0% ± 10.1, significantly lower than that calculated for spray-dried complex prepared in ammonium carbonate, which was measured at 82.1% ± 2.6. A 1.5-fold increase in the respirable fraction of spray-dried complex prepared in ammonium carbonate (41.8% ± 6.5%) was measured in comparison to spray-dried complex prepared in sodium hydroxide (27.7% ± 9.17%). This may be attributed to the higher surface area of spray-dried complex prepared in ammonium carbonate in comparison to spray-dried complex prepared from sodium hydroxide. This was in agreement with Nolan (2008) who studied the correlation between the surface area and aerosolisation performance of spray dried porous particles of sulfa compounds and sodium cromoglicate, where there was a strong positive correlation between the surface are and the respirable fraction, with r2 = 0. 0.92.

Table 5.4 Summary of results from next generation impactor analysis; mean ± s.d.; n = 3.

	Complexation in NaOH	Complexation in $(NH_4)_2CO_3$
MMAD μm	3.11 ± 0.56	3.11 ± 0.10
GSD	2.07 ± 0.06	2.04 ± 0.03
Percentage of emitted powder recovered (no capsule and device)	65.0% ± 10.1	82.1% ± 2.6
Percentage of drug recovered from stages 1 to filter only	41.0% ± 8.84	65.1% ± 4.5
FPF as per nominal dose	27.7% ± 9.17	41.8% ± 6.5
FPF as per emitted recovered dose	39.7% ± 3.53	51.5% ± 2.5

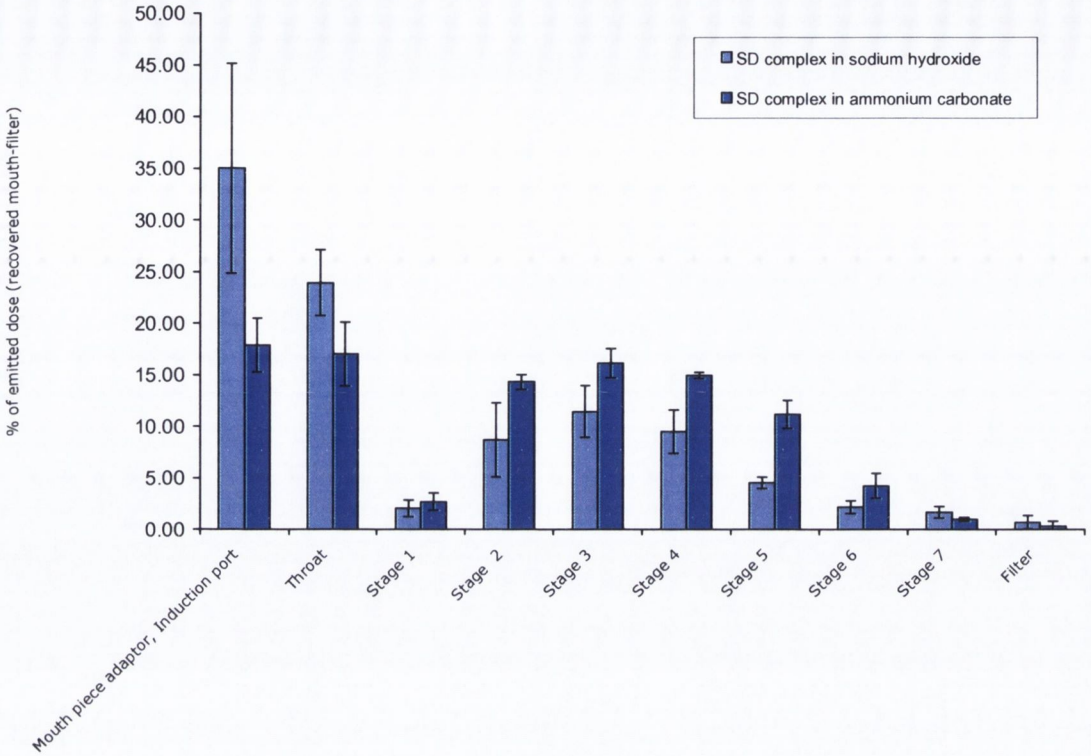

Figure 5.35- Deposition patterns on the stages of the NGI apparatus, SD complex= spray dried rifampicin-HP-β-CD complex.

Conclusion

Spray drying of rifampicin with HP-β-CD resulted in X-ray amorphous composites for the rifampicin/ HP-β-CD complex or mixture, in spite of the fact that peaks due to rifampicin were clearly present in the XRD scan of physical mixtures of rifampicin/ HP-β-CD.

The particle morphology of rifampicin/ HP-β-CD spray dried systems varied depending on the systems spray dried and the spray drying parameters used.

The particle size measurement of spray dried rifampicin/ HP-β-CD complex showed that the recovered particles was seen to fall within the optimal 1-5 μm region. In addition, Using HP-β-CD as a complexing agent for rifampicin resulted in a definite improvement in solubility and dissolution of the rifampicin. Aqueous solubility of rifampicin is particularly important as it may increase the possibility of achieving high concentration in the broncho-alveolar epithelium-lining fluid when administered by inhalation. Furthermore, *in vitro* drug deposition studies using NGI revealed that the aerodynamic properties of the particle were also seen to be favourable.

5.4 SPRAY DRIED PYRAZINAMIDE SYSTEMS

5.4.1 Introduction

Pyrazinamide is a first-line anti-tubercular medication used in the prevention and treatment of tuberculosis. It plays a unique role in shortening the tuberculosis therapy from the previous 9-12 months to 6 months because it kills a population of semi-dormant bacilli that are not killed by other anti-tubercular drugs (Heifets and Lindholm-Levy, 1992).

As shown earlier, the oral dose of pyrazinamide is 15 to 20 mg/kg daily (maximum 2 g daily) (Reynolds, et al., 1996). This is inconvenient to the patient, which leads to the failure of anti-tubercular chemotherapy (Burman et al., 1997), hence the importance of targeting pyrazinamide to the lung, which may increase the local therapeutic effect.

There are numerous reports in the literature regarding formulation of nanoparticles containing antitubercular agents suitable for inhalation. Zahoor, et al. (2005) investigated the use of sodium alginate prepared along with chitosan into nanoparticles encapsulating the three antitubercular agents. The nanoparticles were prepared by cation-induced gelification of alginate. The majority of particles (80.5%) were in the respirable range, with mass median aerodynamic diameter of 1.1 ± 0.4 μm and geometric standard deviation of 1.71 ± 0.1 μm. Drug levels in guinea pigs were detected in the plasma for 10- 14 days and in the lungs for up to 15 days. Efficacy of the three different types of nanoparticle formulations was evaluated in tuberculosis-infected guinea pigs. The animals were exposed to the aerosolised nanoparticles every 10-15 days for a total of 3-5 doses or were given oral drugs daily. At the end of these studies, no tubercle bacilli were detectable in the lungs of animals treated with aerosol nanoparticles or oral drugs, whereas tubercle bacilli were detected in lungs of untreated control animals. The authors reported that 3-5 pulmonary treatments were sufficient to replace the 45–46 daily doses of oral drug. These results confirm the feasibility of inhalation delivery of pyrazinamide.

In the current project, the preparation and properties of spray-dried pyrazinamide systems with and without excipients (PVP) present were investigated.

The objective of this study was to spray dry pyrazinamide to ascertain if nanoporous microparticles could be produced and subsequently to optimise the processing parameters and spray drying conditions to produce nanoporous microparticles.

5.4.2 Pyrazinamide spray dried without excipient

Ethanol and methanol were initially selected for spray drying of pyrazinamide based on previous work of McDonald (2005) which illustrated the use of different mass ratios of ethanol/water or methanol/water in the production of nanoporous microparticles of hydrophobic compounds (bendroflumethiazide and budesonide). The inlet temperature was set to 78 °C for spray-dried systems from ethanolic solutions, because the boiling point of ethanol is 78.5 °C. This was the inlet temperature used by Tajber (2005), when ethanolic solutions of budesonide were spray-dried.

A 1% w/v solution of pyrazinamide was prepared in 90% v/v ethanol 10% water. The particles of the pyrazinamide unprocessed material are seen in Figure 5.36 (a) to be uniform rod like particles. SEM micrographs of spray-dried samples showed that particles were smaller in comparison to the starting material; the recovered particles were spherical, deformed spheres or agglomerates of crystalline particles. Open cycle was used for this sample.

Solutions of pyrazinamide (1% w/v) were prepared in 80% methanol/20% water and 80% methanol/20% butyl acetate. The inlet temperature was set to 110 °C for spray-dried systems from methanolic solutions. This was the inlet temperature used by McDonald (2005), when methanolic solutions of BFMT were spray-dried. SEM micrographs of 1% pyrazinamide system spray dried from methanol/ water showed irregular particles with rough surfaces and different particle sizes while SEM micrographs of pyrazinamide spray dried from methanol/butyl acetate showed non-uniform shape particles with smooth surfaces (Figure 5.36). Closed cycle was used for these samples.

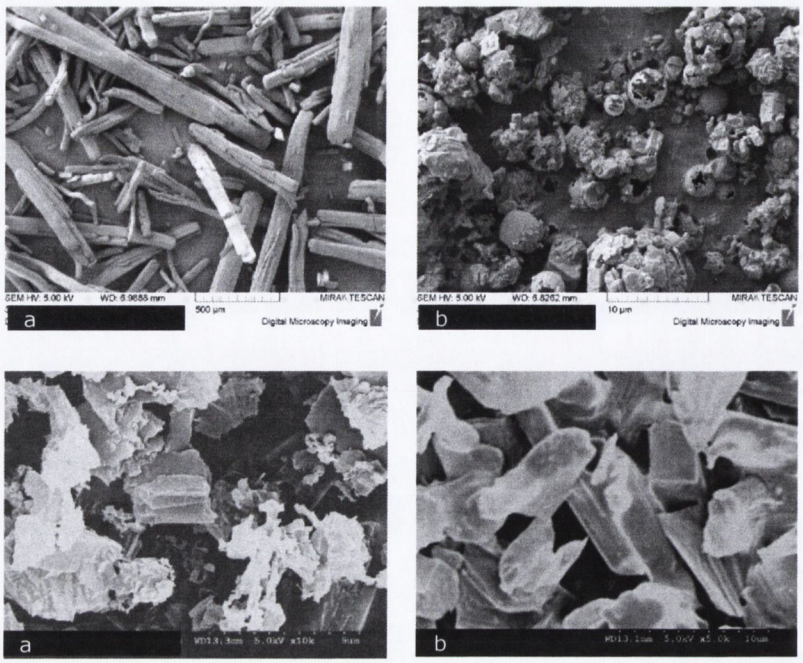

Figure 5.36- SEM micrograph of (a) pyrazinamide starting material (b) 1% pyrazinamide spray dried from 90% v/v ethanol 10% water (c) 1% pyrazinamide spray dried from 80% v/v methanol/20% water (d) 1% pyrazinamide spray dried from 80% methanol /20% butyl acetate.

5.4.3 Pyrazinamide /PVP spray-dried systems

Considering that spray-dried isoniazid/PVP from methanol/butyl acetate produced spherical NPMPs as shown earlier (refer to section 5.2), the same solvent was used for spray drying of pyrazinamide/PVP systems. Pyrazinamide/PVP composite systems consisting of different PVP ratios were spray-dried using the spray drying parameters outlined at Appendix I. This inlet temperature was used for preparation of NPMPs of PVP (Section 5.2.4.2). SEM micrographs of the produced powders are shown in Figure 5.37. It is clear that different PVP concentrations produced significant changes in the morphological characters of the spray-dried samples. At higher proportion of PVP (pyrazinamide/PVP 1:9) the spray-dried particles were roughly spherical porous particles (Figure 5.37c), while at lower proportions of PVP (pyrazinamide/PVP 2:8 and 3:7) it was observed that the particles were non-porous spherical with smooth surfaces (Figure 5.37 (a) and (b)). It can be concluded from these micrographs that significant changes in particle shape of spray-dried pyrazinamide is dependent on the PVP proportion.

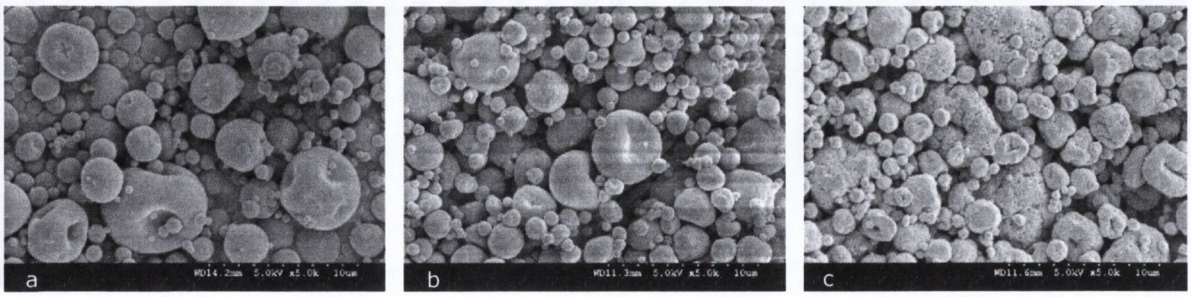

Figure 5.37 - SEM micrographs of pyrazinamide/PVP (a) 3:7 (b) 2:8 (c) 1:9 systems spray-dried from methanol/butyl acetate.

Investigation of the DSC scans of spray dried pyrazinamide/PVP systems are shown in Figure 5.38. The disappearance of the melting endotherm in DSC scans of pyrazinamide/PVP spray-dried systems indicates the miscibility of pyrazinamide and PVP, X-ray diffraction analysis of spray-dried pyrazinamide/PVP systems showed that pyrazinamide/PVP 1:9 spray-dried system were amorphous as indicated by the broad "halo" pattern with no distinct peaks as shown in Figure 5.39. But X-ray diffraction analysis of pyrazinamide/PVP 2:8 and 3:7 spray-dried systems showed the presence of small low intensity peaks indicating the presence of crystalline material, the disappearance of the melting endotherm in DSC scans and presence of peaks in XRD diffractograms was also reported by Patterson et al. (2007), who prepared carbamazepine/PVP 1:2 by either spray drying, melt extrusion, or ball milling. The difference between XRD and DSC could be due to the fact that samples are heated in DSC experiment and that the solubility increases with temperature. Therefore, even if the sample present initially crystalline material, it can be dissolved in the matrix when the temperature reaches the melting point of the drug.

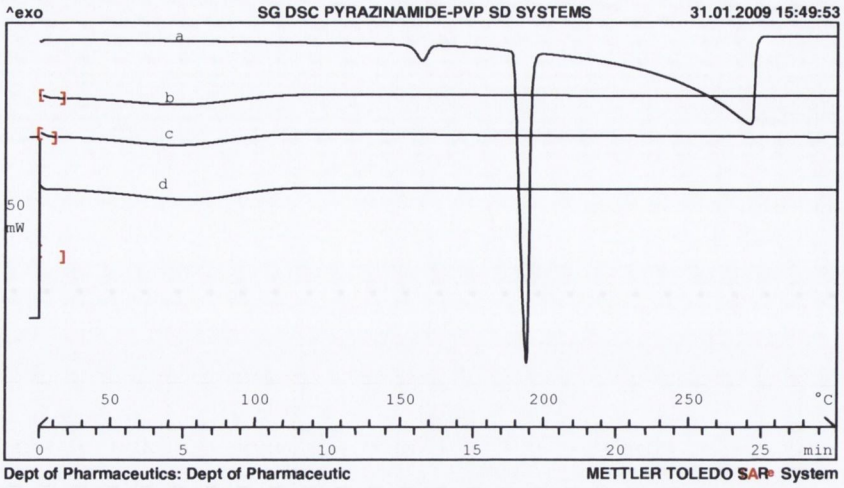

Figure 5.38- DSC scans of (a) pyrazinamide starting material and pyrazinamide/PVP (b) (1:9) (c) (2:8) (d) (3:7) systems spray-dried from methanol/butyl acetate.

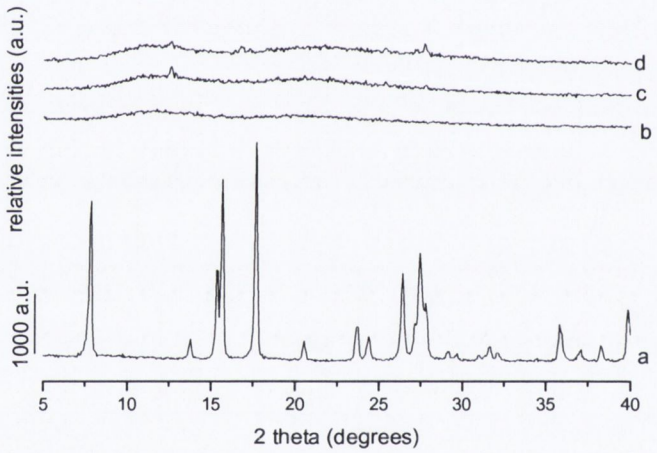

Figure 5.39- XRD scans of (a) pyrazinamide starting material and pyrazinamide/PVP (b) (1:9) (c) (2:8) (d) (3:7) systems spray-dried from methanol/butyl acetate.

Conclusion

Spray drying of pyrazinamide alone from ethanol/water or methanol/water or methanol/butyl acetate was not successful in terms of production of porous particles. Co-spray drying of pyrazinamide: PVP resulted in XRD amorphous systems in high concentration of PVP, lower concentrations of the PVP gave predominantly amorphous phase with weak peaks of the starting pyrazinamide. The morphological characters of co-spray dried pyrazinamide: PVP systems showed that high concentration of PVP was required to produce NPMPs of composite. Therefore, a pharmacokinetic study will be useful to determine the appropriate inhalation dose of this composite.

6. General Discussion

6.1 Introduction

The research presented in this thesis focuses on the application of a pharmaceutical technology, spray-drying method, involving the use of a co-solvent system and potentially a process enhancer, for example, ammonium carbonate or ammonium bicarbonate, to produce particles suitable for inhalation drug delivery, particularly in dry powder inhalation delivery devices. This technology is recently anticipated for different drug compounds/excipients, as it has advantages over current technologies in that it involves a simple one-step particle engineering method and produces microparticles suitable for inhalation. Previous researchers have conducted several studies to explore the potential production of particles suitable for inhalation using this novel method, and these trials were successful, for example budesonide (McDonald, 2005), sodium cromoglicate (Nolan, 2008) and proteins (Ní Ógáin, 2008). However, the feasibility of using this method to produce inhalable particles of antitubercular drugs and full physicochemical characterisation of the recovered particles had not been previously described in the literature. Therefore, it was important to investigate the potential application of this technology on antitubercular agents and to characterise the produced particles in comparison to the unprocessed materials. In addition, this work may be considered as a base for new method for production of porous particles through spray drying of ammonium salts of drug compounds. Five antitubercular drugs: p-aminosalicylic acid (Chapter 3), pyrazinoic acid (Chapter 4), isoniazid, rifampicin and pyrazinamide (Chapter 5), as well as four acidic drugs: benzoic acid, salicylic acid, sulfamethizole and sulfacetamide (Chapter 4) and five ammonium salts, namely ammonium salt of p-aminosalicylic acid (Chapter 3), pyrazinoic acid, benzoic acid, salicylic acid and sulfacetamide (Chapter 4), were selected for analysis. The antitubercular drugs were used to study the feasibility of developing particles of antitubercular drugs suitable for lung delivery (Chapter 5). On the other hand, the series of acidic drugs were selected to investigate the potential of processing a series of similar compounds into novel solid-state and to identify potential similarities in chemical characteristics that could be correlated to novel solid-state production.

The work in this thesis focuses primarily on the effect of changing spray drying parameters/conditions on the physicochemical and morphological characteristics of the recovered spray-dried particles. Drug compounds were spray-dried alone or the process

enhancer, ammonium carbonate, was incorporated into the formulation. Tajber (2005), McDonald (2005) and Nolan (2009) had previously shown that incorporation of ammonium carbonate did not affect the chemical characteristics of spray-dried materials. However, in the current work, a novel solid-state was obtained by spray drying of p-aminosalicylic acid either using ammonium carbonate or ammonium bicarbonate, regardless of the solvent used, as shown in Chapter 3.

A further point of interest illustrated in Chapter 4 is that production of the new solid sate form was also noticed upon using other acidic drugs benzoic acid, salicylic acid and pyrazinoic acid, but no distinct changes in terms of DSC or FTIR was shown when sulfamethizole was spray-dried with the process enhancer, ammonium carbonate. In addition the thermal behaviour and XRD pattern of spray dried sulfamethizole/ammonium carbonate was compared favourably with the findings reported by Nolan, (2008) for spray dried sulfamethizole/ammonium carbonate. Therefore, an in-depth study into the physicochemical characterisation of the solid-state of spray-dried acidic compounds/ammonium carbonate was undertaken. A comparative study between spray-dried and physical mixtures of acidic compounds/ammonium carbonate was also undertaken to study the effect of incorporation of ammonium carbonate or ammonium bicarbonate, as a process enhancer, in the spray drying process.

The solid-states of spray-dried ammonium salts were also characterised in terms of thermal and elemental analysis. These studies were considered important in determining the solid-state characteristics of spray-dried acidic compounds/ammonium carbonate and to investigate the feasibility of production of porous particles of an acidic drug via spray drying of ammonium salts of equivalent compounds.

Production of NPMPs of antitubercular drugs was investigated, where the effect of the process variables of spray drying on the production of NPMPs was explored. Antitubercular drugs were spray dried alone or with excipients (PVP or HP-β-CD) (Chapter 3 and 5).

In addition, selected spray-dried and micronised particles of equivalent material were characterised in terms of physicochemical characterisation and in vitro aerosolisation performance to determine advantages of spray dried particles for inhalation delivery. Micromeritic analysis included density and surface area measurements.

Based on previous discussion this chapter is divided into five sections

- Production of novel solid state upon spray drying of acidic compounds
- Spray drying of ammonium salts
- Morphological characteristics of recovered particles
- Spray drying of active pharmaceutical ingredient/excipient combinations
- Aerosolisation performance of spray dried particles

6.2 Production of novel solid-state upon spray drying of acidic compounds

As reported by Nolan, (2009) excipient-free nanoporous microparticles (NPMPs) of budesonide were produced with the inclusion of the pore-forming agent, ammonium carbonate. Briefly, Nolan, (2009) spray dried budesonide from 90% (v/v) ethanol at an inlet temperature of 78 °C. The total solid concentration in solution was 1% (w/v). The ammonium carbonate was added in a concentration equivalent to 15% of the total weight of solids (such that budesonide concentration in solution was 0.85% w/v). The pore-forming agent, ammonium carbonate, was expected to be volatilised (volatilisation temperature 59 °C) during the spray-drying process, which may in itself promote pore formation, through a type of "blowing" mechanism. As the spray drying process operating above the decomposition temperature of ammonium carbonate, it was expected that the ammonium carbonate is removed from the spray dried system with the exhaust gases, therefore producing essentially excipient-free NPMPs. It should be noted that Nolan, (2009) analysed spray dried budesonide/ammonium carbonate samples and budesonide raw material using an ammonia assay kits (Sigma-Aldrich, Ireland). The authors reported that the amount of ammonia in spray dried budesonide/ammonium carbonate samples was below the limit of detection of the assay (1% w/w).

In another study, Straub et al., (2005) produced porous particles of paclitaxel by spray drying a solution (water/ethanol in ratio of 1:4) containing the drug, a water-soluble excipient such as mannitol and a pore-forming agent, ammonium bicarbonate (volatile salt). The water soluble excipient facilitates wetting of the drug particles during reconstitution, provides proper osmolality to the dosage form, and improves the storage stability of the dry powder. Similarly, the pore forming agent is volatilised and removed during processing.

In addition to the previous studies, Frenkel et al., (1995) reported that ammonium salts undergo thermal decomposition with the formation of gaseous ammonia. This decomposition can proceed both in the solid phase by the heating of the dry salt in a stream of inert gas, and in the liquid phase by heating the solution of the salt. Decomposition of ammonium salts is employed in the industry for the distillation of ammonia-containing waste (Frenkel et al., 1995). Furthermore, ammonium carbonate decomposes into ammonia, carbon dioxide and water at temperatures over 59 °C. Similarly, ammonium bicarbonate decomposes at 36 to 60 °C into ammonia, carbon dioxide and water vapor. Therefore, it is assumed that in a spray drying process operating above this temperature ammonium carbonate is removed, leaving porous particles to be collected in the dryer.

The chemical structures of budesonide (the model drug compound used by Nolan, (2009)), p-aminosalicylic acid (the model drug compound used in this work) and ammonium salt of p-aminosalicylic acid are shown in Figure 6.1. Budesonide is a glucocorticoid, which has no acidic group; therefore, it is not possible to react with ammonia, which means ammonium carbonate will behave in the solution as a free molecule and hence the decomposition and removal of ammonium carbonate during spray drying process is likely. On the other hand, p-aminosalicylic acid is an acidic compound, according to Merck Index, it has a pKa value of 3.25 and the pH of 0.1% aqueous solution of p-aminosalicylic acid is 3.5. Therefore, p-aminosalicylic acid has potential to react with ammonia. The structure of ammonium salt of p-aminosalicylic acid which was prepared by chemical reaction between ammonia and p-aminosalicylic acid is shown if Figure 6.1c. This may explain the reason behind production of excipient free particles reported by Tajber (2005) and Nolan, (2009) using ammonium carbonate, where the drug compounds used by Tajber (2005) and Nolan, (2009) did not react with the process additives; therefore, the process additives were decomposed and removed during spray drying as the inlet temperature used was higher than their decomposition temperature. In contrast, in this work the model drug has the potential to react with the process additives, which resulted in incomplete removal of the process additive and production of a new solid state form.

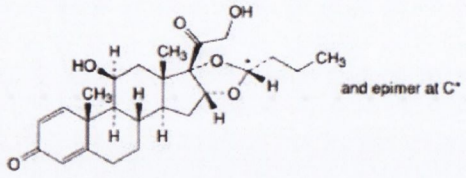

a

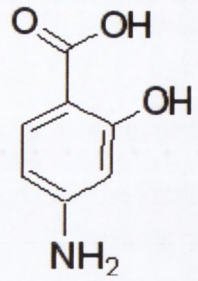

b

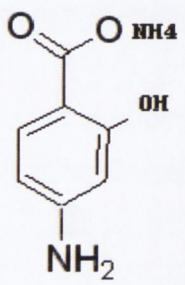

c

Figure 6.1 – Structure of (a) budesonide (b) *p*- aminosalicylic acid (c) ammonium salt of p-aminosalicylic acid

6.2.1 Stoichiometry of the PAS/ammonium carbonate spray-dried systems

The stoichiometric ratio of the solid state produced upon spray drying of PAS with ammonium carbonate or ammonium bicarbonate could be 2:1:0.5 p-aminosalicylic acid: ammonia: water. This was initially estimated from elemental analysis of the recovered particles from spray drying of a solution of p-aminosalicylic acid/ammonium carbonate or p-aminosalicylic acid/ammonium bicarbonate, which gave elemental analysis consistent with this stoichiometric ratio.

It should be noted that the assumption that the recovered particles were simple physical mixture was excluded based on several scans (Chapter 3). A further point of interest was the presence of peaks in the XRD scans of spray dried samples could not be attributed to any of the parent components or to the physical mixture.

An ammonia assay was undertaken for p-aminosalicylic acid raw material and the spray dried composites. In case of the raw material, the amount of ammonia was below the limit of detection of the assay (1%). On the other hand, the amount of ammonia determined in the spray dried composite was approximately 5.8%, which confirmed the stoichiometric ratio of

the solid state as shown in Chapter 3. Water contents were also determined by Karl Fischer titration. The amount of water detected was ~2%. This was consistent with the stoichiometric ratio of the recovered particles as shown in Chapter 3. Another confirmation of the stoichiometry of spray dried samples is TG analysis; TG analysis revealed that the weight loss between 25°C and 100°C was approximately 7.6% for the spray-dried composite. The loss of one ammonia molecule and half water molecule corresponds to a loss of ~7.8% by weight of p-aminosalicylic acid: ammonia: water 2:1:0.5 when determined on a molecular weight basis. Therefore, the weight loss registered in spray dried composites is consistent with the loss of one molecule of ammonia and half molecule of water.

6.2.2 Solid-state characteristics of the acidic compounds/ammonium carbonate spray-dried systems

As shown in Chapter 3, the chemical nature of p-aminosalicylic acid was important with respect to solid-state characteristics of recovered particles, in particular productions of a new solid state upon spray drying with ammonium carbonate. Six different acidic compounds were spray-dried from ethanolic solutions of 90% (v/v) ethanol 10% (v/v) water (Chapter 3 and 4), production of a new solid-state upon spray drying with ammonium carbonate were reported for five of these compounds, with only one compound (sulfamethizole) which gave DSC and FTIR scans similar to the starting material upon spray drying with ammonium carbonate (Chapter 4).

The structure of the acidic compounds and their pKa values are listed in Table 6.1. Four out of six selected model drugs are carboxylic acids, with similar pKa values. These four compounds are similar in structures (aromatic carboxylic acids). It was proposed that these compounds may potentially undergo similar interactions with ammonium carbonate which may contribute to the changes in solid-state of recovered particles.

The solid-state of recovered particles from spray drying of sulfa compounds/ammonium carbonate was dependent on the interaction between the sulfa drug and ammonium carbonate. The recovered particles from spray-drying of sulfacetamide/ammonium carbonate could be a mixture of acid and salt forms of sulfacetamide and there were evidence of sulfacetamide /ammonium carbonate interactions detected by DSC and XRD analysis. On the other hand, there was no interaction between sulfamethizole and ammonium carbonate as indicated by XRD, DSC and FTIR analysis and the solid-state of spray-dried sulfamethizole/ammonium

carbonate was similar to unprocessed sulfamethizole. Although both sulfa compounds have same pKa values, but they differ by substitution on the sulfanilamide structure, sulfacetamide has acetyl group, while sulfamethizole has 5-methyl-1,3,4-thiadiazol group. Bearing in mind that sulfonyl group is the acidic group in the structure, so the lack of interaction between sulfamethizole and ammonium carbonate perhaps due to the presence of bulky group (methyl thiadiazol) which may hinder the interaction. In addition, aqueous solubility of sulfacetamide (1 in 150 of water) is much higher than that of sulfamethizole (1 in 2000 of water). Serajuddin, (2007) reported that the concept of the pH of maximum solubility of certain compound (pH_{max}) plays a major role in acid-base reaction. The author depicted the influence of solubility of the acid and its pK_a on pH_{max} and consequently on salt formation. Furthermore, an increase in solubility and decreases in pK_a of the acidic drug will decrease pH_{max} and therefore, favour salt formation. Consequently, it may be assumed that the potential of salt formation of sulfacetamide (reaction between sulfacetamide and ammonium carbonate) is higher than that of sulfamethizole. A further point of interest was the possibility of synthesis of ammonium salt of sulfacetamide (Chapter 4); meanwhile it was not possible to prepare sulfamethizole salt.

Therefore, it could be concluded that the production of the novel forms of drug compounds upon spray drying with ammonium carbonate was dependent on the interaction of the acidic drug compound with ammonium carbonate. This may explain the results reported by Tajber, (2005); McDonald, (2005) and Nolan, (2008) that produced excipient free particles by spray drying drug compounds with ammonium carbonate, as the drug compound used in their studies has no potential to react with ammonium carbonate. Consequently, ammonium carbonate was totally evaporated upon spray drying.

Table 6.1- list of molecular weights, structures and pKa values of acidic drugs used in the project.

Drug	Mol Wt.	Structure	pKa	solubility
p- Aminosalicylic acid	153.13	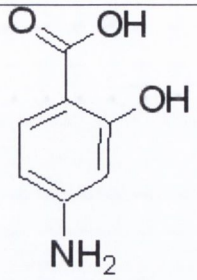	3.25	1 in 500 of water
Benzoic acid	122.1	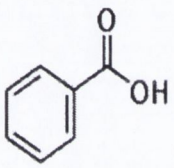	4.19	1 in 300 of water
Salicylic acid	138.1	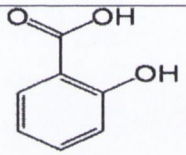	3	1 in 460 of water
Pyrazinoic acid	124.1	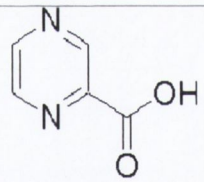	2.92	soluble in cold water
Sulfacetamide	214.24	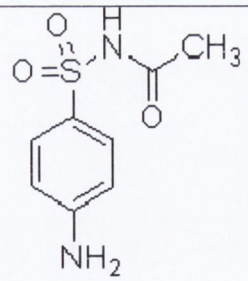	5.4	1 in 150 of water
Sulfamethizole	270.33	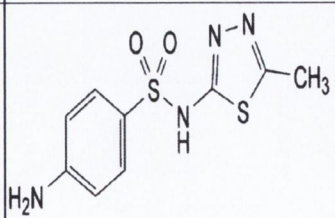	5.4	1 in 2000 of water

6.2.3 Stoichiometry of the acidic compounds/ammonium carbonate spray-dried systems

As shown in Chapter 4, a new solid state was recovered upon spray drying of benzoic acid, salicylic acid and pyrazinoic acid with the process additive, ammonium carbonate, as confirmed by DSC, FTIR and XRD. Elemental analysis of some spray dried acidic compound with ammonium carbonate is shown in Table 6.2. Elemental analysis of spray dried composites showed that the stoichiometric ratio of the recovered particles could be 2:1 acid: ammonia. It should be noted that water contents of spray dried composites were under the limit of detection (1%). It could be concluded that according to elemental analysis the possible stoichiometry for these systems could be 2 molecules of acid: 1 molecule of ammonia.

On the other hand, there were no differences in elemental analysis of spray dried sulfamethizole/ammonium carbonate in comparison with the unprocessed material. This was consistent with the results of DSC and XRD of the spray dried sulfamethizole/ammonium carbonate, which showed that there were no significant changes in the solid state of sulfamethizole upon spray drying with ammonium carbonate.

Table 6.2- Elemental analysis of different acidic compounds systems.

Sample	Analysis			
	C	H	N	S
Benzoic acid unprocessed material	68.87	4.90	0	0
Spray dried benzoic acid/ammonium carbonate 80:20	64.43±0.03	5.89±0.07	5.23±0.16	0
Spray dried benzoic acid/ammonium carbonate 71:29	64.23±0.25	5.96±0.02	5.51±0.23	0
Spray dried benzoic acid/ammonium carbonate 66:34	64.19±0.20	5.95±0.04	5.47±0.28	0
Spray dried benzoic acid/ammonium carbonate 50:50	64.22±0.16	5.93±0.01	5.38±0.15	0
Benzoic acid: ammonia 2:1 (Calculated)	*64.60*	*5.42*	*5.38*	*0*
Salicylic acid unprocessed material	60.87	4.37	0	0
Spray dried salicylic acid/ammonium carbonate 80:20	57.36±1.56	5.02±0.33	5.03±0.40	0
Spray dried salicylic acid/ammonium carbonate 70:30	57.30±0.82	4.91±0.20	4.83±0.56	0
Salicylic acid: ammonia 2:1 (Calculated)	*57.53*	*4.82*	*4.79*	*0*
Sulfamethizole unprocessed material	39.98	3.72	20.72	23.72
Spray dried sulfamethizole/AC 95:5	39.86±0.16	3.70±0.02	20.60±0.16	23.61±0.15
Spray dried sulfamethizole/AC 90:10	39.68±0.07	3.70±0.02	20.57±0.12	23.66±0.22
Spray dried sulfamethizole/AC 80:20	39.61±0.02	3.72±0.01	20.71±0.07	23.56±0.36

6.3 Spray drying of ammonium salts

Frenkel et al., (1995) reported that ammonium salts undergo thermal decomposition with the formation of gaseous ammonia. Additionally, Chuck and Zacher (2000) reported that an aqueous solution of ammonium nicotinate can be converted to nicotinic acid by spray drying. Out of six acidic compounds selected for this work, only sulfamethizole did not show any interaction with ammonium carbonate, and it is neither available nor possible to prepare its ammonium salt. For the other compounds, ammonium salt was either prepared or purchased. Ideally, uniform and porous particles within the size range of 2-5μm are desirable for inhalation systems. The recovered particles from spray drying of ammonium salts of both p-aminosalicylic acid and pyrazinoic acid have a size range of about 1-10μm as estimated from several SEM micrographs; they are uniform, slightly porous spherical agglomerates of

particles. Unfortunately, it was not possible to analyse the actual morphological characteristics of spray-dried ammonium salts of benzoic acid and salicylic acid due to the use of vacuum during the coating and visualisation process. The porosity of particles could be due to decomposition of ammonium salt and release of ammonia. This was confirmed by extensive studies on spray-dried ammonium salt of p-aminosalicylic acid, which showed that the solid-state of spray-dried salt at low inlet temperature (78 °C) was different from either acid or salt forms of p-aminosalicylic acid.

Elemental analyses of spray dried ammonium salt of p-aminosalicylic acid showed that the inlet temperature affected the chemical composition of the recovered particles (Table 6.3). The nitrogen content of the recovered particles was decreased by increasing inlet temperature. This could be due to partial decomposition of the salt upon spray drying and release of ammonia. It should be noted that the ability of ammonium salts to undergo thermal decomposition is well known (Frenkel et al., 1995).

Table 6.3- Elemental analysis of PAS and PAS salt systems

Sample		Analysis% w/w		
		C	H	N
PAS	Calculated	54.90	4.61	9.15
PAS ammonium salt	Calculated	49.41	5.92	16.46
Spray dried ammonium salt at 78°C	Found	50.34±0.07	5.57±0.21	15.53±0.32
PAS ammonium salt spray-dried 120°C	Found	52.91±0.77	5.39±0.48	11.09±0.4

In addition, other ammonium salts also showed differences in solid-state upon spray drying, as confirmed by XRD and DSC scans of spray-dried salt, this could be attributed to decomposition of the ammonium salts upon spray drying.

Furthermore, spray drying of a solution of the ammonium salt of p-aminosalicylic acid at higher temperature (130°C) resulted in spherical particles and aggregates of microcrystalline particles, which gave elemental analysis, DSC and powder-XRD scans consistent with p-aminosalicylic acid. This was confirmed by elemental analysis, which showed that there was no difference between the spray-dried salt and p-aminosalicylic acid. This compares favourably with the results of spray drying of ammonium nicotinate presented by Chuck and Zacher (2000) who prepared pure nicotinic acid by spray drying of ammonium nicotinate.

These findings are useful in terms of production of porous particles suitable for inhalation, where particles, suitable for inhalation, may be obtained by preparation of ammonium salts of chemotherapeutic agents, followed by spray drying of the salt using spray drying method described earlier.

6.4 Morphological characteristics of recovered particles

The work in this thesis includes spray drying of 15 drug compounds, two excipients and mixture of different antitubercular drugs with excipients. Of these compounds, benzoic acid, salicylic acid and their salts are sublimable, so it was not possible to visualise their spray-dried particles.

p-aminosalicylic acid and its salt (Chapter 3), ammonium salt of pyrazinoic acid (Chapter 4), PVP, HP-β-CD and different antitubercular/ excipients (Chapter 5) were successfully processed into porous particles as a result of using spray drying process.

Three solvent systems, namely ethanol: water, ethanol: water: ammonium carbonate and methanol: water: ammonium carbonate were successfully used in this thesis to produce porous particles of hydrophobic compound (p-aminosalicylic acid). As shown in Chapter 3, the choice of these solvent systems was based on the findings reported by McDonald (2005) who successfully used different mass ratios of ethanol/water or methanol/water for production of nanoporous microparticles of hydrophobic compounds (bendroflumethiazide and budesonide) with and without ammonium carbonate. From the morphological characters of various p-aminosalicylic acid spray dried systems, it is obvious that the ethanol: water ratio employed is important in the production of porous particles. In general SEM micrographs were used to examine the morphology of the recovered particles; this method was used by McDonald (2005); Ní Ógáin, (2008) and Nolan, (2008) to examine porous/non porous nature of spray dried samples. It was seen that when the ethanol concentration was 70% and 80% (v/v), some of the particles recovered were spherical porous particles. When the solvent concentration was increased to 90% (v/v), numerous spherical particles was recovered (Chapters 3). Using higher percentage of ethanol (95% and 100%) resulted in spherical particles with visible holes. Solvent composition also affected the recovered particles from spray drying of ammonium salt of p-aminosalicylic acid, where using 90% ethanol, particles were more uniform spherical particles in comparison to the particles obtained by spray drying from aqueous solution.

Rabbani and Seville (2005) used a range of ethanol/water co-solvent containing different concentrations of ethanol (10-50% (v/v)) to study the effect of formulation components on the

characteristics of the resultant spray dried powders. The authors measured the viscosity of the formulations prior to spray drying. They reported that the viscosity was increased when the percentage of ethanol in the ethanol/water solvent system was increased. The authors proposed that the change in viscosity of the solution being spray dried might affect the behaviour of the solution at the spray dryer nozzle, and hence affect the size of the droplet produced, and consequently, affect the morphology of the particles produced.

In addition to investigating the effect of changing the concentration of ethanol employed, the effect of using alternative solvents was also examined. Methanol: water: ammonium carbonate was used as an alternative solvent. As with the ethanolic systems, the water: methanol ratio employed was also seen to be a key parameter when spray drying from methanolic solutions. For p-aminosalicylic acid/ammonium carbonate systems spray dried from 70% (v/v) methanol, none of the particles produced were porous. For p-aminosalicylic acid/ammonium carbonate systems spray dried from 80% and 90% (v/v) methanol, spherical particles were recovered (Chapter 3). This was consistent with finding presented by McDonald, (2005) for spray dried budesonide (hydrophobic drug compound) from methanolic solutions. The author showed that the methanol content is of key importance in the production of porous particles and the optimum solvent concentration is 80% (v/v) methanol.

Other researchers have also reported correlation between the co-solvent composition employed and the ability to produce porous particles (Tajber, 2005 and Nolan, 2008). Therefore, it can be concluded that the solvent composition is of key importance in the production of porous particles.

The operational mode of the spray drying (closed mode or open mode) affected the morphology of spray dried particles. The processing of a sample from the same spray drying conditions, total solid concentration of 3%, ammonium carbonate content of 20%, inlet temperature of 78 °C and using 90% (v/v) ethanol as solvent using both the open and closed mode. Spray drying using open mode produced porous particles and aggregates of microcrystalline particles, on the other hand, spray drying using closed mode configuration irregular shaped and spherical aggregates of particles were produced as shown in Figure 6.2. Nolan (2008) reported that the spray drying mode had an effect on the production of either NPMPs (open mode) or non-porous particles (closed mode) of sulfadimidine and sulfamerazine. McDonald (2005) also studied the effect of spray drying mode on production of NPMPs of bendroflumethiazide, he reported that porous particles were recovered when

open mode was used while recovered particle from spray drying using closed mode were non porous. It should be noted that in the open mode the drying gas is discharged after use, on the other hand, in the closed mode the drying gas is continuously recycled.

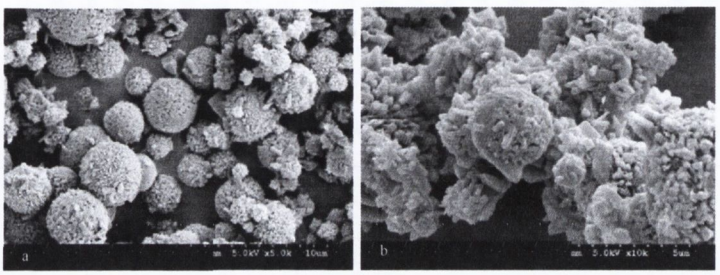

Figure 6.2- SEM micrographs of 3% (w/v) solution of PAS/ammonium carbonate systems spray-dried from 90% v/v ethanol (a) open mode (b) closed mode.

McDonald (2005) reported that the differences in morphology when using different operating modes perhaps due to the fact that when operating in the closed mode the drying gas is recycled through the system so that although the solvent is condensed, the drying gas may not be completely dry of solvent. When operating in the open cycle mode the drying gas exits the system on a continual basis pulling solvent with it. McDonald (2005) anticipated that the gradient for evaporation and thus the driving force may be greater in the open mode, since the solvent is moving into a drier gas.

The following hypothesis for formation of porous particles of p-aminosalicylic acid from EtOH:(H_2O), based on the solubility of the compound and volatility of solvents, and initially proposed by Corrigan (2005), Nolan (2008) based on experiments with several drug compounds.

Spray drying of p-aminosalicylic acid from ethanol: water system involve preparation of a solution of the drug (p-aminosalicylic acid), which was subsequently spray dried. The co-solvent system consisted of two solvents, with different boiling points (boiling point of ethanol is 78 °C, while it is 100 °C for water). p-aminosalicylic acid is more soluble in ethanol (One gram dissolves in 21ml alcohol, while 500 ml water required to dissolve one gram of the drug), so ethanol is a good solvent for the drug, while water is poor solvent (anti-solvent). This combination of co-solvents means that during the drying process the more volatile solvent will evaporate first (ethanol), with the solvent loss from these droplets resulting in an increase in

drug concentration in the less volatile solvent (water) in which the drug is less soluble. Drying process will continue with continued solvent evaporation until the solvent content becomes too low to maintain saturated conditions at the droplet surface, then the drug solidifies out initially as liquid droplets. Several liquid droplets are formed and by solvent evaporation, the drug droplets precipitate and come together and aggregate at the particle surface, leading to formation of aggregates of microcrystalline particles and porous particle.

The processes of spray drying p-aminosalicylic acid with ammonium carbonate or ammonium bicarbonate from ethanolic solutions involve preparation of solution of p-aminosalicylic acid with ammonium carbonate or ammonium bicarbonate. The following hypothesis for formation of porous particles of p-aminosalicylic acid from EtOH: H_2O: ammonium carbonate or EtOH: H_2O: ammonium bicarbonate , based on the solubility of p-aminosalicylic acid, physicochemical properties of ammonium carbonate and ammonium bicarbonate and volatility of solvents. The more volatile solvents (EtOH) is better solvents for the p-aminosalicylic acid and the least volatile solvent (H_2O) is a poor solvent. During the atomisation stage of the spray-drying process, droplets are formed containing the acid and the process additive in the solution. During drying of these droplets are exposed to the drying gas, and the process additive, ammonium carbonate or ammonium bicarbonate, decompose to release ammonia, the produced ammonia may not evaporate completely due to the acidic nature of p-aminosalicylic acid. At the same time the more volatile solvent (EtOH with a boiling point of 78.5 ^{o}C) in which p-aminosalicylic acid is more soluble, may evaporate to a greater extent, resulting in the droplet becoming richer in the less volatile solvent component (H_2O with a boiling point of 100 ^{o}C), in which p-aminosalicylic acid is less soluble. The fall in the solubility of the p-aminosalicylic acid may be dramatic and it may condense out initially as a nano-sized liquid within the droplet. As drying proceeds and further solvent loss occurs, p-aminosalicylic acid droplets become less fluid and come closer together, and may entrap ammonia; the drug may precipitate out as primary nanoparticles and agglomerate together either at the particle surface or within the particle, leading to formation of microparticle.

As detailed throughout this thesis ammonia was not completely evaporated, leading to formation of a new solid state of the acidic drug compound with ammonia. This was confirmed by elemental analysis, Karl Fischer titration, ammonia assay and TGA.

On the other hand, for hydrophilic compounds, the MeOH: BA solvent system or the MeOH: BA: H_2O solvent system was used to produce NPMPs, as shown in Chapter 5 the choice of these solvents based on the successful production of NPMPs of hydrophilic compounds

trehalose by Ní Ógáin (2006) and chitosan glutamate by Katheri (2007) using these solvent systems. Spherical porous particles were obtained on spray drying of PVP from 50:50 MeOH: BA. Spherical porous particles of HP-β-CD were spray-dried from 1:6:6 and 1:15:15 H_2O: MeOH: BA. Attempts to use similar solvent systems to spray-dry isoniazid were unsuccessful in terms of obtaining NPMPs (using either the MeOH: BA or the MeOH: BA: H_2O solvent systems).

Regarding the co-spray drying of drug/ excipients, in the current work different antitubercular drugs were co-spray dried with excipients as outlined in Table 6.4. Generally, two solvent systems, namely MeOH: BA and H_2O: MeOH: BA, were successfully used in this thesis to produce NPMPs of antitubercular drugs and excipients composites as outlined in Table 6.4. Depending on the percentage of excipient (either HP-β-CD or PVP), different particle morphologies were produced. Spray drying of isoniazid with 90% PVP at inlet temperature of 100 °C or 120 °C resulted in amorphous solid states as confirmed by XRD. The recovered particles were uniform spherical NPMPs. Decreasing the proportion of PVP to 80% of total solid, produced spherical porous particles only when the inlet temperature was 100 °C. In contrast, mixtures of porous and non-porous particles were recovered from spray drying of the same system at 120 °C. This confirms the importance of inlet temperature used in spray drying process. It was also observed that using lower proportion of PVP (70% and 50%) resulted in crystalline, smooth surfaces non-porous particles as confirmed by XRD and SEM. These particles were recovered from spray drying at 100 °C or 120 °C.

Similarly, pyrazinamide was co-spray dried from methanol: butyl acetate with PVP constituting 90%, 80% and 70% by weight of solids. Different particle morphologies were produced based on the PVP contents, at higher proportion of PVP (pyrazinamide/PVP 1:9) the spray-dried particles were spherical porous particles, while in lower proportions of PVP (pyrazinamide/PVP 2:8 and 3:7),the recovered particles were non-porous spherical with smooth surfaces and displaying concave depressions. It was observed that significant changes in particle shape of spray-dried pyrazinamide or isoniazid is dependent on the PVP proportion, which could be considered as a key parameter in preparation of NPMPs of isoniazid or pyrazinamide by spray drying.

Isoniazid was spray dried with the excipient HP-β-CD at a concentration of 90%, 80%, 70% and 50% (w/w), producing an XRD amorphous and crystalline powders depending on the concentration of HP-β-CD as shown in Chapter 5. It was concluded that the concentration of

HP-β-CD in the sample is an important factor in preparation of NPMPs of isoniazid/ HP-β-CD.

Table 6.4 Compounds co-spray dried as NPMPs from different solvent feed systems in the present work, and mass ratio of NPMPs composites.

Compound	Feed system	Inlet temperature	Mass ratio (composites)
isoniazid: HP-β-CD	H_2O: MeOH: BA	100 °C	1:9, 2:8
isoniazid: PVP	MeOH:BA	100 °C	1:9, 2:8
isoniazid: PVP	MeOH:BA	120 °C	1:9
pyrazinamide: PVP	MeOH: BA	100 °C	1:9

6.5 spray drying of active pharmaceutical ingredient/excipient combinations

NPMPs are proposed to be particularly suitable for pulmonary delivery and in particular dry powder inhaler formulation (Tajber, 2005; Nolan, 2008). As shown in Chapter 5, the production of porous particles of isoniazid and pyrazinamide required incorporation of high percentage of excipients. This will raise an important question about the feasibility of administration of these porous particles. It should be noted that several researchers studied the pharmacokinetics of inhaled antitubercular drugs and reported that administration of antitubercular agents by inhalation decreases the required dose. Katiyar et al., (2008) compared the oral versus pulmonary administration of antitubercular agents. Briefly, a group of six healthy volunteers aging from 20-50 received antitubercular drugs (isoniazid 15 mg, rifampicin 30 mg and pyrazinamide 75mg with lactose as carrier) using dry powder inhaler, the particle size was 1-10 μm and mass median aerodynamic diameter of 2.79 μm. Another group received oral tablets contain rifampicin 500mg, isoniazid 250 mg and pyrazinamide 1250 mg. the authors reported that the mean concentrations of isoniazid, pyrazinamide and rifampicin in epithelial lining fluid were 220, 15 and 83 times higher in inhaled group than those in the oral group. This confirms the reduction of dose required for treatment of tuberculosis using pulmonary delivered formulations.

In addition, NPMPs of spray dried antitubercular agents with excipients can be characterised by spherical shape and small size which demonstrate superior aerosolisation performance in

comparison to equivalent unprocessed material, higher specific surface area values were also obtained for NPMPs compared to micronised sample. Furthermore, in-vitro deposition data showed the advantage of NPMPs of isoniazid/excipient produced over micronised isoniazid in terms of respirable fraction (Table 6.5).

Pharmacokinetic studies of the spray dried formulations in this thesis were not made and this may be an area worth investigating in future studies of porous particles of antitubercular drugs.

6.6 Aerosolisation performance of spray dried particles

Bosquillon et al., (2001) reported the importance of physical characteristics, and their effect on aerosolisation properties of inhaled particles. Chapters 3 and 5 of this thesis discuss in detail the physical properties (particle size, density, surface area) and in vitro drug deposition profile of different spray-dried systems of p-aminosalicylic acid, ammonium salt of p-aminosalicylic acid, isoniazid and rifampicin. Physical properties and aerosolisation performance of these systems are compared in Table 6.5, to ascertain whether any general trends could be observed in these data.

It should be noted that particle size is important in relation to achieving optimum drug deposition in the lungs. Smyth and Hickey (2003) reported that large size particles (approximately 10 μm and above) are generally accepted to be "nonrespirable". This occurs when the drug is inhaled from a dry powder inhaler or metered dose inhaler. Such particles are swallowed, thus producing negligible, if any, therapeutic response. Particles of sizes ranging from 1-5 μm are deposited in the small airways and alveoli. Over 50% of the 3 μm diameter particles are deposited in the alveolar region (Labris and Dolovich, 2003).

Generally, The median particle size ($d_{(0.5)}$) of the spray dried particles, as determined from laser diffraction particle size analysis, was well within the optimum size-range for pulmonary drug delivery, that being between 1-5 μm (Bosquillon et al., 2004). The smallest median particle size was 2.33±0.031 μm for particles of isoniazid/ HP-β-CD spray dried from H_2O: MeOH: BA 1:15:15 at an inlet temperature of 100 °C. The largest median particle size was 3.673±0.00 μm for ammonium salt of p-aminosalicylic acid spray dried from 90% ethanol. The relationship between the median particle size ($d_{(0.5)}$) of different spray-dried samples and the percentage of respirable fraction is shown in Figure 6.3. It is obvious from the graph that there is no correlation between the median particle size of the spray dried particles and the respirable fraction of the powder particles (r^2 = 0.201). It should be noted that particles

recovered from spray drying of isoniazid/PVP 1:9 at 100 ºC, which exhibited the highest respirable fraction (46.3%) did not have the smallest particle size. These results were compared favorably with the results reported by Nolan (2008) who showed that there was no correlation between the median particle size and the respirable fraction of NPMPs of sulfa compounds, sodium cromoglicate and sulfa or sodium cromoglicate: PVP composites spray-dried systems.

Table 6.5 Physical properties and *in vitro* aerosolisation performance of micronised materials and spray dried systems of p-aminosalicylic acid (PAS), isoniazid (INH) and rifampicin (RIF). * respirable fraction (%) as per NGI study, all other results calculated from twin impinger studies, SD= spray dried, HP-β-CD = Hydroxypropyl-β-cyclodextrin, PVP = polyvinyl pyrrolidone, $d_{(0.5)}$ = median particle size (μm) as determined from laser diffraction particle size analysis.

	Particle size $d_{(0.5)}$ (μm)	**Respirable fraction (%)**	**Surface area (m^2/g)**	**Bulk density (g/cm^3)**	**Tapped density (g/cm^3)**	**Carr's Index (%)**
micronised PAS	2.9±0.026	14.8±2.59	2.83 ± 0.21	0.230±0.024	0.313±0.022	26.5
SD PAS	2.41±0.071	19.2±6.92	6.19 ± 0.26	0.104±0.002	0.168±0.009	38.4
SD PAS /AC80:20	3.38±0.078	24.5±2.86	3.42 ± 0.32	0.122±0.003	0.167±0.008	26.8
SD PAS /AC 73:27	3.33±0.036	17.03±8.55	-	0.081±0.001	0.125±0.002	35
SD PAS salt	3.673±0.00	17.9±5.83	-	0.093±0.002	0.133±0.008	30.1
micronised INH	4.013±0.127	20.3±2.20	1.66±0.06	0.150±0.008	0.265±0.005	43.3
SD INH/ HP-β-CD 1:9	2.33±0.031	43.7±4.31	45.12± 0.29	0.115±0.012	0.171±0.009	32.7
SD INH/PVP 1:9 at 120 °C	2.91±0.121	44.8±1.10	10.70±0.09	0.213±0.004	0.267±0.018	20.2
SD INH/PVP 2:8 at 100 °C	2.97±0.004	33.7±13.01	23.65±0.20	0.161±0.004	0.259±0.022	37.6
SD INH/PVP 1:9 at 100 °C	3.09±0.059	46.3±19.03	30.82±0.26	0.131±0.001	0.201±0.002	35.0
SD RIF complex from NAOH	3.12 ± 0.01	27.7% ± 9.17*	2.30±0.05	-	-	
SD RIF complex from AC	2.79 ± 0.01	41.8% ± 6.5*	9.06±0.08	-	-	

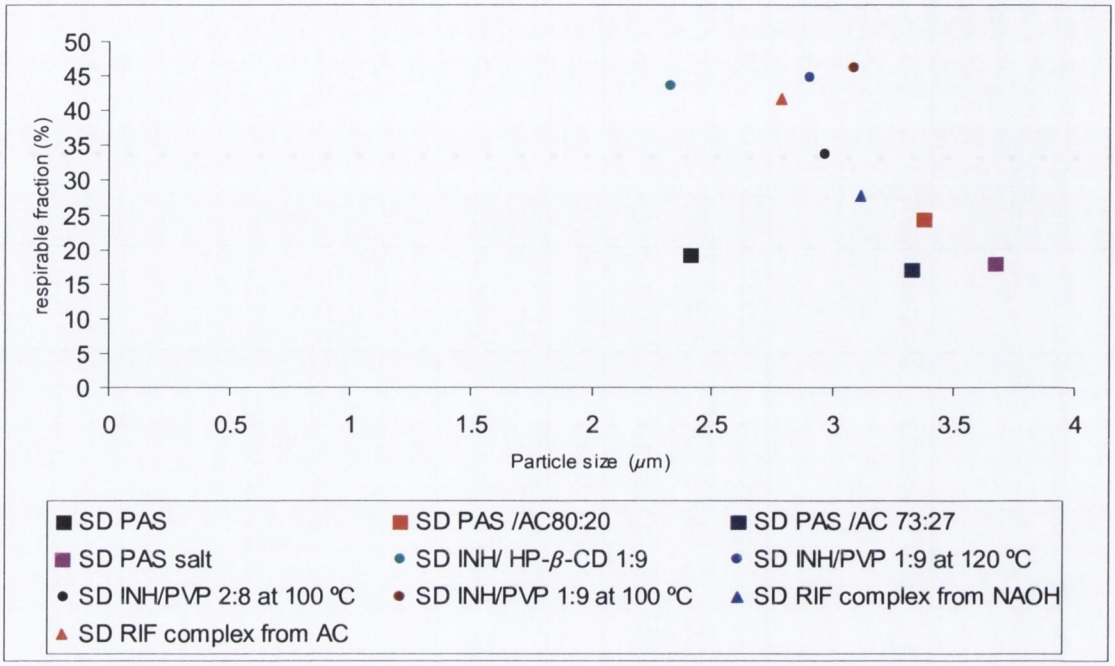

Figure 6.3 effect of median particle size ($d_{0.5}$) (μm) on the respirable fraction (%) of different spray dried powders. General Key: the triangle symbols represent rifampicin spray-dried systems, the square symbols represent spray-dried p-aminosalicylic acid systems and the circular symbols represent spray-dried isoniazid systems.

Carr's Index values may be used as an indication of flow properties of powder, this is based on the fact that compressible powders exhibit poor flow. In addition, Carr's Index values can provide an estimate of the interparticulate forces within particles (Louey et al., 2004). A further point of interest illustrated by Walton and Mumford, (1999) who reported that factors influence the flow properties of powders include particle size, particle size distribution, particle morphology/shape, moisture content and the hygroscopic nature of the material.

Figure 6.4 show the relationship between Carr's Index and the respirable fraction. There was no correlation between the calculated Carr's Index and the respirable fraction of the spray dried powders, with calculated R squared value of 0.077. These results are in agreement with the finding reported by Seville et al., (2007) who reported that the Carr's Index was not predictive of aerosolisation performance of amino acid-modified spray dried powders. In another study, Nolan (2008) studied the correlation between the Carr's

Index and aerosolisation performance of spray dried sulfa compounds and sodium cromoglicate, where there was no correlation between the Carr's Index and the respirable fraction, with $r^2 = 0.132$.

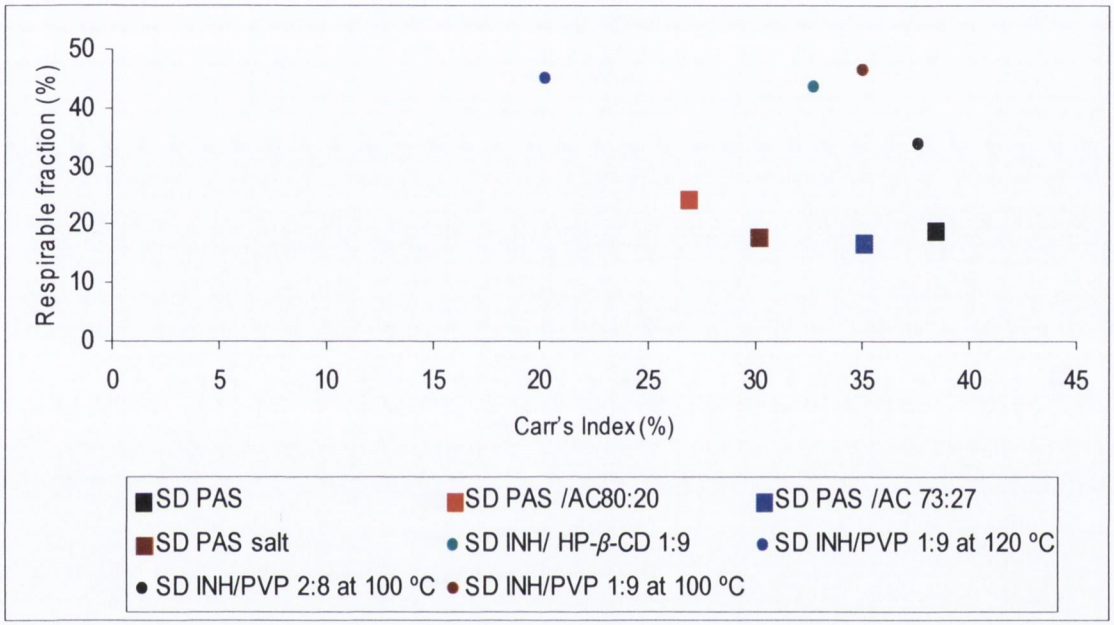

Figure 6.4 effect of Carr's Index (percentage) on the respirable fraction (percentage) of different spray dried powders. General Key: the square symbols represent spray-dried p-aminosalicylic acid systems and the circular symbols represent spray-dried isoniazid systems.

A weak correlations was observed when plotting surface area against respirable fraction of different spray-dried samples (r^2 = 0.39) (Figure 6.5). The lowest surface area measurements were obtained for rifampicin complex prepared in sodium hydroxide and spray-dried from aqueous solution, while this sample did not have the lowest respirable fraction. It was also observed that particles recovered from spray drying of isoniazid/ HP-β-CD 1:9, which demonstrated the highest surface area (45.12 (m^2/g)) did not have the highest respirable fraction.

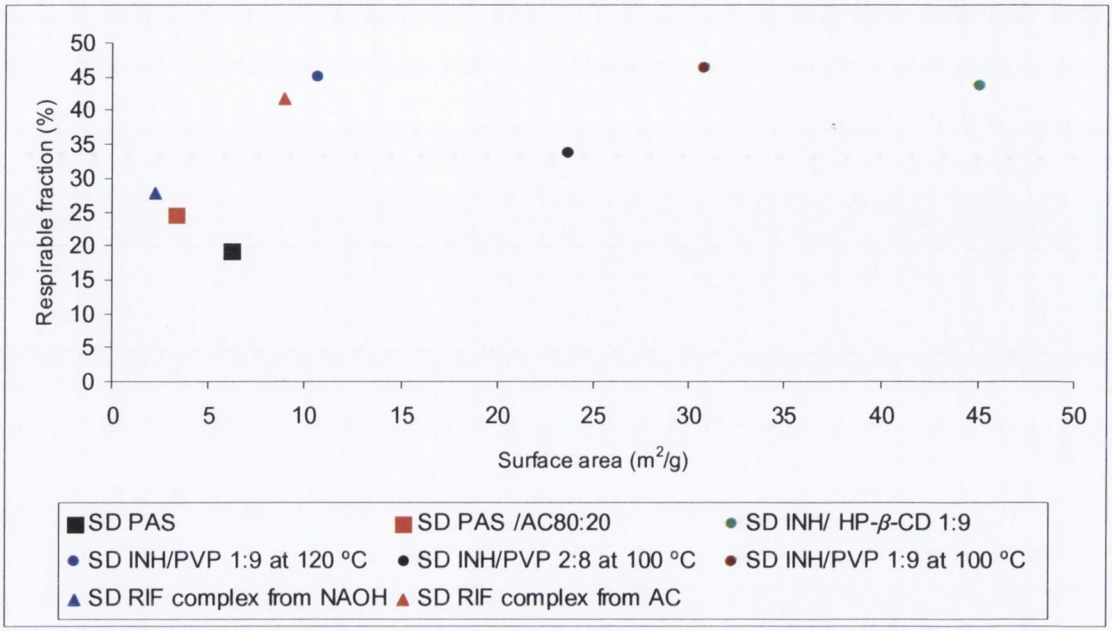

Figure 6.5 effect of surface area (m^2/g) on the respirable fraction (percentage) of different spray dried powders. General Key: the square symbols represent spray-dried p-aminosalicylic acid systems and the circular symbols represent spray-dried isoniazid systems.

6.7 Main findings from this thesis

- Spray drying of p-aminosalicylic acid/ammonium carbonate did not result in production of the main degradation product of p-aminosalicylic acid (3-aminophenol). But a solid state was recovered, the stoichiometry of the recovered particles could be p-aminosalicylic acid: ammonia: water 2:1:0.5, this was calculated from elemental analysis of the recovered particles and confirmed by Karl Fischer titration, ammonia assay and TGA.
- Spray drying of the acidic compounds without ammonium carbonate did not change the chemical composition of the acidic compounds, however, spray drying with ammonium carbonate resulted in a new solid state, and the stoichiometry of recovered particles could be 2:1 acid: ammonia. This was estimated from several elemental analyses of the spray dried samples.
- The production of the new solid state upon spray drying of acidic compounds and ammonium carbonate depends on the interaction between the acidic compound and ammonium carbonate. The solid state of spray dried acidic compounds/ammonium carbonate was altered upon spray drying whenever the compound reacts with ammonium carbonate. Furthermore, in absence of such interaction, there was no alteration in solid state of co-spray dried acidic compound/ammonium carbonate.
- Spray dried p-aminosalicylic acid ammonium salt show good potential for pulmonary delivery as indicated by the increase in emitted dose relative to the micronised p-aminosalicylic acid.

- Production of NPMPs of co-spray drying of isoniazid: excipient (PVP and HP-ß-CD) was dependent on the excipient contents, as high contents of the excipient was required to produce NPMPs. The recovered particles were XRD amorphous in high concentration of the excipient (80% and 90%), while, lower concentrations of the excipient (50%) gave predominantly crystalline phase with peaks of the starting isoniazid.
- Spray dried rifampicin complex have a greater dissolution rate than rifampicin unprocessed material which can be attributed to the increased surface area and smaller particle size of the spray dried particles.
- This spray drying process can produce particles suitable for inhalation of p-aminosalicylic acid, isoniazid and rifampicin.
- Spray drying proved a successful method of producing microspherical particles which, displayed favourable particle characteristics and in-vitro deposition, indicating good potential for pulmonary delivery, as indicated by the increase in emitted dose relative to micronised equivalent drug.
- This type of new inhalation dry powder can be characterised by spherical porous particles, these particles have small size and large surface area. Therefore, they exhibit superior aerosolisation performance in comparison to micronised equivalent systems.

6.8 Future work

- Further study is required to investigate the benefits of using ammonium salts of different acids, as a new technique for preparation of porous particles suitable for inhalation.
- Pharmacokinetic study of the recovered spray-dried particles in comparison with the unprocessed materials, and comparison between pulmonary, oral and intravenous route of administration of the spray-dried particles.
- Further study is required to investigate the benefits of this spray drying process for the co-spray drying of drug-excipient particles.
- Further optimisation of the other spray drying parameters (i.e., pump rate, aspirator rate etc.) for the production of NPMPs.

References

References

- Aaltonen, J., Allesø, M., Mirza, S., Koradia, V., Gordon, K.C. and Rantanen, J. "Solid form screening - A review" European Journal of Pharmaceutics and Biopharmaceutics 71 (1) (2009) 23-37.
- Abounassif, M., Mian. M. S., and Miam, N. A. "Salicylic acid" in Brittain, H, G., (Ed.) "Analytical profiles of drug substances and excipients" Academic Press, New York, 23(1994) 421-470.
- Adler, M. and Lee, G. "Stability and surface activity of lactate dehydrogenase in spray dried trehalose" J Pharm Sci. 88(2) (1999)199-208.
- Agrawal, S., Ashokraj, Y., Bharatam, P V., Pillai, O., Panchagnula, R; Solid-state characterisation of rifampicin samples and its biopharmaceutic relevance. European Journal of Pharmaceutical Sciences 22 (2004) 127-144.
- Akkaya, Y. and Akyuz, S. "Infrared and Raman spectra, ab initio calculations vibrational assignment of 4-aminosalicylic acid" Vibrational Spectroscopy 42 (2006) 292–301.
- Bailey, M.M. and Berkland, C.J. "Nanoparticle formulations in pulmonary drug delivery"
  Medicinal Research Reviews 29 (1) (2009) 196-212.
- Baltimore, R. S., Christie, C. D. C. and Walker Smith, G. J. "Immunohistopathologic localization of Pseudomonas aeruginosa in lungs from patients with cystic fibrosis. Implications for the pathogenesis of progressive lung deterioration" Am Rev Respir Dis. 140 (1989) 1650–1661.
- Basavoju, S., Boström, D., Velaga, S.P. "Pharmaceutical cocrystal and salts of norfloxacin" Crystal Growth and Design 6 (12) (2006) 2699-2708.
- Bastin, R. J., Bowker, M. J. and Slater, B. J. "Salt Selection and Optimisation Procedures for Pharmaceutical New Chemical Entities" Organic Proc. Res. & Dev., 4 (2000) 427-435.
- Bastin, R.J., Bowker, M.J., Slater, B.J. "Salt selection and optimisation procedures for pharmaceutical new chemical entities" Organic Process Research and Development 4 (5) (2000) 427-435.
- Bennett, W.D., Brown, J.S., Zeman, K.L., Hu, S.C. Scheuch, G., and Sommerer, K. "Targeting delivery of aerosols to different lung regions" J. Aerosol Med. 15(2002) 179-188.

- Bhatt, P.M., Desiraju, G.R. "Co-crystal formation and the determination of absolute configuration" CrystEngComm 10 (12) (2008) 1747-1749.
- Bosquillon, C., Lombry, C., Préat, V. and Vanbever, R. "Influence of formulation excipients and physical characteristics of inhalation dry powders on their aerosolization performance" Journal of Controlled Release 70 (3) (2001) 329-339.
- Bosquillon, C., Rouxhet, P.G., Ahimou, F., Simon, D., Culot, C., Préat, V. and Vanbever, R. "Aerosolization properties, surface composition and physical state of spray-dried protein powders" J. Control. Release, 99 (2004) 357-367.
- Bottari, B., Maccari, M., Monfort, F., Ottana, R., Rotndo, E. and Vigorita, M.G. "Antimycobacterial in Vitro Activity of Cobalt (II) Isonicotinoylhydrazone Complexes. Part 10" Bioorg. Med. Chem. Lett. 11 (2001) 301-303.
- British Pharmacopoeia, the Stationary Office, Great Britain, (2008).
- Burman, W. J., Cohn, D. L., Rietmeijer, C. A., Judson, F. N., Sbarbaro, J, A. and Reves, R. R. "Noncompliance with directly observed therapy for tuberculosis. Epidemiology and effect on the outcome of treatment" Chest 111 (1997) 1168–1173.
- Byron, P.R. "Determinants of drug and polypeptide bioavailability from aerosols delivered to the lung" Adv. Drug Deliv. Rev. 5 (1990) 107–132.
- Cairns, D., "Essentials of pharmaceutical chemistry" Pharmaceutical Press (2003).
- Carr, R.L. "Evaluating flow properties of solids" Chem. Eng., 18 (1965) 163-168.
- Carstensen, J. T. A. "Pharmaceutical Preformulation" Informa Healthcare, Pennsylvania, (1998) 41-48.
- Chan, H. K., "Dry powder aerosol drug delivery - opportunities for colloid and surface scientists" Colloids and Surfaces A: Physicochem. Eng. Aspects, 284-285 (2006) 50-55.
- Chawla, A, Taylor, K.M.G., Newton, J.M. and Johnson, M.C.R. "Production of spray dried salbutamol sulphate for use in dry powder aerosol formulation" Int. J. Pharm. 108(1994) 233–240.
- Chen, A. M., Ellison, M. E., Peresypkin, A., Wenslow, R. M., Variankaval, N., Savarin, C. G., Natishan, T. K., Mathre, D. J., Dormer, P. G., Euler, D. H., Ball, R. G., Ye, A., Wang, Y. and Santos, I. "Development of a pharmaceutical cocrystal of a monophosphate salt with phosphoric acid" Chem. Commun. (2007) 419–421.
- Chidavaenzi, O.C., Buckton, G., Koosha, F. and Pathak, R. "The use of thermal techniques to assess the impact of feed concentration on the amorphous content and

polymorphic forms present in spray dried lactose" International Journal of Pharmaceutics 159 (1) (1997) 67-74.

- Chodosh, S., Flanders, J.S., Kesten, S., Serby, C.W., Hochrainer, D, and Witek, T.J., "Effective delivery of particles with the Handihaler ® Dry powder Inhalation System over a range of chronic obstructive pulmonary disease severity" J. Aerosol Medicine, 14(2001) 309-315.
- Chow, A. H.L., Tong, H. Y., Chattopadhyay, P. and Shekunov, B. Y. "Particle Engineering for Pulmonary Drug Delivery" Pharm. Res. 24 (3) (2007) 411-437.
- Chowhan, Z.T. "pH–solubility profiles of organic carboxylic acids and their salts" J. Pharm. Sci. 67 (1978) 1257–1260.
- Chrystyn, H. "The Diskus™: a review of its position among dry powder inhaler devices" Int J Clin Pract. 61(6) (2007) 1022–1036.
- Chuck, R.J. and Zacher, U. "Process for the preparation of nicotinic acid" US Patent 6077957 (2000).
- Corrigan, D. O., Corrigan, O.I. and Healy, A.M. "Physicochemical and in vitro deposition properties of salbutamol sulphate/ipratropium bromide and salbutamol sulphate/excipient spray dried mixtures for use in dry powder inhalers" Int. J. Pharm. 322 (1-2) (2006a) 22-30.
- Corrigan, D. O., Healy, A.M. and Corrigan, O.I. "Preparation and release of salbutamol from chitosan and chitosan co-spray dried compacts and multiparticulates" *European Journal of Pharmaceutics and Biopharmaceutics* 62 (3) (2006b) 295-305.
- Corrigan, O. I., "Thermal analysis of spray dried products" Therm. Acta, 248 (1995) 245-258.
- Corrigan, O. I., Nanoporous microparticles (NPMPs) formation: a hypothesis. Dublin, Document from meeting (2005).
- Corrigan, O.I. (School of Pharmacy and Pharmaceutical Sciences, University of Dublin, Trinity College). Personal communication, (2006).
- Corrigan, O.I., Holohan, E.M., "Amorphous spray-dried hydroflumethazide-polyvinylpyrolidone systems: Physiochemical properties." J. Pharm. Pharmacol. 36(1984) 217-221.
- Dahl, A. R. and Lewis, J. L. "Respiratory tract uptake of inhalants and metabolism of xenobiotics" Annu Rev Pharmacol Toxicol. 32 (1993) 383–407.

- Davies, N. M. and Feddah, M. R., A novel method for assessing dissolution of aerosol inhaler products. Int. J. Pharm., 225 (2003) 175-187.
- Davis, M. E. and Brewster, M. E., "Cyclodextrin-based pharmaceutics: past, present and future" Nature Reviews 3 (2004) 1023-1035.
- De Villiers, M. M., Wurster, D. E., Van der Watt, J. G. and Ketkar, A. "X-Ray powder diffraction determination of the relative amount of crystalline acetaminophen in solid dispersions with polyvinylpyrrolidone" *Int. J. Pharm.,* 63 (1998) 219-224.
- Dehn, W. M. and Heuse, E. O. "Decomposition of hydrated ammonium salts" J. Am. Chem. Soc., 29 (8) (1907) 1137–1165.
- Dye, C., Williams, B. G., Espinal, M.A., and Raviglione, M.C. "Erasing the world's slow stain: strategies to beat multidrug-resistant tuberculosis" Science 295 (2002) 2042–2046.
- Edwards, D. A., Ben-Jebria, A. and Langer, R. "Recent advances in pulmonary drug delivery using large, porous inhaled particles" J Appl Physiol 85 (1998) 379-385.
- Edwards, D. A., Hanes, J., Caponetti, G., Hrkach, J., Ben-Jebria, A., Eskew, M. L., Mintzes, J., Deaver, D., Lotan, N. and Langer, R. "Large Porous Particles for Pulmonary Drug Delivery" Science 276 (5320) (1997) 1868-1872.
- Enright, G. D., Udachin, K. A., Moudrakovski, I. L. and Ripmeester, J. A. "Thermally Programmable Gas Storage and Release in Single Crystals of an Organic van der Waals Host" J. Am. Chem. Soc. (2003)125, 9896-9897.
- Erlenmeyer, H., Prijs, B., Sorkin, E. and Suter, E. *Helu. Chim. Ada,* 31, (1948)988-992. Through Seaman, W., Allen, W., Pasternak, R.L. and Pollara, A. "The Melting Point of 4-Aminosalicylic Acid" J. Am. Chem. Soc., 71 (8) (1949), 2940–2941.
- European Pharmacopoeia, 5th Edition, (2007)
- Evrard, B., Bertholet, P., Gueders, M., Flament, M.P., Piel, G., Delattre, L. Gayot, A., Leterme, P., Foidart, J.M. and Cataldo, D. "Cyclodextrins as a potential carrier in drug nebulization" Journal of Controlled Release 96 (3) (2004) 403–410.
- Felder, E. and Pitre, D "Pyrazinamide" in Florey, K., (Ed.) "Analytical profiles of drug substances" Academic Press, New York, 12(1983) 433-462.
- Fiegel, J., Garcia-Contreras, L., Thomas, M., Verberkmoes, J., Elbert, K., Hickey, A. and Edwards, D. "Preparation and in vivo evaluation of a dry powder for inhalation of capreomycin" *Pharmaceutical Research* 25 (4) (2008) 805-811.

- Forbes, R. T., York, P. and Davidson, J. R., "Dissolution Kinetics and Solubilities of p- Aminosalicylic Acid and Its Salts" Int. J. Pharm. 126(1995) 199-208.
- Fox, W., Ellard, G. A. and Mitchison, D. A. "Studies on the treatment of tuberculosis undertaken by the British Medical Research Council tuberculosis units, 1946–1986, with relevant subsequent publications" Int J Tuberc Lung Dis **3** (suppl 2) (1999) S231–S279.
- French, D. L., Edwards, D. A. and Niven, R. W., "The influence of formulation on emission, deaggregation and deposition of dry powders for inhalation" Journal of Aerosol Sciences, 27, 5 (1996) 769-783.
- Frenkel, A. V., Kaliya, I. M. L. and Guseinov, E. M. "Thermal Decomposition Of Ammonium Salts Of Nicotinic Acid And Its Analogs In The Liquid Phase" Pharmaceutical Chemistry Journal 29 (7) (1995) 480-484.
- Fris□čić, T., and MacGillivray, L.R."Single-crystal-to-single-crystal [2+2] photodimerizations: From discovery to design" Z. Kristallogr. 220 (2005) 351–363.
- Gagnière, E., Mangin, D., Puel, F., Rivoire, A., Monnier, O., Garcia, E., Klein, J.P. "Formation of co-crystals: Kinetic and thermodynamic aspects" Journal of Crystal Growth 311 (9) (2009) 2689-2695
- Garcia-Contreras, L., Fiegel, J., Telko, M.J., Elbert, K., Hawi, A., Thomas, M., VerBerkmoes, J. and Edwards, D.A. "Inhaled large porous particles of capreomycin for treatment of tuberculosis in a guinea pig model "Antimicrobial Agents and Chemotherapy 51 (8) (2007) 2830-2836.
- Gelperina, S., Kisich, K., Iseman, M. D. and Heifets, L. "The Potential Advantages of Nanoparticle Drug Delivery Systems in Chemotherapy of Tuberculosis" Am J Respir Crit Care Med 172 (2005) 1487–1490.
- Giron, D. "Characterisation of salts of drug substances" J. Therm. Anal. Cal., 73 (2003) 441–457.
- Giron, D., Goldbronn, C., Mutz, M., Pfeffer, S., Piechon, P. and Schwab, P. "Solid State Characterizations of Pharmaceutical Hydrates" J. Therm. Anal. Cal., 68 (2002) 453-465.
- Giron, D., Remy, P., Thomas, S. and Vilette, E., "Quantitation of amorphicity by microcalorimetry" J. of Therm. Anal., 48(1997) 465-472.
- Goldman, R. C., Plumley, K. V. and Laughon, B. E. "The evolution of extensively drug resistant tuberculosis (XDR-TB): history, status and issues for global control" Infect Disord Drug Targets 7 (2007)73-91.

- Grimes, P.E. "The Safety and Efficacy of Salicylic Acid Chemical Peels in Darker Racial-ethnic Groups" Dermatologic Surgery 25(1999) 18–22.
- Gunasekaran, S., Sailatha, E., Seshadri, S and Kumaresan, S "FTIR, FT Raman spectra and molecular structural confirmation of isoniazid" Indian Journal of pure & applied physics 47 (2009)12-18
- Guseinov, E.M., Sokolovskii, A.A., Kondrat'eva, N.M., Zarutskii, V.V., Oslyakov, G.V. "Thermal decomposition of ammonium nicotinate" Pharmaceutical Chemistry Journal 15 (10) (1981) 749-752.
- Hancock, B.C., Zografi, G. "Characteristics and significance of the amorphous state in pharmaceutical systems" J. Pharm. Sci. 86 (1997) 1–12.
- Hassan, M.M. A., Jado, A. I., and Uppal Zubair, M "Aminosalicylic acid" in Florey, K., (Ed.) "Analytical profiles of drug substances" Academic Press, New York, 10(1981) 1-28.
- Healy, A.M., McDonald, B., Corrigan, O.I. and Tajber, L. "A method of production porous microparticles" PCT patent WO 2007/086039 (2007).
- Hearle, J. W. S., Sparrow, J. T. and Cross, P. M. "The Use of Scanning Electron Microscope" Pergamon, New York (1972).
- Heifets L.B., Flory M.A. & Lindholm-Levy P.J., "Does pyrazinoic acid as an active moiety of pyrazinamide have specific activity against Mycobacterium tuberculosis?" Antimicrobial Agents Chemotherapy 33(8) (1989) 1252-1254.
- Heifets, L. and Lindholm-Levy, P. "Pyrazinamide sterilizing activity in vitro against semidormant Mycobacterium tuberculosis bacterial populations" Am Rev Respir Dis 145 (1992) 1223-1225.
- Henwood, S. Q., Liebenberg, W., Tiedt, L. R., Lötter, A. P. and de Villiers, M.M." Characterization of the solubility and dissolution properties of several new rifampicin polymorphs, solvates, and hydrates" Drug Development and Industrial Pharmacy 27 (10) (2001) 1017–1030.
- Hickey, A. J. "Inhalation aerosols: Physical and biological basis for therapy" Marcel Dekker, New York (1998).
- Higuchi, T. and Pitman, I. H. "Caffeine complexes with low water solubility: Synthesis and dissolution rates of 1:1 and 1:2 caffeine-gentisic acid complexes" J. Pharm. Sci. 62 (1973) 55-58.
- Hirota, K., Hasegawa, T., Hinata, H., Ito, F., Inagawa, H.,Kochi, C., Soma, G.I., Makino , K. and Terada, H. "Optimum conditions for efficient phagocytosis of

rifampicin-loaded PLGA microspheres by alveolar macrophages" J. Control. Rel. 119 (2007) 69–76.

- Hung, O. R., Whynot, S. C., Varvel, J. R., Shafer, S. L. and Mezei, M. "Pharmacokinetics of inhaled liposome-encapsulated fentanyl" Anesthesiology 83 (1995) 277–284.
- ICH, (International Conference on Harmonisation) Guideline Specification Q1A (R2), Step 4. Draft, Stability testing of new drug substances and products, (2003).
- Indrayanto, G., Syahrani, A., Mugihardjo, Abdul Rahman, Soeharjono, Tanudjojo, W., Susanti, S., Yuwono, M. and Ebel, S. "Benzoic Acid" in Brittain, H, G., (Ed.) "Analytical profiles of drug substances and excipients" Academic Press, New York, 26(1999) 1-46.
- Jacobs, C. and Muller, R. H. "Production and characterisation of a budesonide nanosuspension for pulmonary administration" Pharmaceutical Research 19(2002) 189–194.
- Jain, A.C. and Adeyeye, M.C. "Hygroscopicity, phase solubility and dissolution of various substituted sulfobutylether β -cyclodextrins (SBE) and danazol-SBE inclusion complexes" Int. J. Pharm. 212 (2001) 177–186.
- Jain, N. and Yalkowsky, S.H. "Estimation of the aqueous solubility I: Application to organic nonelectrolytes" Journal of Pharmaceutical Sciences 90 (2) (2001) 234-252.
- Jain, R. A. "The manufacturing techniques of various drug loaded biodegradable poly(lactide-co-glycolide) (PLGA) devices" Biomaterials 21(2000) 2475–2490.
- Jashani, R. N. and Byron, P. R. "Dry powder aerosol generation in different environments: Performance comparisons of albuterol, albuterol sulfate, albuterol adipate and albuterol stearate" Int. J. Pharm., 130 (1996) 13-24.
- Jivani, S. G., Stella, V. J., "Mechanism of Decarboxylation of *p*- Aminosalicylic Acid" J Pharm Sci., 74(1985)1274-1282.
- Karjalainen, M., Airaksinen, S., Rantanen, J., Aaltonen, J., Yliruusi, J. "Characterization of polymorphic solid-state changes using variable temperature X-ray powder diffraction" Journal of Pharmaceutical and Biomedical Analysis 39 (1-2) (2005) 27-32.
- Kassem, N. M., Ho, K. K. L. and Ganderton, D. "The effect of air flow and carrier size on the characteristics of an inspirable cloud" *J. Pharm. Pharmacol.* (41) Suppl. (1989)14.

- Katheri, A. K. (School of Pharmacy and Pharmaceutical Sciences, University of Dublin, Trinity College). Personal communication, (2007).
- Katiyar, S. K., Bihari, S. and Prakash, S. "Low-dose inhaled versus standard dose oral form of anti-tubercular drugs: Concentrations in bronchial epithelial lining fluid, alveolar macrophage and serum" LETTER 54 (3) (2008) 245-246.
- Kawashima, Y., Serigano, T., Hino, T. Yamamoto, H. and Takeuchi, H. "surface-modified antiasthmatic drug powder aerosols inhaled intratracheally reduce the pharmacologically effective dose" Pharm. Res. 15(1998)1753-1759.
- Kent, J. and McLeod, J. "Spray-Dryer Optimization" Powder Bulk Solids, February 2007.
- Kilinc, O., Ucan, E. S., Cakan, M. D. A. et al. "Risk of tuberculosis among health care workers: can tuberculosis be considered as an occupational disease?" Respiratory Medicine 96(2002) 506–10.
- Kramer, S.F. and Flynn, G.L. "Solubility of organic hydrochlorides" J. Pharm. Sci. 61 (1972) 1896–1904.
- Krantz, J. C., Jr.; Holbert, J. M.; Iwamoto, H. K.; Carr, C. J. "Sodium theophylline glycinate" J. Am. Pharm. Assoc. 36 (1947) 248-250.
- Kurunov, I. N., Ursov, I. G., Krasnov, V. A., Petrenko, T.I., Yakovchenko, N.N., Svistelnik, A.V. and Filimonov, P.A. "Effectiveness of liposomal antibacterial drugs in the inhalation therapy of experimental tuberculosis" Problemy Tuberkuleza **1** (1995) 38–40.
- Kurunov, Y. N., Filimonov, P. A., Svistelnik, A. V., Iakovchenko, N. N., Petrenko, T. I., Krasnov, V. A. and Ursov, I. G. ."Efficacy of liposomized antibacterial drugs in inhalation therapy of experimental tuberculosis" Probl. Tuberk 1(1995) 38-40.
- Labris, N.R. and Dolovich, M.B., "Pulmonary Drug Delivery Part 1: Physiological factors affecting therapeutic effectiveness of aerolized medications" British Journal of Clinical Pharmacology 56(2003) 588-599.
- Lahnstein, K., Schmehl, T., Rüsch, U., Rieger, M., Seeger, W. and Gessler, T. "Pulmonary absorption of aerosolized fluorescent markers in the isolated rabbit lung" Int. J. Pharm.351 (1-2) (2008) 158-164
- Li, J., Multiporous microparticles of drugs, pharmaceutical excipients and their mixtures. School of Pharmacy and Pharmaceutical Sciences, Trinity College, (2005), unpublished data.

- Louey, M.D. and Garcia-Contreras, L. "Controlled release products for respiratory delivery" American Pharmaceutical Review 7 (4) (2004) 82–87.
- Maa, Y.-F., Nguyen, P.-A., Sweeney, T., Shire, S. J. and Hsu, C. C. "Protein inhalation powders: spray drying vs spray freeze drying. Pharmaceutical Research" 16, 2 (1999) 249-254.
- Malcolmson, R. J. and Embleton, J. K. "Dry powder formulations for pulmanory delivery" Pharma. Sci.Tech.index 1(1998)394-398.
- Mandell, G.L. and Sande, H.A., "Antimicrobial agents" In: Gilman, G.A., Goodman, A. (Eds.), "The Pharmacological Basis of Therapeutics" 7th ed. Macmillan, New York, (1985) 1202–1205.
- Martin J Telko, M. J. and Hickey, A. J., "Dry Powder Inhaler Formulation" Respir Care 50(9) (2005)1209–1227.
- Masood, A. R., Thomas, S. H. L. "Systemic absorption of nebulized morphine compared with oral morphine in healthy subjects" Br J Clin Pharmacol 41 (1996) 250–252.
- Masters, K. Spray Drying Handbook. 5th Edition, Longman Scientific and Technical., (1991).
- McDonald, B., 2005. Preparation and characterisation of multiporous microparticles manufactured using a novel spray drying process. Thesis PhD Pharmaceutics, TCD
- Mehta, S. K., Bhasin, K. K., Dham, S. and Mehta, N. "Behavior of rifampicin in association with b-cyclodextrin in aqueous media: a spectroscopic and conductometric study" Colloid Polym Sci 283 (2005) 532–538.
- Merck Index, 11th Edition, the Merck and Co., Inc, N.J., USA, 1989.
- Miklia, V., Käerdi, H., kulu, P. and Besterci, M. "Characterization of powder particle morphology" Proc. Estonian Acad. Sci. Eng., 7 (1) (2001) 22–34.
- Mizoe, T., Ozeki, T. and Okada, H. "Preparation of drug nanoparticle-containing microparticles using a 4-fluid nozzle spray drier for oral, pulmonary, and injection dosage forms" J Control Release 122(1) (2007) 10–15.
- Moffat. A. C., Osselton, M. D. and Widdop, B., "Clarke's analysis of drugs and poisons" Pharmaceutical Press (2004).
- Morris, K. R., Griesser, U. J., Eckhardt, C. J. and Stowell, J. G. "Theoretical approaches to physical transformations of active pharmaceutical ingredients during manufacturing processes" Advanced Drug Delivery Reviews 48 (1) (2001) 91-114.

- Muehling, J.K., Arnold, H.R. and House Jr., J.E. "Effects of particle size on the decomposition of ammonium carbonate" Thermochimica Acta 255 (C) (1995) 347-353.
- Muttil, P., Kaur, J., Kumar, K., Yadav, A.B., Sharma, R. and Misra, A. "Inhalable microparticles containing large payload of anti-tuberculosis drugs" European Journal of Pharmaceutical Sciences 32 (2) (2007) 140-150.
- Najafabadi, A., Gilani, K., Barghi, M. and Rafiee-Tehrani, M. "The effect of vehicle on physical properties and aerosolisation behaviour of disodium cromoglycate microparticles spray dried alone or with L-leucine" Int. J. Pharm. 285 (2004) 97–108.
- Newman, A. W. and Byrn, S. R. "Solid-state analysis of the active pharmaceutical ingredient in drug products " Drug Discovery Today 8 (19) (2003) 898-905.
- Newman, S. P. "Principles of Metered-Dose Inhaler Design" RESPIR. CARE 50 (9) (2005) 1177–1188.
- Newman, S. P., Weisz, A. W., Talaee, N. and Clarke, S. W. "Improvement of drug delivery with a breath actuated pressurised aerosol for patients with poor inhaler technique" Thorax 46(10) (1991) 712–716.
- Ní Ógáin, O. (School of Pharmacy and Pharmaceutical Sciences, University of Dublin, Trinity College). Personal communication, (2006).
- Ní Ógáin, O., 2008. "Investigations of a spray-drying method for producing nanoporous/nano-particulate microparticles (NPMPs) of proteins and protein-excipient composites" Thesis PhD Pharmaceutics, TCD
- Nishioka, F., Nakanishi, I., Fujiwara, T. and Tomita, K. "The crystal and molecular structure of the β-cyclodextrin inclusion complex with aspirin and salicylic acid" J. Incl. Phenom. 2 (1984) 701–714.
- Nolan, L., 2008. The production and characterisation of spray dried nanoporous microparticles (NPMPs) intended for dry powder inhalation drug delivery systems. Thesis PhD Pharmaceutics, TCD
- Nolan, L., Tajber, L., Corrigan, O.I. and Healy, A.M., The physicochemical characterisation of spray dried nanoporous microparticles (NPMPs) of sulfa compounds, EUFEPS Conference: When Poor Solubility Becomes an Issue: From Early Stage to Proof of Principles, Verona, Italy, 26-27 April, 2006
- Nolan, L., Tajber, L., McDonald, B., Barham, A., Corrigan, O. I. and Healy, A. M. "Excipient-free nanoporous microparticles of budesonide for pulmonary delivery" European Journal of Pharmaceutical Sciences 37 (5) (2009) 593-602.

- O'Connor, *Lancet,* 254 (1948) 191. Through Seaman, W., Allen, W., Pasternak, R.L. and Pollara, A. "The Melting Point of 4-Aminosalicylic Acid" J. Am. Chem. Soc., 71 (8) (1949), 2940–2941.
- O'Hara. P. and Hickey. A. J. "Respirable PLGA microspheres containing rifampicin for the treatment of tuberculosis: manufacture and characterization" Pharm. Res. 17(2000)955-961.
- Oxtont, I., Amerona, S., NOP, O. and Mcculloc, A. W. "Ammonium salts of benzoic acid and the crystal structure of ammonium hydrogen bisbenzoatel" J. Chem. 55 (1977) 3831-3837.
- Pandey, R and Khuller, G. K. "Antitubercular inhaled therapy: opportunities, progress and challenges" J. Antimicrob. Chemother. 55 (2005a) 430–435.
- Pandey, R. and Khuller, G. K. "Polymer based drug delivery systems for mycobacterial infections" Current Drug Delivery 1 (2004) 195–201.
- Pandey, R. and Khuller, G. K. "Solid lipid particle-based inhalable sustained drug delivery system against experimental tuberculosis" Tuberculosis (Edinb.) 85 (2005b) 227–234.
- Pandey, R., Sharma, A., Zahoor, A., Sharma, S., Khuller, G. K and Prasad B. "Poly (DL-lactide-co-glycolide) nanoparticle-based inhalable sustained drug delivery system for experimental tuberculosis" Journal of Antimicrobial Chemotherapy52 (2003) 981-986.
- Pandey, R., Sharma, S. and Khuller, G. K. "Nebulization of liposome encapsulated antitubercular drugs in guinea pigs" International Journal of Antimicrobial Agents 24 (2004) 93–94.
- Patterson, J. E., James, M. B., Forster, A. H., Lancaster, R. W., Butler, J. M. and Rades, T. "Preparation of glass solutions of three poorly water soluble drugs by spray drying, melt extrusion and ball milling" Int. J. Pharm. 336 (2007) 22-34.
- Patton, J. S. "Mechanisms of macromolecular absorption by the lungs" Adv Drug Deliv Rev (1996) 3–36.
- Patton, J. S., Fishburn, C. S. and Weers, J. G." The Lungs as a Portal of Entry for Systemic Drug Delivery" Proc Am Thorac Soc 1(2004)338–344.
- Pelizza, G., Nebuloni, M., Ferrari, P. and Gallo, G. G "Polymorphismof rifampicin" Il Farmaco 32(1977) 471–481.

- Peloquin, C.A., Berning, S.E., Huitt, G.A., Childs, J.M., Singleton, M.D. and James, G.T. "Once-daily and twice-daily dosing of *p*-aminosalicylic acid granules" Am J Respir Crit Care Med 159 (1999) 932–934.
- Pirttimäki, J., Laine, E., Ketolainen, J. and Paronen, P. "Effects of grinding and compression on crystal structure of anhydrous caffeine" Int. J. Pharm. 95 (1993) 93–99.
- Pop, M., Sieger, P., Cains, P.W. "Tiotropium fumarate: An interesting pharmaceutical co-crystal" Journal of Pharmaceutical Sciences 98 (5) (2009)1820-1834.
- Prinn, K.B., Constantino, H.R., Tracy, M. "Statistical modeling of protein spray drying at the lab scale" AAPS PharmSciTech 3 (2002) 1-8.
- Qiang, Z. and Adams, C., "Potentiometric determination of acid dissociation constants (pK_a) for human and veterinary antibiotics" Water Res. 38 (2004) 2874-2890.
- Rabbani, N.R. and Seville, P.C. "The influence of formulation components on the aerosolisation properties of spray-dried powders" J. Control. Release. 110(2005) 130-140.
- Ramis, G., Yi, L., Busca, G. "Ammonia activation over catalysts for the selective catalytic reduction of NOx and the selective catalytic oxidation of NH3. An FT-IR study "Catalysis Today 28 (4) (1996) 373-380.
- Rane, S. S. and Anderson, B. D. "What determines drug solubility in lipid vehicles: Is it predictable?" Advanced Drug Delivery Reviews 60 (6) (2008) 638-656.
- Rao, B.S. and Murthy, K.V.R. "Studies on rifampicin release from ethylcellulose coated nonpareil beads" Int. J. Pharm. 231 (2002) 97–106.
- Rau, J. L. "The inhalation of drugs: Advantages and Problems" Respir Care 50 (3) (2005) 367-382.
- Rekker, R.F., Nauta,W.T. "The UV absorption spectra of p-aminosalicylic acid and some related compounds" Pharmaceutisch Weekblad 19 (1948) 693–732.
- Rengarajan, J., Sassetti, C., Naroditskaya, V., Sloutsky, A., Bloom, B. R. and Rubin, E. J. "The folate pathway is a target for resistance to the drug para-previous termaminosalicylicnext term acid (PAS) in mycobacteria, Mol Microbiol 53 (2004), pp. 275–282.
- Reynolds, J. E. F., Parfitt, K., Parsons, A. V. and Sweetman, S. C. "Martindale, The Extra Pharmacopoia" Royal Pharmaceutical society, London, (1996).

- Richardson, C.H., De Matas, M., Hosker, H., Mukherjee, R., Wong, I. and Chrystyn, H. "Determination of the relative bioavailability of salbutamol to the lungs following inhalation from dry powder inhaler formulations containing drug substance manufactured by supercritical fluids and micronization" Pharmaceutical Research 24 (11) (2007) 2008-2017.
- Ro, G. and Sorum, H. "Crystal and Molecular Structure of Beta-Pyrazincarboxamide" Acta Crystall B Stru B28 (1972 a) 991–998.
- Ro, G. and Sorum, H. "Crystal and molecular structure of delta-pyrazincarboxamide" Acta Crystall B Stru B28 (1972 b) 1677–1684.
- Roberts W. E. "Chemical peeling in ethnic/dark skin". Dermatologic Therapy 17 (2) (2004) 196-205.
- Rotich, M. K., Brown, M. E. and Glass, B. D. "Thermal studies on mixtures of aminosalicylic acids with cyclodextrins" Journal of Thermal Analysis and Calorimetry, 73 (2003a) 687-706.
- Rotich, M. K., Brown, M. E. and Glass, B. D. "Thermal studies on mixtures of benzoic and salicylic acids with cyclodextrins" Journal of Thermal Analysis and Calorimetry, 73 (2003b) 671-686.
- Rotich, M. K., Glass, B. D. and Brown, M. E. "Thermal studies on some substituted aminobenzoic acids" Journal of Thermal Analysis and Calorimetry, 64 (2001) 681-688.
- Roy, J. "Pharmaceutical impurities—A mini review" AAPS PharmSci Tech 3 (2002) article 6.
- Ruffin, R. E., Dolovich, M. B., Wolff, R. K. and Newhouse, M. T. "The effects of preferential deposition of histamine in the human airway" Am Rev Respir Dis.117 (1978) 485–492.
- Schaller,A., Guo, M., Gisanrin,O., Zhang, Y., "Escherichia coli genes involved in resistance to pyrazinoic acid, the active component of the tuberculosis drug pyrazinamide" FEMS Microbiology Letters. 211(2) (2002) 265-270.
- Schanker, L. S. "Drug absorption from the lung" Biochem Pharmacol 27(1978)381–385.
- Schultheiss, N. and Newman, A. "Pharmaceutical cocrystals and their physicochemical properties" Crystal Growth and Design 9 (6) (2009) 2950-2967.

- Scott, E.R. et al., "Electrotransport Systems for transdermal delivery" in Wise, D. L. (Ed.) Handbook of pharmaceutical controlled release technology, Marcel Dekker, New York (2000).
- Seaman, W., Allen, W., Pasternak, R.L. and Pollara, A. "The Melting Point of 4-Aminosalicylic Acid" J. Am. Chem. Soc., 71 (8) (1949), 2940–2941
- Sebhatu, T., Angberg, M. and Ahlneck, C. "Assessment of the degree of disorder in crystalline solids" Int. J. Pharm. 101 (1994) 237–247.
- Serajuddin, A.T.M "Salt formation to improve drug solubility" Advanced Drug Delivery Reviews 59 (7) (2007) 603-616.
- Serajuddin, A.T.M. and Pudipeddi, M. "Salt-selection strategies" In: Stahl, P.H. and Wermuth, C.G., Editors, Handbook of Pharmaceutical Salts: Properties, Selection, and Use, Wiley-VCH, Weinheim (2002), pp. 135–160.
- Sham, J.O.H., Zhang, Y., Finlay, W.R., Roa, H.R., and Lobenberg, R., "Formulation and characterisation of spray-dried powders containing nanoparticles for aerosol delivery to the lung" Int. J. Pharm. 269(2004)457-467.
- Sharma, A., Sharma, S. and Khuller, G. K. "Lectin-functionalized poly (lactide-co-glycolide) nanoparticles as oral/aerosolised antitubercular drug carriers for treatment of tuberculosis" Journal of Antimicrobial Chemotherapy 54(2004) 761–766.
- Sharma, R., Muttil, P., Yadav, A., Rath, S., Bajpai, V., Mani, U. and Misra, A. "Uptake of inhalable microparticles modifies defense responses of macrophages infected with Mycobacterium tuberculosis h37ra" J. Antimicrob. Chemother. 59 (2007) 499–506
- Sharma, R., Saxena, D., Dwivedi, A. K. and Misra, A. "Inhalable microparticles containing drug combinations to target alveolar macrophages for treatment of pulmonary tuberculosis" Pharmaceutical Research 18(2001b) 1405–1410.
- Sharma, S., White, D., Imondi, A.R., Placke, M.E., Vail, D.M., and Kris, M.G. "Development of inhalation agents for oncologic use" J. Clin. Oncol. 19(2001) 1839-1847.
- Singh, M., Kamble, R. and Viswanadham, N. "Effect of crystal size on physico-chemical properties of ZSM-5" Catalysis Letters 120 (3-4) (2008) 288-293.
- Smith, C. V., Sharma, V. and Sacchettini, J. C. "TB drug discovery: addressing issues of persistence and resistance" Tuberculosis 84 (1-2) (2004) 45–55.

- Smyth, H. D. C and Hickey, A. J. "Multimodal Particle Size Distributions Emitted From HFA-134a Solution Pressurized Metered-Dose Inhalers" *AAPS PharmSciTech*. 2003; 4(3): article 38.
- Socrates G., "Infrared and Raman characteristic group frequencies" John Wiley & Sons, Chichester, (2001).
- Socrates G., Infrared and Raman characteristic group frequencies, John Wiley & Sons, Chichester, (2001).
- Song, W., Justice, R. E., Jones, C. A., Grassian, V. H. and Larsen, S. C. "Size-Dependent Properties of Nanocrystalline Silicalite Synthesized with Systematically Varied Crystal Sizes" Langmuir 20 (2004) 4696-4702
- Stahl, K., Claesson, M., Lilliehorn, P., Linden H. and Backstorm, K. "The effect of process variables on the degradation and physical properties of spray dried insulin intended for inhalation" Int. J. Pharm. 233 (2002) 227–237.
- Stahl, P. H. and Wermuth, C. G. (Eds) "Handbook of Pharmaceutical Salts, Properties, Selection and Use" IUPAC, Wiley-VCH, Verlag Helvetica Chimica Acta, Zürich 2002.
- Stahly, G. P. "Diversity in single- and multiple-component crystals the search for and prevalence of polymorphs and cocrystals" Crystal Growth and Design 7 (6) (2007) 1007-1026.
- Stefely J. S. "Novel excipients for inhalation drug delivery: expanding the capability of MDI". Drug Del.Tech. 2(6) (2002).
- Stone, K.C., Mercer, R.R., Gehr, P., Stockstill, B. and Crapo, J.D. "Allometric relationship of cell numbers and size in the mammalian lung" Am J Respir Cell Mol Biol. 6(1992) 235–243.
- Straub, J.A., Chickering, D. E., Lovely, J. C., Zhang, H., Shah, B., Waud, W. and Bernstein, H., "Intravenous hydrophobic drug delivery: A porous particle formulation of paclitaxel (AI-850)". Pharm. Res., 22 (2005) 347-355.
- Suarez, S., O'Hara, P., Kazantseva, M., Newcomer, C. E., Hopfer, R., McMurray, R. and Hickey, A. "Airways delivery of rifampicin microparticles for the treatment of tuberculosis" Journal of Antimicrobial Chemotherapy 48(2001b) 431–434.
- Suarez, S., O'Hara, P., Kazantseva, M., Newcomer, C. E., Hopfer, R., McMurray, R. and Hickey, A. "Respirable PLGA microspheres containing rifampicin for the treatment of tuberculosis: screening in an infectious disease model. Pharmaceutical Research 18 (2001a) 1315–1319.

- Sung, J. C., Padilla, D.J., Garcia-Contreras, L., VerBerkmoes, J.L., Durbin, D., Peloquin, C.A., Elbert, K.J. and Edwards, D.A. "Formulation and Pharmacokinetics of Self-Assembled Rifampicin Nanoparticle Systems for Pulmonary Delivery" Pharmaceutical Research, (2009) 1-9.
- Sung, J. C., Pulliam, B. L. and Edwards, D. A. "Nanoparticles for drug delivery to the lungs" Trends in Biotechnology 25(12) (2007) 563-70.
- Tajber, L., 2005. Investigations of physiochemical properties of spray dried drug-excipient composites directed to inhalable products. Thesis PhD Pharmaceutics, TCD.
- Takaki, Y., Sasada, Y. and Watanabe, T. "The crystal structure of alpha-pyrazinamide" Acta Crystallogr 13(1960) 693–702.
- Takenaka, H., Kawashima, Y. and Lin, S. Y. "Polymorphism of spray dried microencapsulated sulfamethoxazole with cellulose acetate phthalate and colloidal silica, montmorillonite, or talc" J. Pharm. Sci., 70 (1981) 1256-1260.
- Tamura, C., Sasada, Y. and Kuwano, H. "Crystallographic data of carboxylic acids and carboxyamides of picoline and pyrazine derivatives" Acta Crystallogr 14(1961) 693.
- Tan, S., Hung, O. and Whynot, S. C. "Sustained tissue drug concentrations following inhalation of liposome-encapsulated fentanyl in rabbits" Drug Deliv. 3 (1996) 251–254.
- Thomas, C. "A literature review of the problems of delayed presentation for treatment and non-completion of treatment for tuberculosis in less developed countries and ways of addressing these problems using particular implementations of the DOTS strategy" Journal of management in medicine 16 (2002) 371-400
- Ticehurst, M.D., Basford, P.A., Dallman, C.I., Lukas, T.M., Marshall, P.V., Nichols, G., Smith, D., "Characterisation of the influence of micronisation on the crystallinity and physical stability of revatrope hydrobromide" Int. J. Pharm. 193(2000) 247– 259.
- Timsina, M.P., Martin, G.P., Marriott, C., Ganderton, D. and Yianneskis, M. "Drug delivery to the respiratory tract using dry powder inhalers" Int. J. Pharm. 101(1994)1–13.
- Tronde, A., Norden, B., Marchner, H., Wendel, A. K., Lennernas, H. and Bengtsson, U. H. "Pulmonary absorption rate and bioavailability of drugs in vivo in

rats: structure-absorption relationships and physicochemical profiling of inhaled drugs" J Pharm Sci 92 (2003)1216–1233.

- Tsapis N., Bennett, D., O'Driscoll, K., Shea, K., Lipp, M. M., Fu, K., Clarke, R. W., Deaver, D., Yamins, D., Wright, J.., Peloquin, C. A., Weitz, D. A. and Edwards, D. A. "Direct lung delivery of para-aminosalicylic acid by aerosol particles' Tuberculosis 83(2003) 379-385.
- United States Pharmacopoeia, 2007. United States Pharmacopoeial Convention Inc., Rockville, Maryland.
- Vanbever, R., Mintzes, J.D., Wang, J., Nice, J., Chen, D., Batycky, R., Langer, R., Edwards, D.A. "Formulation and physical characterization of large porous particles for inhalation" Pharmaceutical Research 16 (11) (1999) 1735-1742.
- Variankaval, N., Wenslow, R., Murry, J., Hartman, R., Helmy, R., Kwong, E., and Santos, I. "Preparation and solid-state characterization of nonstoichiometric cocrystals of a phosphodiesterase-IV inhibitor and L-tartaric acid" Crystal Growth and Design 6 (3) (2006) 690-700.
- Vasbinder, E., Van der Weken, G., Vander Heyden, Y., Baeyens, W.R.G., Debunne, A., Remon, J.P., Garcia-Campana, A.M. "Quantitative determination of p-aminosalicylic acid and its degradation product aminophenol in pellets by ion-pair high-performance liquid chromatography applying the monolithic Chromolith Speedrod RP-18e column" Biomed. Chromatogr. 18 (2004) 55–63.
- Verreck, G., Decorte,A., Heymansa, K., Adriaensen,J., Dehua Liu b, David Tomasko b, Arien, A., Peeters, J., den Mooter, G. V. and Brewster, M. E. "Hot stage extrusion of p-amino salicylic acid with ECusing CO2 as a temporary plasticizer" Int. J. Pharm. 327 (2006) 45–50
- Vidgrén, P., Vidgren, M. and Paronen, P., "Physical stability and inhalation behaviour of mechanically micronised and spray dried disodium cromoglycate in different humidities" Acta Pharm. Fennica 98(1989) 71–78.
- Vyas, S. P., Kannan, M. E., Jain, S. , Mishra, V. and Singh, P. "Design of liposomal aerosol for improved delivery of rifampicin to alveolar macrophages" International Journal of Pharmaceutics 269(2004) 37–49.
- Walkling, W. D., Reynolds, B. E., Fegely, B. Y. and Janicki, C. "Xilobam: Effect of salt form on pharmaceutical properties" Drug Dev. Ind. Pharm., 9 (1983) 809-819.
- Walton, D.E. and Mumford, C. J. Spray dried products-characterisation of particle morphology. Trans IChemE, 77(A) (1999) 21-38.

- Wang, W., Zhang, J., Huang, H., Wu, Z., Zhang, Z. "Investigation of monolayer dispersion of benzoic acid supported on the surface of H-titanate nanotubes" Applied Surface Science 253 (12) (2007) 5393-5399.
- Wermuth, C.G. and Stahl, P.H. "Selected procedures for the preparation of pharmaceutically acceptable salts" In: Stahl, P.H. and Wermuth, C.G. Editors, "Handbook of Pharmaceutical Salts: Properties, Selection, and Use" Wiley-VCH, Weinheim (2002) 249–263.
- West, A. R., "Basic Solid State Chemistry" Wiley, New York (1999).
- Whittet, *Lancet,* 254 (1948) 268. Through Seaman, W., Allen, W., Pasternak, R.L. and Pollara, A. "The Melting Point of 4-Aminosalicylic Acid" J. Am. Chem. Soc., 71 (8) (1949), 2940–2941.
- Yamamoto, H., Hoshina, W., Kurashima, H., Takeuchi, H., Kawashima, Y., Yokoyama, T. and Tsujimoto H. "Engineering of poly(DL-lactic-co-glycolic acid) nanocomposite particles for dry powder inhalation dosage forms of insulin with the spray-fluidized bed granulating system" Adv Powder Technol 18 (2007) 215–228.
- Yang, S. S. and Guillory, J. K. Polymorphism in sulfonamides. *J. Pharm. Sci.*, 61 (1972) 26-40.
- Yeo, S-D. and Lee, J-C., Crystallisation of sulfamethizole using the supercritical and liquid antisolvent processes. *J. Supercrit. Fluids*, 30 (2004) 315-323.
- Yokota, S. and Miki, K. "Effects of INH (Isoniazid) inhalation in patients with endobronchial tuberculosis (EBTB)" Kekkaku [Tuberculosis] 74(12)(1999) 873-7
- York, P. "Solid-state properties of powders in the formulation and processing of solid dosage forms" Int. J. Pharm. 14 (1983) 1–28.
- Young, P.M., Thompson, J., Woodcock, D., Aydin, M. and Price, R. "The Development of a Novel High-Dose Pressurized Aerosol Dry-Powder Device (PADD) for the Delivery of Pumactant for Inhalation Therapy" J. Aerosol Med., 17(2), 123–128 (2004).
- Zahoor, A., Sharma, S. and Khuller, G.k. "Inhalable alginate nanoparticles as antitubercular drug carriers against experimental tuberculosis" Int. J. Antimicrob. Agents 26 (2005) 298–303.
- Zeng, X.M., Martin, G.P. and Marriott, C. "Particulate Interactions in Dry Powder Formulations for Inhalation" Taylor and Francis, London (2001).
- Zukerman-Schpector, J., and Tiekink, E.R.T. "What is a co-crystal?" Zeitschrift fur Kristallographie 223 (3) (2008) 233-234.

Appendix

APPENDIX I

All experiments are listed as discussed in each chapter.

Key: PAS = p-aminosalicylic acid EtOH = Ethanol, MeOH = Methanol, BA = butyl acetate, AC = ammonium carbonate, AHC = ammonium hydrogen carbonate, PVP= polyvinylpyrrolidone, HP-ß-CD = hydroxypropyl-ß-cyclodextrin OM = open mode configuration, CM = closed mode configuration, EC = efficiency cyclone, N_2 = nitrogen gas drying medium, Air = compressed air drying medium,

Table1. Spray drying conditions for p-aminosalicylic acid systems

System (sample no)	Solvent % v/v Volume (ml)	Spray Drying Mode	Solid Conc (%w/v)	Drying Gas	Blowing Agent Conc (%w/w)	Inlet Temp (°C)	Outlet Temp (°C)	Airflow rate (Nl/h)	Aspirator (%)	Yield (%)	Notes
PAS (R6)	70% EtOH (100)	OM	1.0	Air	-	78	48	4	100	66.4	
PAS (R3)	80% EtOH (100)	OM	1.0	Air	-	78	45	4	100	55.6	
PAS (R35)	70% EtOH (100)	OM	1.0	Air	-	78	48	4	100	62.7	Lot: S35728-346
PAS (R40)	90% EtOH (100)	OM	1.0	Air	-	78	45	4	100	64.4	Lot: S35728-346
PAS (R36)	70% EtOH (100)	OM	1.0	Air	-	78	44	4	100	47.2	Sample was filtered

System (sample no)	Solvent % v/v Volume (ml)	Spray Drying Mode	Solid Conc (%w/v)	Drying Gas	Blowing Agent Conc (%w/w)	Inlet Temp (°C)	Outlet Temp (°C)	Airflow rate (Nl/h)	Aspirator (%)	Yield (%)	Notes
PAS (R5)	90% EtOH (100)	OM	1.0	Air	-	78	53	4	100	64.4	
PAS (R8)	90% EtOH (100)	OM	3.0	Air	-	78	55	4	100	51.3	
PAS (R12)	90% EtOH (100)	OM	4.0	Air	-	78	42	4	100	73.8	
PAS (R9)	95% EtOH (100)	OM	3.0	Air		78	51	4	100	37.8	
PAS (R7)	100% EtOH (100)	CM	4.0	N2	-	78	58	4	100	26.3	
PAS (R17)	90% EtOH (100)	OM	4.0	Air	3.8% AC	78	44	4	100	77.7	
PAS (R18)	90% EtOH (100)	OM	4.0	Air	10% AC	78	46	4	100	70.6	

System (sample no)	Solvent % v/v Volume (ml)	Spray Drying Mode	Solid Conc (%w/v)	Drying Gas	Blowing Agent Conc (%w/w)	Inlet Temp (°C)	Outlet Temp (°C)	Airflow rate (Nl/h)	Aspirator (%)	Yield (%)	Notes
PAS (R19)	90% EtOH (100)	OM	4.0	Air	15% AC	78	39	4	100	61.4	
PAS (R13)	90% EtOH (100)	OM	4.0	Air	20% AC	78	51	4	100	53.2	Lot: S26559-365
PAS (R37)	90% EtOH (100)	OM	4.0	Air	20% AC	78	55	4	100	67.1	Lot: S35728-346
PAS (R38)	90% EtOH (100)	OM	4.0	Air	20% AC	78	55	4	100	66.1	Lot: S35728-346
PAS (R10)	90% EtOH (100)	OM	3.0	Air	20% AC	78	44	4	100	44.7	Lot: S26559-365
PAS (R27)	90% EtOH (100)	OM	3.0	Air	27% AC	78	50	4	100	38.1	
PAS (R26)	90% EtOH (100)	OM	3.0	Air	38% AC	78	46	4	100	43.4	
PAS (R21)	90% EtOH (100)	OM	3.0	Air	38% AC	78	34	4	100	34.0	

System (sample no)	Solvent % v/v Volume (ml)	Spray Drying Mode	Solid Conc (%w/v)	Drying Gas	Blowing Agent Conc (%w/w)	Inlet Temp (°C)	Outlet Temp (°C)	Airflow rate (Nl/h)	Aspirator (%)	Yield (%)	Notes
PAS (R29)	90% EtOH (100)	OM	3.0	Air	50% AC	78	50	4	100	28.3	
PAS (R10a)	90% EtOH (100)	CM	3.0	N2	20% AC	78	48	4	100	86.6	
PAS (R28)	90% EtOH (100)	OM	3.0	Air	20% AC	78	50	4	100	40.6	Lot: S35728-346
PAS (R39)	90% EtOH (100)	OM	3.0	Air	20% AC	78	54	4	100	64.4	Lot: S35728-346
PAS (R20)	90% EtOH (100)	OM	4.0	Air	20% AHC	78	34	4	100	55.9	
PAS (R15)	90% MeOH (100)	CM	1.0	N2	20% AC	78	50	4	100	42.6	
PAS (R11)	80% MeOH (100)	CM	1.0	N2	20% AC	78	50	4	100	30.7	
PAS (R16)	70% MeOH (100)	CM	1.0	N2	20% AC	78	42	4	100	24.7	

System (sample no)	Solvent % v/v Volume (ml)	Spray Drying Mode	Solid Conc (%w/v)	Drying Gas	Blowing Agent Conc (%w/w)	Inlet Temp (°C)	Outlet Temp (°C)	Airflow rate (Nl/h)	Aspirator (%)	Yield (%)	Notes
PAS (R32)	90% EtOH (100)	CM	3.0	N2	50% AC	130	85	4	100	16.8	
PAS (R31)	90% MeOH (100)	CM	3.0	N2	50% AC	130	79	4	100	-	
PAS (R30)	90% EtOH (100)	CM	3.0	N2	50% AC	130	79	4	100	-	
PAS (R33)	90% EtOH (100)	CM	3.0	N2	50% AHC	130	81	4	100	22.1	
PAS (R34)	90% EtOH (100)	OM	3.0	Air	20% AC	120	78	4	100	20.6	
9:1 PAS/PVP (R25)	90% EtOH (100)	OM	3.0	Air	-	78	39	4	100	36	

Table 2. Spray drying conditions for p-aminosalicylic acid ammonium salt systems

System (sample no)	Solvent % v/v Volume (ml)	Spray Drying Mode	Solid Conc (%w/v)	Drying Gas	Blowing Agent Conc (%w/w)	Inlet Temp (°C)	Outlet Temp (°C)	Airflow rate (Nl/h)	Aspirator (%)	Yield (%)	Notes
PAS (AS1)	90% EtOH (33)	OM	3.0	Air	-	78	45	4	100	47	
PAS (AS7)	90% EtOH (20)	OM	3.0	Air	-	78	55	4	100	51.3	
PAS (AS5)	100% H2O (50)	OM	1.0	Air	-	120	52	4	100	19.6	
PAS (AS6)	90% EtOH (20)	CM	3.0	Air	-	130	76	4	100	43.3	

Table 3. Spray drying conditions for benzoic acid systems

System (sample no)	Solvent % v/v Volume (ml)	Spray Drying Mode	Solid Conc (%w/v)	Drying Gas	Blowing Agent Conc (%w/w)	Inlet Temp (°C)	Outlet Temp (°C)	Airflow rate (Nl/h)	Aspirator (%)	Yield (%)	Notes
Benzoic acid (B2)	90% EtOH (100)	OM	3.0	Air	20% AC	78	54	4	100	21.6	
Benzoic acid (B4)	90% EtOH (100)	OM	3.0	Air	34% AC	78	53	4	100	21.5	
Benzoic acid (B5)	90% EtOH (100)	OM	3.0	Air	50% AC	78	56	4	100	7.8	
Am. benzoate (A1)	90% EtOH (100)	OM	3.0	Air	-	78	50	4	100	54	
Benzoic acid (B1)	90% EtOH (100)	OM	3.0	Air	-	78	49	4	100	15.1	

Table 3. Spray drying conditions for salicylic acid systems

System (sample no)	Solvent % v/v Volume (ml)	Spray Drying Mode	Solid Conc (%w/v)	Drying Gas	Blowing Agent Conc (%w/w)	Inlet Temp (°C)	Outlet Temp (°C)	Airflow rate (Nl/h)	Aspirator (%)	Yield (%)	Notes
Salicylic acid (S3)	90% EtOH (200)	OM	3.0	Air	20% AC	78	52	4	100	28.3	V=200ml
Salicylic acid (S5)	90% EtOH (100)	OM	3.0	Air	30% AC	78	54	4	100	23.5	V=200ml
Salicylic acid (S4)	90% EtOH (100)	OM	3.0	Air	42% AC	78	53	4	100	21.1	V=200ml
Salicylic acid (S2)	90% EtOH (200)	OM	3.0	Air	50% AC	78	56	4	100	20.2	V=200ml
Salicylic acid (S1)	90% EtOH (100)	OM	3.0	Air	-	78	54	4	100	7.2	V=100ml
Ammonium salicylate (AA1)	90% EtOH (100)	OM	3.0	Air	-	78	54	4	100	36.0	
Ammonium salicylate (AA2)	100% H2O (100)	OM	3.0	Air	-	120	72	4	100	24.6	

Table 4. Spray drying conditions for pyrazinoic acid systems

System (sample no)	Solvent % v/v Volume (ml)	Spray Drying Mode	Solid Conc (%w/v)	Drying Gas	Blowing Agent Conc (%w/w)	Inlet Temp (°C)	Outlet Temp (°C)	Airflow rate (Nl/h)	Aspirator (%)	Yield (%)	Notes
Pyrazinoic acid (Y5)	90% EtOH (200)	OM	1.0	Air	20% AC	78	55	4	100	43.5	V=200ml
Pyrazinoic acid (Y6)	90% EtOH (100)	OM	1.0	Air	27% AC	78	53	4	100	16.5	
Pyrazinoic acid (Y7)	90% EtOH (100)	OM	1.0	Air	34% AC	78	57	4	100	26.0	
Pyrazinoic acid (Y9)	90% EtOH (100)	OM	1.0	Air	50% AC	78	59	4	100	21.9	
Ammonium salt of pyrazinoic (AP6)	90% EtOH (33)	OM	3.0	Air	-	78	52	4	100	46.5	
Ammonium salt of pyrazinoic (AP5)	100% H2O (25)	OM	1.0	Air	-	120	39	4	100	21.2	

Table 5. Spray drying conditions for sulfacetamide systems

System (sample no)	Solvent % v/v Volume (ml)	Spray Drying Mode	Solid Conc (%w/v)	Drying Gas	Blowing Agent Conc (%w/w)	Inlet Temp (°C)	Outlet Temp (°C)	Airflow rate (Nl/h)	Aspirator (%)	Yield (%)
Sulfacetamide (T2)	90% EtOH (100)	OM	1.0	Air	10% AC	78	51	4	100	30.7
Sulfacetamide (T3)	90% EtOH (100)	OM	1.0	Air	20% AC	78	52	4	100	25.1
Sulfacetamide (T4)	90% EtOH (100)	OM	1.0	Air	30% AC	78	52	4	100	28.0
Sulfacetamide (T5)	90% EtOH (100)	OM	1.0	Air	50% AC	78	51	4	100	14.0
Ammonium salt of Sulfacetamide (AT1)	90% EtOH (33)	OM	3.0	Air	-	78	51	4	100	49.8
Ammonium salt of Sulfacetamide (AT2)	100% H2O (50)	OM	1.0	Air	-	78	55	4	100	32.8
Sulfacetamide (T1)	90% EtOH (100)	OM	1.0	Air	-	78	49	4	100	43.4

Table 6. Spray drying conditions for sulfamethizole systems

System (sample no)	Solvent % v/v Volume (ml)	Spray Drying Mode	Solid Conc (%w/v)	Drying Gas	Blowing Agent Conc (%w/w)	Inlet Temp (°C)	Outlet Temp (°C)	Airflow rate (Nl/h)	Aspirator (%)	Yield (%)	Notes
Sulfamethizole (F17)	90% EtOH (100)	OM	0.5	Air	5% AC	78	55	4	100	29.8	
Sulfamethizole (F18)	90% EtOH (100)	OM	0.5	Air	10% AC	78	56	4	100	41.8	200ml
Sulfamethizole (F19)	90% EtOH (100)	OM	0.5	Air	20% AC	78	56	4	100	39.5	
Sulfamethizole (F11)	90% EtOH (100)	OM	1.0	Air	5% AC	78	57	4	100	36.7	
Sulfamethizole (F12)	90% EtOH (100)	OM	1.0	Air	10% AC	78	57	4	100	43.5	
Sulfamethizole (F13)	90% EtOH (100)	OM	1.0	Air	20% AC	78	57	4	100	24	

System (sample no)	Solvent % v/v Volume (ml)	Spray Drying Mode	Solid Conc (%w/v)	Drying Gas	Blowing Agent Conc (%w/w)	Inlet Temp (°C)	Outlet Temp (°C)	Airflow rate (Nl/h)	Aspirator (%)	Yield (%)	Notes
Sulfamethizole (F6)	90% EtOH (100)	OM	1.5	Air	5% AC	78	55	4	100	51.7	
Sulfamethizole (F5)	90% EtOH (100)	OM	1.5	Air	10% AC	78	57	4	100	44.6	
Sulfamethizole (F2)	90% EtOH (100)	OM	1.5	Air	20% AC	78	56	4	100	44.9	
Sulfamethizole (F15)	90% EtOH (100)	OM	0.5	Air	-	78	59	4	100	24.0	
Sulfamethizole (F10)	90% EtOH (100)	OM	1.0	Air	-	78	59	4	100	34.0	
Sulfamethizole (F14)	90% EtOH (100)	OM	1.5	Air	-	78	57	4	100	32.8	
Sulfamethizole (F1)	90% EtOH (100)	OM	1.5	Air	-	78	56	4	100	44.2	
Sulfamethizole (F16)	90% EtOH (100)	OM	1.8	Air	-	78	59	4	100	45.4	

Table 7. Spray drying conditions for spray dried isoniazid (INH) systems.

System (sample no)	Solvent % v/v Volume (ml)	Spray Drying Mode	Solid Conc (%w/v)	Drying Gas	Blowing Agent Conc (%w/w)	Inlet Temp (°C)	Outlet Temp (°C)	Airflow rate (Nl/h)	Aspirator (%)	Yield (%)	Notes
INH I1	80:20 MeOH:BA (50)	CM	0.5	N2	-	78	45	4	100	30.4	
INH I2	50:50 MeOH:BA (50)	CM	0.5	N2	-	78	51	4	100	8.0	
INH I3	80:20 MeOH:BA (50)	CM	0.5	N2	-	100	56	4	100	16.8	
INH I4	50:50 MeOH:BA (100)	CM	0.5	N2	-	100	66	4	100	27.8	
INH I18	1:15:15 H20: MeOH:BA (100)	CM	0.5	N2	-	100	61	4	100	51.2	
INH I19	1:6:6 H20: MeOH:BA (100)	CM	0.5	N2	-	100	61	4	100	55.2	
1:9 INH/ HP-β-CD I29	1:15:15 H20: MeOH:BA (100)	CM	1.9	N2	-	100	56	4	100	71.1	

System (sample no)	Solvent % v/v Volume (ml)	Spray Drying Mode	Solid Conc (%w/v)	Drying Gas	Blowing Agent Conc (%w/w)	Inlet Temp (°C)	Outlet Temp (°C)	Airflow rate (Nl/h)	Aspirator (%)	Yield (%)	Notes
2:8 INH/ HP-β-CD I30	1:15:15 H20: MeOH: BA (100)	CM	1.9	N2	-	100	59	4	100	78.8	
3:7 INH/ HP-β-CD I31	1:15:15 H20: MeOH: BA (100)	CM	1.9	N2	-	100	60	4	100	28.2	
1:1 INH/ HP-β-CD I28	1:15:15 H20: MeOH: BA (100)	CM	1.9	N2	-	100	59	4	100	50.1	
1:9 INH/ PVP I23	50:50 MeOH: BA (100)	CM	2	N2	-	100	63	4	100	66.8	
2:8 INH/ PVP I22	50:50 MeOH: BA (100)	CM	2	N2	-	100	58	4	100	55.9	
3:7 INH/ PVP I21	50:50 MeOH: BA (100)	CM	2	N2	-	100	56	4	100	17.0	
1:1 INH/ PVP I20	50:50 MeOH: BA (100)	CM	2	N2	-	100	60	4	100	17.7	
1:9 INH/ PVP I9	50:50 MeOH: BA (100)	CM	2	N2	-	120	81	4	100	42.9	

System (sample no)	Solvent % v/v Volume (ml)	Spray Drying Mode	Solid Conc (%w/v)	Drying Gas	Blowing Agent Conc (%w/w)	Inlet Temp (°C)	Outlet Temp (°C)	Airflow rate (Nl/h)	Aspirator (%)	Yield (%)	Notes
2:8 INH/ PVP I16	50:50 MeOH: BA (100)	CM	2	N2	-	120	71	4	100	64.0	
3:7 INH/ PVP I17	50:50 MeOH: BA (100)	CM	2	N2	-	120	72	4	100	25.3	
1:1 INH/ PVP I11	50:50 MeOH: BA (50)	CM	2	N2	-	120	80	4	100	32.5	

Table 8. Spray drying conditions for spray dried rifampicin (RIF) systems.

System (sample no)	Solvent % v/v	Spray Drying Mode	Solid Conc (%w/v)	Drying Gas	Blowing Agent Conc (%w/w)	Inlet Temp (°C)	Outlet Temp (°C)	Airflow rate (Nl/h)	Aspirator (%)	Notes
RIF/ HP-β-CD Complex (NAOH) C1	100% H20	OM	10 gm from complex	Air	-	120	55	4	100	
RIF/ HP-β-CD Complex (AC) C8	100% H20	OM	10 gm from complex	Air	-	120	51	4	100	
RIF/ HP-β-CD Complex (NAOH) C2	1:5:5 H20: MeOH: BA	CM	10 gm from complex	N2	-	100	65	4	100	
RIF/ HP-β-CD Complex (AC) C6	1:5:5 H20: MeOH: BA	CM	10 gm from complex	N2	-	100	59	4	100	
RIF/ HP-β-CD (NAOH) C10	100% H20	OM	8:100 Rifampicin: HP-β-CD	Air	-	120	46	4	100	
RIF/ HP-β-CD (AC) C11	100% H20	OM	22:100 Rifampicin: HP-β-CD	Air	-	120	46	4	100	
RIF C9	100% H20	OM	0.5% rifampicin	Air	-	120	47	4	100	
RIF C5	1:5:5 H20: MeOH: BA	OM	0.5% rifampicin	Air	-	100	52	4	100	

Table 9. Spray drying conditions for spray dried pyrazinamide (PZD) systems.

System (sample no)	Solvent % v/v	Spray Drying Mode	Solid Conc (%w/v)	Drying Gas	Blowing Agent Conc (%w/w)	Inlet Temp (°C)	Outlet Temp (°C)	Airflow rate (Nl/h)	Aspirator (%)	Yield (%)	Notes
PZD P9	80:20 MeOH: H20	CM	1.0	N2	-	110	68	4	100	44.8	
PZD P7	80:20 MeOH: BA	CM	1.0	N2	-	110	71	4	100	17.9	
1:9 PZD/PVP P17	50:50 MeOH: BA	CM	1.0	N2	-	120	76	4	100	80.2	
2:8 PZD/PVP P14	50:50 MeOH: BA	CM	1.0	N2	-	120	78	4	100	61.2	
3:7 PZD/PVP P15	50:50 MeOH: BA	CM	1.0	N2	-	120	78	4	100	20.5	

APPENDIX II

Calibration curves used to determine the concentration of drug in solution.

(1) p-aminosalicylic acid in 80% (v/v) ethanol (chapter 2, section 2.2.10)

Instrument: Shimadzu UV-1700

Analytical wavelength: 280 nm

Absorbance = 0.0884*Concentration (mg/L) +0.0088

$R^2 = 0.999$

(2) Spray dried *p*-aminosalicylic acid/ammonium carbonate system in 80% (v/v) ethanol (Chapter 2, section 2.2.10)

Instrument: Shimadzu UV-1700

Analytical wavelength: 271 nm

Absorbance = 0.064*Concentration (mg/L)-0.0503

(3) Ammonium salt of p-aminosalicylic acid in 80% (v/v) ethanol (Chapter 2, section 2.2.10)

Instrument: Shimadzu UV-1700

Analytical wavelength: 280 nm

Absorbance = 0.537*Concentration (mg/100ml) -0.024

$R^2 = 0.999$

(4) Spray dried ammonium salt of p-aminosalicylic acid system in 80% (v/v) ethanol (Chapter 2, section 2.2.10)

Instrument: Shimadzu UV-1700

Analytical wavelength: 267 nm

Absorbance = 0.684*Concentration (mg/100ml)+0.037

$R^2 = 0.999$

(6) Isoniazid in deionised water (Chapter 5, section 2.2.10)

Instrument: Shimadzu UV-1700

Analytical wavelength: 262 nm

Absorbance = 0.684*Concentration (mg/100ml)+0.037

$R^2 = 0.999$

(7) HPLC calibration curves used to determine the concentration of rifampicin (Chapter 2, section 2.2.18).

Peak area = 35673*Concentration (μg/ml)

$R^2 = 0.999$